INELASTIC BEHAVIOUR OF REINFORCED CONCRETE MEMBERS WITH CYCLIC LOADING

A thesis presented for
the degree of Doctor of Philosophy
in Civil Engineering
in the University of Canterbury,
Christchurch, New Zealand.

---

by
D. C. KENT
1969

ABSTRACT

This thesis is concerned with the inelastic behaviour of reinforced concrete members subjected to cyclic overload.

Theoretical methods for predicting the flexural behaviour of reinforced concrete members have been advanced and compared with experimental evidence at each stage in the development. Particular attention has been paid to the influence of conventional rectangular binding steel on the stress-strain properties of concrete and the effect on ductility in reinforced concrete beams and columns. The Bauschinger Effect in cyclically-stressed structural grade reinforcing steel was studied in some detail, both experimentally and theoretically, and a mathematical model for this behaviour was derived and is incorporated in the analyses.

Since cyclic loading predictions require the complete loading histories of the component materials to be known, and since both materials have complex responses to this type of load, all of the analyses have been programmed for computer use.

A further experimental programme using cyclically-loaded beams was conducted in order to compare theoretical and experimental moment-curvature and load-deflection behaviour. These beams were simply-supported and cyclically-loaded to simulate seismic response in beams at connections with columns. Close agreement between experiment and the proposed theories was found.

- oOo -

ACKNOWLEDGEMENTS

This investigation was conducted in the Civil Engineering Department of the University of Canterbury, of which Professor H.J. Hopkins is Head.

I gratefully acknowledge the assistance that I have received during the course of this project and extend my thanks to:

Professor R. Park, supervisor for this study, for his valued encouragement and guidance throughout the project and for his helpful advice during the preparation of this thesis;

Members of the academic staff, including Dr A.J. Carr for assistance with Least Squares Analyses;

The technical assistance given me by Mr H.T. Watson, Technical Officer, Messrs N.W. Prebble and K.L. Marrion, Senior Technicians, and many others in the Department of Civil Engineering. I particularly wish to thank Mr J.N. Byers, Senior Technician, for his practical advice and conscientous preparation of the testing equipment and test specimens;

Members of the University Computer Centre, for punching cards and for executing programs;

The University Grants Committee for financial assistance in the form of a Post-Graduate Scholarship and a research grant;

The typist, Mrs J.M. Keoghan;

and Certified Concrete Limited, Christchurch, for providing materials.

For her forbearance and encouragement I thank my Wife.

- oOo -

CONTENTS

- oOo -

LIST OF FIGURES

Page

- oOo -

LIST OF TABLES

- oOo -

LIST OF PLATES

- oOo -

INDEX OF NOTATION

A_c = Area of concrete section confined by stirrups or ties

A_{eff} = Effective area of deformed reinforcing bar

A_g = Gross area of concrete section

A_s = Area of bottom steel

A'_s = Area of top steel

A''_s = Area of binder steel

B = Minimum dimension of confined concrete core

b = Width of rectangular section or web width of T section

b" = Ratio of confined core width to total section (or web) width

C_u = Cube strength of concrete

D = Diameter of longitudinal reinforcing steel

D" = Diameter of lateral reinforcing steel

d = Effective depth of section

d' = Ratio of compression steel depth to effective depth

d" = Height of confined concrete core

d_F = Ratio of flange thickness to effective depth for T sections

E_c = Initial tangent modulus for concrete

E_{cr} = Energy absorption of section at crushing

E_s = Young's Modulus for reinforcing steel

E_t = Tangent Modulus for reinforcing steel

E_y = Energy absorption of section at yield

e_p = Ratio of eccentricity of point of action of axial load measured from top face of member, to effective depth

F_y = Yield force for reinforcing bar

F_u = Ultimate force for reinforcing bar

f = Stress

f_c = Concrete stress

f'_c = Cylinder strength of concrete

f_{ch} = Characteristic stress for reinforcing steel

f_r = Modulus of Rupture for concrete

f_s = Tension steel stress

f'_s = Compression steel stress

f_y = Tension steel yield stress

f'_y = Compression steel yield stress

f_u = Tension steel ultimate stress

f'_u = Compression steel ultimate stress

h = Ratio of total section depth to effective depth of section

k = Ratio of neutral axis depth to effective depth of section

k_1, k_2, k_3 = Ultimate strength design parameters of Hognestad, Hanson and McHenry (Figure 2.2)

L_p = Equivalent plastic hinge length

l_c = Ratio of length of cantilever to effective depth

M = Bending moment of section

M_{cr} = Bending moment of section at crushing

M_{max} = Maximum bending moment of section

M_{ult} = Ultimate bending moment of section

M_y = Bending moment of section at yield

N = Cycle number for Bauschinger Effect in reinforcing steel

N_s = Number of sections of finite length describing a cantilever

P = Ratio of axial load on a section to the product of b and d

p = Tension steel ratio

p' = Compression steel ratio

p" = Binding steel ratio

p_t = Total longitudinal steel ratio for symmetrically-reinforced columns

R_{ch} = Characteristic Ratio for Bauschinger Effect in reinforcing steel

r = Ramberg-Osgood parameter for Bauschinger-Effect in reinforcing steel

S = Stirrup or tie spacing

t = Overall dimension of column perpendicular to the plane of bending

W = Uniformly distributed load

W_a, W_h = Parameters for strain-hardening in reinforcing steel

W_F = Ratio of flange width to web width for T sections

Z = Slope of falling branch of concrete stress-strain curve

α = Ratio of average concrete stress in stress block to concrete cylinder strength

γ = Distance of resultant concrete force from top of stress block, as a fraction of the neutral axis depth kd

ϵ = Strain

$\bar{\epsilon}$ = Strain corresponding to centroid of area of concrete stress block

ϵ_c = Concrete strain

ϵ_{ch} = Characteristic strain for Bauschinger Effect in Reinforcing steel

ϵ_{cm} = Strain in concrete fibre at top of section

ϵ_{cr} = Crushing strain for concrete

ϵ_{ipl} = Plastic strain in previous cycle for cyclically-stressed reinforcing steel

ϵ_r = Tension rupture strain for concrete

ϵ_s = Strain in tension steel

ϵ'_s = Strain in compression steel

ϵ_{sh} = Strain hardening strain for tension steel

ϵ'_{sh} = Strain hardening strain for compression steel

ϵ_{su} = Strain at ultimate stress in tension steel

ϵ'_{su} = Strain at ultimate stress in compression steel

ϵ_o = Concrete strain at maximum stress

ϵ_{20} = Concrete strain for the falling branch of the stress-strain curve at 20 per cent maximum stress

ϵ_{50b} = $\epsilon_{50t} - \epsilon_{50c}$

ϵ_{50c} = Strain at 50 per cent maximum stress on the falling branch of the stress-strain curve for unconfined concrete

ϵ_{50t} = Strain at 50 per cent maximum stress on the falling branch of the stress-strain curve for confined concrete

θ_p = Plastic rotation at beam plastic hinge

ϕ = Curvature

ϕ_{cr} = Section curvature at crushing

ϕ_{u} = Section curvature at ultimate

ϕ_{y} = Section curvature at yield

- oOo -

CHAPTER 1

INTRODUCTION AND SCOPE OF RESEARCH

1.1 GENERAL

This country is among those in which provision for the possibility of earthquakes must be made in the design of structures. Most design procedures recommended by codes of practice are based on experimental evidence, yet most previous researches into ductility, plastic hinging and other post-elastic characteristics of reinforced concrete sections, have consisted of applying monotonically-increasing loads to test specimens until failure. Under most circumstances, and particularly in the case of seismic loading, the likelihood of a building being failed in this fashion is slight. That the recommendations of the codes of practice may not be applicable to the cyclic behaviour associated with seismic loading has long been recognised.

1.2 OBJECT AND SCOPE

The growing use of electronic computers as a design tool has resulted in a very rapid advance in the dynamic analyses of structures. Perhaps because this application is

attractive to researchers, a study of the factors on which such analyses should be based, the behaviour of the component materials, has fallen well behind the computer analyses. That this is so is well illustrated by the inaccurate and even apparently unsafe, idealised models that are currently being used to predict cyclic, inelastic behaviour of high rise structures to seismic loading.

Three previous experimental investigations[50,62,67] have been solely concerned with the cyclic behaviour of reinforced concrete sections. The first, conducted by Agrawal, Tulin and Gerstle[50] has concerned itself with the behaviour of beam sections and has proposed a simple mathematical expression for the Bauschinger Effect in reinforcing steel. This study is discussed more fully in Chapter 3. The second investigation was reported on by Hanson and Conner[62] and is purely an experimental programme, in which the Bauschinger Effect is mentioned briefly, but in the writer's view not recognised as being of great significance. Bertero and Bresler[67] have contributed with a descriptive paper in which the work of the previous authors is also summarised.

The scope of the investigation reported herein was restricted to the study of the cyclic, flexural behaviour of concrete and steel, both individually and when combined to form beams and columns. As such it was intended to make a wide study into the effects that the various features of

steel and concrete stress-strain behaviour have on the response to cyclic loading, and to assess the relevance of each of these factors. Therefore this thesis is a preliminary study and its objective is to indicate the more immediate needs for research in this topic rather than to propose changes in existing seismic design techniques. However, experimental and theoretical evidence is presented in the text that could justify modifications to current practice.

Other features of reinforced concrete behaviour under cyclic loading, for example shear and bond capacities, have not been studied in detail but have been mentioned briefly herein.

1.3 FORMAT

The chapters of this thesis have been arranged as far as possible to represent the individual studies within this investigation.

In Chapter 2, the results of previously-published experimental results for the stress-strain behaviour of concrete are collated. The behaviour of plain concrete has been considered and a method for modifying the falling branch of the stress-strain curve for confinement afforded by conventional rectangular stirrups or ties has been proposed.

Chapter 3 describes an experimental and theoretical investigation into the behaviour of structural-grade reinforcing steel. Special significance has been attached to the response of reinforcing steel to alternating stress cycles and this factor has been studied in some detail.

Theories developed in these two chapters are combined in Chapter 4 and used to study the monotonic behaviour of reinforced concrete sections. The consequent theory is shown to compare favourably with published test results and then used to illustrate the effects of lateral confinement of concrete on the ductility of beam and column sections.

Chapter 5 extends the theory further to enable predictions of cyclic behaviour of reinforced concrete beam sections. Again this analysis is compared with experimentally-obtained moment-curvature results.

The theory of Chapter 5 is utilised in Chapter 6 to enlarge the scope of the investigation by considering the deflection behaviour of simple beams, comprising a number of discrete elements of length.

The experiments that were performed to provide comparisons for the analyses of the previous two chapters are described in Chapter 7.

The conclusions that have been reached and the suggestions for future reseach are summarised in Chapter 8. Generally, conclusions appear with discussions in the body of

the thesis and therefore the formal conclusions in this chapter are comparatively brief.

1.4 PRESENTATION OF RESULTS

Many diagrams and tables supplement the text of this thesis. In many cases, these diagrams have been used rather than text to conserve space and are therefore discussed very briefly or even simply referred to.

Many of the experimental results have been plotted and appear in conjunction with the theoretical analyses with which they are compared, rather than in the chapter discussing the experimental programme.

1.5 COMPUTER FACILITIES

For the major part of this investigation, the University of Canterbury's principal computer was an I.B.M. 360 model 44 with 16^K, 32-bit words core storage. This central storage was doubled towards the end of this study. Peripheral storage comprised two 2311 disc drives, each capable of storing $250{,}000^K$ words. This is a third generation machine designed specifically for scientific use and thus has a very rapid execution speed.

A large part of this investigation was devoted to the development of computer programs. The workings of these programs are dealt with only briefly in the text of this thesis, and listings and instructions for their use appear in Appendix B.

CHAPTER 2

STRESS-STRAIN CHARACTERISTICS OF CONCRETE

SUMMARY

The behaviour of concrete under monotonic, repeated and cyclic loading is considered. Compressive stress-strain curves for plain and confined concrete based on previously-published test data are presented and an approximate method of predetermining concrete stress-strain characteristics for flexural and axial loading conditions is proposed.

2.1 INTRODUCTION

Many stress-strain curves for concrete have been postulated in recent years[5,9,10,12,13,16,23,27] and probably no other single aspect of Civil Engineering has been the subject of such a vast amount of research as has this material. An inherent problem in determining compressive stress-strain curves has been the difficulty of directly measuring stress in concrete subject to flexure. Consequently, empirical expressions have evolved that are either based in some way on the load-deformation responses

obtained from axially-loaded specimens or indirectly from beam and column tests using numerical integration of moment-load-strain observations. The validity of the first method has been questioned from time to time[9,51], but the fact remains that any reasonable shape of stress-strain expression for compressed concrete produces sufficiently accurate estimates of ultimate bending moments in under-reinforced beam sections. The explanation is simply that reinforcing steel, which has an easily defined stress-strain expression, has by far the greater influence on flexural moments for such beams.

Soon after Whitney's Ultimate Strength Theory, based on the idealised rectangular stress block, was published[3,4], research into factors influencing the flexural stress-strain curve for concrete lapsed, and the subject was for some time considered as of only academic interest. More recently however, the plastic hinge theories have resulted in a renewed interest in the topic, for the ultimate curvature, and hence the energy absorption capacity of a monotonically-loaded section, is greatly dependent on the maximum strain to which concrete can be subjected. Consequently many formulae for the determination of ultimate concrete strain have been proposed[17,18,19,32,42,43,55], many of which are based on the cylinder strength. As Rüsch[28] has shown, the ultimate strain in concrete depends to a larger extent on the shape of the section, the position of the neutral axis, and the

rate of loading.

Most of the developments to date have arisen from monotonic loading tests and this approach is now inadequate. A clearer picture of concrete behaviour at all stages of the stress-strain relation is required for analyses concerned with cyclic behaviour.

2.2 HISTORICAL REVIEW

Excellent historical reviews on previous concrete research have been published by Hognestad[10,12,24] in the early 1950's and there seems little point in repeating them here. Since that time, however, there have been a number of notable contributions to the literature and some should be mentioned briefly.

2.2.1 Unconfined Concrete

In 1950, Herr and Vandegrift[8] studied the compression zones of singly-reinforced concrete beams with constant moment zone using a photo-elastic method incorporating isotropic glass. This investigation was beset with experimental difficulties caused by varying humidity and changes of moisture content in the concrete. Consequently their findings should be interpretted with caution. Using concrete with a 4,500 p.s.i. cylinder strength, they found the maximum flexural stress to be 6,500 p.s.i.; an increase in strength of 45 per cent. No further experimental work using this approach has been published since these pilot tests.

At about the same time, Hognestad[10,12] carried out eccentric and concentric loading tests on one hundred and twenty short column specimens of both rectangular and cylindrical section and his well known stress-strain expression resulted (Figure 2.1).

Parme[11] reported on U.S. Bureau of Reclamation beam tests that utilised small pressure cells and thus stresses in the compression zone were obtained directly. These experiments showed the measured maximum concrete stress to be equal to the cylinder strength. The complexity of instrumentation and cost probably account for no further work being undertaken using this technique.

The now classical Portland Cement Association tests conducted by Hognestad, Hanson and McHenry[18] were reported in 1955. Using eccentrically-loaded specimens, the compression zone of a beam was simulated by maintaining zero strain at one face of the specimen. Their resulting parameters k_1, k_2 and k_3, are based exclusively on cylinder strength. Again, the ratio of maximum flexural stress to cylinder strength is sufficiently close to unity for structural grade concretes (Figure 2.2). In fact, the stress-strain curves for their cylinders were very similar to those obtained from their eccentrically-loaded specimens. Hognestad et al., therefore concluded that "The true general characteristics of stress-strain relations for concrete in concentric compression are indeed applicable to flexure".

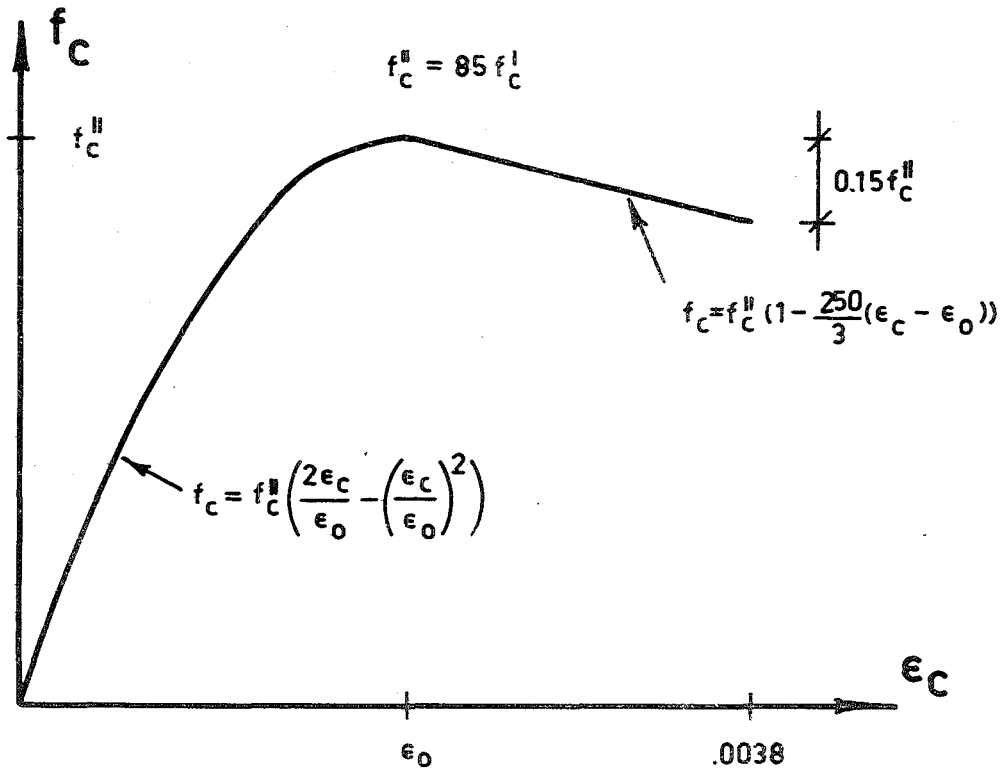

FIG.2.1 - HOGNESTAD'S[10] STRESS-STRAIN MODEL

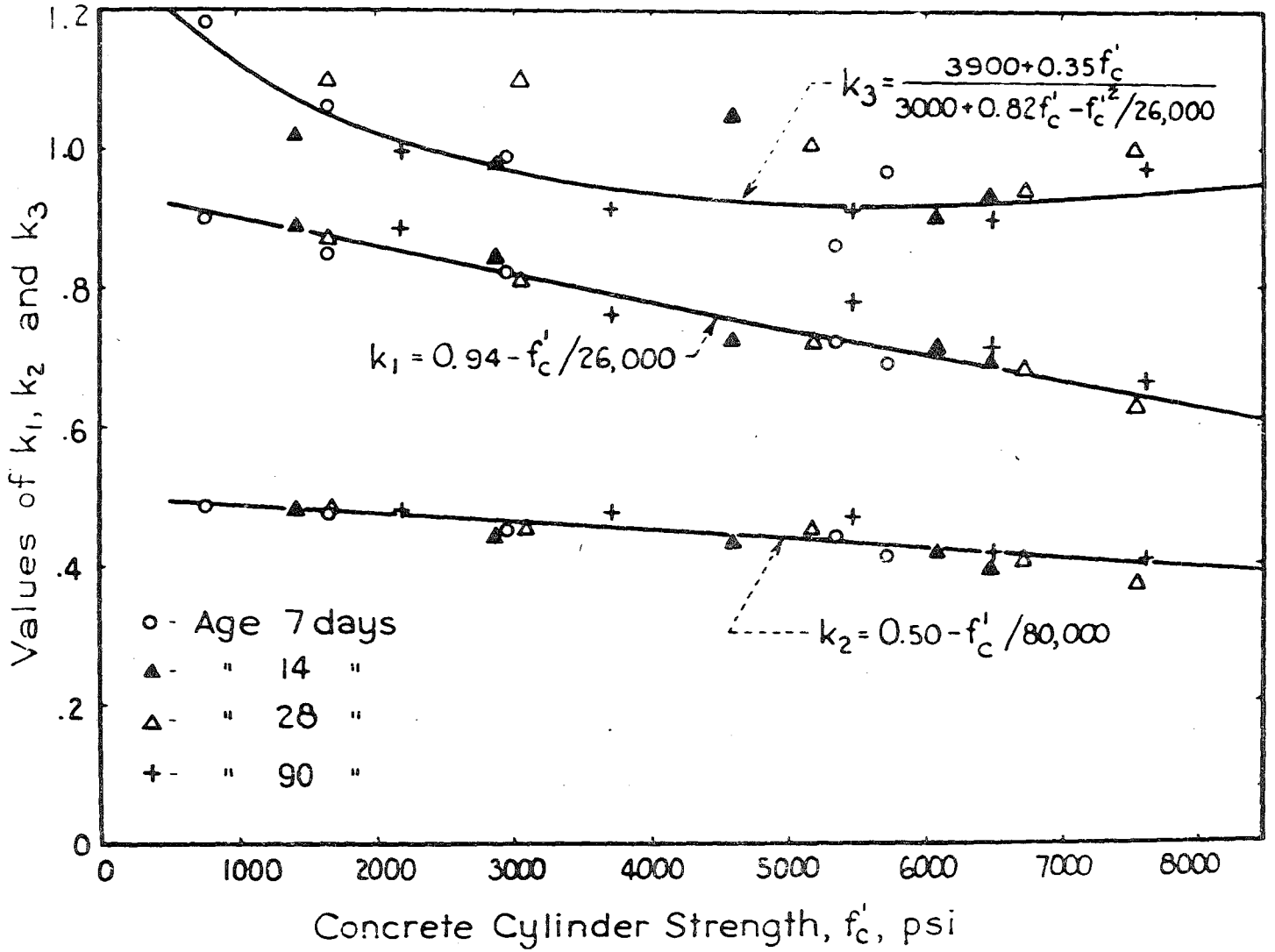

FIG.2.2 - ULTIMATE STRENGTH FACTORS[18]

An extremely thorough experimental programme on this subject was introduced by Rüsch[28] in 1960. His objective was to determine which variables affected the stress-strain curve and to what extent. On the basis of this more complete knowledge, rational simplifications could be made for design purposes. Up until this time, the simplifying assumptions had been made in advance, and Rüsch's "grass-roots" approach was most enlightening, showing the effects of time on the material to be very marked. Unfortunately this work is not yet completed, but a simplified design curve for one concrete strength was published and is compared with expressions derived by Hognestad et al.[18] in Figure 2.3.

Sinha, Gerstle and Tulin[39] proposed a method in 1964 for modifying the cylinder stress-strain curve for repeated loading. Expressions were developed for envelope, unloading and reloading curves. It is significant that they later[41, 50] found the accuracy of the stress-strain curves to be of minor importance in beams subjected to repeated loading.

In 1965, the question of using the concentric compression curve for flexure was again aired, this time by Sturman, Shah and Winter[51] of Cornell University. By studying microcracks, the initial cause of failure in concrete, as observed by Richart, Brandtzaeg and Brown[1,2] in 1928, they noted that a flexural strain gradient across the section appeared to "retard and reduce" microcracking,

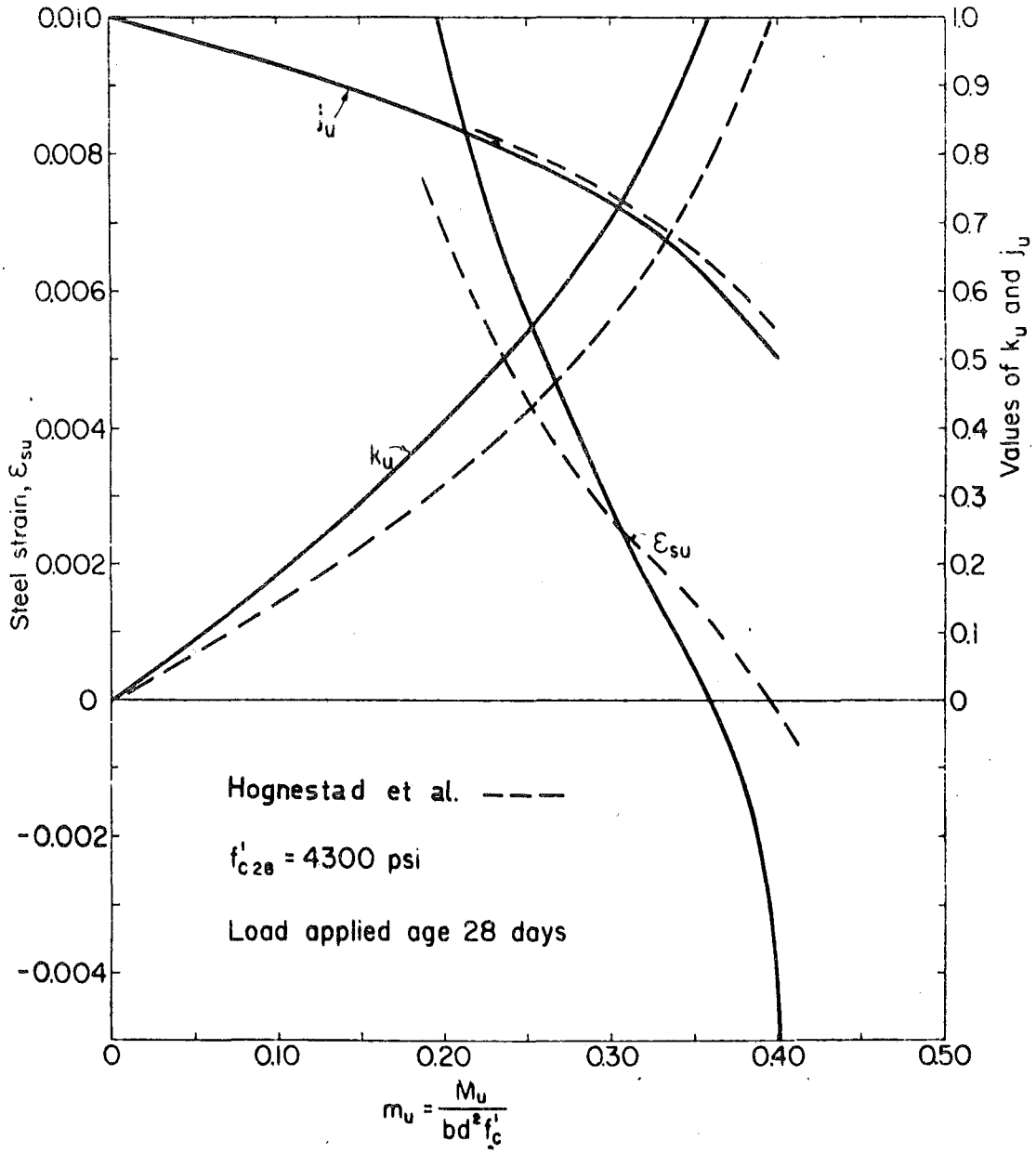

FIG.2.3 - RÜSCH'S[28] DESIGN PARAMETERS

and that this resulted in quite different stress-strain curves for concrete in flexural and uniaxial compressions. With maximum flexural stresses 20 per cent in excess of maximum concentric stresses, their findings reinforced, to some degree, the results of Herr and Vandegrifts'[8] photo-elastic tests.

2.2.2 Concrete Confined by Lateral Steel

Chan's[17] tri-linear idealised expression for confined concrete appeared in 1955 with the suggestion that the "falling" branch of the stress-strain curve did not always exist (Figure 2.4). This "curve" was based on results from tests on short columns. Unfortunately, values for Chan's experimental parameters did not appear in his paper, although he did publish curves relating percentage binders, ultimate concrete strain, and the ratio of ultimate flexural strength to control specimen strength for rectangular and spiral binding steel.

It was not until 1964 that any significant research into lateral reinforcing steel was published. Roy and Sozen[45] conducted tests on 60 axially-loaded 5 in. x 5 in. x 25 in. concrete prisms. These tests led Roy and Sozen to believe that the binding ratio was linearly related to the strain at 50 per cent of the maximum stress on the falling branch of the stress-strain curve. The work of these investigators is further discussed in Section 2.5.

In 1965, Base and Read[52] published results from tests

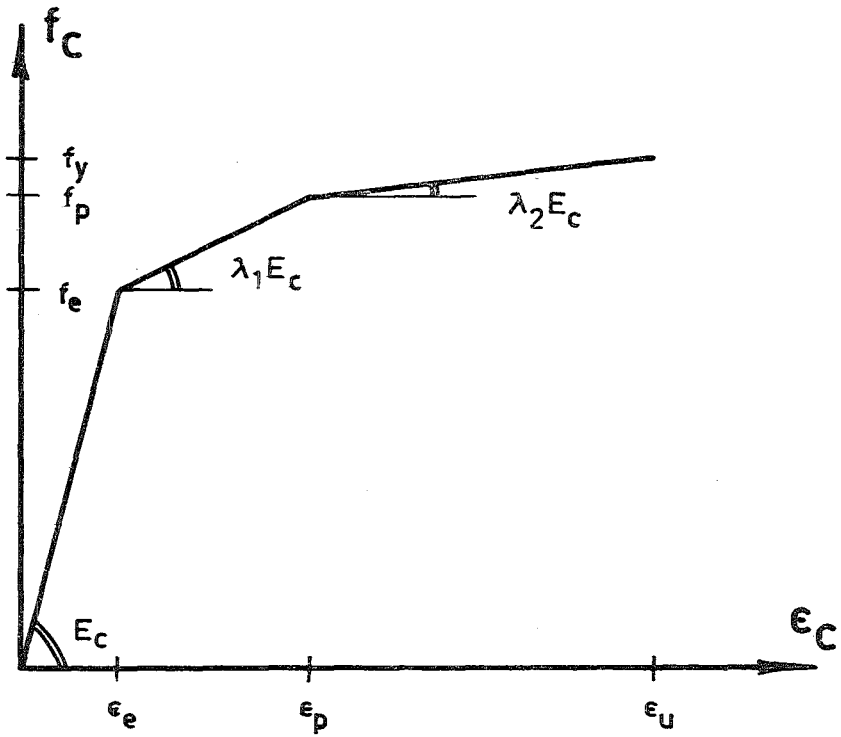

FIG.2.4 - CHAN'S[17] STRESS-STRAIN MODEL

on beams with helical and conventional binding reinforcement in the compression zone. They found that for under-reinforced beams, the moment-curvature characteristics were affected only to a very slight extent by the percentage binders (Figure 2.5). The effect was, however, most marked for over-reinforced beams.

A further study into lateral reinforcement effects on the concrete stress-strain curve was published by Soliman and Yu[64] in 1967. Using an experimental technique similar to that employed by Hognestad et al.[18], their tests led to a bilinear-parabolic expression of the type shown in Figure 2.6. The work of Soliman and Yu is also discussed more fully later.

Other work on confined concrete has been published by Rüsch and Stöckl[37], Bertero and Felippa[46] and Nawy et al.[66].

2.3 STRESS-STRAIN RELATION FOR PLAIN CONCRETE

The plain concrete uniaxial stress-strain relationship used in this thesis is shown in Figure 2.7. Reasons for the adoption of this curve are as follows:

2.3.1 Ascending Portion of Curve

Most investigators agree that the ascending portion of the stress-strain curve can be represented by a parabola. This thesis, in common with Hognestad[10] and others, utilizes Ritter's second degree parabola which has the form:

$$f_c = f''_c \left[\frac{2\epsilon_c}{\epsilon_o} - \left(\frac{\epsilon_c}{\epsilon_o} \right)^2 \right] \qquad \ldots\ldots(2.1)$$

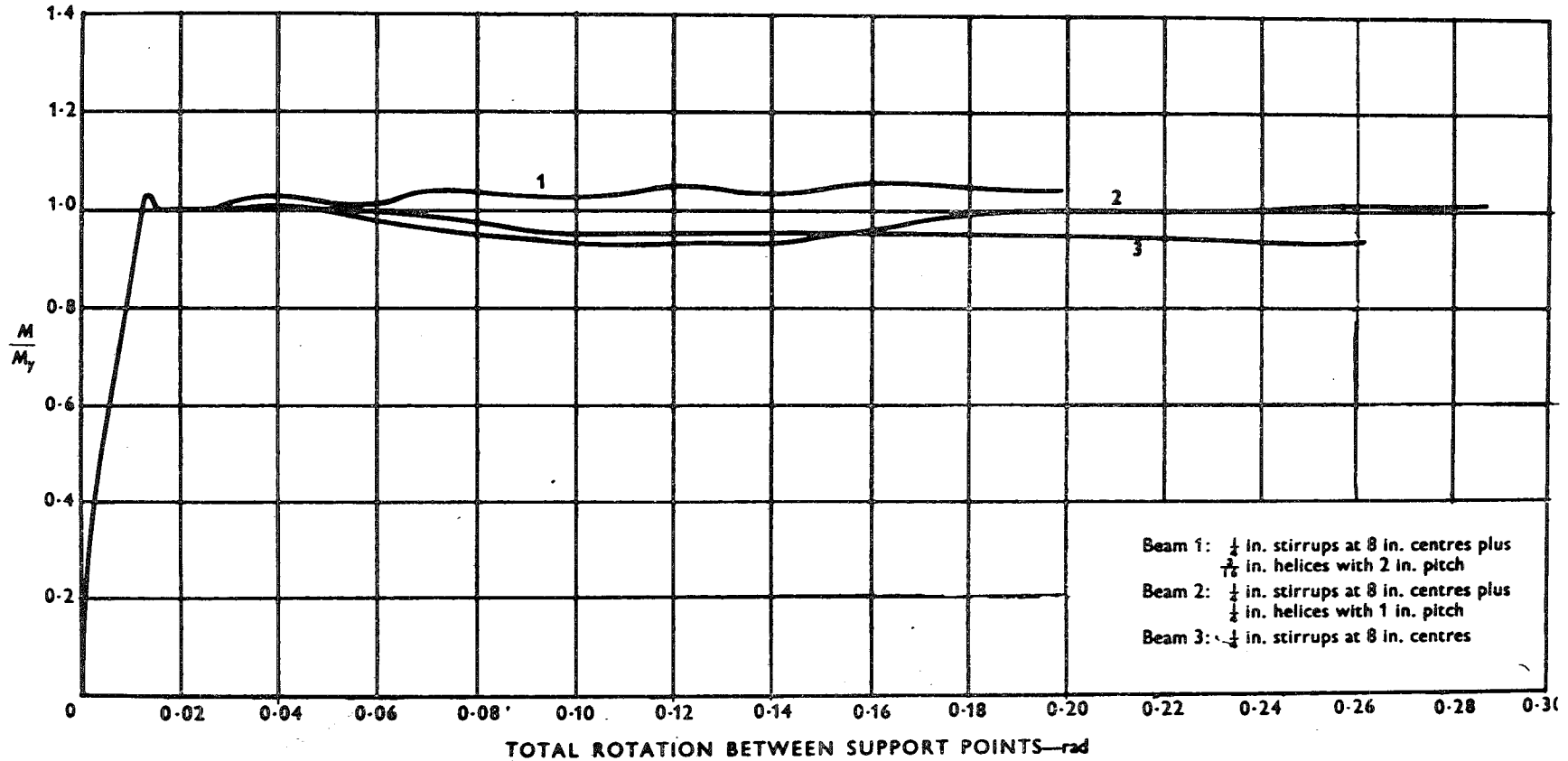

FIG.2.5 - MOMENT-ROTATION CURVES[52]

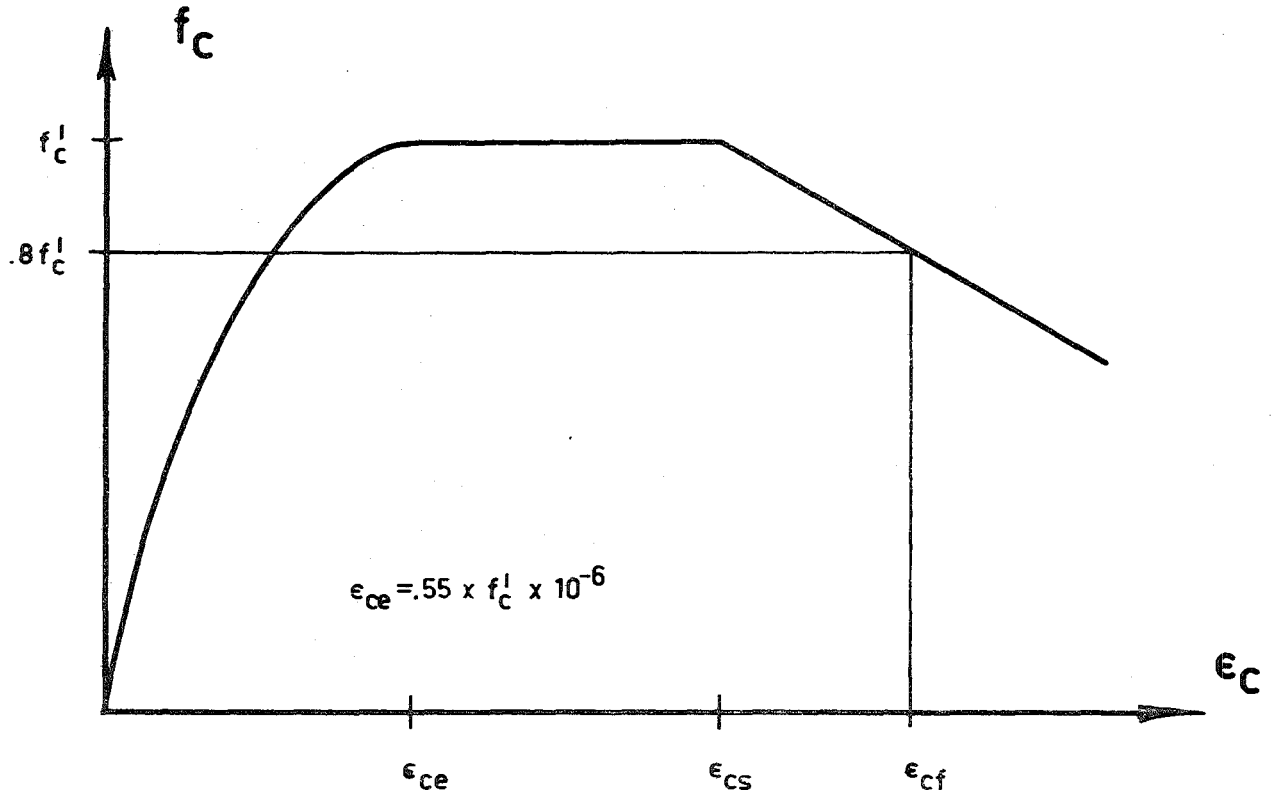

FIG.2.6 - SOLIMAN AND YUS'[64] STRESS-STRAIN MODEL

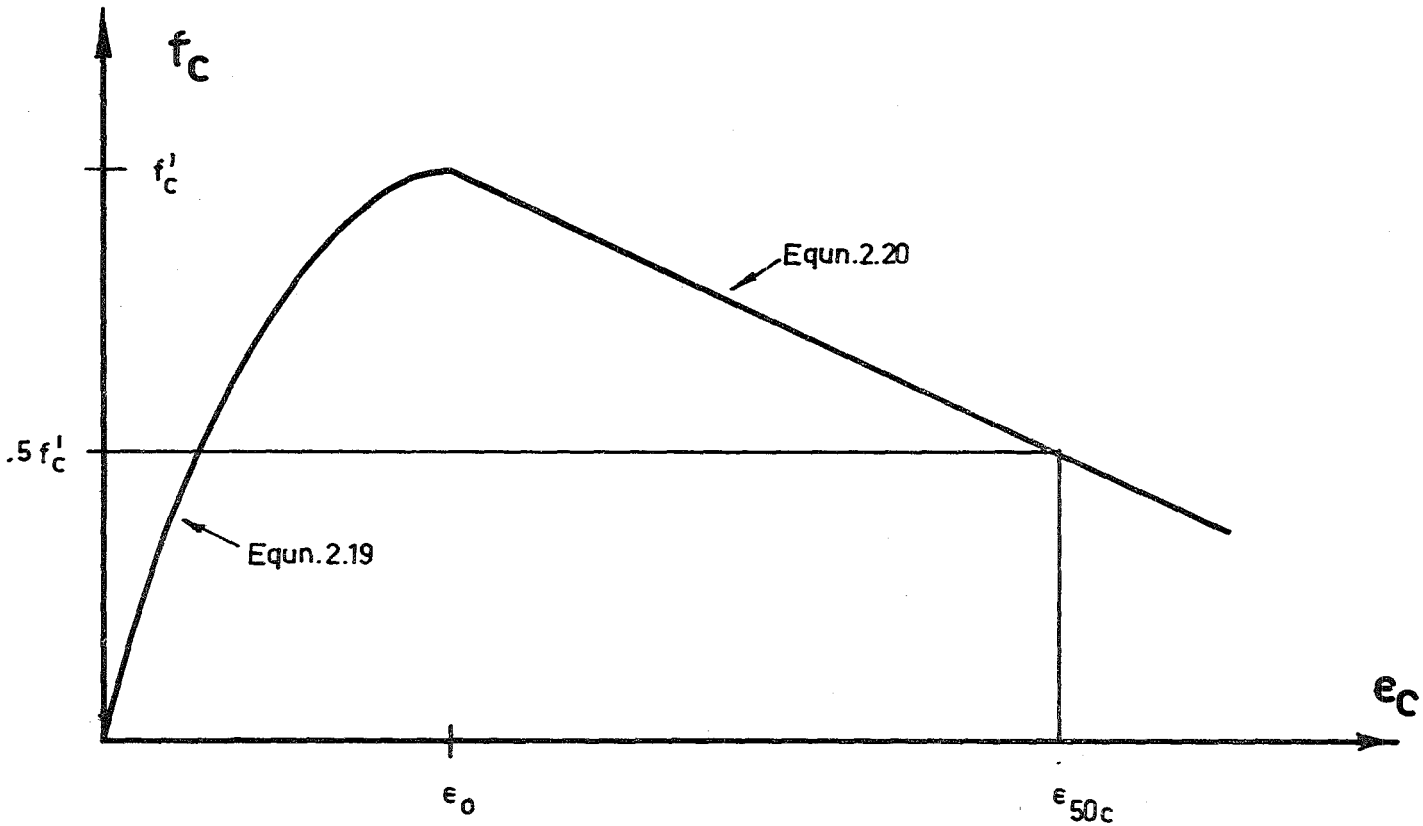

FIG.2.7 - ASSUMED COMPRESSIVE STRESS-STRAIN RELATION FOR UNCONFINED CONCRETE

where f''_c = maximum concrete compressive stress

ϵ_o = corresponding concrete strain

Differentiating this expression and equating ϵ_c to zero gives the initial tangent modulus as:

$$E_{c_o} = \frac{2f''_c}{\epsilon_o} \qquad \ldots\ldots(2.2)$$

2.3.2 Maximum Flexural Stress

The following reasons are listed in support of the author's use of cylinder strength as the maximum flexural stress (i.e. $f''_c = f'_c$):-

1. The $f''_c = 0.85f'_c$ used by Hognestad[10] was based on column tests.

2. The Portland Cement Association tests on compression zones with strain gradients, conducted by Hognestad et al.[18] show that $k_3 = 1$ appears to be as good a fit to experimental results as their expression for concrete strengths in excess of 2,500 p.s.i. (Figure 2.2).

3. The pressure cell tests reported by Parme[11] and using direct stress measurements have found this to be the case.

4. The observations of Sturman, Shah and Winter[51], showing that the effect of a strain gradient makes the flexural stress-strain relation substantially different from concentrically-loaded cylinders is recognised. However, it is felt that this theory has not yet been advanced to the extent of being generally applicable. On their

findings, use of the cylinder strength as the maximum flexural stress is a conservative assumption.

2.3.3 Strain at Maximum Stress

The strain, ϵ_o, corresponding to maximum stress, is taken as a constant value. The tests on concrete cylinders in the present investigation did not find a consistent dependence on cylinder strength as observed by Lee[15]:

$$\epsilon_o = (1220 + \frac{1}{6}f'_c) \times 10^{-6} \qquad \ldots\ldots(2.3)$$

but found $\epsilon_o = 0.002$ to be a safe limiting value.

2.3.4 "Falling" Branch Behaviour

It is in this region of the stress-strain curve that mathematical expressions are lacking. Various investigators[16,23,27,34,39,40,51] have proposed functions for a continuous stress-strain curve from zero load, through maximum stress, to ultimate failure, but in most cases, this advantage is outweighed by the complex expressions resulting from integration. Furthermore, as shown later in this chapter, such expressions cannot be easily modified for the increase in ductility arising from lateral confinement.

Figure 2.7 shows that the falling branch has been idealised as a linear relationship. This approximation has a negligible effect on moment-curvature response as has been shown by other investigators[5,9,10,12,13,35,36,43,44]. In order to determine the falling branch characteristics the results of other investigators will be used.

Figure 2.8 shows a plot of experimental results with maximum stress, f'_c, and the strain at 50 per cent maximum stress on the falling branch compared. It can be seen that for rapid loading rates, the experimental points[6,10,18,27,33,45] plotted on this graph conform quite closely to the expression:

$$\epsilon_{50c} = \frac{3 + 0.002 f'_c}{f'_c - 1000} \quad \text{[psi]} \qquad \ldots\ldots(2.4)$$

Rüsch[28] has shown that as the rate of straining is decreased, an increase in ϵ_{50c} is obtained.

The implications of this relationship are that a truly generalised dimensionless plot of (f_c/f'_c) versus ϵ_c cannot be achieved because the higher strength concretes have considerably lower values for ϵ_{50c}, i.e., they are more brittle, and the falling branch then has a steeper average slope. It would appear then, that the ductility of concrete depends significantly on the strength of the concrete itself. The neglect of this factor was probably responsible for the discrepancies in results obtained by Roy and Sozen[45] and by Bertero and Fellipa[46], since concrete strengths were considerably higher in Bertero and Felippas' tests.

2.3.5 Spalling Strain

It seems that the strain at which spalling of concrete commences depends mainly on the strain gradient over the cross-section. A wide variety of spalling strains has been

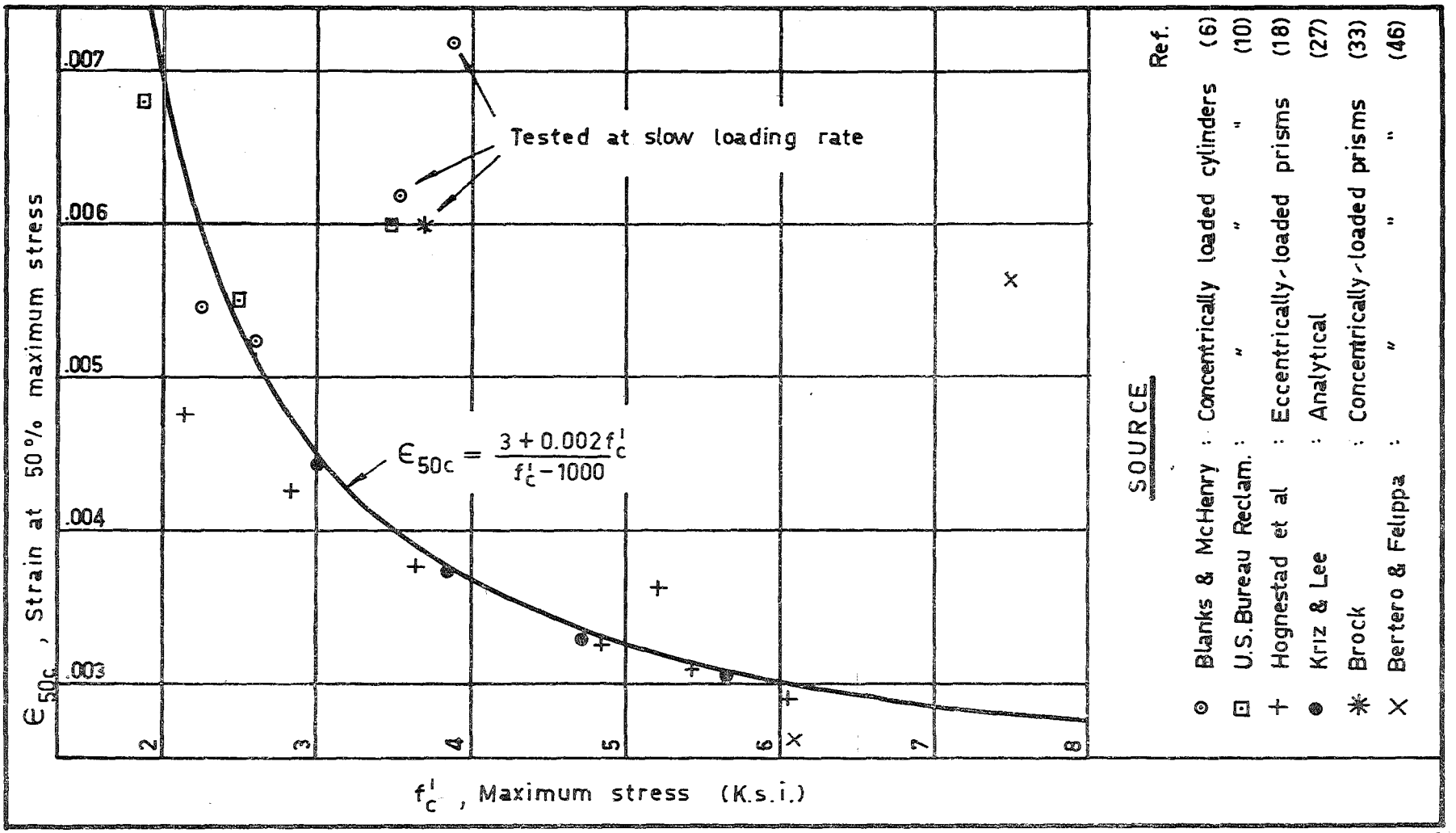

FIG.2.8 - FALLING BRANCH PROPERTY FOR UNCONFINED CONCRETE

observed and this thesis assumes a value of ϵ_{cr} = .004 as being conservative in most cases.

2.4 FACTORS INFLUENCING INCREASED DUCTILITY FOR CONFINED CONCRETE IN COMPRESSION

It is evident that lateral reinforcement has a beneficial effect on the stress-strain response of concrete and results in a reduced slope for the falling branch of the stress-strain curve. There is considerable speculation regarding the question of an increase in maximum compressive stress due to binders, and experimental work reported to date[17,45,52,64] produces conflicting results. Roy and Sozen[45] did not observe any maximum strength increase due to rectangular binders but others[17,46] have. There is, however, little doubt that circular spiral binders are more efficient than conventional rectangular stirrups or ties, and the more efficient restraint to radial stresses intuitively supports this observation.

This thesis assumes that lateral binding steel has no effect on the rising portion of the stress-strain curve or on the maximum stress. Brock[33] has shown (Figure 2.9) that Poisson's ratio for concrete remains reasonably constant up to about 90 per cent of the maximum stress (the "Critical" stress) and it is therefore contended that lateral strains are minimal in this region. Base and Read[52] have also stated this and it appears that most investigators

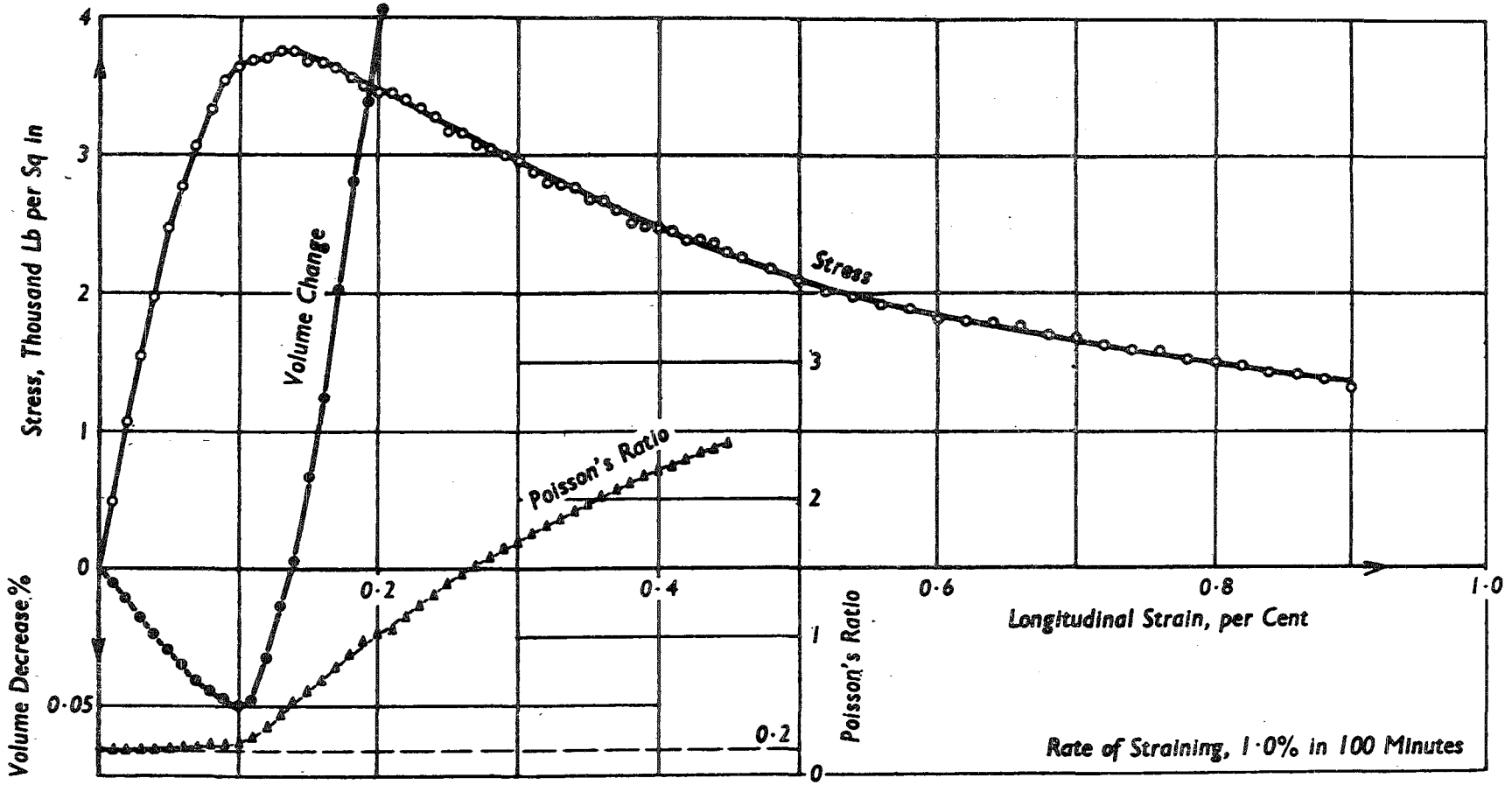

FIG.2.9 - BROCK'S[33] STRESS-STRAIN CURVE

implicitly accept that the ascending portion of the curve is unaffected by lateral steel. For this reason the author feels that the triaxial stress tests on concrete performed by Richart et al.[1,2] which used a fluid pressure loading are not strictly comparable with the confining effect provided by lateral confining steel; this latter confinement being the result of passive pressure at advanced longitudinal strains. The experiments of Richart et al.[1,2] utilised active pressure which were applied before the commencement of longitudinal deformation. It can be argued that in the limiting case, this active pressure is analogous to the constant confinement afforded by stirrups or ties at yield, but since it is not yet clear when, in the concrete stress-strain history, the confining steel yields, this approach, and mathematical expressions resulting from it[29] are, in the writer's opinion, open to serious criticism. The work of Balmer[7] supports this view to some extent.

The question of whether or not the stirrups or ties do yield is an interesting one. Frequently they do not and in such cases a smaller binding steel percentage should produce an identical concrete stress-strain response. Future research aimed at an expression for concrete ductility predictions will need to consider the consequences of this.

Conventional rectangular stirrups or ties are the only type of lateral reinforcement studied in this thesis.

The following variables are relevant when considering falling branch behaviour of the stress-strain curve for concrete confined in this way:-

1. Diameter of lateral reinforcement, D",
2. Spacing of lateral reinforcement, S,
3. Number of stirrups or ties at one point, N_T,
4. Relationship between stirrup or tie spacing and minimum dimension of confined core, B,
5. Strength of concrete itself,
6. Strain gradient over section and adjacent to it,
7. Longitudinal reinforcement,
8. Rate of loading,
9. Stress in lateral reinforcement.

The first two variables are usually considered by using the simple binding steel ratio:

$$p'' = \frac{A_s'' \cdot 2(b'' + d'')}{b''d''S} \qquad \ldots\ldots(2.5)$$

where A_s'' = area of stirrup or tie

b'' = width of confined core

d'' = depth of confined core.

The importance of the third and fourth variables may be illustrated with Figures 2.10(i) and 2.10(ii). Figure 2.10(i) shows an elevation of a beam with pairs of stirrups at S_1 centres. Figure 2.10(ii) shows an elevation of a beam with identical b", d" and p" such that $S_2 = \frac{1}{2} S_1$. It is evident that the confinement of concrete between the stirrups relies

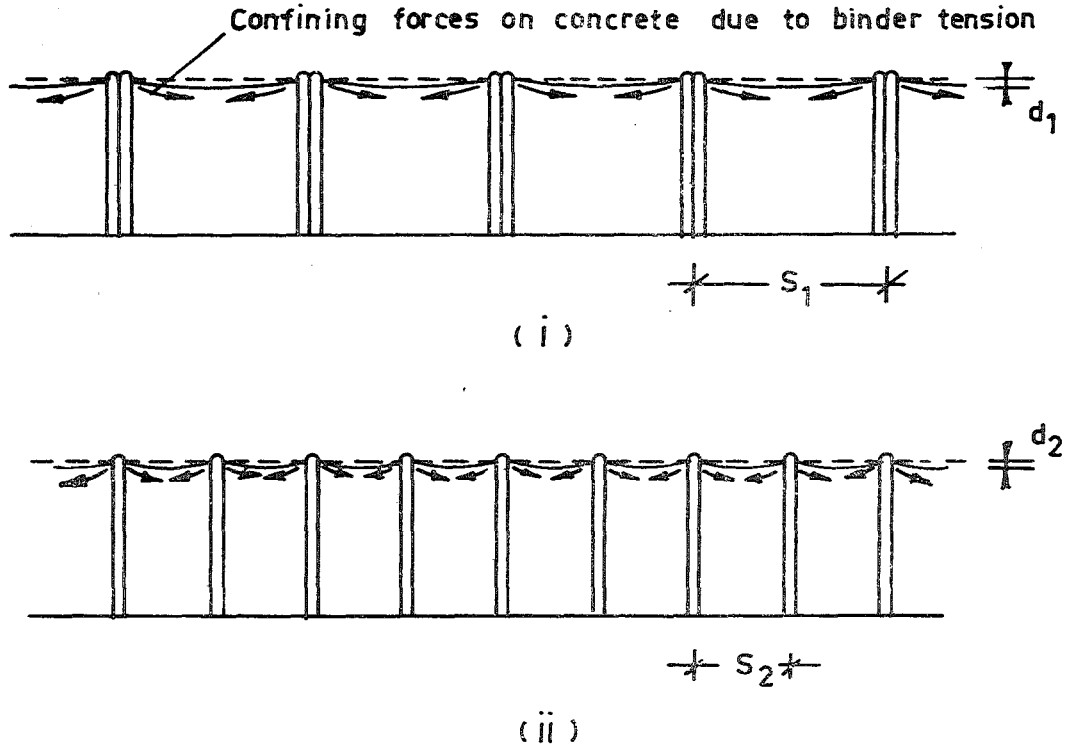

FIG.2.10 - EFFICIENCY OF LATERAL REINFORCEMENT

on the arching action developed by the binder forces on the concrete. Clearly the confinement provided for the concrete is greater for the beam shown in Figure 2.10(ii), because there is less concrete lost due to the arching action between stirrups. For the simple one-dimensional cases illustrated here, the volume of concrete lost due to arching action can be shown to be:

$$V_{CA} = \frac{b'' \psi s^2}{6} \qquad \ldots\ldots(2.6)$$

if the arch is assumed to be parabolic and where ψ = a constant.

Therefore the use of the p" term alone is insufficient for a prediction of concrete ductility and a means is required of allowing for the <u>efficiencies</u> of similar binding steel ratios. Notice that it is not only grouped stirrups or ties that are inefficient, for the pair of stirrups shown in Figure 2.10(i) could be replaced by a single, larger bar such that p" is unaltered.

In this thesis the ratio $\sqrt{B/S}$ is used as a measure of efficiency. The choice of $\sqrt{B/S}$ rather than B/S is discussed in Section 2.5.

The fifth variable has been discussed in Section 2.3.4 and is illustrated in Figure 2.8.

The remaining four variables have not been studied as it was felt that insufficient experimental data was available.

Other investigators[42,55] have considered the strain gradient over and adjacent to the section in expressions for ultimate concrete strain. Similarly, expressions exist[32] that take longitudinal reinforcement into account. There appears to be nothing in the literature indicating a study of stresses in the lateral reinforcement of beams although pilot tests on spacing and size of column ties have been reported[30].

2.5 DIMENSIONLESS ANALYSIS FOR CONFINED CONCRETE

Published experimental results from confined concrete tests[45,46,64] were studied and values for ϵ_{50t} (see Figure 2.13) measured from the load-strain curves shown in the references. When obtaining ϵ_{50t} for confined concrete alone it was assumed that spalling of the specimens commenced after maximum load and that spalling of the cover concrete was complete at a load corresponding to ϵ_{50t}; i.e., the load is distributed over the gross section, A_g, at maximum load, and at ϵ_{50t} is distributed only over the confined core area, A_c.

$$\therefore f'_c = \frac{P_{max}}{A_g}$$

Thus the load at which ϵ_{50t} occurs is given by P_{50} and is related to P_{max} as follows:

$$\tfrac{1}{2} f'_c = \frac{P_{50}}{A_c} = \frac{P_{max}}{2A_g}$$

$$\therefore P_{50} = \frac{P_{max}}{2} \cdot \frac{A_c}{A_g} \qquad \ldots\ldots(2.7)$$

In this way, loads corresponding to 50 per cent maximum core stress were computed and used to obtain values from previous investigations for ϵ_{50t} (Table 2.1). These ϵ_{50t} values were scaled off the diagrams provided in the references.

In all cases, f'_c could be determined and ϵ_{50c} was computed using Equation (2.4). The measure of additional strain at 50 per cent maximum stress on the falling branch of the stress-strain expression and being provided by binders is then given by:

$$\epsilon_{50b} = \epsilon_{50t} - \epsilon_{50c} \qquad \ldots\ldots(2.8)$$

and this ϵ_{50b} is therefore independent of the concrete strength.

Values of p" and B/S were then computed and a plot of ϵ_{50b} versus p" (B/S) was made. It was found that in this form, (B/S) had too large an influence on ϵ_{50b} and to reduce this effect, square, cube and fourth roots of (B/S) were combined with p" and compared with ϵ_{50b}. Each set of points was then subjected to least squares analyses using two equations:

TABLE 2.1

TEST RESULTS FOR CONFINED CONCRETE

Source	Ref. No.	Spec. No.	f'_c	ϵ_{50c}	$\frac{1}{2}A_b/A_c$	ϵ_{50t}	ϵ_{50b}	B/S	$\sqrt[2]{B/S}$	$\sqrt[3]{B/S}$	$\sqrt[4]{B/S}$	p"	p" B/S	p"$\sqrt[2]{B/S}$	p"$\sqrt[3]{B/S}$	p"$\sqrt[4]{B/S}$
SOLIMAN & YU**	64	2	3660	.00388	.460	.00793*	.00405	.475	.690	.780	.830	.0035	.00166	.00242	.00273	.00290
		3	3980	.00368	.460	.00740	.00372	.633	.795	.860	.892	.0046	.00291	.00366	.00396	.00410
		4	3460	.00445	.460	.00959	.00514	.950	.975	.981	.986	.0069	.00655	.00672	.00673	.00680
		5	3730	.00385	.460	.01210	.00827	1.267	1.125	1.081	1.061	.0092	.01164	.01035	.00995	.00976
		6	3740	.00382	.460	.01912*	.01530	1.900	1.378	1.240	1.172	.0137	.02600	.01885	.01700	.01610
		7	3630	.00390	.460	.04085*	.03695	3.800	1.950	1.560	1.396	.0274	.10400	.05345	.04275	.03820
		8	3720	.00382	.455	.01500	.01118	.937	.966	.977	.983	.0108	.01011	.01043	.01055	.01060
		9	3590	.00393	.455	.02165*	.01772	1.875	1.370	1.231	1.170	.0215	.04033	.02945	.02650	.02520
		10	3190	.00428	.450	.01440	.01012	.925	.961	.974	.980	.0171	.01581	.01643	.01665	.01675
		11	3810	.00378	.450	.02320*	.01942	1.850	1.360	1.228	1.167	.0341	.06305	.04640	.04180	.03980
		12	3740	.00382	.460	.01836*	.01454	1.850	1.360	1.228	1.167	.0137	.02535	.01862	.01680	.01600
		13	3980	.00368	.455	.01785*	.01417	1.400	1.182	1.120	1.090	.0166	.02325	.01970	.01860	.01810
		14	3930	.00367	.475	.01945*	.01578	2.400	1.550	1.340	1.245	.0119	.02855	.01845	.01595	.01481
		15	3860	.00375	.340	.01195*	.00820	1.600	1.265	1.170	1.127	.0160	.02560	.02025	.01870	.01802
		16	3840	.00375	.260	.01500	.01125	1.300	1.140	1.091	1.069	.0187	.02435	.02130	.02045	.01997
ROY & SOZEN	45	A1	3080	.00440	.450	.03750	.03310									
		A2	2980	.00453	.450	.01930	.01477	2.375	1.540	1.335	1.240	.0206	.04890	.03180	.02750	.02560
		A3	3690	.00386	.450	.03000	.02614									
		B1	3490	.00401	.450	.02360	.01959									
		B2	3490	.00401	.450	.02000	.01599	1.188	1.090	1.060	1.041	.0207	.02450	.02250	.02195	.02160
		B3	3380	.00410	.450	.02170	.01760									

TABLE 2.1 (Cont'd).

Source	Ref. No.	Spec. No.	f'_c	ϵ_{50c}	$\frac{1}{2}A_b/A_c$	ϵ_{50t}	ϵ_{50b}	B/S	$\sqrt[2]{B/S}$	$\sqrt[3]{B/S}$	$\sqrt[4]{B/S}$	p"	p" B/S	p"$\sqrt[2]{B/S}$	p"$\sqrt[3]{B/S}$	p"$\sqrt[4]{B/S}$
ROY & SOZEN	45	C1	3320	.00415	.428	.02290	.01875									
⊡		C2	3440	.00405	.428	.02780	.02375	1.156	1.072	1.050	1.037	.0241	.02785	.02590	.02530	.02500
		C3	3390	.00409	.428	.02100	.01691									
		D1	3160	.00432	.450	.02650	.02218									
		D2	3200	.00427	.450	.01790	.01363	.780	.883	.920	.940	.0206	.01610	.01820	.01895	.01940
		D3	3380	.00410	.450	.01840	.01430									
		E1	3350	.00415	.450	.00850	.00435									
		E2	3420	.00407	.450	.01700	.01293	.594	.771	.840	.880	.0146	.01222	.01129	.01227	.01285
		E3	3460	.00403	.450	.01370	.00967									
BERTERO & FELIPPA	46	3x3x2½	8460	.00267	.440	.00750	.00483	1.165	1.080	1.052	1.040	.0090	.01049	.00973	.00947	.00936
X		4¼sqx1½	4120	.00360	.460	.01910	.01550	2.710	1.650	1.396	1.285	.0103	.02790	.01695	.01440	.01322
		4¼sqx2½	8050	.00271	.460	.00970	.00699	1.630	1.276	1.178	1.130	.0062	.01010	.00791	.00730	.00700

* = estimated values; ** = f'_c obtained from private communication with authors.

$$\epsilon_{50b} = a + b \left[p'' \left(\frac{B}{S} \right)^{\frac{1}{N}} \right]^{C} \quad \text{....(2.9)}$$

$$\epsilon_{50b} = bp'' \left(\frac{B}{S} \right)^{\frac{1}{N}} \quad \text{....(2.10)}$$

Computer Program 2.1 ("CORE") was used for this purpose.

Equation (2.9) cannot be partitioned into matrices for least squares analysis of a, b and c. Therefore it was necessary to predetermine a and find best values for b and c; a taking values from 0.0 to 0.0035 in increments of 0.0005. Note that a = 0 is necessary to satisfy the boundary condition $\epsilon_{50b} = 0$ when p" = 0.

Equation (2.10) is a special linear case of Equation (2.9) involving only one unknown (since a = 0 and c = 1).

In both equations, values of N = 2, 3, 4,∞ were used.

The results of these analyses, and the standard deviations of theoretical from experimental ϵ_{50b} values, are shown in Table 2.2. Two sets of analyses were performed, the first using all specimens and the second neglecting Soliman and Yus' Specimen 11. The results for this latter analysis are shown in parenthesis in Table 2.2.

Least squares analysis of all specimens gave a = 0, b = .305, c = .778 and N = 2 as the best fit with a standard deviation of .00423.

$$\epsilon_{50b} = .305 \left(p'' \sqrt{\frac{B}{S}} \right)^{0.778} \quad \text{....(2.11)}$$

This equation is shown as a dashed line in Figure 2.11

TABLE 2.2

LEAST SQUARES ANALYSIS FOR CONFINED CONCRETE

$$\epsilon_{50b} = a + b\left[p''\left(\frac{B}{S}\right)^{\frac{1}{N}}\right]^{C}$$

N =	2			3			4			∞		
a	b	c	Std. Devn.	b	c	Std. Devn.	b	c	Std. Devn.	b	c	Std. Devn.
0**	.703 (.744)	1.0	.00448 (.00380)*	.770 (.812)	1.0	.00446 (.00382)	.799 (.842)	1.0	.00457 (.00401)	.871 (.907)	1.0	.00533 (.00506)
0	.305 (.349)	.778 (.808)	.00423* (.00389)	.407 (.475)	.841 (.876)	.00443 (.00407)	.461 (.542)	.867 (.903)	.00460 (.00426)	.572 (.668)	.907 (.941)	.00538 (.00522)
.0005	.350 (.404)	.824 (.856)	.00423* (.00386)	.476 (.560)	.891 (.927)	.00443 (.00403)	.543 (.645)	.919 (.957)	.00460 (.00423)	.684 (.807)	.961 (.998)	.00539 (.00521)
.0010	.412 (.481)	.877 (.911)	.00424 (.00383)	.573 (.683)	.949 (.988)	.00443 (.00400)	.660 (.793)	.979 (1.020)	.00460 (.00419)	.847 (1.011)	1.025 (1.064)	.00540 (.00519)
.0015	.504 (.597)	.941 (.978)	.00426 (.00381)	.719 (.870)	1.018 (1.060)	.00444 (.00395)	.838 (1.023)	1.050 (1.095)	.00461 (.00414)	1.098 (1.332)	1.000 (1.143)	.00541 (.00517)
.0020	.652 (.784)	1.019 (1.060)	.00431 (.00380)*	.958 (1.181)	1.103 (1.150)	.00448 (.00390)	1.132 (1.411)	1.139 (1.187)	.00463 (.00408)	1.525 (1.885)	1.194 (1.241)	.00544 (.00514)
.0025	.919 (1.129)	1.121 (1.167)	.00440 (.00383)	1.406 (1.778)	1.214 (1.266)	.00453 (.00386)	1.692 (2.164)	1.253 (1.308)	.00469 (.00402)	2.358 (2.993)	1.315 (1.368)	.00548 (.00510)
.0030	1.523 (1.934)	1.267 (1.320)	.00466 (.00399)	2.468 (3.238)	1.372 (1.433)	.00471 (.00385)	3.047 (4.053)	1.417 (1.481)	.00483 (.00396)	4.457 (5.887)	1.488 (1.550)	.00557 (.00505)
.0035	4.008 (5.431)	1.535 (1.603)	.00560 (.00486)	7.222 (10.206)	1.664 (1.741)	.00539 (.00419)	9.363 (13.465)	1.719 (1.800)	.00539 (.00405)	15.014 (21.475)	1.808 (1.888)	.00588 (.00498)

* = Best values; ** = Parameter c fixed at 1.0.

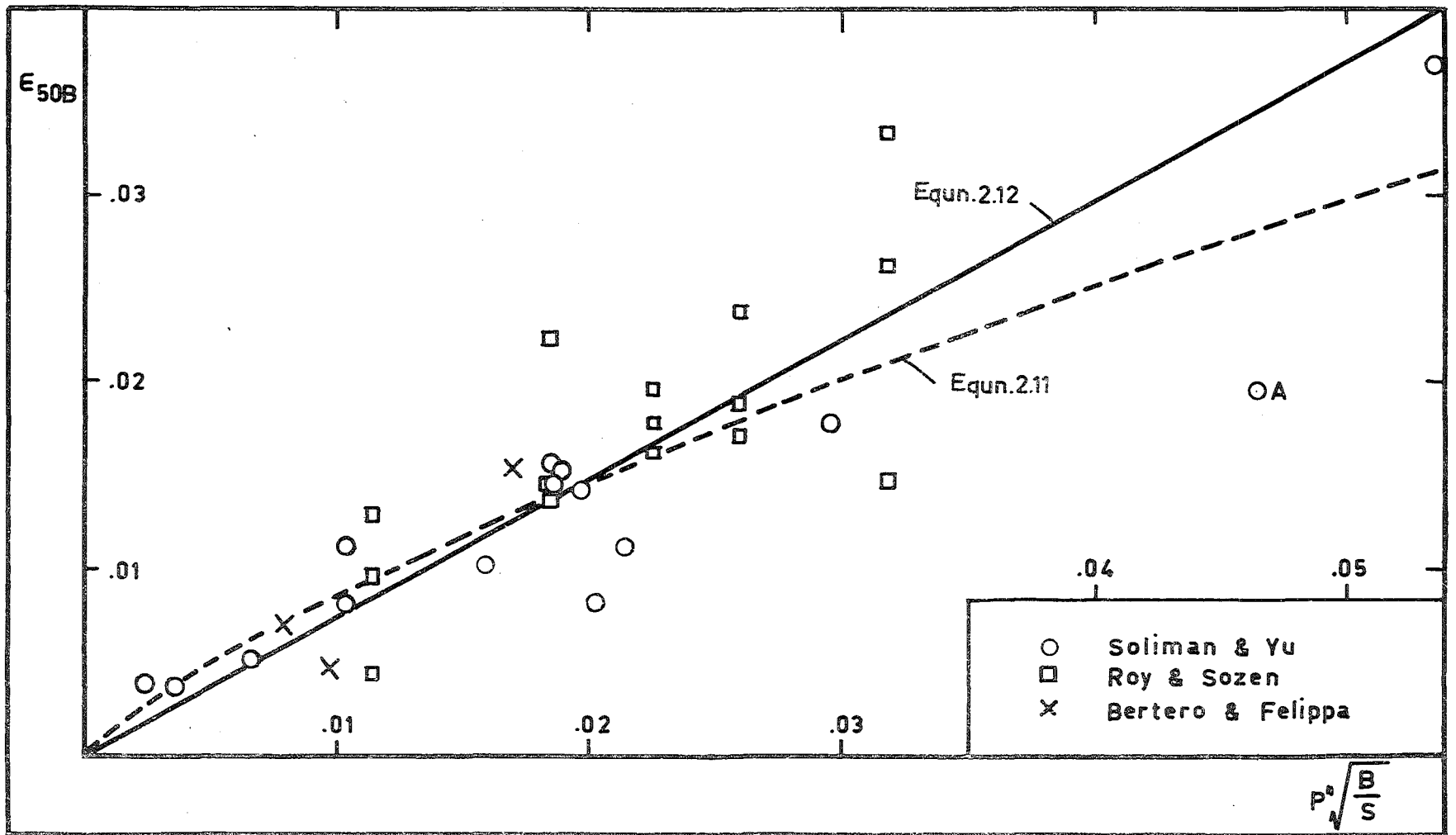

FIG.2.11 - EXPERIMENTAL RESULTS FOR BOUND CONCRETE

which plots ϵ_{50b} vs $p''\sqrt{\frac{B}{S}}$. It is to be noted that the points in Figure 2.11 are from tests covering both uniform strain and strain gradients across the specimens.

The full line in Figure 2.11 results when the point marked A (Soliman and Yus' Specimen 11) is neglected. Although this point is within the scatter band (approximately $\pm$ 40 per cent) there is no corresponding point of similar distance from, and on the other side of, the analytical lines, and therefore the point was too influential on an analysis of this type. Least squares analysis gave the coefficients for this line as a = 0, c = 1 (fixed), b = .744, N = 2. The standard deviation was lower at .00380. Accordingly the following expression was chosen as representing the relationship between ϵ_{50b}, p" and B/S (see also Figure 2.12):

$$\epsilon_{50b} = \tfrac{3}{4}p''\sqrt{\frac{B}{S}} \qquad \ldots\ldots(2.12)$$

Being linear, this expression is probably not realistic for large values of p" such as those encountered in steel columns in-filled with concrete. It is of interest at this point to compare Equation (2.12) with the expression derived by Roy and Sozen[45]:

$$\epsilon_{50t} = \tfrac{3}{4}p''\ \frac{B}{S} \qquad \ldots\ldots(2.13)$$

Inspection of Figure 2.11 shows that:

$$\epsilon_{50b} = \tfrac{3}{8}p''\sqrt{\frac{B}{S}} \qquad \ldots\ldots(2.14)$$

produced a line above which all experimental points lie and therefore Equation (2.14) would be suitable for design purposes.

2.6 PROPOSED STRESS-STRAIN RELATION FOR CONCRETE

The proposed stress-strain relationship for concrete is illustrated in Figure 2.13.

2.6.1 Tension Stress-Strain Curve (OD of Figure 2.13)

A linear response for concrete in tension is assumed. The maximum tensile stress is termed the Modulus of Rupture and an expression for this has been proposed by Warwaruk[59] as:

$$f_r = \frac{1000\ f'_c}{4000+f'_c} \qquad \ldots\ldots(2.15)$$

In the course of the author's tests on concrete prisms, it was found that this expression was conservative and the following equation resulted in a better fit:

$$f_r = \frac{1400\ f'_c}{4000+f'_c} \qquad \ldots\ldots(2.16)$$

Traditionally, the modulus of rupture is given by the product of a constant and the square root of the cylinder strength, but Equation (2.15) has considerable experimental support. It would appear that aggregate size and local conditions, particularly curing, have a greater effect on

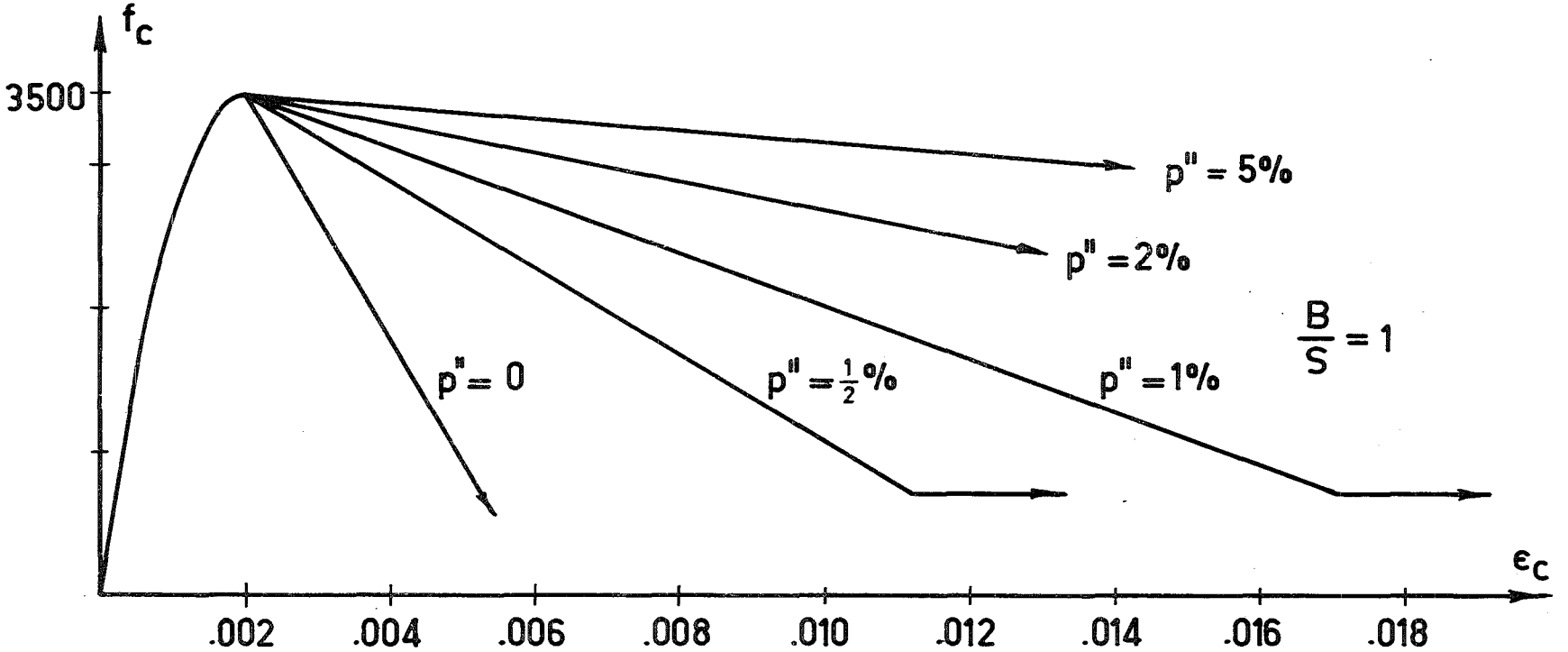

FIG.2.12 - INFLUENCE OF BINDING STEEL ON STRESS-STRAIN RESPONSE

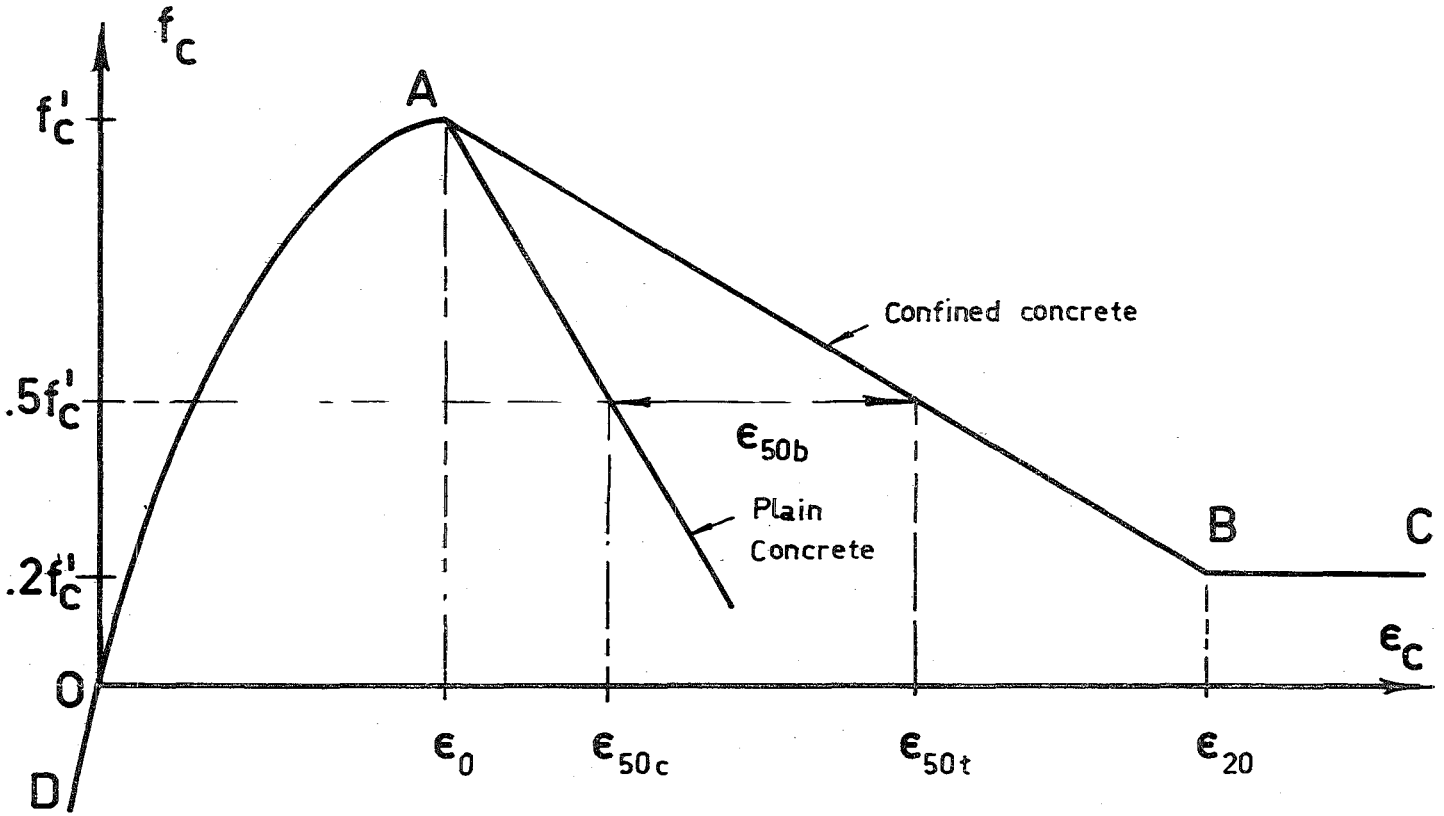

FIG.2.13 - ASSUMED COMPRESSIVE STRESS-STRAIN RELATION FOR CONFINED CONCRETE

modulus of rupture than is allowed for in either of these expressions. This conclusion is borne out by the tests of other investigators at this University. In this thesis, Equation (2.15) is used and the additional tensile stress available is assumed to compensate for shrinkage effects in reinforced concrete members.

E_c is obtained by differentiating Ritter's parabola for $\epsilon_c = 0$:

$$E_c = \frac{2f'_c}{\epsilon_o} \qquad \ldots\ldots(2.17)$$

Consequently,

$$\epsilon_r = \frac{500\epsilon_o}{4000+f'_c} \qquad \ldots\ldots(2.18)$$

2.6.2 Compressive Stress-Strain Curve: Ascending Branch

The ascending portion of the compressive stress-strain curve is given by Ritter's second degree parabola:

$$f_c = f'_c \left[\frac{2\epsilon_c}{\epsilon_o} - \left(\frac{\epsilon_c}{\epsilon_o}\right)^2\right] \qquad \ldots\ldots(2.19)$$

2.6.3 Compressive Stress-Strain Curve: Falling Branch

The falling branch of the compressive stress-strain curve is given by:

$$f_c = f'_c\,(1 - Z(\epsilon_c - \epsilon_o)) \qquad \ldots.(2.20)$$

$$(\text{for } \epsilon_o \leq \epsilon_c \leq \epsilon_{20})$$

where Z may be defined as follows:

For $f_c = \frac{1}{2}f'_c$, and $\epsilon_c = \epsilon_{50t} = \epsilon_{50c} + \epsilon_{50b}$;

$$\tfrac{1}{2}f'_c = f'_c\,(1 - Z(\epsilon_{50b} + \epsilon_{50c} - \epsilon_o))$$

$$\text{whence } Z = \frac{0.5}{\epsilon_{50b} + \epsilon_{50c} - \epsilon_o} \qquad \ldots.(2.21)$$

Where $\epsilon_o = .002$, ϵ_{50c} is obtained from Equation (2.4) and ϵ_{50b} is obtained from Equation (2.12).

Table 2.3 shows Z values for a variety of concrete strength, B/S ratios and p" ratios. Equations used were (2.4), (2.12), (2.21).

2.6.4 Compressive Stress-Strain Curve - Large Strains (BC of Figure 2.13)

It is assumed that bound concrete can sustain 20 per cent maximum stress from ϵ_{20} to infinite strain. This has been assumed previously[36] and is suitable for analysis in that other causes of failure, viz. buckling of compression steel, buckling of the member as a whole, or fracture of the tension steel, will occur before concrete strains become unrealistic. Barnard[47] has shown that concrete can sustain almost indefinitely large strains.

TABLE 2.3 - TABLE OF Z VALUES

B/S	PDD	FCD										
		2500	3000	3500	4000	4500	5000	5500	6000	6500	7000	7500
0.50	0.0	150	200	250	300	350	400	450	500	550	600	650
	0.0100	58	64	68	72	74	76	78	79	80	81	82
	0.0200	36	38	40	41	42	42	43	43	43	44	44
	0.0300	26	27	28	28	29	29	29	30	30	30	30
	0.0400	20	21	22	22	22	22	22	23	23	23	23
	0.0500	17	17	18	18	18	18	18	18	18	18	18
	0.0600	14	15	15	15	15	15	15	15	15	15	15
	0.0700	12	13	13	13	13	13	13	13	13	13	13
	0.0800	11	11	11	11	11	11	11	12	12	12	12
	0.0900	10	10	10	10	10	10	10	10	10	10	10
	0.1000	9	9	9	9	9	9	9	9	9	9	9
0.75	0.0100	51	56	59	61	63	65	66	67	68	68	69
	0.0200	31	32	33	34	35	35	35	36	36	36	36
	0.0300	22	23	23	24	24	24	24	24	25	25	25
	0.0400	17	18	18	18	18	18	18	19	19	19	19
	0.0500	14	14	15	15	15	15	15	15	15	15	15
	0.0600	12	12	12	12	12	12	12	13	13	13	13
	0.0700	10	10	11	11	11	11	11	11	11	11	11
	0.0800	9	9	9	9	9	9	9	9	9	9	9
	0.1000	7	7	7	8	8	8	8	8	8	8	8
1.00	0.0100	46	50	53	55	56	57	58	59	59	60	60
	0.0200	27	29	29	30	30	31	31	31	31	32	32
	0.0300	19	20	20	21	21	21	21	21	21	21	21
	0.0400	15	15	16	16	16	16	16	16	16	16	16
	0.0500	12	13	13	13	13	13	13	13	13	13	13
	0.0600	10	11	11	11	11	11	11	11	11	11	11
	0.0700	9	9	9	9	9	9	9	9	9	9	9
	0.0800	8	8	8	8	8	8	8	8	8	8	8
	0.1000	6	6	6	7	7	7	7	7	7	7	7
1.25	0.0100	43	46	48	50	51	52	53	53	54	54	55
	0.0200	25	26	27	27	27	28	28	28	28	28	29
	0.0300	18	18	18	19	19	19	19	19	19	19	19
	0.0400	14	14	14	14	14	14	14	14	15	15	15
	0.0500	11	11	11	11	12	12	12	12	12	12	12
	0.0600	9	9	10	10	10	10	10	10	10	10	10
	0.0700	8	8	8	8	8	8	8	8	8	8	8
	0.0800	7	7	7	7	7	7	7	7	7	7	7
	0.1000	6	6	6	6	6	6	6	6	6	6	6
1.50	0.0100	40	43	45	46	47	48	49	49	50	50	50
	0.0200	23	24	25	25	25	25	26	26	26	26	26
	0.0300	16	17	17	17	17	17	17	18	18	18	18
	0.0400	12	13	13	13	13	13	13	13	13	13	13
	0.0500	10	10	10	11	11	11	11	11	11	11	11
	0.0600	9	9	9	9	9	9	9	9	9	9	9
	0.0700	7	7	8	8	8	8	8	8	8	8	8
	0.0800	7	7	7	7	7	7	7	7	7	7	7
	0.1000	5	5	5	5	5	5	5	5	5	5	5
1.75	0.0100	38	40	42	43	44	45	45	46	46	46	47
	0.0200	22	22	23	23	24	24	24	24	24	24	24
	0.0300	15	15	16	16	16	16	16	16	16	16	16
	0.0400	12	12	12	12	12	12	12	12	12	12	12
	0.0500	9	10	10	10	10	10	10	10	10	10	10
	0.0600	8	8	8	8	8	8	8	8	8	8	8
	0.0700	7	7	7	7	7	7	7	7	7	7	7
	0.0800	6	6	6	6	6	6	6	6	6	6	6
	0.1000	5	5	5	5	5	5	5	5	5	5	5
2.00	0.0100	36	38	40	41	42	42	43	43	43	44	44
	0.0200	20	21	22	22	22	22	22	23	23	23	23
	0.0300	14	15	15	15	15	15	15	15	15	15	15
	0.0400	11	11	11	11	11	11	11	12	12	12	12
	0.0500	9	9	9	9	9	9	9	9	9	9	9
	0.0600	7	8	8	8	8	8	8	8	8	8	8
	0.0700	6	7	7	7	7	7	7	7	7	7	7
	0.0800	6	6	6	6	6	6	6	6	6	6	6
	0.1000	5	5	5	5	5	5	5	5	5	5	5

TABLE 2.3 - TABLE OF Z VALUES

B/S	PDD	FCD										
		2500	3000	3500	4000	4500	5000	5500	6000	6500	7000	7500
0.50	0.0	150	200	250	300	350	400	450	500	550	600	650
	0.0100	58	64	68	72	74	76	78	79	80	81	82
	0.0200	36	38	40	41	42	42	43	43	43	44	44
	0.0300	26	27	28	28	29	29	29	30	30	30	30
	0.0400	20	21	22	22	22	22	22	23	23	23	23
	0.0500	17	17	18	18	18	18	18	18	18	18	18
	0.0600	14	15	15	15	15	15	15	15	15	15	15
	0.0700	12	13	13	13	13	13	13	13	13	13	13
	0.0800	11	11	11	11	11	11	11	12	12	12	12
	0.0900	10	10	10	10	10	10	10	10	10	10	10
	0.1000	9	9	9	9	9	9	9	9	9	9	9
0.75	0.0100	51	56	59	61	63	65	66	67	68	68	69
	0.0200	31	32	33	34	35	35	35	36	36	36	36
	0.0300	22	23	23	24	24	24	24	24	25	25	25
	0.0400	17	18	18	18	18	18	18	19	19	19	19
	0.0500	14	14	15	15	15	15	15	15	15	15	15
	0.0600	12	12	12	12	12	12	12	13	13	13	13
	0.0700	10	10	11	11	11	11	11	11	11	11	11
	0.0800	9	9	9	9	9	9	9	9	9	9	9
	0.1000	7	7	7	8	8	8	8	8	8	8	8
1.00	0.0100	46	50	53	55	56	57	58	59	59	60	60
	0.0200	27	29	29	30	30	31	31	31	31	32	32
	0.0300	19	20	20	21	21	21	21	21	21	21	21
	0.0400	15	15	16	16	16	16	16	16	16	16	16
	0.0500	12	13	13	13	13	13	13	13	13	13	13
	0.0600	10	11	11	11	11	11	11	11	11	11	11
	0.0700	9	9	9	9	9	9	9	9	9	9	9
	0.0800	8	8	8	8	8	8	8	8	8	8	8
	0.1000	6	6	6	7	7	7	7	7	7	7	7
1.25	0.0100	43	46	48	50	51	52	53	53	54	54	55
	0.0200	25	26	27	27	27	28	28	28	28	28	29
	0.0300	18	18	18	19	19	19	19	19	19	19	19
	0.0400	14	14	14	14	14	14	14	14	15	15	15
	0.0500	11	11	11	11	12	12	12	12	12	12	12
	0.0600	9	9	10	10	10	10	10	10	10	10	10
	0.0700	8	8	8	8	8	8	8	8	8	8	8
	0.0800	7	7	7	7	7	7	7	7	7	7	7
	0.1000	6	6	6	6	6	6	6	6	6	6	6
1.50	0.0100	40	43	45	46	47	48	49	49	50	50	50
	0.0200	23	24	25	25	25	25	26	26	26	26	26
	0.0300	16	17	17	17	17	17	17	18	18	18	18
	0.0400	12	13	13	13	13	13	13	13	13	13	13
	0.0500	10	10	10	11	11	11	11	11	11	11	11
	0.0600	9	9	9	9	9	9	9	9	9	9	9
	0.0700	7	7	8	8	8	8	8	8	8	8	8
	0.0800	7	7	7	7	7	7	7	7	7	7	7
	0.1000	5	5	5	5	5	5	5	5	5	5	5
1.75	0.0100	38	40	42	43	44	45	45	46	46	46	47
	0.0200	22	22	23	23	24	24	24	24	24	24	24
	0.0300	15	15	16	16	16	16	16	16	16	16	16
	0.0400	12	12	12	12	12	12	12	12	12	12	12
	0.0500	9	10	10	10	10	10	10	10	10	10	10
	0.0600	8	8	8	8	8	8	8	8	8	8	8
	0.0700	7	7	7	7	7	7	7	7	7	7	7
	0.0800	6	6	6	6	6	6	6	6	6	6	6
	0.1000	5	5	5	5	5	5	5	5	5	5	5
2.00	0.0100	36	38	40	41	42	42	43	43	43	44	44
	0.0200	20	21	22	22	22	22	22	23	23	23	23
	0.0300	14	15	15	15	15	15	15	15	15	15	15
	0.0400	11	11	11	11	11	11	11	12	12	12	12
	0.0500	9	9	9	9	9	9	9	9	9	9	9
	0.0600	7	8	8	8	8	8	8	8	8	8	8
	0.0700	6	7	7	7	7	7	7	7	7	7	7
	0.0800	6	6	6	6	6	6	6	6	6	6	6
	0.1000	5	5	5	5	5	5	5	5	5	5	5

2.7 CYCLIC AND REPEATED LOADING OF PLAIN AND CONFINED CONCRETE

Cyclic loading of concrete may occur in such places as beam-column joints in structures subjected to earthquakes. Repeated loading occurs daily in most structures as human activity within them fluctuates. To a very small extent, repeated loading occurs in some discrete concrete elements in reinforced concrete members under monotonic loading, as the neutral axis moves up and down the cross section. Figure 2.14 shows the effect of repeated compression loading on concrete.

An investigation into repeated loading on structural concrete has been reported by Sinha, Gerstle, and Tulin[39]. They proposed a method for following the loops of the repeated load curves but their approach is considered to be too complex in view of the comparitively low importance of this effect on this particular material.

In this thesis, a simplified idealised repeated and cyclic loading response is assumed, and is illustrated in Figure 2.14. On unloading from point A it is considered that 75 per cent of the previous stress is lost with no decrease in strain and the remaining 25 per cent stress follows a linear path of slope $.25E_c$ to point C. If the discrete concrete element has not cracked it is capable of carrying tensile stress to point G, but if the concrete in

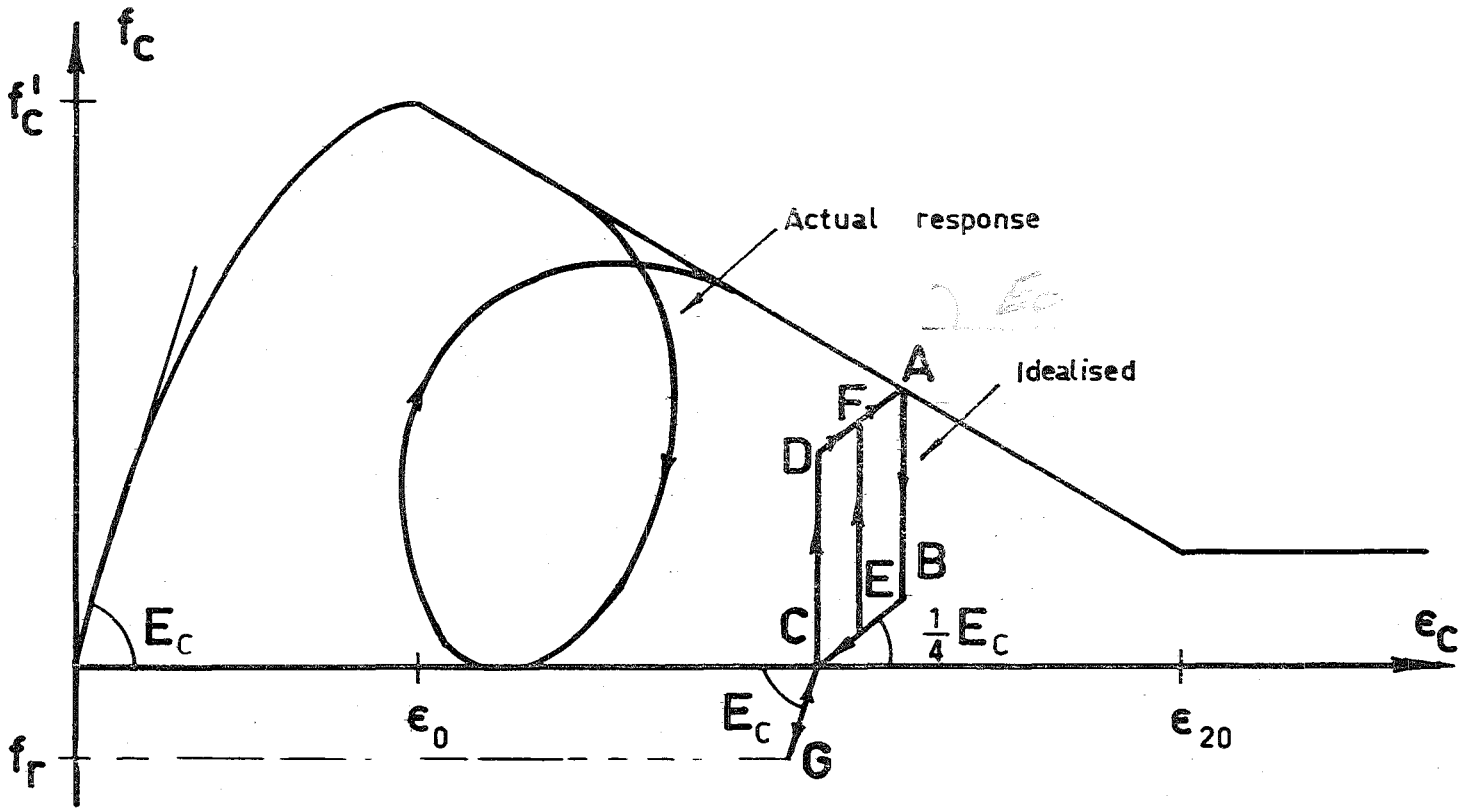

FIG.2.14 - CYCLIC BEHAVIOUR OF CONCRETE

this element has previously cracked, or cracks form during this unloading stage, then the strain reduces at zero stress such that strain compatability with surrounding elements is maintained. On reloading from this state, the strain must regain the value at C before compressive stress can be sustained again.

If reloading commences before unloading produces zero stress, then reloading follows one of the infinite number of paths bounded by BC and DA, one of which is shown as ABEFA in Figure 2.14.

It is to be noted that the average slope of the assumed (trapezoidal) loop between A and C is parallel to the initial tangent modulus of the stress-strain curve. It is thought that more complicated idealizations of the loop are unwarranted.

For the purposes of the analyses presented in subsequent chapters of this thesis, it is further assumed that the behaviour described above is characteristic of unloading-reloading throughout the entire strain history.

2.8 COMPUTER PROGRAMS

Program 2.1 ("CORE"): This program was used to carry out the least squares analysis described in Section 2.5.

Program 2.2 ("ZTABLE"): Tables of Z values for varying concrete strengths and B/S and p" ratios are produced (see Table 2.3).

Listings of both programs appear in Appendix B.

2.9 CONCLUSIONS

It has been shown that the stress-strain behaviour of concrete may be represented by the following equations:-

For $-\epsilon_r \leq \epsilon_c \leq 0$, $f_c = E_c \epsilon_c$ ....(2.22)

where $E_c = \dfrac{2f'_c}{\epsilon_o}$ ....(2.17)

and $\epsilon_o = 0.002$

$$\epsilon_r = \frac{500\epsilon_o}{4000 + f'_c} \quad \text{....(2.18)}$$

For $0 \leq \epsilon_c \leq \epsilon_o$, $f_c = f'_c \left[\dfrac{2\epsilon_c}{\epsilon_o} - \left(\dfrac{\epsilon_c}{\epsilon_o} \right)^2 \right]$ ....(2.19)

For $\epsilon_o \leq \epsilon_c \leq \epsilon_{20}$, $f_c = f'_c(1 + Z(\epsilon_c - \epsilon_o))$ ....(2.20)

where $Z = \dfrac{0.5}{\epsilon_{50b} + \epsilon_{50c} - \epsilon_o}$ ....(2.21)

and $\epsilon_{50c} = \dfrac{3 + 0.002f'_c}{f'_c - 1000}$ ....(2.4)

and $\epsilon_{50b} = \frac{3}{4}p''\sqrt{\dfrac{B}{S}}$ ....(2.12)

For $\epsilon_{20} \leq \epsilon_c$, $f_c = .2f'_c$ ....(2.23)

CHAPTER 3

STRESS-STRAIN BEHAVIOUR OF STRUCTURAL-GRADE REINFORCING STEEL

SUMMARY

The behaviour of reinforcing steel under monotonic, repeated and cyclic loading is considered. A modification to Burns and Seiss'[32] stress-strain expression for the strain-hardening range is proposed and compared with test results. Tests on cyclically-loaded steel coupons are described and a theory for the Bauschinger Effect is presented.

3.1 INTRODUCTION

The stress-strain relation for structural steel subjected to monotonic loading is well known and easily defined. The expression, with the notation used in this thesis, is shown in Figure 3.1. Under repeated loading of the same sign, the unloading and reloading stress-strain paths closely follow the initial elastic slope and when the strain regains the value at which unloading commenced, the stress-strain curve continues as if unloading

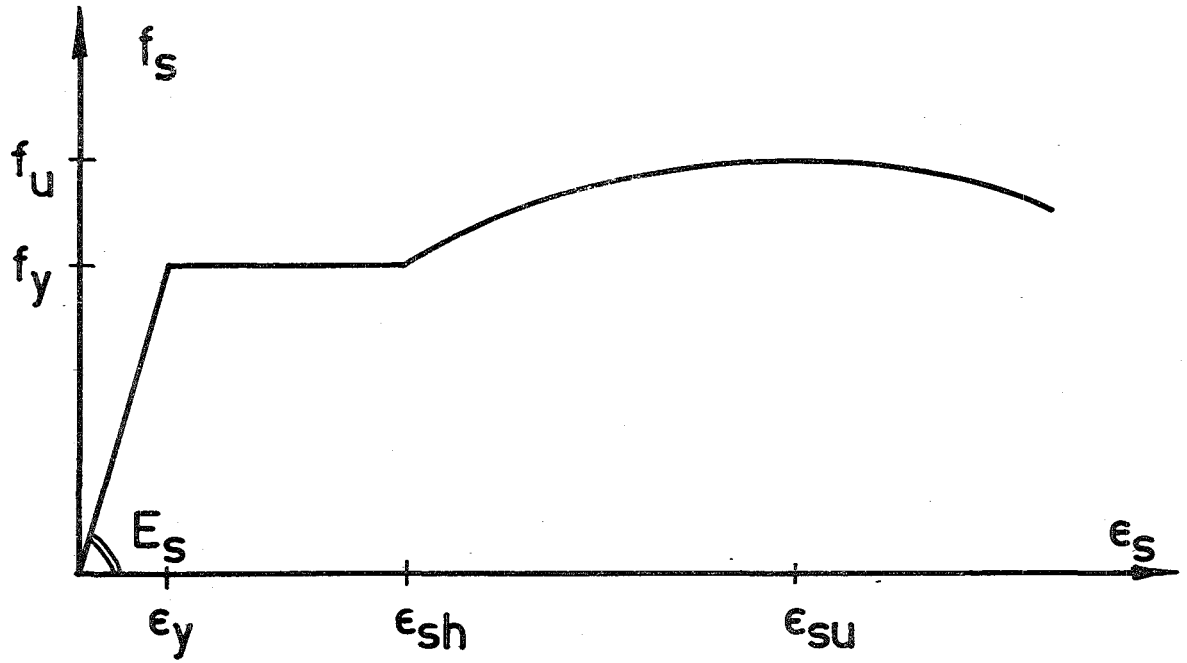

FIG.3.1 NOTATION FOR STEEL

had not occurred. Hence the monotonic stress-strain relation forms an envelope for repeated loadings, regardless of whether unloading is initiated in the elastic, plastic or strain-hardening regions. However, this property cannot be extended to cover situations in which the sign of the stress is reversed, as will become evident later.

3.2 STRAIN HARDENING

A stress-strain expression for the strain-hardening region has been postulated by Burns and Seiss[32]:

$$f_s = f_y \left[\frac{112\left|\epsilon_s - \epsilon_{sh}\right| + 2}{60\left(\epsilon_s - \epsilon_{sh}\right) + 2} + \frac{\left|\epsilon_s - \epsilon_{sh}\right|}{\epsilon_{su} - \epsilon_{sh}} \left\{ \frac{f_u}{f_y} - 1.7 \right\} \right] \quad \ldots\ldots (3.1)$$

Close inspection of this expression shows that limitations for its proper use are implied. Examination of the two boundary conditions:-

(i) $f_s = f_u$, when $\epsilon_s = \epsilon_{su}$, and

(ii) $\dfrac{df_s}{d\epsilon_s} = 0$, when $\epsilon_s = \epsilon_{su}$

shows that the equation leads to the following restraints:-

(i) $\dfrac{f_u}{f_y} = 1.5654$

(ii) $\epsilon_{su} = \epsilon_{sh} + .14$

Neither of these restraints is particularly unrealistic, but it is possible to generalise the expression for any ratio of f_u/f_y and value of ϵ_{su} as follows:

$$f_s = f_y \left[\frac{W_h(\epsilon_s - \epsilon_{sh}) + 2}{60(\epsilon_s - \epsilon_{sh}) + 2} + \frac{\epsilon_s - \epsilon_{sh}}{\epsilon_{su} - \epsilon_{sh}} \left\{ \frac{f_u}{f_y} - W_a \right\} \right] \quad \ldots\ldots(3.2)$$

From $f_s = f_u$, when $\epsilon_s = \epsilon_{su}$,

$$\frac{f_u}{f_y} = \frac{W_h(\epsilon_{su} - \epsilon_{sh}) + 2}{60(\epsilon_{su} - \epsilon_{sh}) + 2} + \frac{f_u}{f_y} - W_a$$

$$\therefore \quad W_a = \frac{W_h(\epsilon_{su} - \epsilon_{sh}) + 2}{60(\epsilon_{su} - \epsilon_{sh}) + 2}$$

$$= \frac{W_h b + 2}{60b + 2} \quad \ldots\ldots(3.3)$$

where $b = \epsilon_{su} - \epsilon_{sh}$

Also, from $\frac{df_s}{d\epsilon_s} = 0$, when $\epsilon_s = \epsilon_{su}$

$$W_a = \frac{f_u}{f_y} + \frac{W_h b - 60b}{2(30b + 1)^2} \quad \ldots\ldots(3.4)$$

From (3.3) and (3.4)

$$W_h = \frac{\frac{f_u}{f_y}(30b + 1)^2 - 60b - 1}{15b^2} \quad \ldots\ldots(3.5)$$

Substituting W_h into Equation (3.3) gives W_a.

3.3 TEST SPECIMEN FOR STRAIN HARDENING

To test the validity of Equations (3.2), (3.3) and

(3.5) a deformed bar, nominal $\frac{7}{8}$" diameter was machined and tension tested to A.S.T.M. specifications A370-61T. An Avery 25,000 lb hydraulic testing machine and an Instron G-51-14 Strain Gauge extensometer coupled to a Budd Bridge were used. Owing to the inherent difficulty in measuring strain near ultimate with this type of machine, it was necessary to make an estimate for the ultimate strain. This appeared to have a value of the order of 0.26. Figure 3.2 shows the experimental values compared with the Burns and Seiss expression and with the modified expression proposed in Section 3.2. The standard deviations for the Burns and Seiss expression and the modified expression are 3,313 p.s.i. and 2,205 p.s.i. respectively. Not too much importance should be attached to these values as the standard deviations include values in the elastic and plastic ranges and therefore show the Burns and Seiss Expression in a correspondingly better light. Also, there is a preponderance of experimental points near the onset of strain hardening. Consequently a visual assessment of the two theories is probably more meaningful.

It is recognised that one specimen alone does not constitute proof of a better expression. However, good agreement is obtained in this comparison and it is expected that the general expression is more accurate than Burns and Seiss' expression since account is taken of the actual

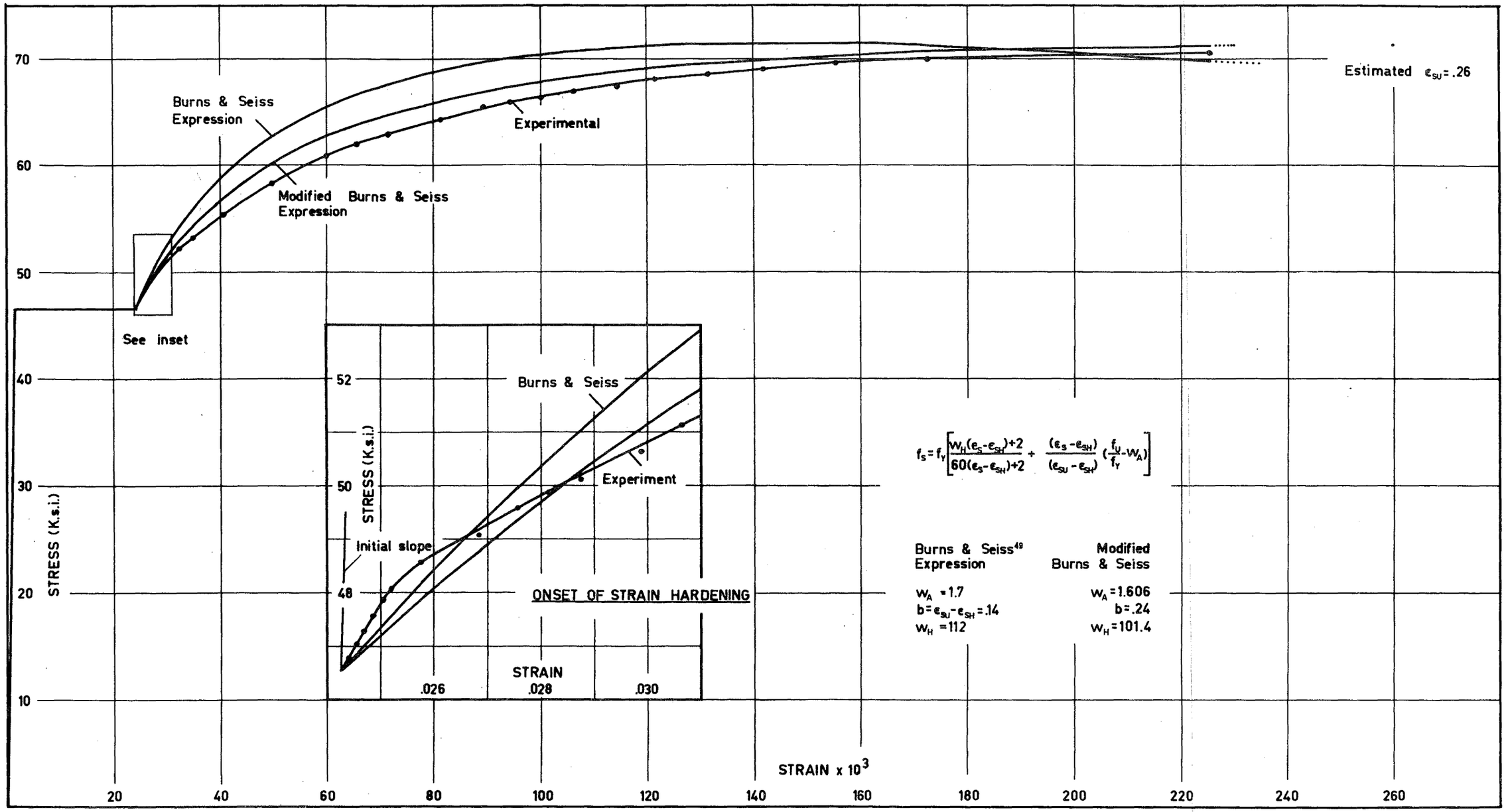

FIG.3.2 - STRESS-STRAIN RELATIONS IN THE STRAIN-HARDENING RANGE : EXPERIMENTAL AND THEORETICAL PLOTS

f_u/f_y ratio and the value of ϵ_{su}.

3.4 COMPRESSION STRESS

Most investigators subject their steel coupons to more convenient tension tests and assume the same response in compression. This has been shown[32] to be the case except that strain-hardening occurs at a lower strain than in the same specimen subjected to tension. Whether this behaviour is a property of compressed steel or is a consequence of using a necessarily short test coupon is not known.

However there is one steel characteristic relating to compression stress that is still not adequately defined and this is the point of buckling. The familiar Euler formula, later modified by Engesser for inelastic materials, can be stated as

$$\sigma_{cr} = \frac{\pi^2 E_t D^2}{L^2} \qquad \ldots\ldots(3.6)$$

$\therefore$ E_t = Tangent modulus

D = Bar diameter

L = Effective length

For steel reinforcement acting as compression steel in beams a rough estimate of the buckling stress could be obtained by assuming that the bar is axially loaded, that it receives no lateral support from the concrete, and that the effective length is the stirrup spacing. Then L = S in Equation (3.6).

When the compression steel enters the plastic range, the tangent modulus becomes zero, and therefore so does the critical stress. However, in the case of reinforced concrete beams, the steel cannot buckle at the yield point because the surrounding concrete provides lateral support. Moreover, when the concrete does spall away, the steel has followed the curvature of the concrete member and therefore, in order to buckle, the curvature of the bar must change sign.

It seems also that at less than a given stirrup spacing, compressed steel buckles between alternate stirrups, laterally displacing the intermediate binder. Other complications that arise are the pre-loaded curvature of the steel and the extent to which buckling actually advances spalling.

Clearly, a theoretical description of this behaviour would be difficult to evolve and no attempt is made to do so here, but the problem is raised because this situation arises frequently in cyclically-loaded reinforced concrete beams which often rely on only a steel couple to provide moment resistance (q.v. Chapter 5).

3.5 PROPERTIES OF BAUSCHINGER EFFECT

Little information is available regarding the behaviour of reinforcing steel when subjected to alternating tensile and compressive strains. This condition may occur

in beam-column joints of reinforced concrete framed structures during earthquake loading. Under this cyclic loading the stress-strain properties of steel become quite different from those associated with purely tensile or compressive stress and are strongly dependent upon the previous strain history.

This is known as the Bauschinger Effect and results in a lowering of the reversed yield strength. Once this phenomenon has been initiated by a yield excursion, the steel behaviour is affected by time and temperature, and linearity between stress and strain is lost over much of the range.

Figure 3.3 illustrates the properties of the Bauschinger Effect. Of interest here is that the steel is able to demonstrate some properties common to repeated loading; namely that unloading of both signs follows the initial elastic slope, as does reloading, after which the stress-strain curve resumes as if unloading had not occurred. This is of more than academic interest in that in a structure after an earthquake, there will not be incremental failure in the steel due to repeated live loadings. Figure 3.4 illustrates the incremental deformation property that was initially thought to occur.

Clearly there must be some reversed stress on unloading, at which the Bauschinger Effect must commence and below which, repeated loading characteristics apply. This has been termed

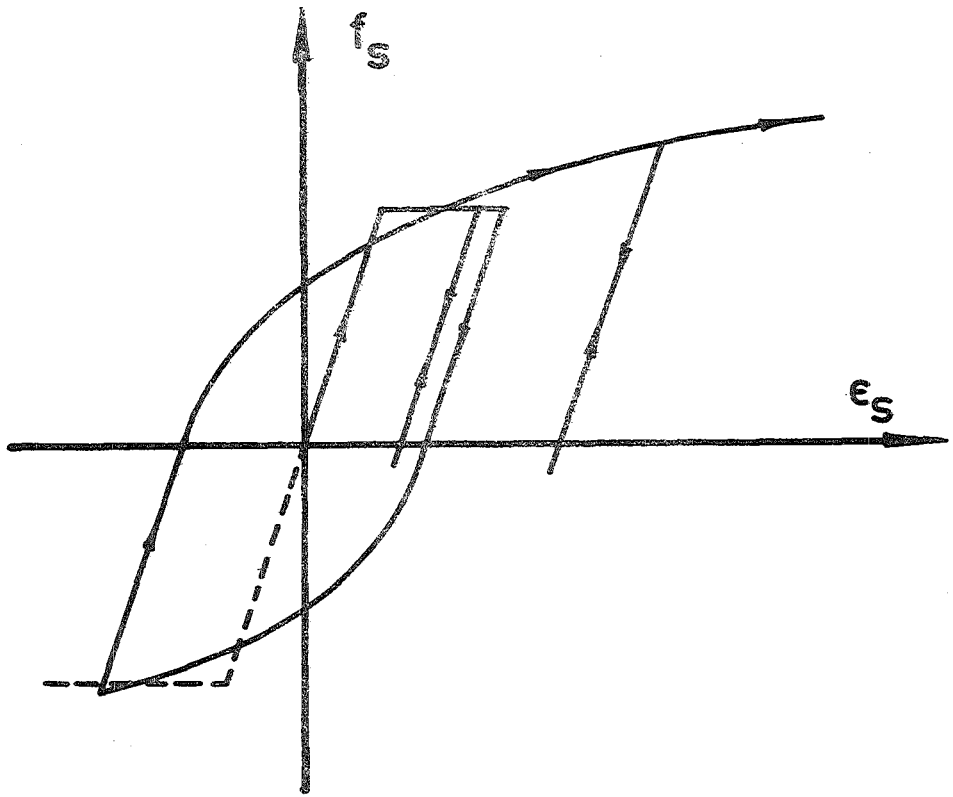

FIG.3.3 - BAUSCHINGER EFFECT PROPERTIES

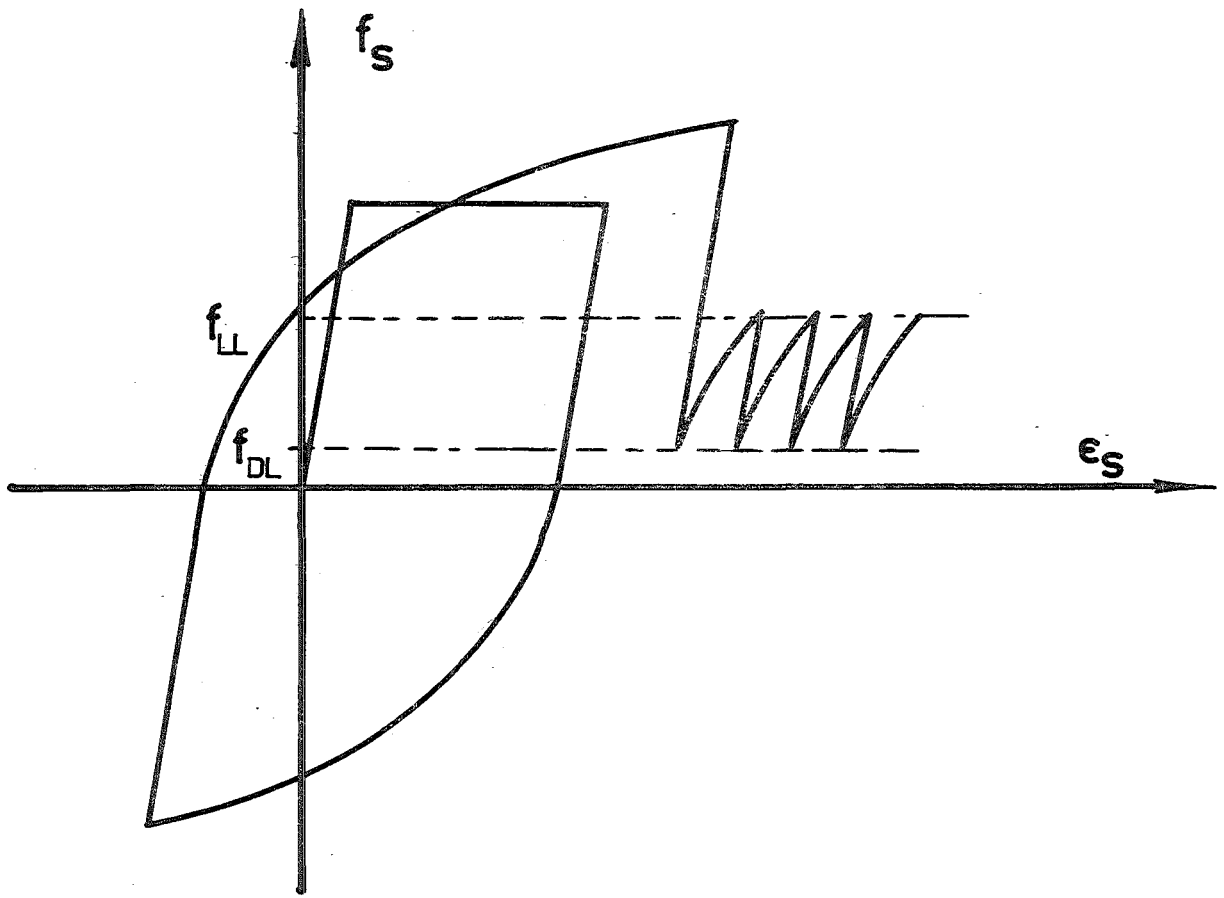

FIG.3.4 - STEEL STRESS-STRAIN CURVE SHOWING POSSIBLE INCREMENTAL DEFORMATION CYCLES

the "transition stress" and although in practice a definite "point" may not exist, some estimate must be made for theoretical analysis.

3.6 BAUSCHINGER EXPRESSION OF SINGH, GERSTLE AND TULIN

A preliminary study into this effect has been conducted by Singh, Gerstle and Tulin[49] and they assess the following as the relevant factors responsible for the difference between the virgin stress-strain curve and that obtained after previous cycles of inelastic loading:-

1. Virgin properties of the material,
2. Entire previous load history,
3. Rate of straining,
4. Elapsed time, or ageing, between cycles,
5. Temperature.

Since the temperature range in Reinforced Concrete members is not great, this variable was not studied by Singh et al.[49], and it was found that over the usual range of test speeds, the rate of straining did not produce a noticeable effect.

For a detailed account of the work of Singh et al., readers are referred to their paper[49] but their conclusions are repeated here for completeness.

It was found that the slope of the curved part of the reversed stress-strain curve was reduced with larger values

of plastic strain in the previous cycle. Also, cyclic loading and ageing tended to increase the value of this slope and in certain circumstances became larger than the initial elastic modulus, i.e., there is a general trend toward an increase in stiffness with increasing number of prior cycles.

From their experiments, Singh et al[49] arrived at a simple equation representing an average of the family of reversed loading curves.

Their expression:

$$\left|f_s\right| = 64500 - 52700\ (.838)^{1000\epsilon} \qquad \ldots.(3.7)$$

represents an exponential curve which is extended backwards to meet an initial elastic slope at the transition stress (see Figure 3.5).

The elastic and exponential regions of this response meet at the transition stress, the value for which must be found using a suitable iterative technique.

3.7 CYCLIC LOADING TESTS ON STEEL COUPONS

In the tests performed by Singh et al.[49], great care was taken in choosing their test specimens in that they all came from the same heat. In other words, they eliminated considerations of virgin properties in their experiments. Consequently their formula is theoretically of limited application.

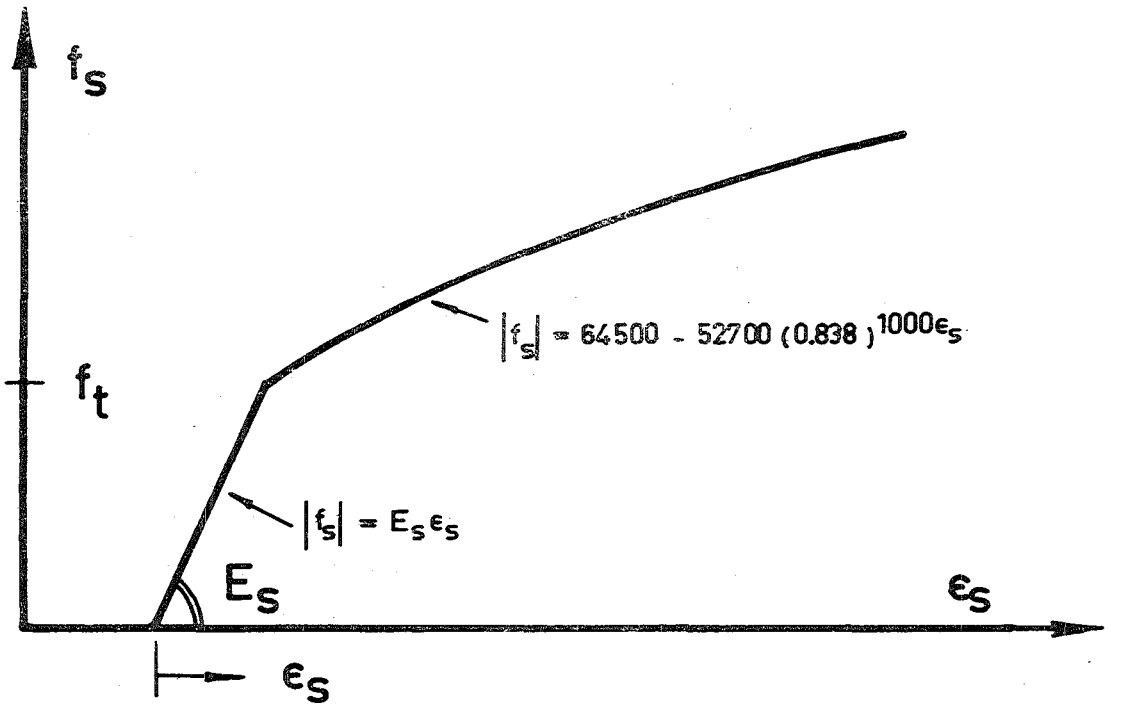

FIG.35 - SINGH, TULIN & GERSTLE[49] MODEL

To test Equation (3.7) it was decided to carry out tests on a variety of steel bars from different heats to establish whether or not Singh's et al. expression was suitable for general application. As it transpired, it was felt that the expression was not sufficiently accurate, and following the writer's tests a number of other functions were examined as possible mathematical representations of the Bauschinger Effect.

Some 19 deformed bar, steel coupons were tested of which 8 had to be abandoned owing to difficulties mainly with the test rig and procedure (see Appendix C). The remaining 11 specimens comprised 7 - $\frac{1}{2}$", 1 - $\frac{5}{8}$", 1 - $\frac{3}{4}$", and 2 - $\frac{7}{8}$" dia. bars.

It is fairly evident that a full study of the Bauschinger Effect requires very sophisticated test equipment in order that all the variables can be studied. Also such a study is considered to be an extensive research investigation in itself and consequently the theory advanced here does not pretend to be the result of a rigorous testing programme.

The number of variables studied was reduced by removing those that were not relevant to this study, being earthquake-based; temperature changes and time between cycles. Neither of these factors have significance in seismic considerations. The effect of the rate of

straining could not be studied with the available equipment and anyway, Singh et al.[49] have reported this to be not noticeable over the usual range of test speeds. Hopefully this observation can be extrapolated to cover speeds associated with earthquake loading. At worst, static loading tests have shown to be conservative. There only remains then, the virgin properties of the material and the previous strain history.

3.8 FURTHER EXPRESSIONS FOR BAUSCHINGER EFFECT

In order to find a more general formula for the Bauschinger Effect, each cycle of all eleven specimens was isolated and subjected to least squares analysis for a variety of expressions. Most of these expressions proved unsuccessful but they are presented here to illustrate the complexity of the Bauschinger Effect and as a background for other investigators who intend to examine this behaviour.

3.8.1 Modified Singh, Gerstle and Tulin Expression

The most obvious starting place for this phase of the investigation seemed to be a modification of the expression proposed by Singh et al.[49], in that the virgin properties of the steel could be included.

Therefore, the chosen equation was:

$$|f_s| = C_1 f_u - C_2 f_y C_3^{C_4 \epsilon} \qquad \ldots\ldots(3.8)$$

A number of these coefficients can be quickly disposed

of here. A graph in Singh's et al. paper shows f_y to be approximately 52.7 K.s.i. and therefore coefficient C_2 was chosen as unity on comparison with Equation (3.7).

From the tests of the present investigation it appears that, for a small number of cycles, the value of the ultimate stress is not affected by the means of reaching it. That is, specimens loaded directly to failure give the same ultimate stress as those subjected to reversed loading. This means that if $C_3 < 1$ then as $\epsilon \to \infty$ then $|f_s| \to C_1 f_u$.

$\therefore C_1 = 1$

If this same conclusion was reached by Singh et al. then their ultimate stress was 64500 p.s.i. On reflection this appears to be a very low ultimate stress for the comparatively high yield stress, but 52700/64500 = 0.818 which is close to the 0.838 value used in Equation (3.7).

Therefore, Equation (3.8) has been simplified to:

$$|f_s| = f_u - f_y \left(\frac{f_y}{f_u}\right)^{C_4 \epsilon} \qquad \ldots\ldots(3.9)$$

There is a strong relationship between C_3 and C_4 in that the initial plastic strain has a large effect on the shape of the stress-strain curve on reversal (q.v. Section 3.6). It was intended that C_4 would embody this effect and toward this end the experimental results obtained by the author were subjected to least squares analysis to find C_4 for each cycle.

Two main factors discounted this approach. Firstly, the transition stress where the initial linear response joined the exponential response of Equation (3.9) was too high, being about $\frac{3}{4}$ yield and therefore twice as high as the transition stress for Singh's et al. expression. Secondly, C_4 did not show any correlation with initial or previous plastic strains and was in fact very random.

3.8.2 Exponential Function

An exponential function was next attempted of the form:

$$f = \frac{2E\,\epsilon}{1 + e^{k_1\epsilon}} + k_2(1 - e^{-k_3\epsilon}) \qquad \ldots.(3.10)$$

This function has several apparent advantages. It can be differentiated and manipulated to comply with the three boundary conditions:-

(1) $\frac{df_s}{d\epsilon_s} = E_s$ when $\epsilon_s = 0$

(2) $\frac{df_s}{d\epsilon_s} = 0$ when $\epsilon_s = \epsilon_{su}$

(3) $f_s = f_u$ when $\epsilon_s = \epsilon_{su}$

However, the resultant expression is unduly complex and insufficiently general to allow for considerations of initial plastic strain or virgin properties such as the yield stress.

3.8.3 Quartic Polynomial Expression

An expression of the form:

$$f = E(\epsilon - \alpha\epsilon^2 + \beta\epsilon^3 - \gamma\epsilon^4) \qquad \ldots\ldots(3.11)$$

was also tried and least squares analysis performed on experimental cycles. Again, this expression can be made to comply with the boundary conditions listed in Section 3.8.2. For experimental cycles with low strain range ($< 2\epsilon_y$) this expression produced remarkably low standard deviations of theoretical from experimental values. However, the cubic term caused difficulty when large strains were involved in that points of contraflexure, and maxima and minima appeared.

3.8.4 Sixth Power Polynomial Expression

To remove the points of discontinuity from the theoretical expression, the cubic term in Equation (3.11) was replaced with a power six term to give:

$$f = E(\epsilon - \alpha\epsilon^2 + \beta\epsilon^6 - \gamma\epsilon^4) \qquad \ldots\ldots(3.12)$$

This change resulted in very good fits of theoretical to experimental curves when α , β and γ were subjected to least squares analysis. Unfortunately as was the case with the quartic, these coefficients could not be correlated with any of the factors influencing Bauschinger behaviour and the polynominal approach had to be discontinued.

3.9 PROPOSED EXPRESSION FOR BAUSCHINGER EFFECT

Finally an expression was chosen that has been used by

other investigators[61] as a moment-curvature formula for structural steel sections. The equation, the Ramberg-Osgood function, has the form:

$$\frac{\phi}{\phi_{ch}} = \frac{M}{M_{ch}} \left(1 + \left|\frac{M}{M_{ch}}\right|^{r-1}\right) \qquad \ldots\ldots(3.13)$$

$\therefore$ M_{ch} and ϕ_{ch} are "characteristic" moment and curvature respectively,

r is the Ramberg-Osgood parameter.

This function can be modified for stress-strain formulation as follows:

$$\frac{\epsilon}{\epsilon_{ch}} = \frac{f}{f_{ch}} \left(1 + \left|\frac{f}{f_{ch}}\right|^{r-1}\right) \qquad \ldots\ldots(3.14)$$

$\therefore$ f_{ch} and ϵ_{ch} are "characteristic" stress and strain respectively,

r is the Ramberg-Osgood parameter.

Depending on the value of r, the function has the advantage of either having the form of a sweeping curve, or of having two almost linear "limbs" joined by a sharp elbow (see Figure 3.6).

For all values of r, the function passes through the point:

$$\frac{\epsilon}{\epsilon_{ch}} = 2 \text{ and } \frac{f}{f_{ch}} = 1$$

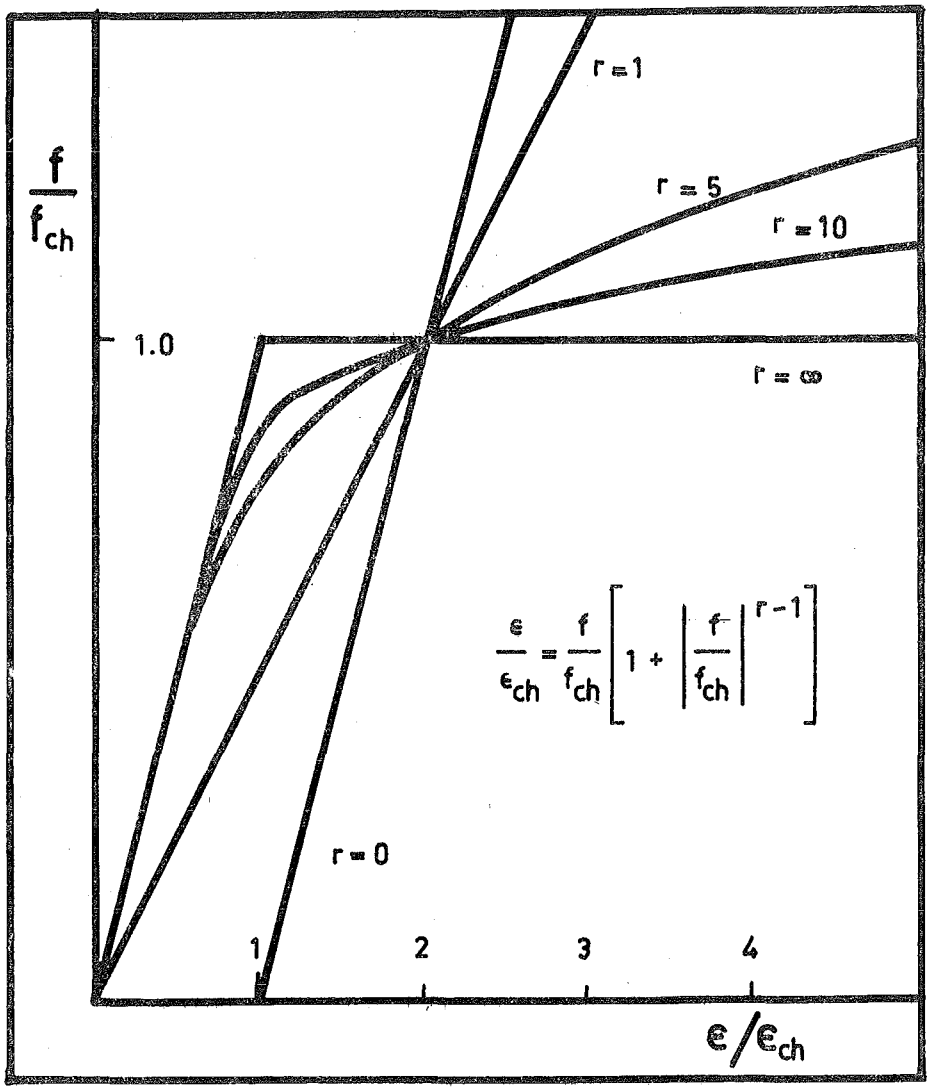

FIG.3.6 - RAMBERG-OSGOOD FUNCTION

ϵ_{ch} and f_{ch} are related such that $f_{ch} = \epsilon_{ch} E_s$.

Therefore, given E_s, the function simplifies to an equation involving only two unknowns, f_{ch} and r.

$$\epsilon E_s = f \left(1 + \left|\frac{f}{f_{ch}}\right|^{r-1}\right) \qquad \ldots\ldots(3.15)$$

3.9.1 Boundary Conditions for the Ramberg-Osgood Function

As shown in Section 3.8, most expressions can be simplified by considering boundary conditions and thereby reducing the number of unknowns. For this application, boundary conditions are:-

$$\frac{df_s}{d\epsilon_s} = E_s \text{ when } \epsilon_s = 0$$

$$\frac{df_s}{d\epsilon_s} = 0 \text{ when } \epsilon_s = \epsilon_{su}$$

$$f_s = f_u \text{ when } \epsilon_s = \epsilon_{su}$$

Differentiating Equation (3.15) gives:

$$\frac{df_s}{d\epsilon_s} = \frac{E_s}{1 + r\left|\frac{f_s}{f_{ch}}\right|^{r-1}} \qquad \ldots\ldots(3.16)$$

The first boundary conditions is true by definition.

Using the second boundary condition above does not produce a unique solution.

Either $f_{ch} = 0$ or $r = \infty$, neither of which is true.

This then is a disadvantage of the Ramberg-Osgood function in that an increase in strain will always result in an increase in stress. As this is unrealistic in the real situation, the condition that $\epsilon_s \ll \epsilon_{su}$, has to be imposed on the use of this function.

The third boundary condition cannot be applied for the same reason and therefore the equation remains as a function involving two unknowns.

3.9.2 Experimental and Theoretical Comparisons: The Method of Least Squares

As with previous functions, a least squares analysis was performed on individual cycles in an attempt to find a means of predetermining f_{ch} and r.

From Equation (3.15)

$$\epsilon_s E_s = f_s + f_{ch} \left| \frac{f_s}{f_{ch}} \right|^r$$

$$\text{or } (\epsilon_s E_s - f_s) = f_{ch} \left| \frac{f_s}{f_{ch}} \right|^r$$

$$\therefore \log (\epsilon_s E_s - f_s) = \log f_{ch} + r \log f_s - r \log f_{ch} \quad \ldots\ldots(3.17)$$

This particular form, Equation (3.17), is not immediately useful for least squares analysis as $r \log f_{ch}$ is a term involving both unknowns and therefore cannot be partitioned into matrices.

Therefore let:

$$\log(\epsilon_s E_s - f_s) = \log f_{ch} + r \log f_s - a \log f_{ch} \quad \ldots\ldots(3.18)$$

where a represents a trial value for r.

Now ϵ_s and f_s are experimental values and we require the difference between these and theoretical values to be minimised.

$$\therefore\ s = (1 - a)\log f_{ch} + r \log f_s - \log(\epsilon_s E_s - f_s) \ldots\ldots(3.19)$$

where s = difference.

For n experimentally-obtained values of f_s and ϵ_s, Equation (3.19) can be written as:

$$\{s\} = \begin{bmatrix} (1-a)\log f_{s1} \\ (1-a)\log f_{s2} \\ (1-a)\log f_{s3} \\ \vdots \\ (1-a)\log f_{sn} \end{bmatrix} \begin{Bmatrix} \log f_{ch} \\ r \end{Bmatrix} - \begin{Bmatrix} \log(\epsilon_{s1} E_s - f_{s1}) \\ \log(\epsilon_{s2} E_s - f_{s2}) \\ \log(\epsilon_{s3} E_s - f_{s3}) \\ \vdots \\ \log(\epsilon_{sn} E_s - f_{sn}) \end{Bmatrix}$$

This simplifies to:

$$\{s\} = [A]\{B\} - \{C\}$$

where vector $\{B\}$ contains the two unknowns.

Now the square of the difference is required:

$$S = \{s\}^T\{s\} = \left[[A]\{B\} - \{C\}\right]^T\left[[A]\{B\} - \{C\}\right]$$

$$= \{B\}^T[A]^T[A]\{B\} - \{B\}^T[A]^T\{C\} - \{C\}^T[A]\{B\} + \{C\}^T\{C\} \quad \ldots\ldots(3.20)$$

For the least value of $S = \{s\}^T\{s\}$, Equation (3.20) is differentiated with respect to the unknowns f_{ch} and r, that is, with respect to $\{B\}^T$

$$\frac{\partial S}{\partial \{B\}^T} = 2[A]^T[A]\{B\} - 2[A]^T\{C\} = \{0\}$$

$$\therefore [A]^T[A]\{B\} = [A]^T\{C\} \quad \ldots\ldots(3.21)$$

Equation (3.21) then gives:

$$[\phi]\{B\} = \{w\}$$

$$\text{and } \{B\} = [\phi]^{-1}\{w\} \quad \ldots\ldots(3.22)$$

Equation (3.22) gives the 2 x 1 vector $\{B\}$ with first term $\log f_{ch}$ and second term r.

$$\therefore \quad r = B2$$

$$f_{ch} = e^{B1}$$

At this stage, r is compared with the trial value a. If $|r - a| \leq .05$ then r and f_{ch} have been obtained to suitable accuracy but if $|r - a| > .05$ then a is equated to the average of the previous a and the computed r value, and the analysis performed again. A computer program (Program 3.1) was written for this operation.

A fuller account of the technique of least squares is given in Reference 48.

3.9.3 Solution for Stress, given Strain

Having obtained values for f_{ch} and r, theoretical and experimental stresses are compared (using experimental

strains) to find mean and standard deviations (Table 3.1). Here a further disadvantage of the function becomes apparent, in that it cannot be written to give stress explicitly in terms of strain.

Consequently, stress is found by trial and error using Taylor's Method:

$$x_1 = x_o - \frac{f(x_o)}{f'(x_o)}$$

where x_o = a trial value

x_1 = a better value.

This method works particularly well for continuous functions and if the trial value is close to the final result.

In the case of a Ramberg-Osgood function:

$$f(f_s) = -\epsilon_s E_s + f_s + f_{ch} \left| \frac{f_s}{f_{ch}} \right|^r$$

$$\text{and } f'(f_s) = 1 + r \left| \frac{f_s}{f_{ch}} \right|^{r-1}$$

$$\therefore f_{s1} = f_{s0} - \frac{f_{s0} + \left| \frac{f_{s0}}{f_{ch}} \right|^r f_{ch} - \epsilon_s E_s}{1 + r \left| \frac{f_{s0}}{f_{ch}} \right|^{r-1}} \qquad \ldots\ldots(3.23)$$

If $\left| f_{s1} - f_{s0} \right| \leq 10$ then f_{s1} is accurate to within 10 p.s.i. If not, then f_{s0} is set equal to f_{s1} and a new

TABLE 3.1

LEAST SQUARES ANALYSIS FOR r AND f_{ch}

Specimen	Cycle	r	f_{ch}/f_y	Mean Devn.	Std. Devn.
6	1	2.792	.707	-2478	3359
8	1	3.227	1.004	2192	4378
	2	4.192	.628	-1663	4695
	3	2.798	.341	-1911	2623
9	1	2.776	.963	-1607	1915
	2	4.355	.824	-1915	6078
	3	2.843	.464	-2406	3076
11	1	2.923	.737	-569	1222
12	1	2.871	.579	-1429	1746
	2	4.678	.565	-5094	7931
17	1	2.209	.670	-878	1420
	2	6.146	1.187	798	3128
	3	3.721	.625	-841	1164
	4	4.402	1.183	518	2999
	5	3.047	.590	-828	1080
	6	4.010	1.019	-686	2577
	7	2.244	.569	-348	699
	8	4.248	.708	-2960	5274
20	1	3.367	.724	-289	418
	2	2.892	1.693	168	4670
	3	3.424	.632	-785	932
	4	2.476	1.721	-537	3357
	5	3.037	.625	-1059	1221
	6	2.624	1.607	-68	3594
	7	3.342	.664	22	253
	8	3.375	1.039	-1684	2494
	9	3.651	.605	-324	823
21	1	2.160	1.971	-1202	1372
	2	2.068	3.708	-1048	2577
	3	1.896	3.697	814	936
	4	2.069	4.780	74	3160
	5	1.986	3.625	-67	689
	6	9.156	1.172	-226	785
	7	2.440	2.046	-579	1010
	8	6.485	.838	-2617	5482
25	1	3.212	.585	-1868	2321
	2	8.211	.745	-1586	4135
	3	4.773	.580	491	2462
29	1	1.824	1.759	-485	655
	2	2.780	2.363	-1524	6986
	3	2.036	.589	-2213	2579
	4	3.460	.967	-2616	3956
	5	3.394	.622	-1343	1597
	6	2.991	1.118	-738	3006
	7	2.454	.490	-1780	2138
	8	3.975	.736	-1895	5580
30	1	1.813	1.528	-2154	2790
	2	2.249	1.419	-1968	2320
	3	1.876	6.511	3061	4139
	4	4.198	1.025	653	5720

value for f_{s1} computed.

An initial value of $f_{s0} = \epsilon_s E_s$ gives convergence within two or three cycles for low strains and up to fifteen cycles for very high strain (c.2%).

3.9.4 Characteristic Ratio, R_{ch}

$$R_{ch} = \frac{f_{ch}}{f_y}$$

Inspection of the results of the least squares analysis discussed in Section 3.9.3 indicates that the characteristic ratio is dependent on the plastic strain produced in the previous cycle, ϵ_{ipl}. This is shown in Figure 3.7 which plots the characteristic ratio against ϵ_{ipl}. This relationship complies with reported observations in that the reversed "yield" stress is lowered with increasing prior plastic strain.

The shape of the curve in Figure 3.7 is similar to $y = \log^{-1}x$, $y = e^{-x}$ and $y = x^{-4}$ and therefore a least squares analysis (Program 3.2) was carried out on the following function:

$$R_{ch} = \frac{\alpha}{\log(1 + 1000\epsilon_{ipl})} + \frac{\beta}{(e^{1000\epsilon_{ipl}} - 1)} + \frac{\gamma}{\epsilon_{ipl}^4} + \delta \quad \ldots.(3.24)$$

Results from the least squares analysis of Section 3.9.3 were weighted according to the inverse of the standard deviations. Weighting, in terms of least squares analysis,

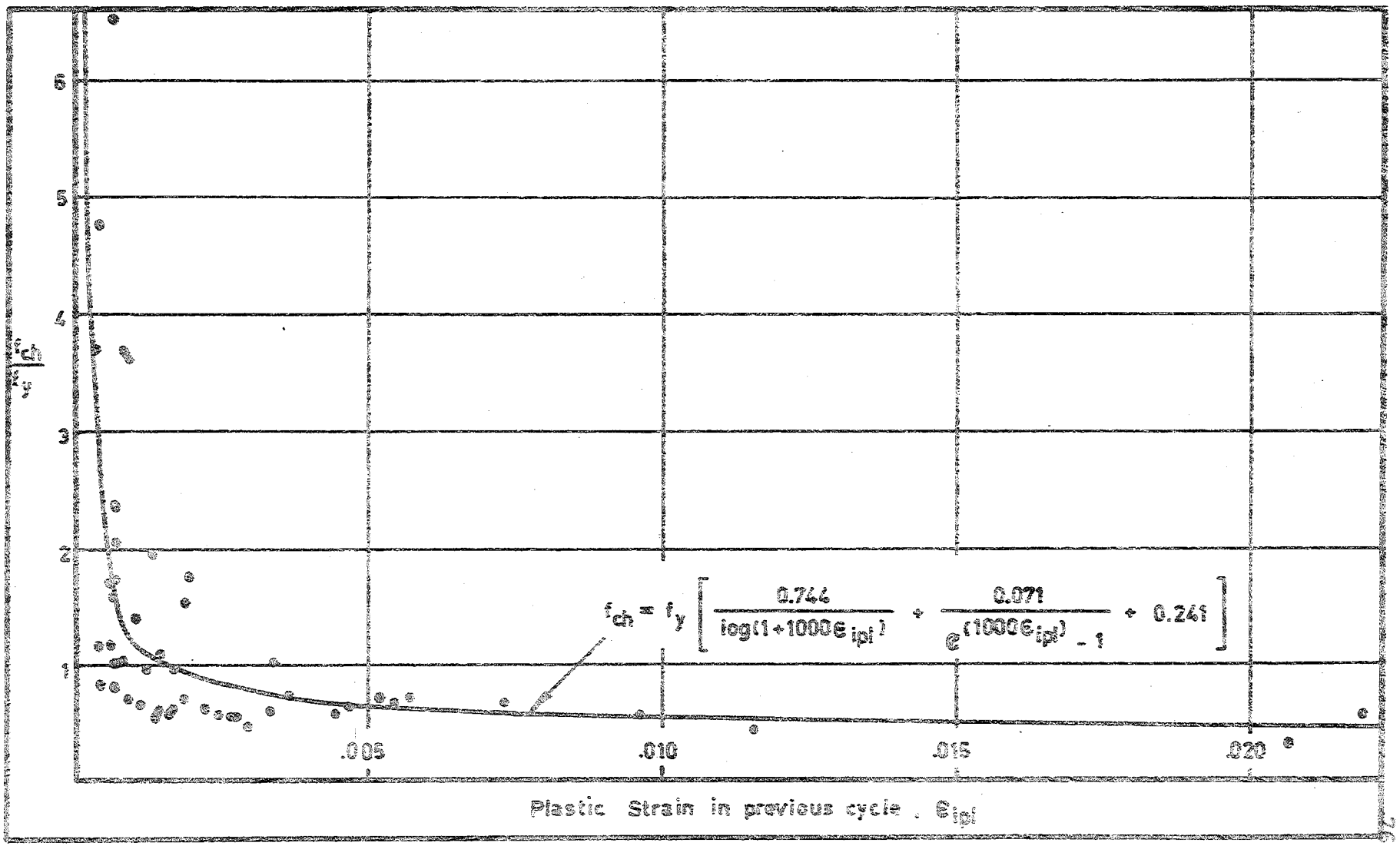

FIG.3.7 - CHARACTERISTIC RATIO vs STRAIN IN PREVIOUS CYCLE

required generation of more points for values with low standard deviations. This technique produced the following values for the unknown coefficients in Equation (3.24).

α = 0.744

β = 0.071

γ = 0.0

δ = 0.241

Therefore the following relation is adopted and is shown in Figure 3.7:

$$f_{ch} = f_y \left[\frac{.744}{\log(1 + 1000\epsilon_{ipl})} + \frac{.071}{(e^{1000\epsilon_{ipl}} - 1)} + .241 \right] \quad \ldots\ldots(3.25)$$

$$\epsilon_{ch} = f_{ch}/E_s \quad \ldots\ldots(3.26)$$

A condition was imposed whereby $f_{ch} \leqslant f_y$. Although Figure 3.7 shows several values of characteristic ratios in excess of unity, these were all obtained on specimens with a low strain range, i.e., the deviation from elastic response was not marked, and therefore the least squares analysis for a Ramsberg-Osgood function was particularly insensitive for these cycles.

3.9.5 Ramberg-Osgood Parameter, r

Having found a reasonably accurate method for predetermining characteristic stress, a further least squares analysis was carried out on the individual experimental

cycles to find best values for r. The results of this analysis (Program 3.3) are shown in Table 3.2.

Comparing standard deviations in Tables 3.1 and 3.2 shows that some standard deviations have been improved by fixing values for characteristic stress. The reason for this is that in both analyses, when f_{ch} and r were found, and when r was found given f_{ch}, experimental strain values were weighted so that large strain values had a greater effect on the analysis.

The values of r in Table 3.2 were then plotted against various factors, and of these, only the cycle number showed any correlation with the Ramberg-Osgood parameter (Figure 3.8). It can be seen that the odd-numbered cycles show lower values of r than do the even-numbered cycles. First yield occurs in cycle 0 and cycle 1 is the first post-yield stress reveral. Also there is a noticeable trend towards lower values of r with increasing number of prior cycles. This behaviour is reinforced by observations reported by Singh et al.[49]: that stiffness increases with increasing number of prior cycles. Figure 3.6 shows that a reduction in r corresponds to an increase in stiffness.

A least squares analysis (Program 3.2A) using N and r values shown in Figure 3.8 was carried out and extra values were generated according to the strain range in cycle N to standard deviation ratio. The analysis resulted in the following expressions:-

TABLE 3.2

LEAST SQUARES ANALYSIS FOR r GIVEN f_{ch}

Specimen	Cycle	r	f_{ch}/f_y	Mean Devn.	Std. Devn.
6	1	2.167	.597	-3885	4987
8	1	3.395	.747	-1239	2515
	2	4.803	.672	-1160	3874
	3	3.407	.483	814	1354
9	1	3.268	1.000	-446	863
	2	4.463	1.000	692	7178
	3	2.791	.535	-730	1740
11	1	2.258	.730	-674	1305
12	1	3.148	.556	-1554	1987
	2	3.862	1.000	5634	14675
17	1	2.306	.639	-915	1534
	2	8.192	1.000	-898	1904
	3	2.994	.886	517	769
	4	5.297	1.000	-903	2139
	5	2.522	.856	570	880
	6	4.409	1.000	-558	2248
	7	1.809	.810	333	561
	8	3.848	1.000	2767	8126
20	1	4.140	.632	-457	736
	2	4.900	1.000	-2230	3144
	3	2.538	1.000	535	1177
	4	3.811	1.000	-1924	2947
	5	2.518	1.000	537	1146
	6	3.924	1.000	-1662	2582
	7	2.444	1.000	852	1631
	8	4.137	1.000	-1142	1918
	9	1.320	1.000	9124	18382
21	1	3.708	1.000	-840	1456
	2	4.349	1.000	-3006	4385
	3	2.934	1.000	-826	1708
	4	4.322	1.000	-3276	4576
	5	3.542	1.000	-903	1582
	6	16.796	1.000	-1459	2013
	7	4.241	1.000	-654	1065
	8	6.098	1.000	1202	6534
25	1	3.642	.680	-31	1054
	2	4.849	.651	-1461	4059
	3	3.686	.479	387	1433
29	1	2.580	.945	-795	1381
	2	4.179	1.000	-3298	4917
	3	2.089	.825	-265	510
	4	4.061	1.000	-1716	3049
	5	2.976	.756	440	630
	6	3.478	1.000	-1492	2795
	7	1.872	.787	1157	2199
	8	4.368	.968	2910	7046
30	1	2.659	1.000	-2148	3173
	2	3.456	1.000	-1647	2507
	3	3.061	1.000	-3441	4476
	4	4.350	1.000	270	5244

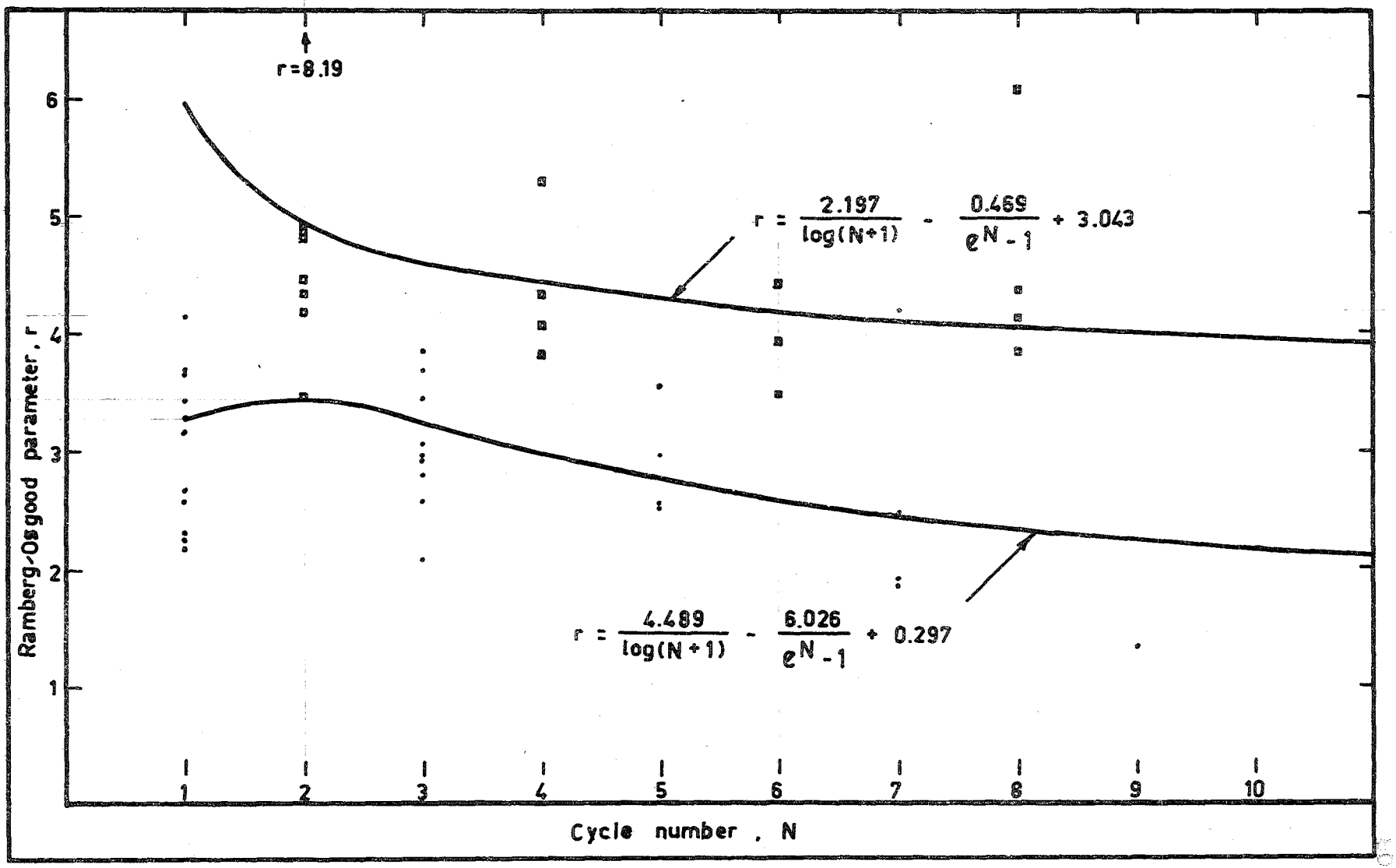

FIG.3.8 - RAMBERG-OSGOOD PARAMETER vs CYCLE NUMBER

For odd-numbered cycles:

$$r = \frac{4.489}{\log(1+N)} - \frac{6.026}{e^N - 1} + 0.297 \qquad \ldots\ldots(3.27)$$

For even-numbered cycles:

$$r = \frac{2.197}{\log(1+N)} - \frac{0.489}{e^N - 1} + 3.043 \qquad \ldots\ldots(3.28)$$

Equations (3.27) and (3.28) are shown in Figure 3.8.

3.10 THEORY AND EXPERIMENT COMPARED

The theory for Bauschinger Effect advanced in this chapter is based on individual cycles from the eleven test specimens. Fuller details on the derivation of the experimental results are given in Appendix C.

To test the theory and the experimentally-derived constants advanced in Section 3.9 with the expression proposed by Singh et al.[49] and with the complete range of experimental stress-strain curves, the individual cycles of the eleven test specimens were recombined and run through a computer program to obtain stress standard deviations from experimental strains (Program 3.4).

Although the programming for the Singh et al. expression presented no difficulty, the algorithm required for the modified Ramberg-Osgood model proved to be considerably complex. The difficulties that arose stemmed mainly from provisions for repeated loading from stress of one sign to

a stress, less than transition stress, of the opposite sign. On reloading to the starting stress, care had to be taken to ensure that the stress-strain history did not become lost or confused. This particular problem was aggravated by allowance having to be made for such an occurrence near the origin, where signs changed.

The results for this analysis are plotted against experimental points and the Singh et al.[49] expression in Figures 3.9 to 3.20. Mean and standard deviations for stress for the Singh et al. expression and for the modified Ramberg-Osgood expression are shown in Table 3.3.

Table 3.3 shows that in all but two cases the modified Ramberg-Osgood function is more accurate than the Singh, Gerstle and Tulin expression. In cycles of large strain range, the Singh et al. model tends to be less inaccurate but in the cycles of lower strain range, the modified Ramberg-Osgood function is clearly better.

It can be seen in Figures 3.9 to 3.20 that if the difference between theoretical and actual stresses immediately prior to stress reversal is large, then the theoretical expression becomes "out-of-phase" with the observed response and significant errors can arise.

TABLE 3.3

COMPARISON OF THEORIES AND EXPERIMENT

Specimen No.	Singh et al.		Modified Ramberg-Osgood	
	Mean Dev. (p.s.i.)	Std. Dev. (p.s.i.)	Mean Dev. (p.s.i.)	Std. Dev. (p.s.i.)
6	-1090	2629	-1869	3628
8	45	4577	442	2644
9	-945	4654	-1759	4699
11	360	4422	-601	3106
12	534	4497	-1450	3469
17	2699	6049	-625	3366
20	4016	6754	2241	4477
21	2098	7072	254	4604
25	-1360	6405	-86	3115
29	2726	5550	316	2993
30	1922	7241	1546	3351

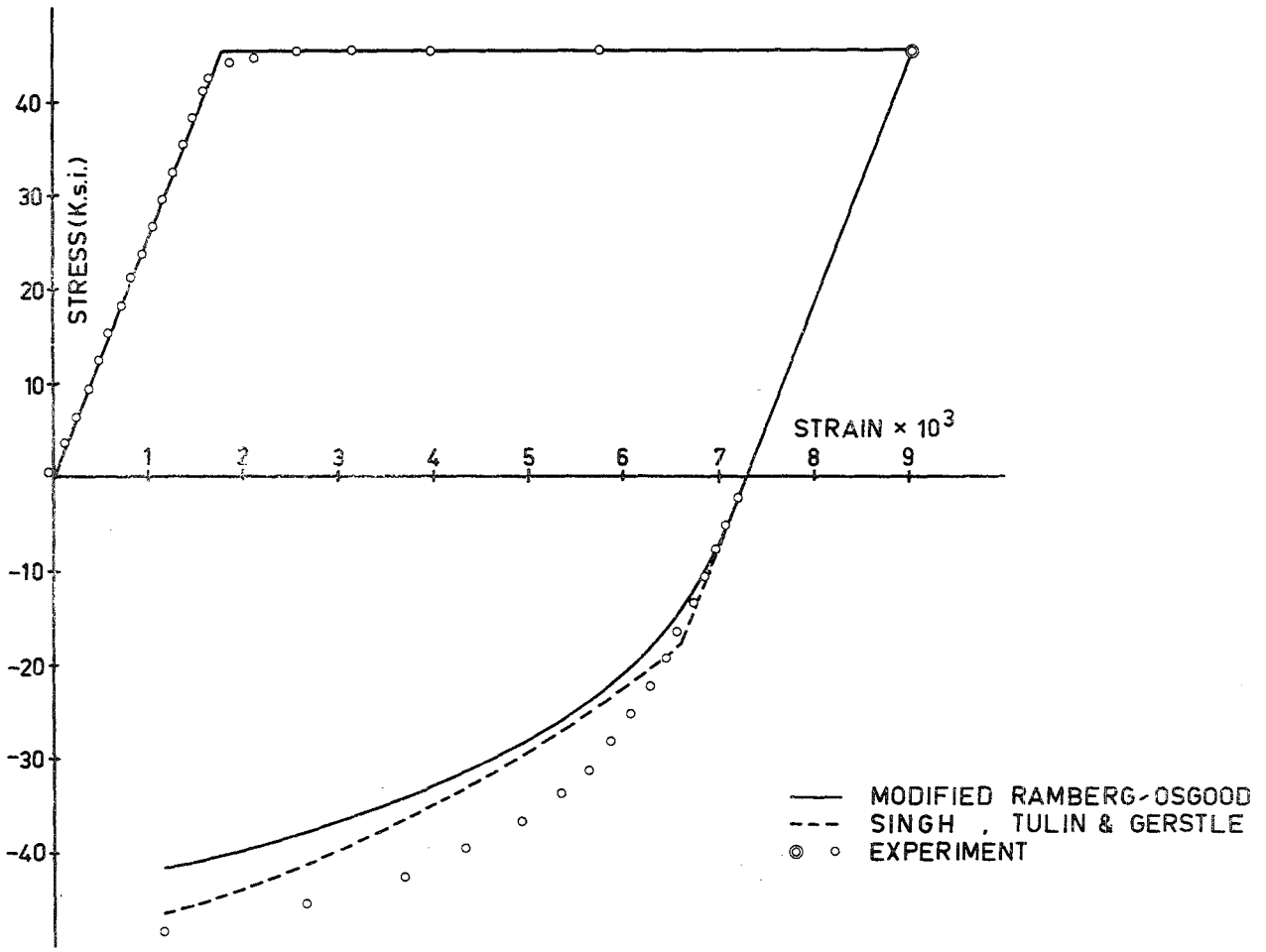

FIG.3.9 - BAUSCHINGER SPECIMEN 6

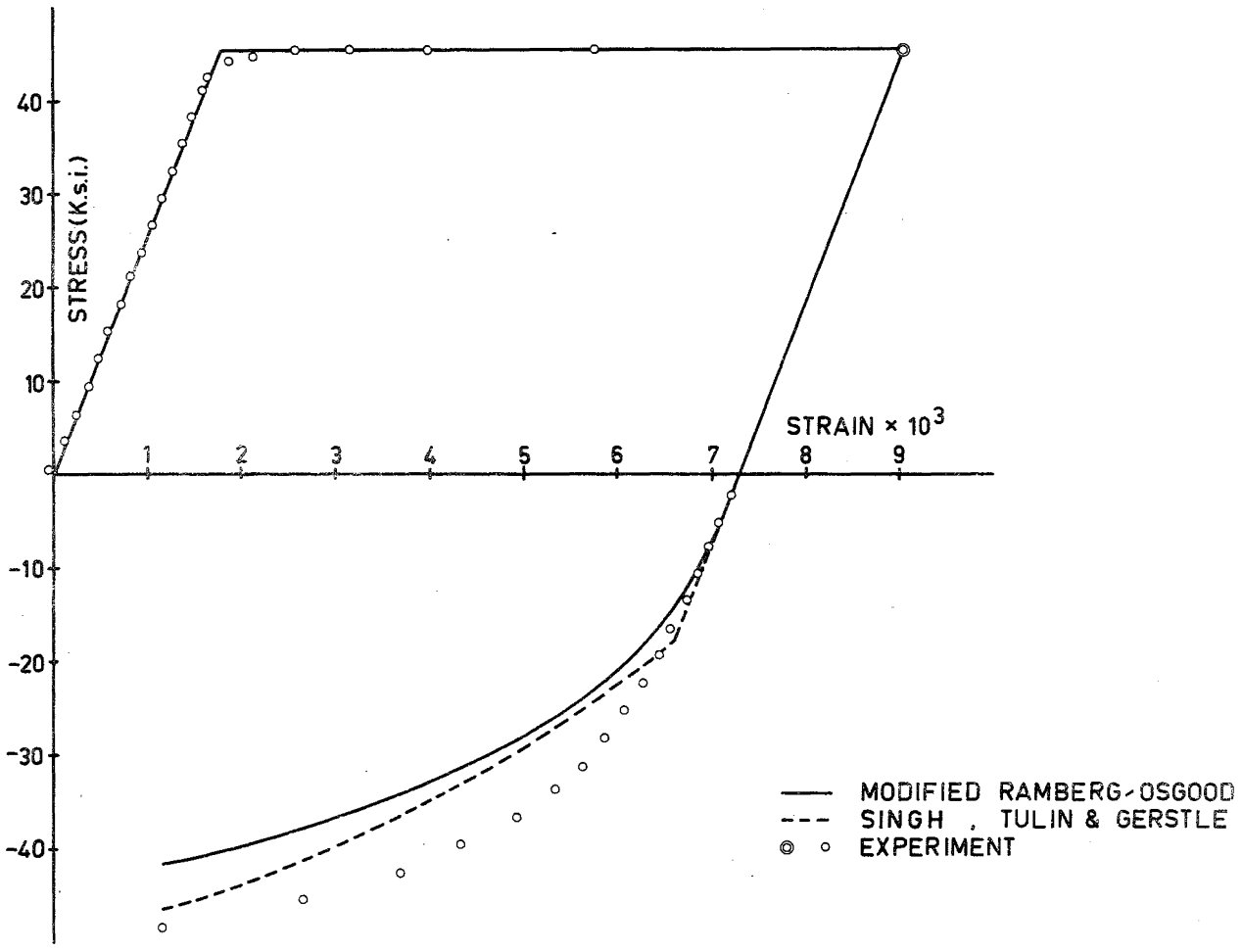

FIG.3.9 - BAUSCHINGER SPECIMEN 6

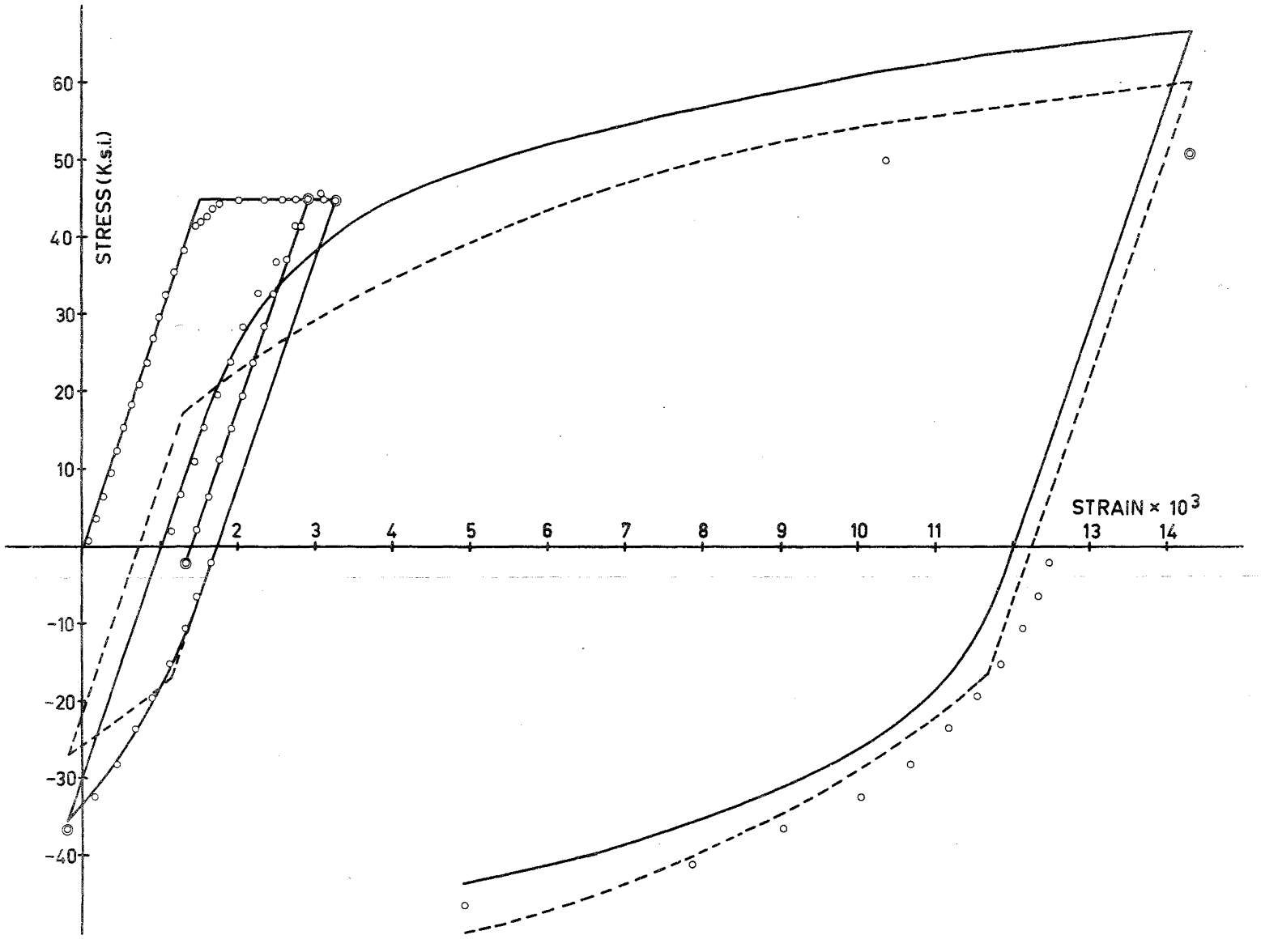

FIG.3.11 - BAUSCHINGER SPECIMEN 9

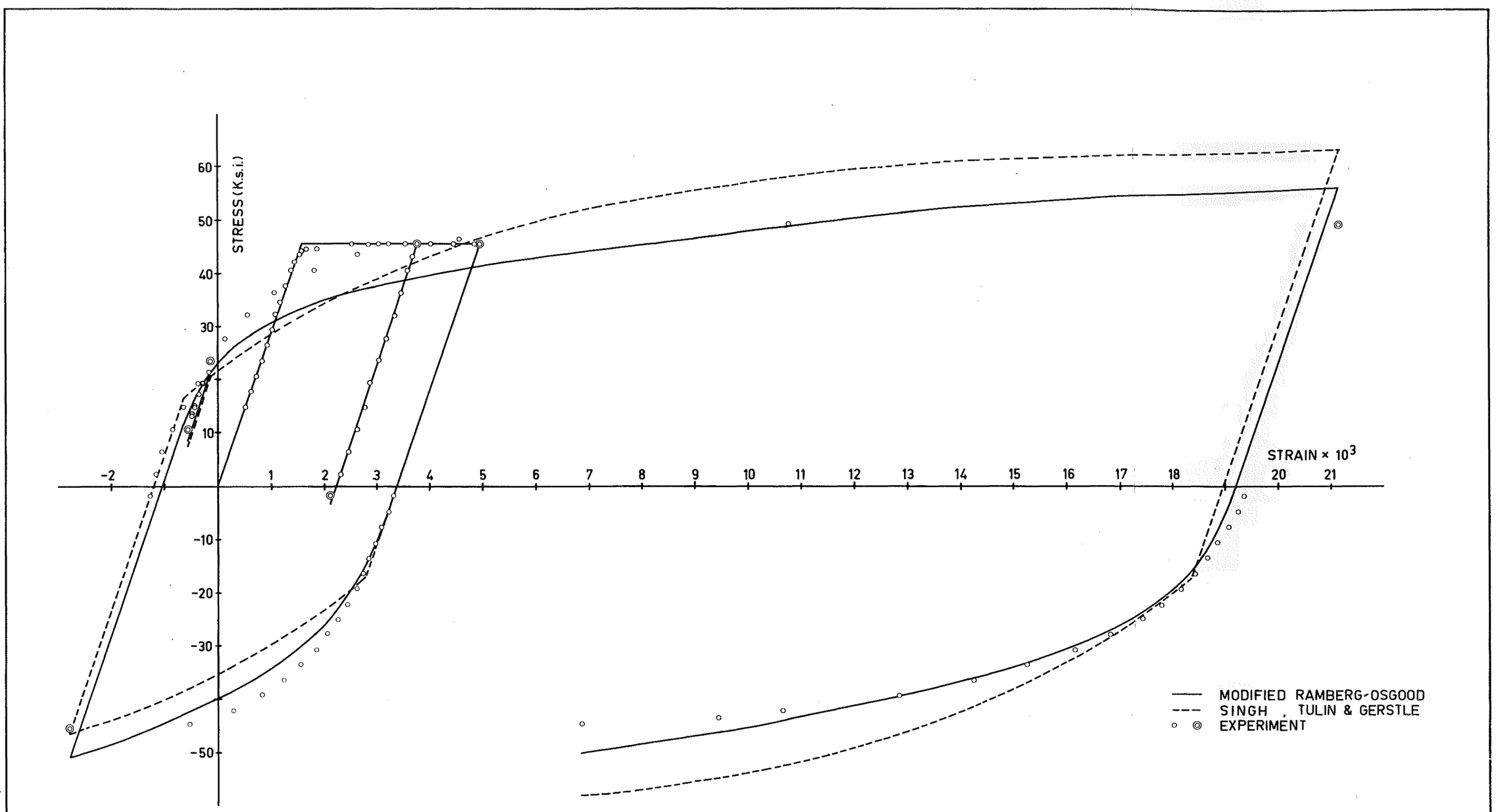

FIG.3.10 - BAUSCHINGER SPECIMEN 8

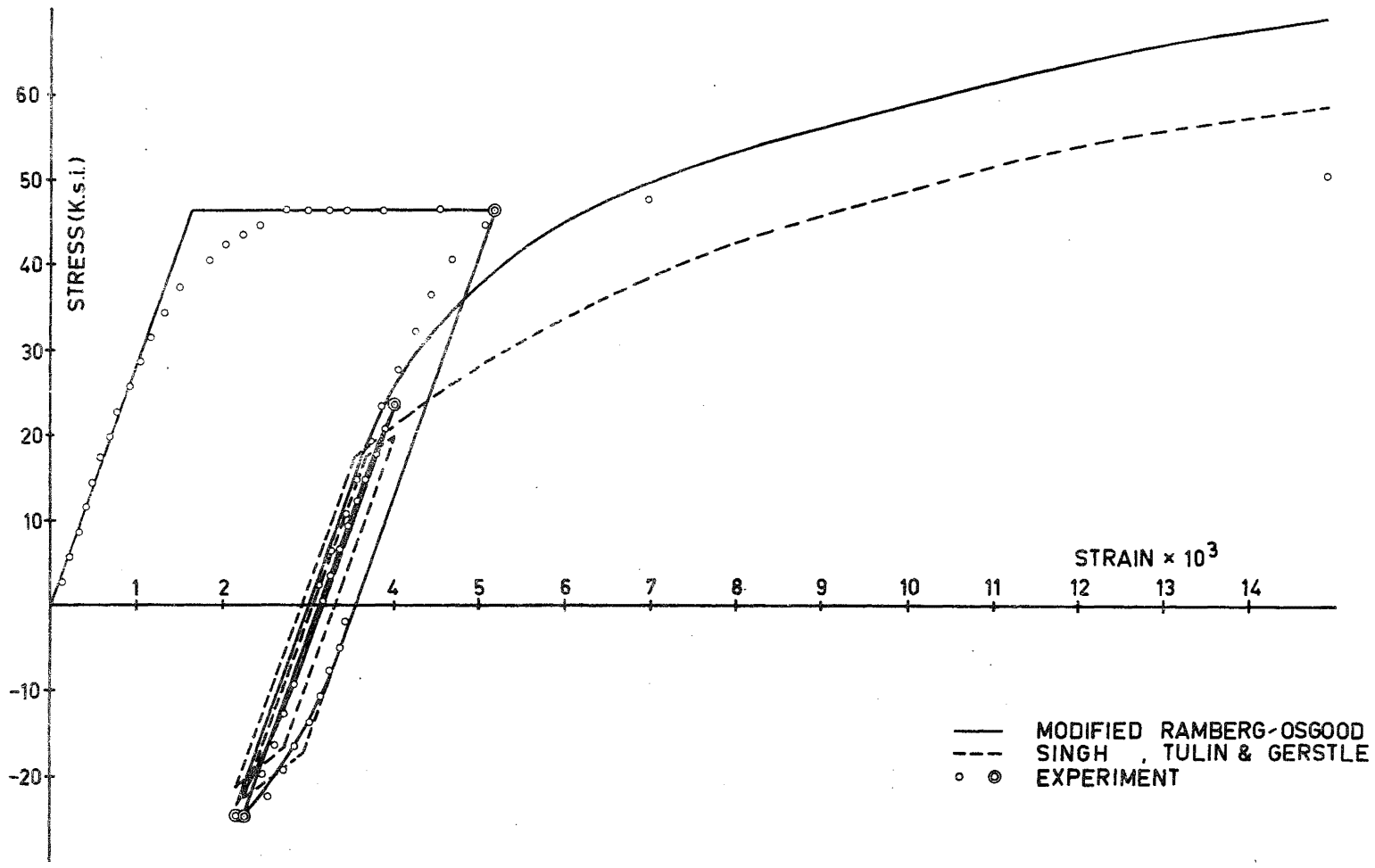

FIG.3.12 - BAUSCHINGER SPECIMEN 11

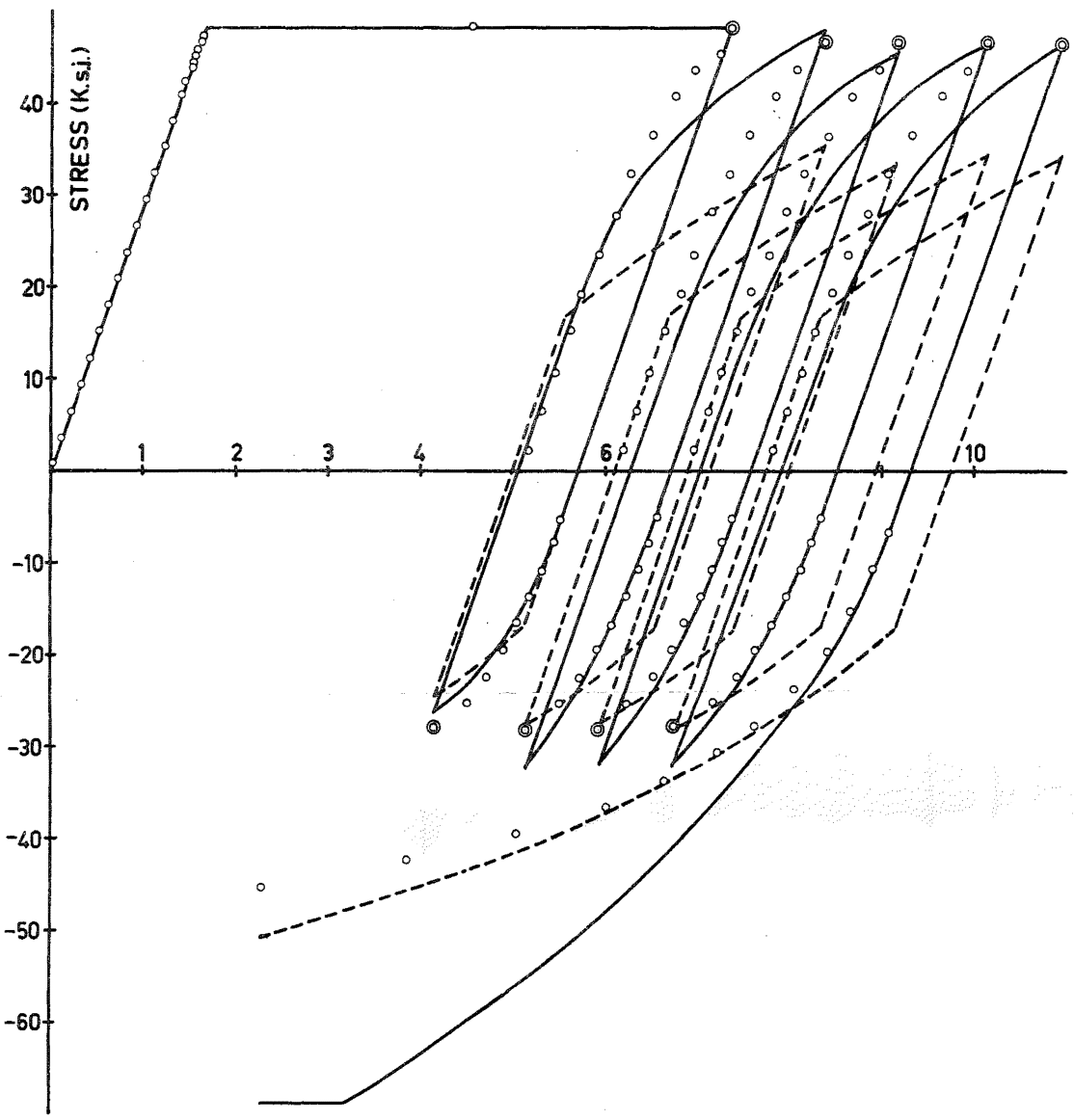

FIG.3.15 - BAUSCHINGER SPECIMEN 20

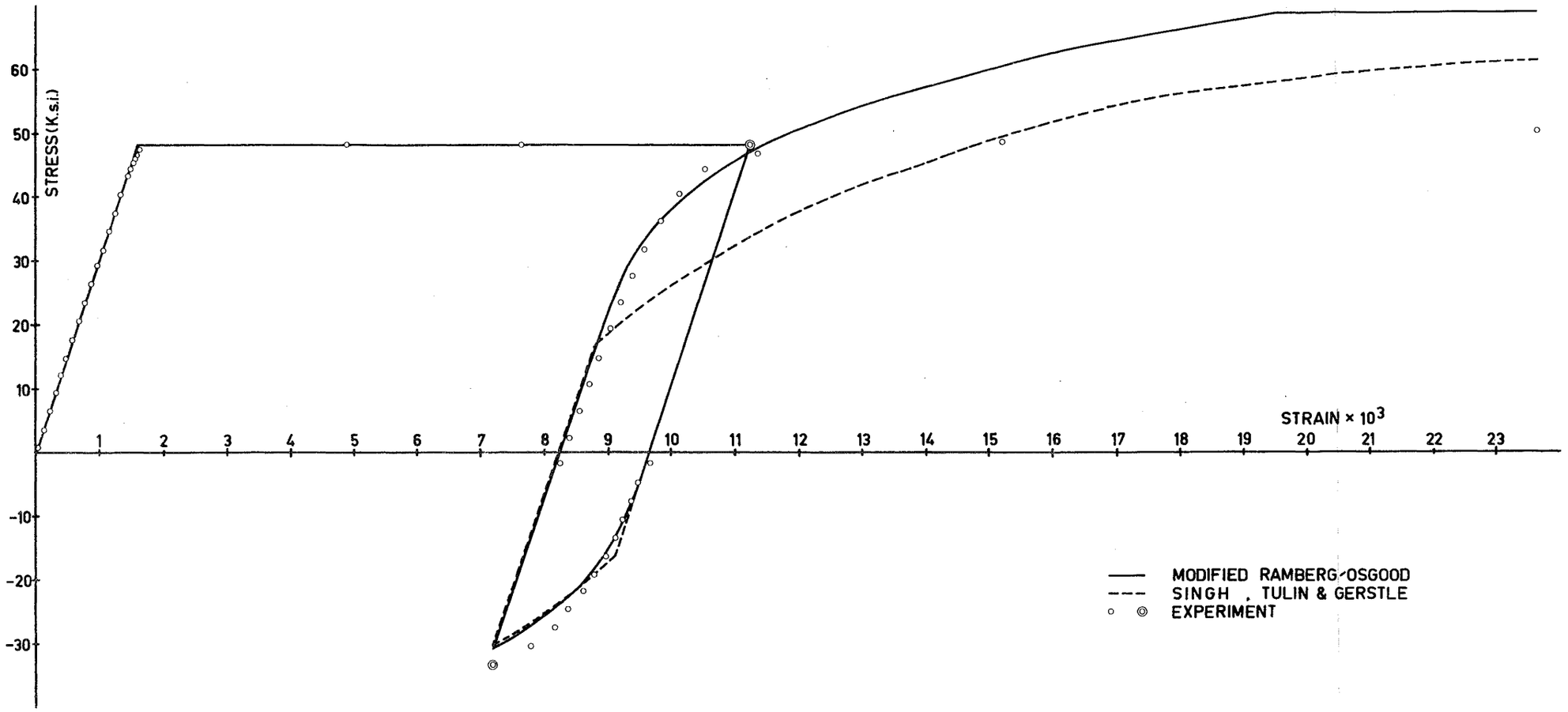

FIG.3.13 - BAUSCHINGER SPECIMEN 12

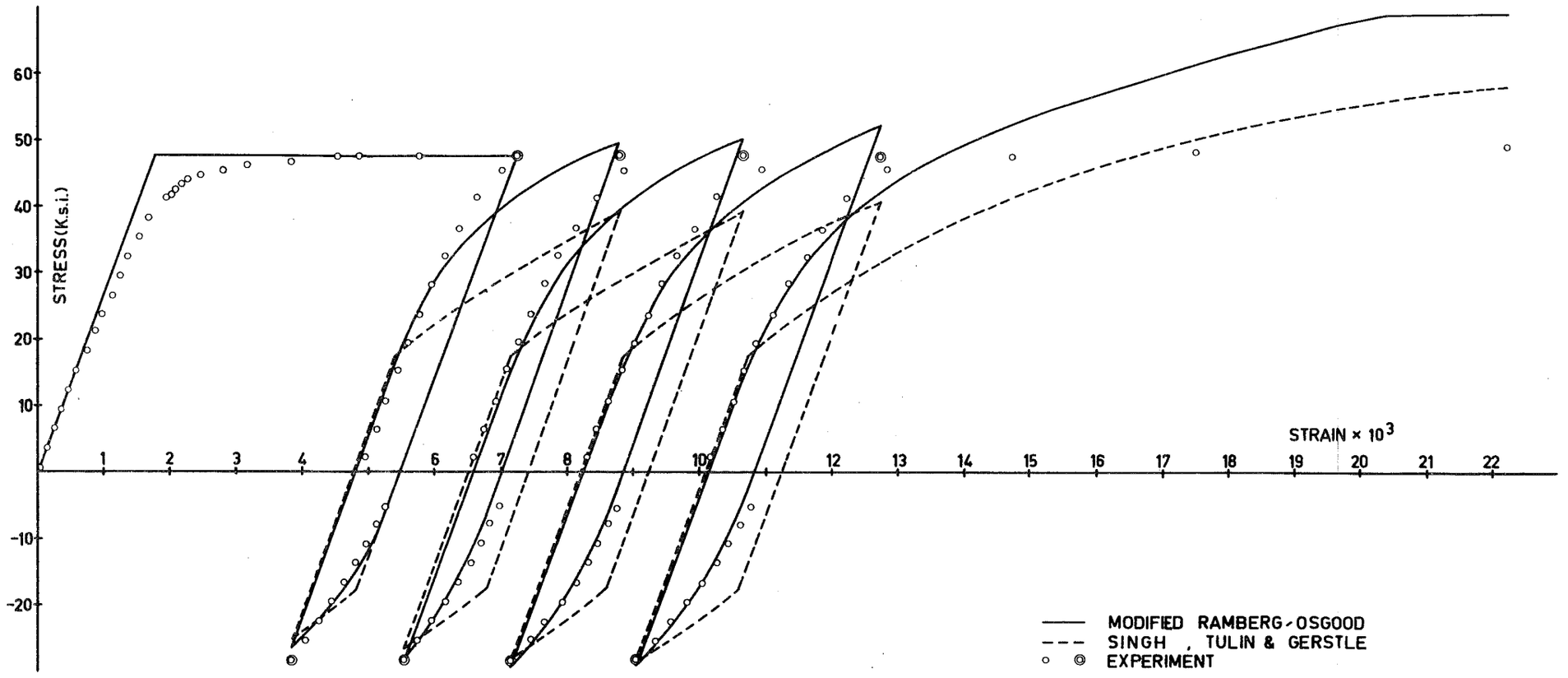

FIG.3.14 - BAUSCHINGER SPECIMEN 17

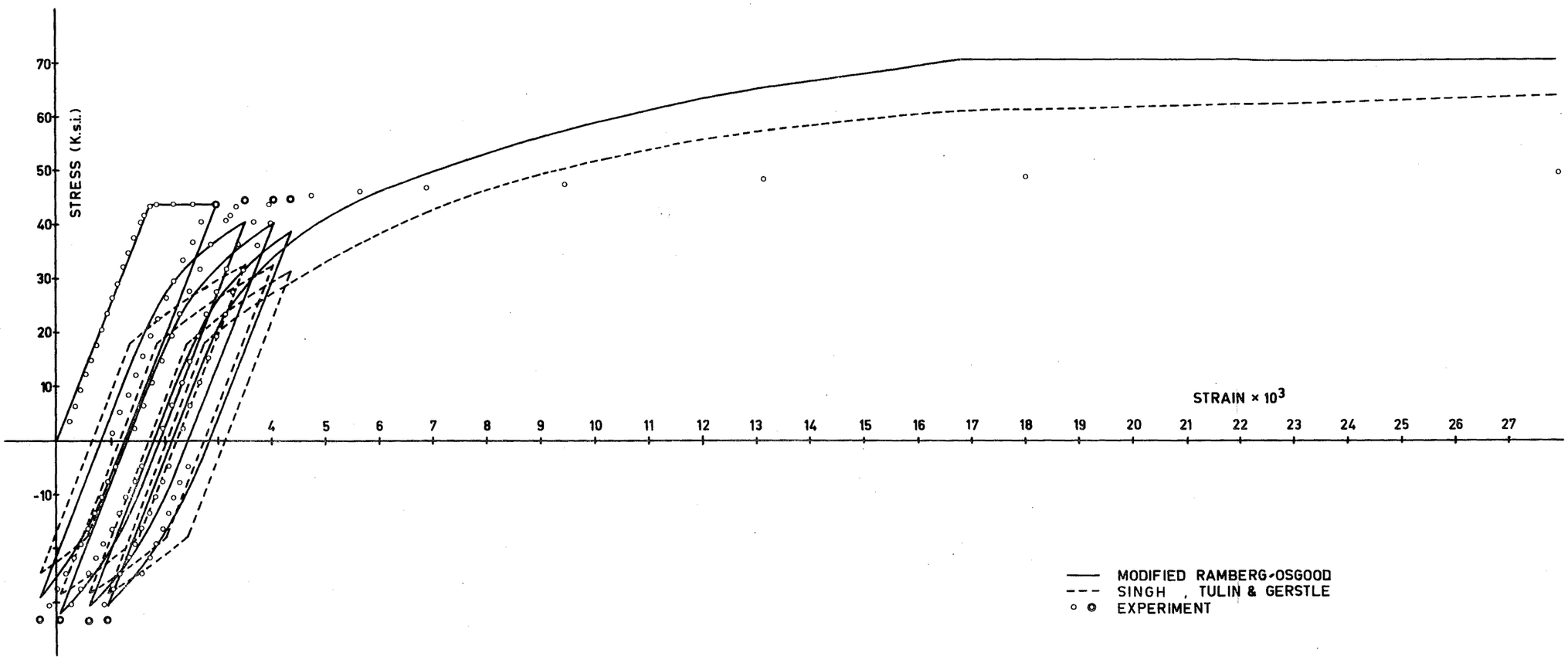

FIG.3.16 - BAUSCHINGER SPECIMEN 21

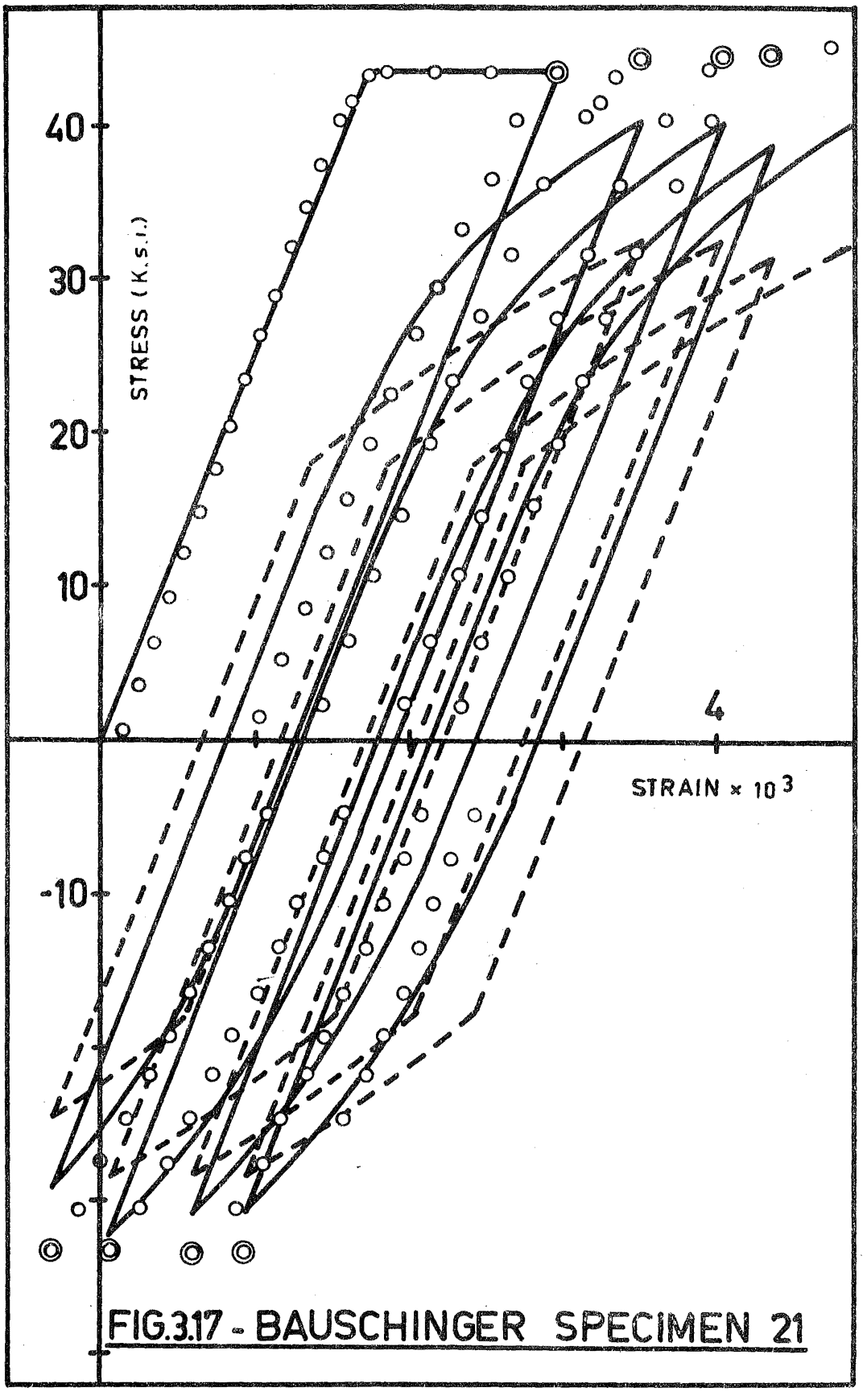

FIG.3.17 - BAUSCHINGER SPECIMEN 21

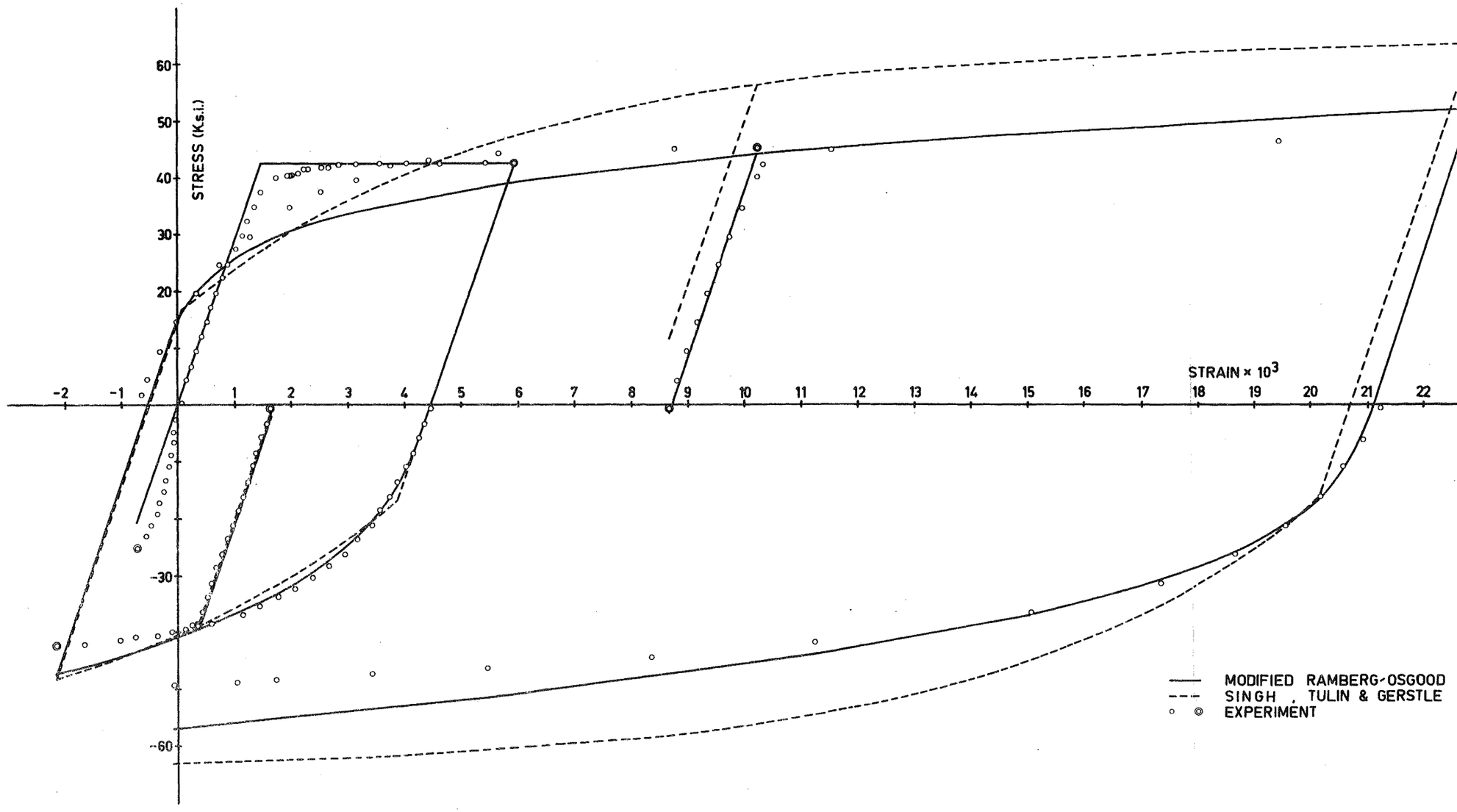

FIG.3.18 - BAUSCHINGER SPECIMEN 25

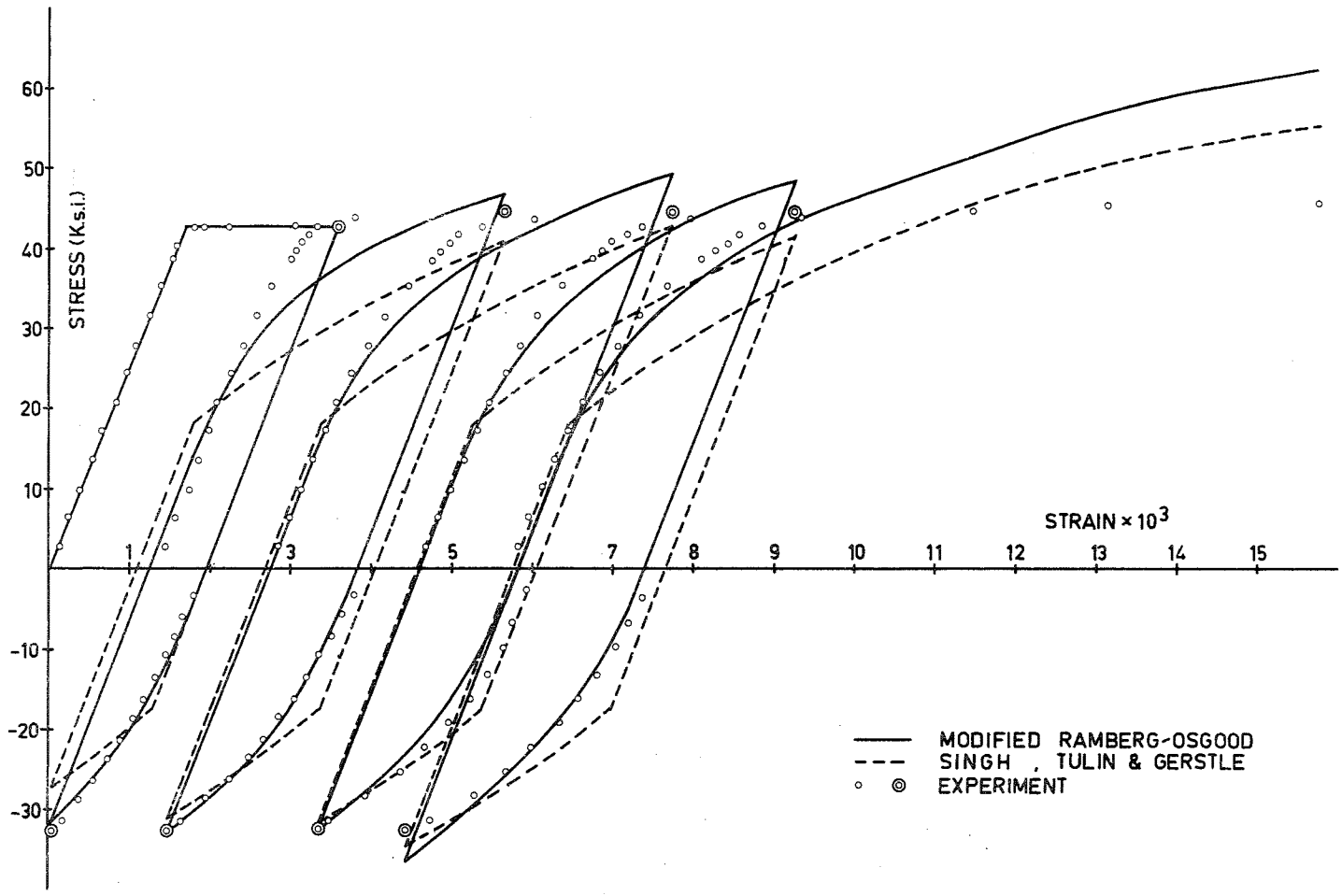

FIG.3.19 - BAUSCHINGER SPECIMEN 29

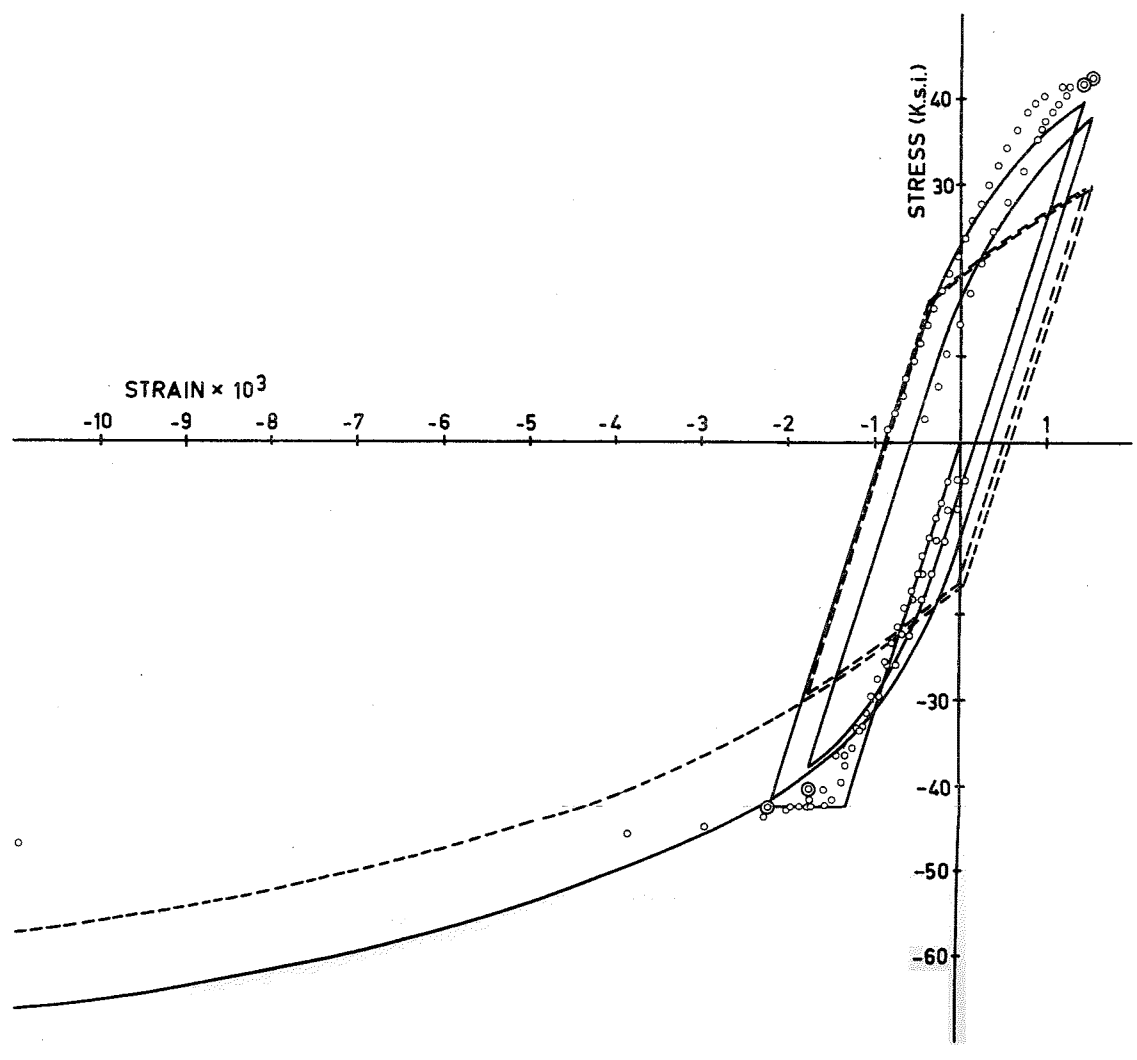

FIG.3.20 - BAUSCHINGER SPECIMEN 30

3.11 COMPUTER PROGRAMS

A number of computer programs were written for theoretical analyses of structural reinforcing steel properties. The programs written for the unsuccessful functions discussed in Section 3.8 are not included in this thesis and only those referred to in the text are described briefly below. Listings of these programs appear in Appendix B.

Program 3.1 ("FCHANDR"): Least squares analysis to find characteristic stress and Ramberg-Osgood parameter given individual experimental Bauschinger cycles (refer Section 3.9.2).

Program 3.2 ("FCOR"): Least squares analysis to find expression relating characteristic ratio and plastic strain in the previous cycle for steel (refer Section 3.9.4).

Program 3.3 ("FINDR"): Least squares analysis to find Ramberg-Osgood parameter, r, given characteristic stress (Equation 3.25) (refer Section 3.9.5).

Program 3.2A ("FCOR"): Least squares analysis to find Ramberg-Osgood parameter, r, in terms of cycle number N. Program 3.2 was modified for this analysis (refer Section 3.9.5).

Program 3.4 ("STEEL"): Comparison of modified Ramberg-Osgood and Singh et al.[49] with experimental results for each specimen. Ramberg-Osgood expression uses r and f_{ch} values found from previous programs (refer

Section 3.10).

3.12 CONCLUSIONS

A mathematical expression of the Bauschinger Effect in structural reinforcing steel has been presented and uses a Ramberg-Osgood function to describe the stress-strain response. It has been shown that for the eleven specimens tested, the proposed function is generally more accurate than that derived by Singh et al.[49]; the exceptions occurring when cycles of very large strain deformation took place.

The Singh et al.[49] expression has the apparent advantage of being easier to apply but, as will be shown later in this thesis, the importance of an accurate steel stress-strain model cannot be over-emphasised and this advantage is considered to be outweighed by the resulting inaccuracy.

The modified Ramberg-Osgood model is summarised below:-

$$\epsilon_s E_s = f_s\left(1 + \left|\frac{f_s}{f_{ch}}\right|^{r-1}\right) \qquad \ldots\ldots(3.15)$$

where

$$f_{ch} = f_y \left[\frac{0.744}{\log(1 + 1000\,\epsilon_{ipl})} + \frac{0.071}{(e^{1000\,\epsilon_{ipl}} - 1)} + 0.241\right] \qquad \ldots\ldots(3.25)$$

but $f_{ch} \leq f_y$

and for odd-numbered cycles (initial yield occurs in cycle 0):

$$r = \frac{4.489}{\log_e(1+N)} - \frac{6.026}{e^N - 1} + 0.297 \qquad \ldots\ldots(3.27)$$

or for even-numbered cycles:

$$r = \frac{2.197}{\log_e(1+N)} - \frac{0.489}{e^N - 1} + 3.043 \qquad \ldots\ldots(3.28)$$

and N = cycle number.

CHAPTER 4

MOMENT-CURVATURE RELATIONS FOR MONOTONICALLY-LOADED T AND RECTANGULAR REINFORCED CONCRETE SECTIONS

SUMMARY

Moment-curvature models for T and rectangular sections are developed and the resulting theory is compared with published test results. Design charts for stress block parameters α and γ are presented and nomograms for section curvatures and ductility at the crushing of the concrete have been constructed. The effect of axial stress, compression steel, and parameter Z on curvature of sections is discussed and tables for moment and curvature after crushing are included.

4.1 INTRODUCTION

Using the concrete theories developed in Chapter 2, it is possible to obtain moment-curvature responses for monotonically-loaded T sections with or without axial load. Rectangular sections can be considered as special cases of the generalised T-shape with flange width equal to web width and flange depth equal to any percentage of

effective depth.

Using the analyses discussed in this chapter, a computer program was written for the solution of these moment-curvature relations and the effects of steel content, parameter Z, and axial load on ductility were studied.

4.2 STRESS BLOCK FOR CONCRETE

Two simplifying assumptions were made when considering the stress block for concrete:

1. Tension capacity of concrete was neglected because it was felt that the additional programming was not warranted, there being twelve general section types for consideration anyway and the effect of concrete tension after cracking is negligible in practical cases.

2. The stress-strain response of unconfined concrete is assumed to follow the stress-strain response of the bound concrete in the section up to spalling strain, after which the unbound concrete makes no contribution. The reason for this simplification is discussed fully in Chapter 5.

The stress-strain response for concrete adopted in this thesis is reproduced in Figure 4.1.

4.2.1 Region 1: $\epsilon_c \leq \epsilon_o$

In this region the stress is given as:

$$f_{c_1} = f'_c \left[\frac{2\epsilon_c}{\epsilon_o} - \left(\frac{\epsilon_c}{\epsilon_o} \right)^2 \right] \qquad \ldots\ldots(2.19)$$

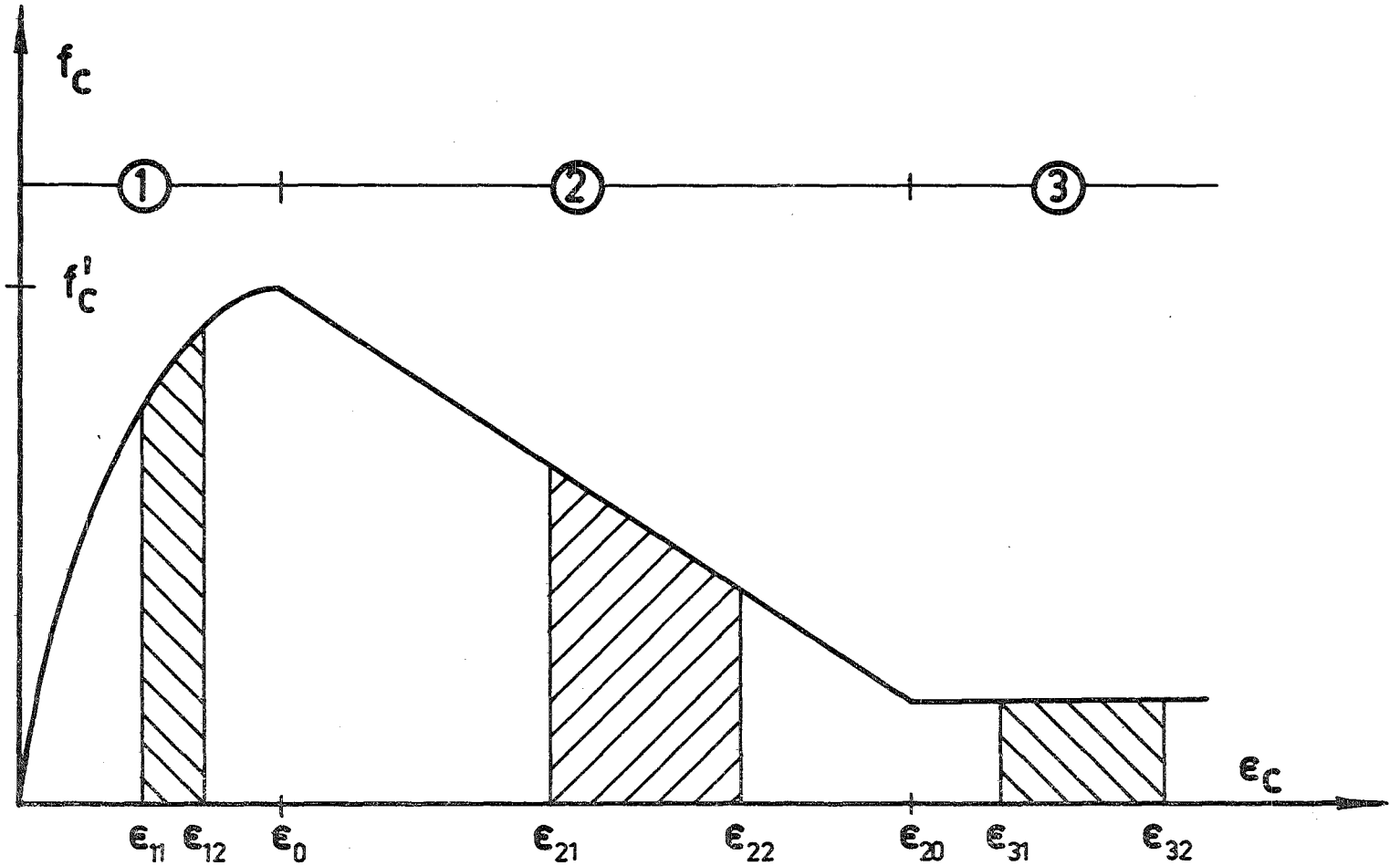

FIG.4.1 - ASSUMED STRESS-STRAIN FOR CONCRETE

The area under the stress-strain curve between limits ϵ_{11} and ϵ_{12} is:

$$A = \int_{\epsilon_{11}}^{\epsilon_{12}} f_c \cdot d\epsilon_c = \int_{\epsilon_{11}}^{\epsilon_{12}} f'_c \left[\frac{2\epsilon_c \epsilon_o}{\epsilon_c^2} - \frac{\epsilon_c^2}{\epsilon_o^2} \right] d\epsilon_c$$

$$= \frac{f'_c}{\epsilon_o^2} \left[\epsilon_c^2 \epsilon_o - \tfrac{1}{3}\epsilon_c^3 \right]_{\epsilon_{11}}^{\epsilon_{12}}$$

Therefore the average stress, f_{a_1}, between ϵ_{11} and ϵ_{12} is:

$$f_a = \frac{A}{\epsilon_{12} - \epsilon_{11}} = \frac{f'_c}{\epsilon_o^2(\epsilon_{12} - \epsilon_{11})} \left[\epsilon_c^2 \epsilon_o - \tfrac{1}{3}\epsilon_c^3 \right]_{\epsilon_{11}}^{\epsilon_{12}}$$

....(4.1)

The strain, $\bar{\epsilon}_1$, corresponding to the centroid of area of this stress is then:

$$\bar{\epsilon}_1 = \frac{\int \epsilon_c f_c \, d\epsilon_c}{\int f_c \, d\epsilon_c}$$

$$= \frac{\int (2\epsilon_c^2 \epsilon_o - \epsilon_c^3) d\epsilon_c}{\int (2\epsilon_c \epsilon_o - \epsilon_c^2) d\epsilon_c}$$

$$= \frac{\left[8\epsilon_c^3 \epsilon_o - 3\epsilon_c^4 \right]_{\epsilon_{11}}^{\epsilon_{12}}}{\left[12\epsilon_c^2 \epsilon_o - 4\epsilon_c^3 \right]_{\epsilon_{11}}^{\epsilon_{12}}}$$

....(4.2)

The distance, q, from the neutral axis to the centroid of this compression area is given by:

$$q = kd \frac{\bar{\epsilon}}{\epsilon_{cm}} \qquad \ldots\ldots(4.3)$$

and the concrete force, C_1, is:

$$C_1 = f_{a_1} bkd \frac{\epsilon_{12} - \epsilon_{11}}{\epsilon_{cm}} \qquad \ldots\ldots(4.4)$$

where ϵ_{cm} = concrete strain in the extreme compressed fibre.

4.2.2 Region 2: $\epsilon_o < \epsilon_c \leq \epsilon_{20}$

The falling branch stress is given by:

$$f_{c_2} = f'_c(1 - Z(\epsilon_c - \epsilon_o)) \qquad \ldots\ldots(2.20)$$

Therefore, the average stress, f_{a_2}, between ϵ_{21} and ϵ_{22} is:

$$f_{a_2} = \tfrac{1}{2}\left[f'_c(1 - Z(\epsilon_{21} - \epsilon_o)) + f'_c(1 - Z(\epsilon_{22} - \epsilon_o))\right]$$

$$= f'_c(1 - \tfrac{1}{2}Z(\epsilon_{21} + \epsilon_{22} - 2\epsilon_o)) \qquad \ldots\ldots(4.5)$$

and the concrete force, C_2, is:

$$C_2 = f_{a_2} bkd \frac{\epsilon_{22} - \epsilon_{21}}{\epsilon_{cm}} \qquad \ldots\ldots(4.6)$$

The strain, $\bar{\epsilon}_2$, corresponding to the point of action of this force is then:

$$\bar{\epsilon}_2 = \epsilon_{21} + \frac{f_{c_{22}}(\epsilon_{22}-\epsilon_{21})\frac{1}{2}(\epsilon_{22}-\epsilon_{21})+\frac{1}{2}(f_{c_{21}}-f_{c_{22}})(\epsilon_{22}-\epsilon_{21})^2(\frac{1}{3})}{f_{c_{22}}(\epsilon_{22}-\epsilon_{21})+\frac{1}{2}(f_{c_{21}}-f_{c_{22}})(\epsilon_{22}-\epsilon_{21})}$$

$$= \epsilon_{21} + (\epsilon_{22}-\epsilon_{21}) \frac{\frac{1}{2}f_{c_{22}} + \frac{1}{6}(f_{c_{21}}-f_{c_{22}})}{\frac{1}{2}(f_{c_{21}}+f_{c_{22}})}$$

$$= \epsilon_{21} + (\epsilon_{22}-\epsilon_{21}) \frac{3(1+Z\epsilon_o)-Z\epsilon_{21}-2Z\epsilon_{22}}{6(1+Z\epsilon_o)-3Z(\epsilon_{21}+\epsilon_{22})} \quad ....(4.7)$$

Equation (4.3) may be used to obtain the distance of the point of action of the concrete force from the neutral axis.

4.2.3 Region 3: $\epsilon_c > \epsilon_{20}$

$$f_{a_3} = 0.2f'_c \quad ....(4.8)$$

$$\bar{\epsilon}_3 = \epsilon_{31} + \frac{1}{2}(\epsilon_{32}-\epsilon_{31}) = \frac{1}{2}(\epsilon_{31} + \epsilon_{32}) \quad ....(4.9)$$

$$C_3 = f_{a_3} bkd \frac{\epsilon_{32}-\epsilon_{31}}{\epsilon_{cm}} \quad ....(4.10)$$

4.3 STRESS BLOCK PARAMETERS FOR RECTANGULAR SECTIONS

When designing rectangular sections, it is convenient

to specify the concrete stress-block in terms of α and γ, where:-

α = ratio of average concrete stress in stress block to concrete cylinder strength.

γ = distance of resultant concrete force from top of stress block, as a fraction of the neutral axis depth, kd.

Using the equations developed in the preceding sections and the Z values in Table 2.3, it is a simple matter to calculate values for α and γ. Figure 4.2 shows the three general stress block shapes considered here.

4.3.1 Mode 1, $\epsilon_{cm} \leq \epsilon_o$ (Figure 4.2(i))

From Equation (4.1) for $\epsilon_{12} = \epsilon_{cm}$ and $\epsilon_{11} = o$

$$f_{a_1} = \frac{f'_c \epsilon_{cm}}{\epsilon_o^2} \left(\epsilon_o - \frac{\epsilon_{cm}}{3}\right)$$

$$\therefore \alpha_1 = \frac{f_{a_1}}{f'_c} = \frac{\epsilon_{cm}}{\epsilon_o^2} \left(\epsilon_o - \frac{\epsilon_{cm}}{3}\right) \qquad \ldots\ldots(4.11)$$

From Equation (4.2) and (4.3)

$$\bar{\epsilon}_1 = \frac{8\epsilon_{cm}\epsilon_o - 3\epsilon_{cm}^2}{12\epsilon_o - 4\epsilon_{cm}}$$

and $q = kd \frac{\bar{\epsilon}}{\epsilon_{cm}}$

Hence $\gamma_1 kd = kd - q$

$$\therefore \gamma_1 = 1 - \frac{\bar{\epsilon}}{\epsilon_{cm}} \qquad \ldots\ldots(4.12)$$

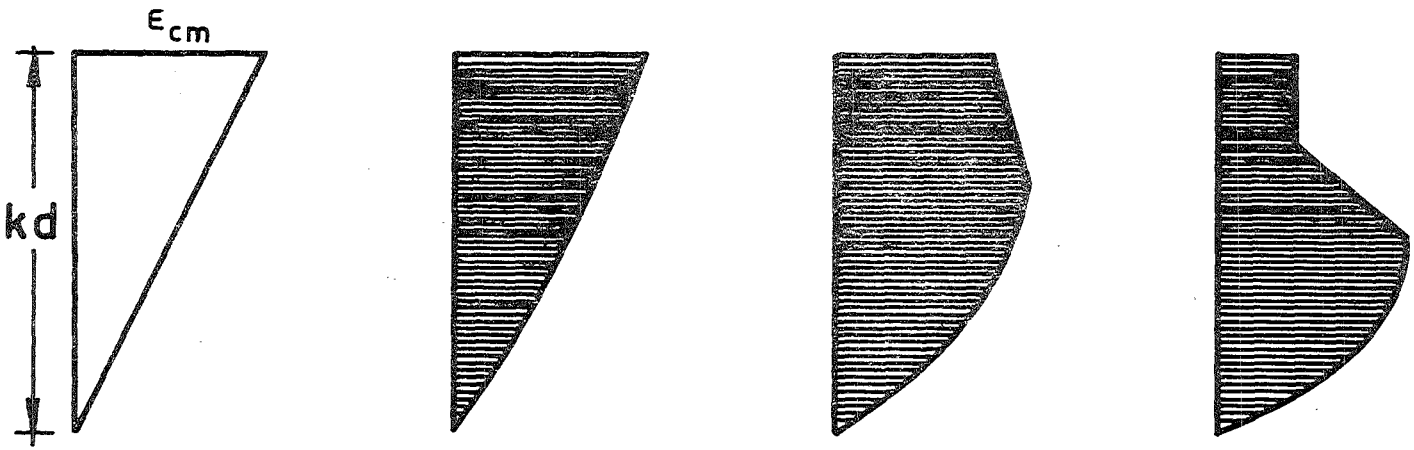

FIG. 4.2 TYPICAL CONCRETE STRESS BLOCKS

4.3.2 Mode 2, $\epsilon_o < \epsilon_{cm} \leq \epsilon_{20}$ (Figure 4.2(ii))

Region 1: $\epsilon_c \leq \epsilon_o$

$$f_{a_1} = \tfrac{2}{3} f'_c \quad , \quad C_1 = f_{a_1} bkd \frac{\epsilon_o}{\epsilon_{cm}}$$

$$\bar{\epsilon}_1 = \tfrac{5}{8}\epsilon_o \quad , \quad q_1 = kd \frac{\bar{\epsilon}_1}{\epsilon_{cm}}$$

Region 2: $\epsilon_o < \epsilon_c \leq \epsilon_{cm}$

From Equation (4.5) for $\epsilon_{21} = \epsilon_o$ and $\epsilon_{22} = \epsilon_{cm}$:

$$f_{a_2} = f'_c(1 - \tfrac{1}{2}Z(\epsilon_{cm} - \epsilon_o))$$

$$C_2 = f_{a_2} bkd \frac{\epsilon_{cm} - \epsilon_o}{\epsilon_{cm}}$$

From Equations (4.7) and (4.3):

$$\bar{\epsilon}_2 = \epsilon_o + (\epsilon_{cm} - \epsilon_o) \frac{3 - 2Z(\epsilon_{cm} - \epsilon_o)}{6 - 3Z(\epsilon_{cm} - \epsilon_o)}$$

$$q_2 = kd \frac{\bar{\epsilon}_2}{\epsilon_{cm}}$$

Parameters α and γ

$\therefore C = C_1 + C_2$

$$\alpha_2 = \frac{C}{bkdf'_c} = \frac{2}{3}\frac{\epsilon_o}{\epsilon_{cm}} + (1 - \tfrac{1}{2}Z(\epsilon_{cm} - \epsilon_o))\frac{\epsilon_{cm} - \epsilon_o}{\epsilon_{cm}} \quad \ldots\ldots(4.13)$$

$$q = \frac{C_1 q_1 + C_2 q_2}{C_1 + C_2}$$

$$\gamma_2 = 1 - \frac{q}{kd} \quad \ldots\ldots(4.14)$$

4.3.3 Mode 3, $\epsilon_{20} < \epsilon_{cm}$ (Figure 4.2(iii))

Region 1: $\epsilon_c \leq \epsilon_o$

As for Mode 2

Region 2: $\epsilon_o \leq \epsilon_c \leq \epsilon_{20}$

From Equations (4.5) and (4.6) for $\epsilon_{21} = \epsilon_o$ and $\epsilon_{22} = \epsilon_{20}$:

$$f_{a_2} = f'_c(1 - \tfrac{1}{2}Z(\epsilon_{20} - \epsilon_o))$$

$$C_2 = f_{a_2} bkd \frac{\epsilon_{20} - \epsilon_o}{\epsilon_{cm}}$$

From Equations (4.7) and (4.3):

$$\bar{\epsilon}_2 = \epsilon_o + (\epsilon_{20} - \epsilon_o)\frac{3 - 2Z(\epsilon_{20} - \epsilon_o)}{6 - 3Z(\epsilon_{20} - \epsilon_o)}$$

$$q_2 = kd\frac{\bar{\epsilon}_2}{\epsilon_{cm}}$$

Region 3: $\epsilon_{20} \leq \epsilon_c \leq \epsilon_{cm}$

From Equations (4.8) and (4.10) for $\epsilon_{31} = \epsilon_{20}$ and $\epsilon_{32} = \epsilon_{cm}$:

$$f_{a_3} = 0.2f'_c \text{ and } C_3 = f_{a_3} bkd \frac{\epsilon_{cm} - \epsilon_{20}}{\epsilon_{cm}}$$

From Equations (4.9) and (4.3):

$$\bar{\epsilon}_3 = \tfrac{1}{2}(\epsilon_{20} + \epsilon_{cm}) \ , \ q_3 = kd \frac{\bar{\epsilon}_3}{\epsilon_{cm}}$$

Parameters α and γ

$$\alpha_3 = \frac{C_1 + C_2 + C_3}{bkdf'_c} \qquad \ldots\ldots(4.15)$$

$$q = \frac{C_1q_1 + C_2q_2 + C_3q_3}{C_1 + C_2 + C_3}$$

$$\gamma_3 = 1 - \frac{q}{kd} \qquad \ldots\ldots(4.16)$$

4.3.4 Tables of α and γ Values

Tables 4.1 and 4.2 show values of α and γ respectively, computed for Modes 2 and 3 (i.e. $\epsilon_{cm} \geqslant \epsilon_o$, where ϵ_o = 0.002). Note that if a value of ϵ_{cm} greater than the spalling strain, ϵ_{cr}, where ϵ_{cr} = 0.004, is chosen, then the stress-block should refer only to the bound concrete section.

For Mode 1, i.e. $\epsilon_{cm} < \epsilon_o$, α and γ can be found simply from Equations (4.11) and (4.12).

TABLE 4.1 - TABLE OF ALPHA VALUES

	Z VALUES																		
EC	10	20	30	40	50	60	70	80	100	120	140	160	180	200	250	300	350	400
.0020	0.667	0.667	0.667	0.667	0.667	0.667	0.667	0.667	0.667	0.667	0.667	0.667	0.667	0.667	0.667	0.667	0.667	0.667
.0022	0.697	0.697	0.697	0.697	0.697	0.696	0.696	0.696	0.696	0.696	0.696	0.696	0.695	0.695	0.695	0.694	0.694	0.693
.0024	0.722	0.722	0.721	0.721	0.721	0.720	0.720	0.720	0.719	0.718	0.718	0.717	0.716	0.716	0.714	0.712	0.711	0.709
.0026	0.743	0.742	0.742	0.741	0.740	0.739	0.739	0.738	0.737	0.735	0.734	0.733	0.731	0.730	0.726	0.723	0.719	0.716
.0028	0.761	0.760	0.758	0.757	0.756	0.755	0.754	0.753	0.750	0.748	0.746	0.744	0.741	0.739	0.733	0.728	0.722	0.716
.0030	0.776	0.774	0.773	0.771	0.769	0.768	0.766	0.764	0.761	0.758	0.754	0.751	0.748	0.744	0.736	0.728	0.719	0.711
.0032	0.789	0.787	0.785	0.783	0.780	0.778	0.776	0.774	0.769	0.765	0.760	0.756	0.751	0.747	0.735	0.724	0.713	0.702
.0034	0.801	0.798	0.795	0.792	0.790	0.787	0.784	0.781	0.775	0.769	0.764	0.758	0.752	0.746	0.732	0.717	0.703	0.689
.0036	0.811	0.808	0.804	0.801	0.797	0.793	0.790	0.786	0.779	0.772	0.765	0.758	0.751	0.744	0.726	0.708	0.690	0.673
.0038	0.820	0.816	0.812	0.808	0.803	0.799	0.795	0.790	0.782	0.773	0.765	0.756	0.748	0.739	0.718	0.697	0.675	0.654
.0040	0.828	0.823	0.818	0.813	0.808	0.803	0.798	0.793	0.783	0.773	0.763	0.753	0.743	0.733	0.708	0.683	0.658	0.633
.0042	0.836	0.830	0.824	0.818	0.812	0.807	0.801	0.795	0.784	0.772	0.761	0.749	0.738	0.726	0.697	0.668	0.640	0.613
.0044	0.842	0.835	0.829	0.822	0.816	0.809	0.803	0.796	0.783	0.770	0.757	0.744	0.731	0.718	0.685	0.652	0.620	0.594
.0046	0.848	0.840	0.833	0.826	0.818	0.811	0.804	0.796	0.782	0.767	0.752	0.738	0.723	0.708	0.671	0.635	0.602	0.577
.0048	0.853	0.845	0.837	0.828	0.820	0.812	0.804	0.796	0.779	0.763	0.747	0.730	0.714	0.698	0.657	0.617	0.585	0.561
.0050	0.858	0.849	0.840	0.831	0.822	0.813	0.804	0.795	0.777	0.759	0.741	0.723	0.705	0.687	0.642	0.600	0.570	0.547
.0052	0.862	0.852	0.842	0.832	0.823	0.813	0.803	0.793	0.773	0.754	0.734	0.714	0.695	0.675	0.626	0.585	0.555	0.533
.0054	0.866	0.855	0.844	0.834	0.823	0.812	0.802	0.791	0.770	0.748	0.727	0.705	0.684	0.662	0.610	0.570	0.542	0.521
.0056	0.869	0.858	0.846	0.835	0.823	0.812	0.800	0.788	0.765	0.742	0.719	0.696	0.673	0.650	0.595	0.557	0.530	0.510
.0058	0.873	0.860	0.848	0.835	0.823	0.810	0.798	0.785	0.761	0.736	0.711	0.686	0.661	0.636	0.582	0.545	0.519	0.499
.0060	0.876	0.862	0.849	0.836	0.822	0.809	0.796	0.782	0.756	0.729	0.702	0.676	0.649	0.622	0.569	0.533	0.508	0.489
.0062	0.878	0.864	0.850	0.836	0.821	0.807	0.793	0.779	0.750	0.722	0.693	0.665	0.636	0.609	0.557	0.523	0.498	0.480
.0064	0.881	0.866	0.850	0.835	0.820	0.805	0.790	0.775	0.745	0.714	0.684	0.654	0.624	0.596	0.546	0.513	0.489	0.471
.0066	0.883	0.867	0.851	0.835	0.819	0.803	0.787	0.771	0.739	0.707	0.675	0.643	0.611	0.584	0.535	0.503	0.480	0.463
.0068	0.885	0.868	0.851	0.834	0.817	0.800	0.783	0.766	0.733	0.699	0.665	0.631	0.599	0.573	0.525	0.494	0.472	0.455
.0070	0.887	0.869	0.851	0.833	0.815	0.798	0.780	0.762	0.726	0.690	0.655	0.619	0.587	0.562	0.516	0.486	0.464	0.448
.0072	0.889	0.870	0.851	0.832	0.814	0.795	0.776	0.757	0.720	0.682	0.645	0.607	0.577	0.552	0.507	0.478	0.457	0.441
.0074	0.890	0.871	0.851	0.831	0.811	0.792	0.772	0.752	0.713	0.673	0.634	0.596	0.566	0.542	0.499	0.470	0.450	0.434
.0076	0.892	0.871	0.850	0.830	0.809	0.788	0.768	0.747	0.706	0.665	0.623	0.586	0.557	0.533	0.491	0.463	0.443	0.428
.0078	0.893	0.871	0.850	0.828	0.807	0.785	0.764	0.742	0.699	0.656	0.613	0.576	0.548	0.525	0.484	0.456	0.437	0.422
.0080	0.894	0.872	0.849	0.827	0.804	0.782	0.759	0.737	0.692	0.647	0.602	0.567	0.539	0.517	0.477	0.450	0.431	0.417
.0082	0.895	0.872	0.848	0.825	0.802	0.778	0.755	0.731	0.684	0.637	0.593	0.558	0.531	0.509	0.470	0.444	0.425	0.411
.0084	0.896	0.872	0.847	0.823	0.799	0.774	0.750	0.726	0.677	0.628	0.583	0.549	0.523	0.502	0.463	0.438	0.420	0.406
.0086	0.897	0.872	0.847	0.821	0.796	0.771	0.745	0.720	0.669	0.619	0.574	0.541	0.515	0.495	0.457	0.433	0.415	0.402
.0088	0.898	0.872	0.845	0.819	0.793	0.767	0.740	0.714	0.662	0.609	0.566	0.533	0.508	0.488	0.452	0.427	0.410	0.397
.0090	0.899	0.871	0.844	0.817	0.790	0.763	0.735	0.708	0.654	0.600	0.558	0.526	0.501	0.481	0.446	0.422	0.405	0.393
.0092	0.899	0.871	0.843	0.815	0.787	0.758	0.730	0.702	0.646	0.591	0.550	0.519	0.495	0.475	0.441	0.417	0.401	0.388
.0094	0.900	0.871	0.842	0.813	0.783	0.754	0.725	0.696	0.638	0.583	0.542	0.512	0.488	0.470	0.435	0.413	0.397	0.384
.0096	0.900	0.870	0.840	0.810	0.780	0.750	0.720	0.690	0.630	0.575	0.535	0.506	0.482	0.464	0.431	0.408	0.392	0.381
.0098	0.901	0.870	0.839	0.808	0.777	0.746	0.715	0.684	0.622	0.567	0.528	0.499	0.477	0.459	0.426	0.404	0.389	0.377
.0100	0.901	0.869	0.837	0.805	0.773	0.741	0.709	0.677	0.613	0.560	0.522	0.493	0.471	0.453	0.421	0.400	0.385	0.373
.0102	0.902	0.869	0.836	0.803	0.770	0.737	0.704	0.671	0.605	0.553	0.516	0.488	0.466	0.448	0.417	0.396	0.381	0.370
.0104	0.902	0.868	0.834	0.800	0.766	0.732	0.698	0.665	0.597	0.546	0.510	0.482	0.461	0.444	0.413	0.392	0.378	0.367
.0106	0.902	0.867	0.832	0.798	0.763	0.728	0.693	0.658	0.590	0.540	0.504	0.477	0.456	0.439	0.409	0.389	0.374	0.364
.0108	0.902	0.867	0.831	0.795	0.759	0.723	0.687	0.651	0.583	0.533	0.498	0.472	0.451	0.435	0.405	0.385	0.371	0.360
.0110	0.903	0.866	0.829	0.792	0.755	0.718	0.682	0.645	0.576	0.527	0.493	0.467	0.446	0.430	0.401	0.382	0.368	0.358
.0112	0.903	0.865	0.827	0.789	0.752	0.714	0.676	0.638	0.569	0.521	0.487	0.462	0.442	0.426	0.398	0.379	0.365	0.355
.0114	0.903	0.864	0.825	0.787	0.748	0.709	0.670	0.631	0.563	0.516	0.482	0.457	0.438	0.422	0.394	0.375	0.362	0.352
.0116	0.903	0.863	0.823	0.784	0.744	0.704	0.664	0.625	0.556	0.510	0.478	0.453	0.434	0.418	0.391	0.372	0.359	0.349
.0118	0.903	0.862	0.821	0.781	0.740	0.699	0.659	0.618	0.550	0.505	0.473	0.449	0.430	0.415	0.388	0.369	0.357	0.347
.0120	0.903	0.861	0.819	0.778	0.736	0.694	0.653	0.611	0.544	0.500	0.468	0.444	0.426	0.411	0.384	0.367	0.354	0.344
.0122	0.903	0.860	0.817	0.775	0.732	0.690	0.647	0.604	0.539	0.495	0.464	0.440	0.422	0.408	0.381	0.364	0.351	0.342
.0124	0.903	0.859	0.815	0.772	0.728	0.685	0.641	0.598	0.535	0.490	0.460	0.437	0.419	0.404	0.378	0.361	0.349	0.340
.0126	0.903	0.858	0.813	0.769	0.724	0.680	0.635	0.592	0.528	0.486	0.455	0.433	0.415	0.401	0.376	0.359	0.347	0.338
.0128	0.902	0.857	0.811	0.766	0.720	0.675	0.629	0.585	0.523	0.481	0.451	0.429	0.412	0.398	0.373	0.356	0.344	0.335
.0130	0.902	0.856	0.809	0.763	0.716	0.669	0.623	0.579	0.518	0.477	0.448	0.426	0.409	0.395	0.370	0.354	0.342	0.333
.0132	0.902	0.854	0.807	0.759	0.712	0.664	0.617	0.574	0.513	0.473	0.444	0.422	0.405	0.392	0.368	0.352	0.340	0.331
.0134	0.902	0.853	0.805	0.756	0.708	0.659	0.611	0.568	0.508	0.469	0.440	0.419	0.402	0.389	0.365	0.349	0.338	0.329
.0136	0.902	0.852	0.803	0.753	0.704	0.654	0.605	0.563	0.504	0.465	0.437	0.416	0.399	0.386	0.363	0.347	0.336	0.327
.0138	0.901	0.851	0.800	0.750	0.699	0.649	0.599	0.557	0.500	0.461	0.433	0.413	0.396	0.384	0.360	0.345	0.334	0.326
.0140	0.901	0.850	0.798	0.747	0.695	0.644	0.593	0.552	0.495	0.457	0.430	0.410	0.394	0.381	0.358	0.343	0.332	0.324
.0142	0.901	0.848	0.796	0.743	0.691	0.639	0.588	0.547	0.491	0.454	0.427	0.407	0.391	0.378	0.356	0.341	0.330	0.322
.0144	0.900	0.847	0.794	0.740	0.687	0.633	0.582	0.543	0.487	0.450	0.424	0.404	0.388	0.376	0.354	0.339	0.328	0.320
.0146	0.900	0.846	0.791	0.737	0.682	0.628	0.577	0.538	0.483	0.447	0.420	0.401	0.386	0.374	0.352	0.337	0.327	0.319
.0148	0.900	0.844	0.789	0.734	0.678	0.623	0.572	0.533	0.479	0.443	0.418	0.398	0.383	0.371	0.350	0.335	0.325	0.317
.0150	0.899	0.843	0.787	0.730	0.674	0.618	0.567	0.529	0.476	0.440	0.415	0.396	0.381	0.369	0.348	0.333	0.323	0.316

TABLE 4.2 - TABLE OF GAMMA VALUES

	Z VALUES																	
EC	10	20	30	40	50	60	70	80	100	120	140	160	180	200	250	300	350	400
.0020	0.375	0.375	0.375	0.375	0.375	0.375	0.375	0.375	0.375	0.375	0.375	0.375	0.375	0.375	0.375	0.375	0.375	0.375
.0022	0.381	0.382	0.382	0.382	0.382	0.382	0.382	0.382	0.382	0.382	0.382	0.382	0.382	0.382	0.383	0.383	0.383	0.383
.0024	0.388	0.388	0.388	0.388	0.389	0.389	0.389	0.389	0.389	0.390	0.390	0.390	0.391	0.391	0.392	0.392	0.393	0.394
.0026	0.394	0.394	0.395	0.395	0.395	0.396	0.396	0.396	0.397	0.397	0.398	0.399	0.399	0.400	0.401	0.403	0.405	0.406
.0028	0.400	0.400	0.401	0.401	0.402	0.402	0.403	0.403	0.404	0.405	0.406	0.407	0.408	0.409	0.411	0.414	0.416	0.419
.0030	0.405	0.406	0.407	0.407	0.408	0.409	0.409	0.410	0.411	0.413	0.414	0.415	0.417	0.418	0.421	0.425	0.429	0.432
.0032	0.410	0.411	0.412	0.413	0.414	0.414	0.415	0.416	0.418	0.420	0.421	0.423	0.425	0.427	0.431	0.436	0.441	0.446
.0034	0.415	0.416	0.417	0.418	0.419	0.420	0.421	0.422	0.424	0.426	0.429	0.431	0.433	0.435	0.441	0.447	0.454	0.460
.0036	0.419	0.420	0.422	0.423	0.424	0.425	0.426	0.428	0.430	0.433	0.435	0.438	0.441	0.444	0.451	0.459	0.467	0.475
.0038	0.423	0.424	0.426	0.427	0.429	0.430	0.432	0.433	0.436	0.439	0.442	0.445	0.449	0.452	0.461	0.470	0.480	0.490
.0040	0.427	0.428	0.430	0.431	0.433	0.435	0.436	0.438	0.441	0.445	0.449	0.452	0.456	0.460	0.471	0.482	0.494	0.507
.0042	0.430	0.432	0.433	0.435	0.437	0.439	0.441	0.443	0.447	0.451	0.455	0.459	0.464	0.468	0.480	0.494	0.508	0.522
.0044	0.433	0.435	0.437	0.439	0.441	0.443	0.445	0.447	0.452	0.456	0.461	0.466	0.471	0.476	0.491	0.506	0.523	0.536
.0046	0.436	0.438	0.440	0.442	0.445	0.447	0.449	0.452	0.457	0.462	0.467	0.473	0.479	0.485	0.501	0.519	0.536	0.548
.0048	0.438	0.441	0.443	0.446	0.448	0.451	0.453	0.456	0.461	0.467	0.473	0.479	0.486	0.493	0.511	0.532	0.548	0.559
.0050	0.441	0.444	0.446	0.449	0.452	0.454	0.457	0.460	0.466	0.472	0.479	0.486	0.493	0.501	0.522	0.543	0.558	0.568
.0052	0.443	0.446	0.449	0.452	0.455	0.458	0.461	0.464	0.471	0.478	0.485	0.493	0.501	0.509	0.533	0.554	0.567	0.577
.0054	0.445	0.448	0.451	0.455	0.458	0.461	0.464	0.468	0.475	0.483	0.491	0.499	0.508	0.518	0.544	0.563	0.576	0.584
.0056	0.448	0.451	0.454	0.457	0.461	0.464	0.468	0.472	0.479	0.488	0.496	0.506	0.516	0.527	0.554	0.572	0.583	0.591
.0058	0.450	0.453	0.456	0.460	0.463	0.467	0.471	0.475	0.484	0.493	0.502	0.512	0.524	0.535	0.563	0.579	0.590	0.597
.0060	0.451	0.455	0.459	0.462	0.466	0.470	0.474	0.479	0.488	0.497	0.508	0.519	0.531	0.545	0.571	0.586	0.596	0.602
.0062	0.453	0.457	0.461	0.465	0.469	0.473	0.478	0.482	0.492	0.502	0.514	0.526	0.539	0.554	0.578	0.592	0.601	0.607
.0064	0.455	0.459	0.463	0.467	0.471	0.476	0.481	0.486	0.496	0.507	0.520	0.533	0.548	0.562	0.585	0.598	0.606	0.611
.0066	0.456	0.460	0.465	0.469	0.474	0.479	0.484	0.489	0.500	0.512	0.526	0.540	0.556	0.569	0.591	0.603	0.610	0.615
.0068	0.458	0.462	0.467	0.471	0.476	0.481	0.487	0.492	0.504	0.517	0.532	0.547	0.564	0.576	0.596	0.607	0.614	0.619
.0070	0.459	0.464	0.469	0.473	0.479	0.484	0.490	0.496	0.508	0.522	0.538	0.555	0.571	0.582	0.601	0.611	0.618	0.622
.0072	0.461	0.465	0.470	0.475	0.481	0.487	0.493	0.499	0.512	0.527	0.544	0.562	0.577	0.588	0.606	0.615	0.621	0.624
.0074	0.462	0.467	0.472	0.477	0.483	0.489	0.495	0.502	0.516	0.532	0.550	0.569	0.583	0.593	0.610	0.619	0.624	0.627
.0076	0.463	0.468	0.474	0.479	0.485	0.492	0.498	0.505	0.520	0.537	0.557	0.575	0.589	0.598	0.613	0.622	0.626	0.629
.0078	0.464	0.470	0.475	0.481	0.488	0.494	0.501	0.508	0.524	0.543	0.563	0.581	0.594	0.603	0.617	0.624	0.628	0.631
.0080	0.466	0.471	0.477	0.483	0.490	0.497	0.504	0.512	0.529	0.548	0.570	0.586	0.598	0.607	0.620	0.627	0.630	0.633
.0082	0.467	0.472	0.478	0.485	0.492	0.499	0.507	0.515	0.533	0.553	0.575	0.591	0.603	0.611	0.623	0.629	0.632	0.634
.0084	0.468	0.474	0.480	0.487	0.494	0.501	0.509	0.518	0.537	0.559	0.581	0.596	0.607	0.614	0.625	0.631	0.634	0.635
.0086	0.469	0.475	0.481	0.488	0.496	0.504	0.512	0.521	0.541	0.565	0.586	0.600	0.610	0.617	0.628	0.633	0.635	0.636
.0088	0.470	0.476	0.483	0.490	0.498	0.506	0.515	0.524	0.546	0.570	0.591	0.604	0.614	0.620	0.630	0.635	0.637	0.637
.0090	0.471	0.477	0.484	0.492	0.500	0.508	0.518	0.528	0.550	0.576	0.595	0.608	0.617	0.623	0.632	0.636	0.638	0.638
.0092	0.472	0.478	0.486	0.493	0.502	0.511	0.520	0.531	0.554	0.581	0.599	0.611	0.620	0.626	0.634	0.637	0.639	0.639
.0094	0.472	0.480	0.487	0.495	0.504	0.513	0.523	0.534	0.559	0.585	0.603	0.615	0.622	0.628	0.635	0.639	0.640	0.640
.0096	0.473	0.481	0.488	0.497	0.506	0.515	0.526	0.537	0.563	0.590	0.607	0.618	0.625	0.630	0.637	0.640	0.640	0.640
.0098	0.474	0.482	0.490	0.498	0.508	0.518	0.529	0.541	0.568	0.594	0.610	0.620	0.627	0.632	0.638	0.640	0.641	0.641
.0100	0.475	0.483	0.491	0.500	0.509	0.520	0.531	0.544	0.573	0.598	0.613	0.623	0.629	0.634	0.639	0.641	0.642	0.641
.0102	0.476	0.484	0.492	0.501	0.511	0.522	0.534	0.547	0.577	0.601	0.616	0.625	0.631	0.635	0.641	0.642	0.642	0.641
.0104	0.477	0.485	0.493	0.503	0.513	0.525	0.537	0.551	0.582	0.605	0.619	0.628	0.633	0.637	0.641	0.643	0.642	0.642
.0106	0.477	0.486	0.495	0.504	0.515	0.527	0.540	0.554	0.586	0.608	0.621	0.630	0.635	0.638	0.642	0.643	0.643	0.642
.0108	0.478	0.487	0.496	0.506	0.517	0.529	0.543	0.558	0.590	0.611	0.624	0.632	0.637	0.640	0.643	0.644	0.643	0.642
.0110	0.479	0.488	0.497	0.507	0.519	0.532	0.546	0.561	0.594	0.614	0.626	0.633	0.638	0.641	0.644	0.644	0.643	0.642
.0112	0.479	0.488	0.498	0.509	0.521	0.534	0.548	0.565	0.597	0.617	0.628	0.635	0.639	0.642	0.644	0.644	0.643	0.642
.0114	0.480	0.489	0.499	0.510	0.523	0.536	0.551	0.568	0.601	0.619	0.630	0.637	0.641	0.643	0.645	0.645	0.643	0.642
.0116	0.481	0.490	0.501	0.512	0.525	0.539	0.554	0.572	0.604	0.622	0.632	0.638	0.642	0.644	0.645	0.645	0.643	0.642
.0118	0.481	0.491	0.502	0.513	0.526	0.541	0.557	0.576	0.607	0.624	0.634	0.639	0.643	0.645	0.646	0.645	0.643	0.641
.0120	0.482	0.492	0.503	0.515	0.528	0.543	0.560	0.580	0.610	0.626	0.635	0.641	0.644	0.645	0.646	0.645	0.643	0.641
.0122	0.483	0.493	0.504	0.516	0.530	0.546	0.563	0.583	0.612	0.628	0.637	0.642	0.645	0.646	0.646	0.645	0.643	0.641
.0124	0.483	0.494	0.505	0.518	0.532	0.548	0.566	0.587	0.615	0.630	0.638	0.643	0.645	0.646	0.647	0.645	0.643	0.641
.0126	0.484	0.494	0.506	0.519	0.534	0.551	0.570	0.590	0.617	0.632	0.640	0.644	0.646	0.647	0.647	0.645	0.643	0.640
.0128	0.484	0.495	0.507	0.521	0.536	0.553	0.573	0.594	0.620	0.633	0.641	0.645	0.647	0.647	0.647	0.645	0.642	0.640
.0130	0.485	0.496	0.508	0.522	0.538	0.556	0.576	0.597	0.622	0.635	0.642	0.646	0.647	0.648	0.647	0.645	0.642	0.640
.0132	0.486	0.497	0.509	0.524	0.540	0.558	0.579	0.600	0.624	0.636	0.643	0.646	0.648	0.648	0.647	0.645	0.642	0.639
.0134	0.486	0.498	0.511	0.525	0.542	0.561	0.583	0.602	0.626	0.638	0.644	0.647	0.648	0.648	0.647	0.644	0.642	0.639
.0136	0.487	0.498	0.512	0.527	0.544	0.563	0.586	0.605	0.628	0.639	0.645	0.648	0.649	0.649	0.647	0.644	0.641	0.638
.0138	0.487	0.499	0.513	0.528	0.545	0.566	0.589	0.608	0.630	0.640	0.646	0.648	0.649	0.649	0.647	0.644	0.641	0.638
.0140	0.488	0.500	0.514	0.529	0.547	0.568	0.592	0.610	0.631	0.641	0.646	0.649	0.649	0.649	0.647	0.644	0.640	0.638
.0142	0.488	0.501	0.515	0.531	0.549	0.571	0.595	0.613	0.633	0.643	0.647	0.649	0.650	0.649	0.647	0.643	0.640	0.637
.0144	0.489	0.501	0.516	0.532	0.551	0.574	0.598	0.615	0.634	0.644	0.648	0.650	0.650	0.649	0.646	0.643	0.640	0.637
.0146	0.489	0.502	0.517	0.534	0.553	0.576	0.600	0.617	0.636	0.644	0.648	0.650	0.650	0.649	0.646	0.643	0.639	0.636
.0148	0.490	0.503	0.518	0.535	0.555	0.579	0.603	0.619	0.637	0.645	0.649	0.650	0.650	0.649	0.646	0.642	0.639	0.636
.0150	0.490	0.504	0.519	0.537	0.557	0.582	0.606	0.621	0.638	0.646	0.650	0.651	0.650	0.649	0.646	0.642	0.638	0.635

4.4 MOMENT-CURVATURE ANALYSIS FOR T SHAPES

The nomenclature used for T shapes is illustrated in Figure 4.3. A bilinear-parabolic expression for concrete stress-strain acting upon a generalised T-section with compression reinforcement, has twelve separate modes for concrete compression force. These twelve cases are shown in Figure 4.4 and the differences itemised in Table 4.3.

TABLE 4.3

DIFFERENCES BETWEEN THE TWELVE MODES OF FIGURE 4.4

Mode	Concrete Strain	Neutral Axis	Top Steel
1	$\epsilon_{cm} \leq \epsilon_o$	$d_F=0$ or $k \leq d_F$	
2	$\epsilon_{cm} \leq \epsilon_o$	$k > d_F$	
3	$\epsilon_o < \epsilon_{cm} \leq \epsilon_{cr}$	$d_F=0$ or $k \leq d_F$	
4	$\epsilon_o < \epsilon_{cm} \leq \epsilon_{cr}$	$k > d_F$	
5	$\epsilon_o < \epsilon_{cm} \leq \epsilon_{cr}$	$d_F=0$ or $k \leq d_F$	$\epsilon'_s \leq \epsilon_{cr}$
6	$\epsilon_{cr} < \epsilon_{cm} \leq \epsilon_{20}$	$d_F=0$ or $k \leq d_F$	$\epsilon_{cr} < \epsilon'_s \leq \epsilon_{20}$
7	$\epsilon_{cm} > \epsilon_{20}$	$d_F=0$ or $k \leq d_F$	$\epsilon'_s > \epsilon_{20}$
8	$\epsilon_{cm} > \epsilon_{20}$	$k > d_F$	$\epsilon'_s > \epsilon_{20}$
9*	$\epsilon_o \leq \epsilon_b$	$k > d_F$	$\epsilon_{cr} \leq \epsilon'_s$
10*	$\epsilon_o > \epsilon_b$	$k > d_F$	$\epsilon_{cr} \leq \epsilon'_s$
11	$\epsilon_o \leq \epsilon_b$	$k > d_F$	$\epsilon_{cr} > \epsilon'_s$
12	$\epsilon_o > \epsilon_b$	$k > d_F$	$\epsilon_{cr} > \epsilon'_s$

* (A) $\epsilon_{20} > \epsilon'_s$

(B) $\epsilon_{20} \leq \epsilon'_s$

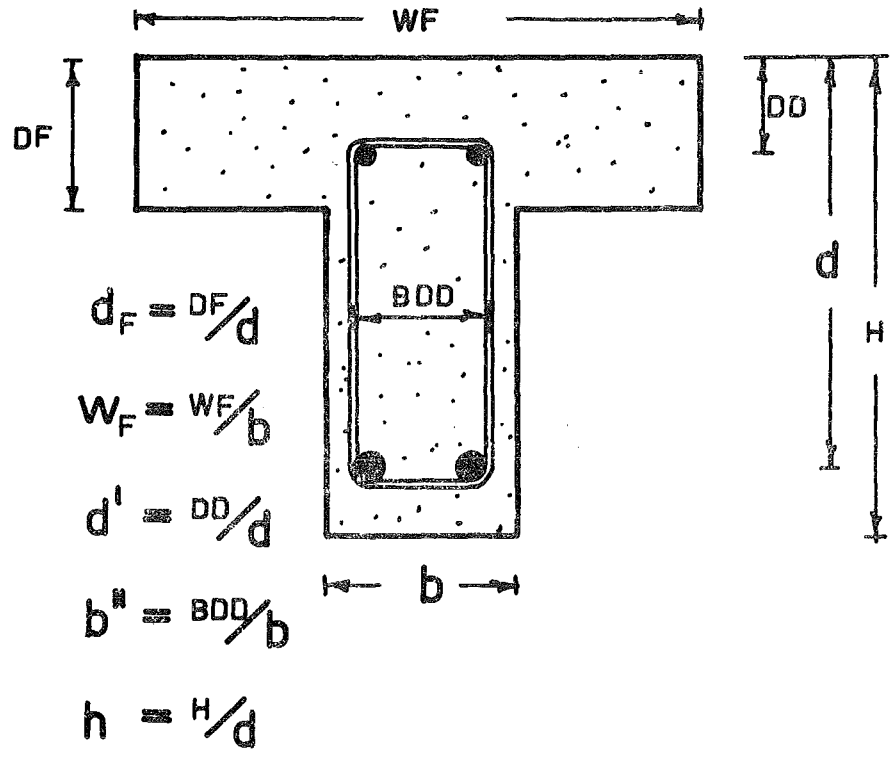

FIG. 4.3 T-BEAM NOMENCLATURE

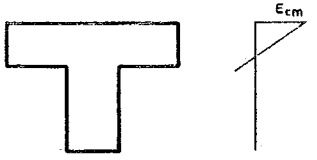

CASE 1

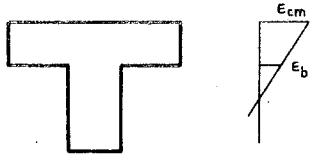

CASE 2

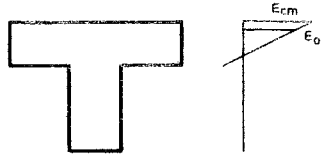

CASE 3

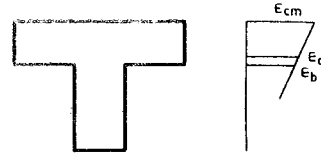

CASE 4

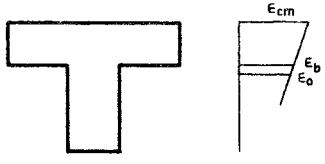

CASE 5

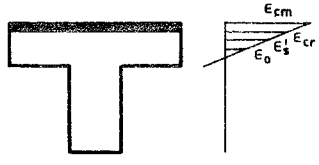

CASE 6

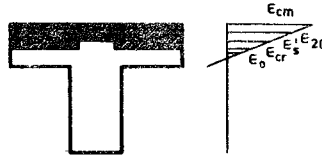

CASE 7

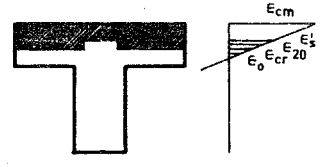

CASE 8

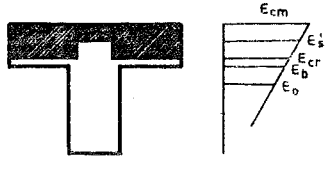

CASE 9

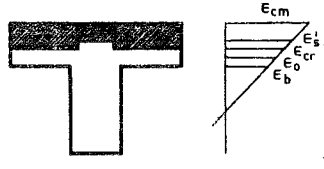

CASE 10

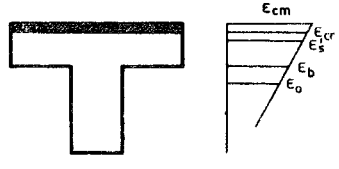

CASE 11

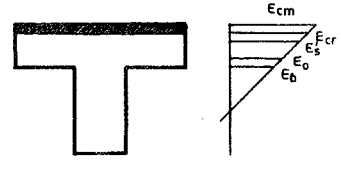

CASE 12

FIG.4.4 - GENERAL TYPES FOR T-SECTIONS

Factors common to all modes are:-

1. Reduction of concrete force for top steel area if $k > d'$;
2. Reduction of concrete force for bottom steel area if $k > 1$;
3. Reduction of concrete force if the neutral axis is outside the section ($k > h$) ;
4. Computation of top and bottom steel forces.

This analysis is subject to two limiations:-

1. Crushing may not extend into the web;
2. Spalling strain, ϵ_{cr}, must not exceed ϵ_{20} (i.e. $Z \leqslant 400$).

Allowance for either of these factors is considered unwarranted in view of the likelihood of occurrence and the more general analysis presented in Chapter 5.

4.4.1 Reduction of Concrete Force for Top Steel Area, C_{SR}

The top steel strain is given by

$$\epsilon'_s = \epsilon_{cm}\left(1 - \frac{d'}{k}\right) \qquad \ldots\ldots(4.17)$$

$$\underline{\text{If } \epsilon'_s \leqslant \epsilon_o}: \quad C_{SR} = p'bdf'_c \left[\frac{2\epsilon'_s}{\epsilon_o} - \left(\frac{\epsilon'_s}{\epsilon_o}\right)^2\right]$$

or in "dimensionless" form:

$$CSR = \frac{C_{SR}}{bd} = p'f'_c \left[\frac{2\epsilon'_s}{\epsilon_o} - \left(\frac{\epsilon'_s}{\epsilon_o}\right)^2\right] \qquad \ldots\ldots(4.18)$$

If $\epsilon_o < \epsilon'_s \leq \epsilon_{cr}$

$$CSR = p' f'_c (1 - Z(\epsilon'_s - \epsilon_{20})) \quad \ldots\ldots(4.19)$$

If $\epsilon'_s > \epsilon_{cr}$

No reduction since unbound concrete stress = 0

4.4.2 Reduction of Concrete Force for Bottom Steel Area, T_{SR}

The bottom steel strain is given by:

$$\epsilon_s = \epsilon_{cm}(1 - \frac{1}{k}) \quad \ldots\ldots(4.20)$$

If $\epsilon_s \leq \epsilon_o$ $\quad TSR = pf'_c \left[\frac{2\epsilon_s}{\epsilon_o} - \left(\frac{\epsilon_s}{\epsilon_o}\right)^2\right]$ $\quad \ldots\ldots(4.21)$

If $\epsilon_o < \epsilon_s \leq \epsilon_{cr}$ $\quad TSR = pf'_c(1 - Z(\epsilon_s - \epsilon_o))$ $\quad \ldots\ldots(4.22)$

If $\epsilon_s > \epsilon_{cr}$ $\quad$ No reduction

4.4.3 Reduction of Concrete Force for Neutral Axis Outside the Section

The strain at the bottom of the section is given by

$$\epsilon_{bot} = \epsilon_{cm}(1 - \frac{h}{k}) \quad \ldots\ldots(4.23)$$

The concrete force acting on this non-existent area must be subtracted from the total concrete force because, in each of the twelve modes, it is simpler for analysis to consider the web depth as being infinite.

If $\epsilon_{bot} \leq \epsilon_o$

$$f_{a_n} = \frac{f'_c \epsilon_{bot}}{\epsilon_o^2} \left(\epsilon_o - \frac{\epsilon_{bot}}{3}\right)$$

$$\therefore CCN = \frac{CC_N}{bd} = f_{a_n} k \frac{\epsilon_{bot}}{\epsilon_{cm}} \qquad \ldots\ldots(4.24)$$

$$\bar{\epsilon} = \frac{8\epsilon_{bot}\epsilon_o - 3\epsilon_{bot}^2}{12\epsilon_o - 4\epsilon_{bot}}$$

If $\epsilon_o < \epsilon_{bot} \leq \epsilon_{cr}$

At top: $\epsilon_o < \epsilon_c \leq \epsilon_{bot}$

$$f_{a_t} = f'_c(1 - \tfrac{1}{2}Z(\epsilon_{bot} - \epsilon_o))$$

$$CCT = f_{a_t} k \frac{\epsilon_{bot} - \epsilon_o}{\epsilon_{cm}} \qquad \ldots\ldots(4.25)$$

$$\bar{\epsilon} = \epsilon_o + (\epsilon_{bot} - \epsilon_o) \frac{3 - 2Z(\epsilon_{bot} - \epsilon_o)}{6 - 3Z(\epsilon_{bot} - \epsilon_o)}$$

At bottom: $\epsilon_c \leq \epsilon_o$

$$f_{a_b} = \tfrac{2}{3}f'_c \quad , \quad \bar{\epsilon} = \tfrac{5}{8}\epsilon_o$$

$$CCB = f_{a_b} k \frac{\epsilon_o}{\epsilon_{cm}} \qquad \ldots\ldots(4.26)$$

4.5 CONCRETE COMPRESSION FORCES FOR GENERAL T SECTIONS

In this section, the equations for concrete compression forces in each of the twelve modes illustrated in Figure 4.4 are developed. In each case, Equation (4.3) is valid for obtaining moments of these forces about the neutral axis. The analysis below has been programmed for computer and appears as Program 4.2 in Appendix B.

4.5.1 CASE 1:

$$f_{a_F} = \frac{f'_c \epsilon_{cm}}{\epsilon_o^2} \left(\epsilon_o - \frac{\epsilon_{cm}}{3}\right)$$

$$CCF_1 = f_{a_F} k W_F \qquad \ldots\ldots(4.27)$$

$$\bar{\epsilon} = \frac{8\epsilon_{cm}\epsilon_o - 3\epsilon_{cm}^2}{12\epsilon_o - 4\epsilon_{cm}}$$

4.5.2 CASE 2:

At the bottom face of the flange:

$$\epsilon_b = \epsilon_{cm}\left(1 - \frac{d_F}{k}\right)$$

(a) In the flange:

$$f_{a_F} = \frac{f'_c}{\epsilon_o^2(\epsilon_{cm} - \epsilon_b)} \left[\epsilon_o(\epsilon_{cm}^2 - \epsilon_b^2) - \tfrac{1}{3}(\epsilon_{cm}^3 - \epsilon_b^3)\right]$$

$$CCF_2 = f_{a_F} W_F k \frac{\epsilon_{cm} - \epsilon_b}{\epsilon_{cm}} \quad \ldots\ldots(4.28)$$

$$\bar{\epsilon} = \frac{8\epsilon_o(\epsilon_{cm}^3 - \epsilon_b^3) - 3(\epsilon_{cm}^4 - \epsilon_b^4)}{12\epsilon_o(\epsilon_{cm}^2 - \epsilon_b^2) - 4(\epsilon_{cm}^3 - \epsilon_b^3)}$$

(b) In the web:

$$f_{a_w} = \frac{f'_c \epsilon_b}{\epsilon_o^2}\left(\epsilon_o - \frac{\epsilon_b}{3}\right)$$

$$CCW_2 = f_{a_w} k \frac{\epsilon_b}{\epsilon_{cm}} \quad \ldots\ldots(4.29)$$

$$\bar{\epsilon} = \frac{8\epsilon_b\epsilon_o - 3\epsilon_b^2}{12\epsilon_o - 4\epsilon_b}$$

4.5.3 CASE 3:

(a) In top of flange:

$$f_{a_T} = f'_c(1 - \tfrac{1}{2}Z(\epsilon_{cm} - \epsilon_o))$$

$$CCT_3 = f_{a_T} W_F k \frac{\epsilon_{cm} - \epsilon_o}{\epsilon_{cm}} \quad \ldots\ldots(4.30)$$

$$\bar{\epsilon} = \epsilon_o + (\epsilon_{cm} - \epsilon_o)\frac{3 - 2Z(\epsilon_{cm} - \epsilon_o)}{6 - 3Z(\epsilon_{cm} - \epsilon_o)}$$

(b) In bottom of flange:

$$f_{a_B} = \tfrac{2}{3}f'_c \quad , \quad \bar{\epsilon} = \tfrac{5}{8}\epsilon_o$$

$$CCB_3 = f_{a_B} W_F k \frac{\epsilon_o}{\epsilon_{cm}} \qquad \ldots\ldots(4.31)$$

4.5.4 CASE 4:

(a) In top of flange:

As for Case 3

(b) In bottom of flange:

$$f_{a_{FB}} = \frac{f'_c}{\epsilon_o^2(\epsilon_o - \epsilon_b)} \left(\tfrac{2}{3}\epsilon_o^3 - \epsilon_b^2\epsilon_o + \tfrac{1}{3}\epsilon_b^3\right)$$

$$CCFB_4 = f_{a_{FB}} W_F k \frac{\epsilon_o - \epsilon_b}{\epsilon_{cm}} \qquad \ldots\ldots(4.32)$$

$$\bar{\epsilon} = \frac{5\epsilon_o^4 - \epsilon_b^3(8\epsilon_o - 3\epsilon_b)}{8\epsilon_o^3 - 4\epsilon_b^2(3\epsilon_o - \epsilon_b)}$$

(c) In web:

As for Case 2

4.5.5 CASE 5:

(a) In the flange:

$$f_{a_F} = f'_c(1 - \tfrac{1}{2}Z(\epsilon_{cm} + \epsilon_b - 2\epsilon_o))$$

$$CCF_5 = f_{a_F} W_F k \frac{\epsilon_{cm} - \epsilon_b}{\epsilon_{cm}} \qquad \ldots\ldots(4.33)$$

$$\bar{\epsilon} = \epsilon_b + (\epsilon_{cm} - \epsilon_b) \frac{3(1 + Z\epsilon_o) - Z\epsilon_b - 2Z\epsilon_{cm}}{6(1 + Z\epsilon_o) - 3Z(\epsilon_b + \epsilon_{cm})}$$

(b) <u>In top of web</u>:

$$f_{a_{WT}} = f'_c(1 - \tfrac{1}{2}Z(\epsilon_b - \epsilon_o))$$

$$CCWT_5 = f_{a_{WT}} k \frac{\epsilon_b - \epsilon_o}{\epsilon_{cm}} \qquad \ldots\ldots(4.34)$$

$$\bar{\epsilon} = \epsilon_o + (\epsilon_b - \epsilon_o) \frac{3 - 2Z(\epsilon_b - \epsilon_o)}{6 - 3Z(\epsilon_b - \epsilon_o)}$$

(c) <u>In bottom of web</u>:

$$f_{a_{WB}} = \tfrac{2}{3}f'_c \quad , \quad \bar{\epsilon} = \tfrac{5}{8}\epsilon_o$$

$$CCWB_5 = f_{a_{WB}} k \frac{\epsilon_o}{\epsilon_{cm}} \qquad \ldots\ldots(4.35)$$

4.5.6 CASE 6:

(a) In top of flange:

No concrete force - spalling has occurred.

(b) In middle of flange:

$$f_{a_{FM}} = f'_c(1 - \tfrac{1}{2}Z(\epsilon_{cr} - \epsilon_o))$$

$$CCFM_6 = f_{a_{FM}} W_F k \frac{\epsilon_{cr} - \epsilon_o}{\epsilon_{cm}} \qquad ....(4.36)$$

$$\overline{\epsilon} = \epsilon_o + (\epsilon_{cr} - \epsilon_o) \frac{3 - 2Z(\epsilon_{cr} - \epsilon_o)}{6 - 3Z(\epsilon_{cr} - \epsilon_o)}$$

(c) In bottom of flange:

As for Case 3.

4.5.7 CASE 7:

(a) Unbound concrete: $\epsilon_c > \epsilon_{cr}$

No concrete force - spalling has occurred.

(b) Bound concrete: $\epsilon_c > \epsilon_{cr}$

$$f_{a_B} = f'_c(1 - \tfrac{1}{2}Z(\epsilon'_s + \epsilon_{cr} - 2\epsilon_o))$$

$$CCB_7 = f_{a_B} b'' k \frac{\epsilon'_s - \epsilon_{cr}}{\epsilon_{cm}} \qquad ....(4.37)$$

$$\bar{\epsilon} = \epsilon_{cr} + (\epsilon'_s - \epsilon_{cr}) \frac{3(1 + Z\epsilon_o) - Z\epsilon_{cr} - 2Z\epsilon'_s}{6(1 + Z\epsilon_o) - 3Z(\epsilon_{cr} + \epsilon'_s)}$$

(c) Top of uncrushed flange:

$$f_{a_{FT}} = f'_c(1 - \tfrac{1}{2}Z(\epsilon_{cr} - \epsilon_o))$$

$$CCFT_7 = f_{a_{FT}} W_F k \frac{\epsilon_{cr} - \epsilon_o}{\epsilon_{cm}} \qquad ....(4.38)$$

$$\bar{\epsilon} = \epsilon_o + (\epsilon_{cr} - \epsilon_o) \frac{3 - 2Z(\epsilon_{cr} - \epsilon_o)}{6 - 3Z(\epsilon_{cr} - \epsilon_o)}$$

(d) Bottom of uncrushed flange:

As for Case 3.

4.5.8 CASE 8:

(a) Unbound concrete: $\epsilon_c > \epsilon_{cr}$

No concrete force - spalling has occurred.

(b) Top of bound concrete: $\epsilon'_s \geqslant \epsilon_c \geqslant \epsilon_{20}$

$$f_{a_{BT}} = \tfrac{1}{5} f'_c \quad , \quad \bar{\epsilon} = \tfrac{1}{2}(\epsilon'_s + \epsilon_{20})$$

$$CCBT_8 = f_{a_{BT}} b'' k \frac{\epsilon'_s - \epsilon_{20}}{\epsilon_{cm}} \qquad ....(4.39)$$

(c) Bottom of bound concrete: $\epsilon_{20} \geqslant \epsilon_c \geqslant \epsilon_{cr}$

$$f_{a_{BB}} = f'_c(1 - \tfrac{1}{2}Z(\epsilon_{20} + \epsilon_{cr} - 2\epsilon_o))$$

$$CCBB_8 = f_{a_{BB}} b''k \frac{\epsilon_{20} - \epsilon_{cr}}{\epsilon_{cm}} \qquad ....(4.40)$$

$$\bar{\epsilon} = \epsilon_{cr} + (\epsilon_{20} - \epsilon_{cr}) \frac{3(1 + Z\epsilon_o) - Z\epsilon_{cr} - 2Z\epsilon_{20}}{6(1 + Z\epsilon_o) - 3Z(\epsilon_{cr} + \epsilon_{20})}$$

(d) Top of uncrushed flange:

As for Case 7.

(e) Bottom of uncrushed flange:

As for Case 3.

4.5.9 CASE 9:

CASE 9A: $\epsilon_{20} > \epsilon'_s$

(a) Unbound concrete: $\epsilon_c > \epsilon_{cr}$

No concrete force - spalling has occurred.

(b) Bound concrete: $\epsilon_c > \epsilon_{cr}$

As for Case 7.

(c) Uncrushed flange concrete:

$$f_{a_F} = f'_c(1 - \tfrac{1}{2}Z(\epsilon_{cr} + \epsilon_b - 2\epsilon_o))$$

$$CCF_9 = f_{a_F} W_F k \frac{\epsilon_{cr} - \epsilon_b}{\epsilon_{cm}} \qquad ....(4.41)$$

$$\bar{\epsilon} = \epsilon_b + (\epsilon_{cr} - \epsilon_b) \frac{3(1 + Z\epsilon_o) - Z\epsilon_b - 2Z\epsilon_{cr}}{6(1 + Z\epsilon_o) - 3Z(\epsilon_b + \epsilon_{cr})}$$

(d) Top of web concrete:

As for Case 5.

(e) Bottom of web concrete:

As for Case 5.

CASE 9B: $\epsilon_{20} \leqslant \epsilon'_s$

This case differs from Case 9A only in that the bound concrete now spans two regions of the concrete compression strain curve. As such, the bound concrete compression forces are those for Case 8, i.e., Equations (4.39) and (4.40).

4.5.10 CASE 10:

CASE 10A: $\epsilon_{20} > \epsilon'_s$

(a) Unbound concrete: $\epsilon_c > \epsilon_{cr}$

No concrete force - spalling has occurred.

(b) Bound concrete:

As for Case 7.

(c) Top of uncrushed flange:

As for Case 7.

(d) Bottom of uncrushed flange:

As for Case 4.

(e) Web concrete:

As for Case 2.

CASE 10B: $\epsilon_{20} \leq \epsilon'_s$

As with Case 9, Case 10B differs from Case 10A only in that the bound concrete strain has exceeded ϵ_{20}. Equations (4.39) and (4.40) apply.

4.5.11 CASE 11:

(a) Unbound flange concrete: $\epsilon_c > \epsilon_{cr}$

No concrete force - spalling has occurred.

(b) Uncrushed flange concrete:

As for Case 9.

(c) Top of web:

As for Case 5.

(d) Bottom of web:

As for Case 5.

4.5.12 CASE 12:

(a) Top of flange: $\epsilon_c > \epsilon_{cr}$

No concrete force - spalling has occurred.

(b) Middle of flange:

As for Case 6.

(c) Bottom of flange:

As for Case 4.

(d) Web concrete:

As for Case 2.

4.6 DEFINITIONS - "ULTIMATE" AND "DUCTILITY"

Frequently the terms "maximum" and "ultimate" moments are used synonymously, and since there is, in many beams considerable capacity for energy absorption available beyond the maximum moment, a distinction must be made between these two terms. There are many opinions regarding a definition of "ultimate" behaviour but in this thesis the following meaning will be attached to this term: that "ultimate" moment corresponds to fracture of the tension steel, in which case maximum usually equals ultimate, or a 20 per cent reduction in moment from the maximum. Clearly, buckling of compression steel would in many cases constitute failure but, as has been mentioned in the previous chapter, no theoretical means of determining the onset of this type of failure exists at present, and so no account is taken of it in this theory.

Also there is some confusion concerning the term "ductility". In this thesis the term "deflection ductility" will refer to a specified ratio of member deflections, while "curvature ductility" will consider section curvature ratios. "Ductility" without a prefix will mean curvature ductility.

4.7 THEORY COMPARED WITH EXPERIMENTAL RESULTS

Very few writers have published complete moment-curvature responses from test beams and it is therefore difficult to subject this theory to a rigorous test. However, Mattock[42] reproduced eight experimental moment-curvature plots from his series and these are shown, compared with Mattock's theory and the theory developed in this chapter in Figure 4.5. It can be seen that the theory described in this chapter predicts low maximum moments for beams C1, C2, C3, C4, C5, and C6 and this may be due to the fact that these beams were tested with a central point load. The resulting confinement afforded to the compressed concrete delays spalling of the concrete and results in an increase in moment that such a beam can sustain at large strains. The theory compares very well with beams C2A and C5A and these were both subjected to two point loads giving a constant moment region with no additional concrete confinement.

Mattock's beam details and test results were particularly well-documented and it was therefore possible to compare the present theory with experiment for yield moments and some maximum moments. It was assumed that point loading had no effect on the yield moment since at this stage, the concrete in the extreme fibre had not reached maximum stress, hence Poisson's ratio is low, and so confinement effects are negligible (q.v. Chapter 2).

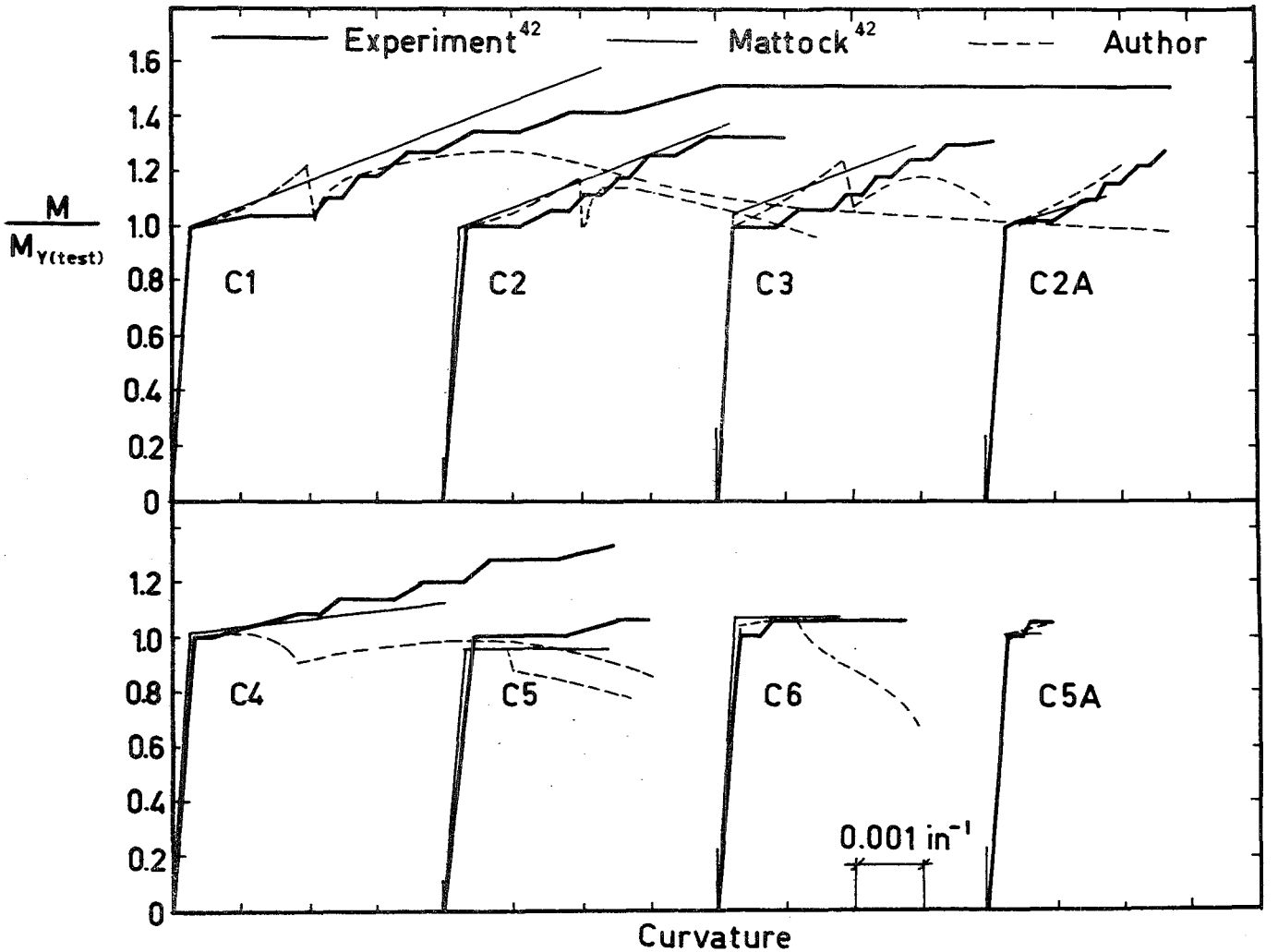

FIG.4.5 - MOMENT-CURVATURE COMPARISONS

For this reason, only those beams with two-point loading are compared at maximum moment.

A summary of these comparisons appears in Table 4.4 and shows the theory developed earlier in this chapter to agree very well with Mattock's experimental results. It is relevant to note that this theory is conservative in predicting maximum moments and corresponding curvatures for beams with point loads.

4.8 MOMENT-CURVATURE RESPONSES FOR REINFORCED AND PRESTRESSED CONCRETE SECTIONS

Figure 4.6 illustrates theoretical moment-curvature responses for typical reinforced concrete sections with varying amounts of longitudinal steel. The effects of concrete confinement are considered by means of two different values for Z. For comparison, prestressed concrete moment-curvature responses from an analytical study by Sherbourne and Parameswar[65] are also shown.

It can be seen in Figure 4.6 that for prestressed and reinforced concrete beams of similar size and effective depth, the reinforced concrete behaves in a more ductile manner. Clearly such comparisons are open to criticism, for the prestressed concrete sections have considerably lower steel percentages and the difference in concrete strengths greatly affects ($M/f'_c bd^2$), but for the same

TABLE 4.4

PROPERTIES OF MATTOCK'S BEAMS

Beam	$M_{y(expt)}$ (K.ft.)	$M_{y(calc)}/M_{y(expt)}$ Mattock	Author	$\phi_{y(expt)}$ $x10^{-5}$	$\phi_{y(calc)}/\phi_{y(expt)}$ Mattock	Author	$M_{m(expt)}$ (K.ft.)	$M_{m(calc)}/M_{m(expt)}$ Mattock	Author	$\phi_{m(expt)}$ $x10^{-5}$	$\phi_{m(calc)}/\phi_{m(expt)}$ Mattock	Author
A1	374	.96	.96	31	.78	.80						
2	392	.93	.93	28	.86	.97						
3	392	.98	.99	28	.93	1.10						
4	677	1.02	1.02	35	.80	.81						
5	676	1.02	1.01	32	.91	.95						
6	693	1.04	1.03	34	.89	.89						
B1	1574	.95	.96	15	.89	.85						
2	1508	.97	.98	14	.86	.91						
3	2647	1.06	1.11	19	.81	.82						
4	2628	1.08	1.12	16	.93	.97						
C1	370	1.00	1.00	28	.93	1.13						
2	373	.99	.99	34	.76	.88						
2A	368	1.00	.99	29	.89	.95	474	.85	.95	263	.62	.77
2B	380	.95	.94	29	.89	1.01	476	.78	.85	268	.48	.64
3	357	1.04	1.03	28	.93	1.05						
4	693	1.02	.99	36	.86	1.04						
5	713	1.00	.96	40	.80	.99						
5A	685	1.02	1.00	34	.91	1.03	720	.96	.98	105	.72	1.00
5B	677	1.02	.99	37	.84	.99	708	.93	.96	117	.55	.71
6	645	1.08	1.04	36	.86	.93						

TABLE 4.4 (Cont'd).

Beam	$M_{y(expt)}$ (K.ft.)	$M_{y(calc)}/M_{y(expt)}$ Mattock	Author	$\phi_{y(expt)}$ x10^{-5}	$\phi_{y(calc)}/\phi_{y(expt)}$ Mattock	Author	$M_{m(expt)}$ (K.ft.)	$M_{m(calc)}/M_{m(expt)}$ Mattock	Author	$\phi_{m(expt)}$ x10^{-5}	$\phi_{m(calc)}/\phi_{m(expt)}$ Mattock	Author
D1	1430	1.01	1.00	14	.93	1.07						
2	1449	.98	.98	15	.87	.97						
2A	1353	1.02	1.02	14	.96	1.06	1505	.98	1.06	87	.79	1.00
3	2677	1.03	1.00	19	.82	.95						
4	2701	1.03	1.00	20	.80	.93						
4A	2666	1.00	.97	19	.79	.89	2666	.98	1.00	40	.88	1.17
E1	451	1.01	1.00	42	.79	.83						
2	467	1.00	.99	38	.87	.91						
3	456	1.02	1.02	35	.94	1.04						
F1	472	.97	.98	42	.74	.75						
2	476	.99	1.00	32	1.00	1.14						
3	492	.95	.96	29	1.10	1.09						
G1	1469	.97	.96	18	.89	1.03						
2	1439	.98	.98	17	.94	.97						
3	1849	1.01	1.00	21	.75	.90						
4	1926	.97	.96	19	.89	.94						
5	1006	.95	.97	16	.94	1.03						
Mean		1.00	1.00		.87	.96		.91	.97		.67	.88
S.D'n.		.035	.012		.074	.092	.074	.074	.063		.138	.188

REINFORCED CONCRETE BEAMS								PRESTRESSED CONC. BEAMS		
Z = 10				Z = 100						
No.	$p'f_y/f'_c$	$p\,f_y/f'_c$	$M_M/f'_c bd^2$	No.	$p'f_y/f'_c$	$p\,f_y/f'_c$	$M_M/f'_c bd^2$	No.	$p f_{SE}/f'_c$	$M_M/f'_c bd^2$
R 1	.250	.375	.341	R 2	.250	.375	.341	P1	.24	.260
R 3	.125	.375	.328	R 4	.125	.375	.327	P2	.20	.236
R 5		.375	.302	R 6		.375	.299	P3	.16	.197
R 7	.125	.250	.229	R 8	.125	.250	.229	P4	.12	.152
R 9		.250	.218	R10		.250	.216	P5	.08	.108
R11	.125	.125	.133	R12	.125	.125	.133	P6	.04	.063
R13		.125	.117	R14		.125	.116			

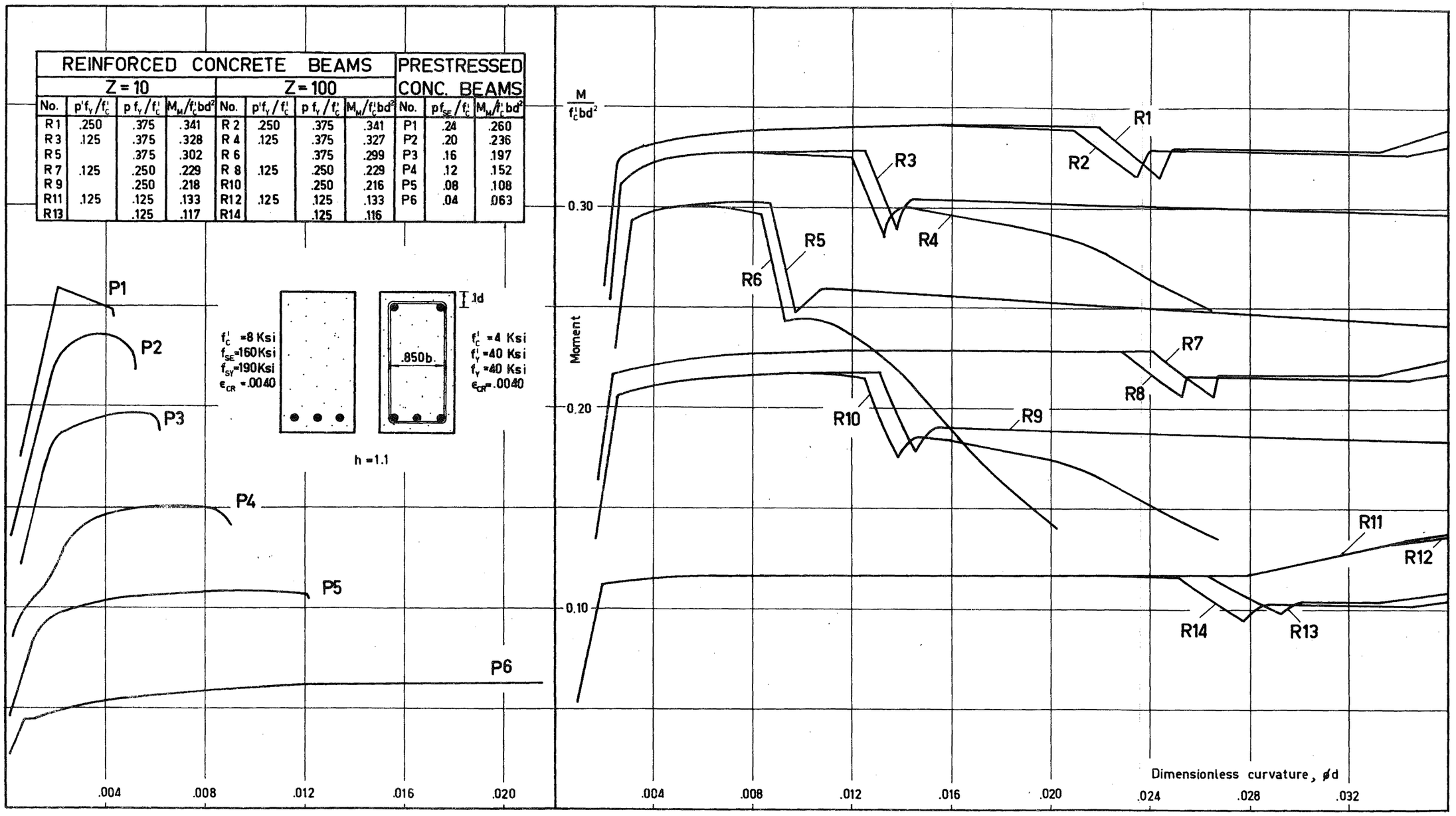

FIG. 4.6 THEORETICAL MOMENT CURVATURE PLOTS

value of maximum moment (and hence design moment), there is more energy-absorption available in the reinforced concrete section than in its prestressed concrete counterpart (c.f. P2 and R10 in Figure 4.6).

The SEAOC Code[31] specifies the following limitation on reinforcement ratio:

$$\frac{pf_y}{f'_c} \leqslant 0.46 \frac{p'}{p}$$

The commentary on the code states the requirement as being based on provision for ductility when higher yield strength steels are used in flexural members. Of the reinforced concrete sections in Figure 4.6, only two comply with this requirement (R11 and R12) and it is interesting to note that in these sections, the rapid loss of moment is not present, since strain hardening of the tension steel occurs before the commencement of crushing. Sections R7 and R8 come close to meeting this requirement and this is illustrated by a comparatively low moment loss at crushing.

A key to significant points on the Reinforced Concrete moment-curvature plot appears in Figure 4.7.

4.9 NOMOGRAMS FOR DUCTILITY AND ENERGY ABSORPTION AT CRUSHING

Using this theory, a nomogram giving the ratio of

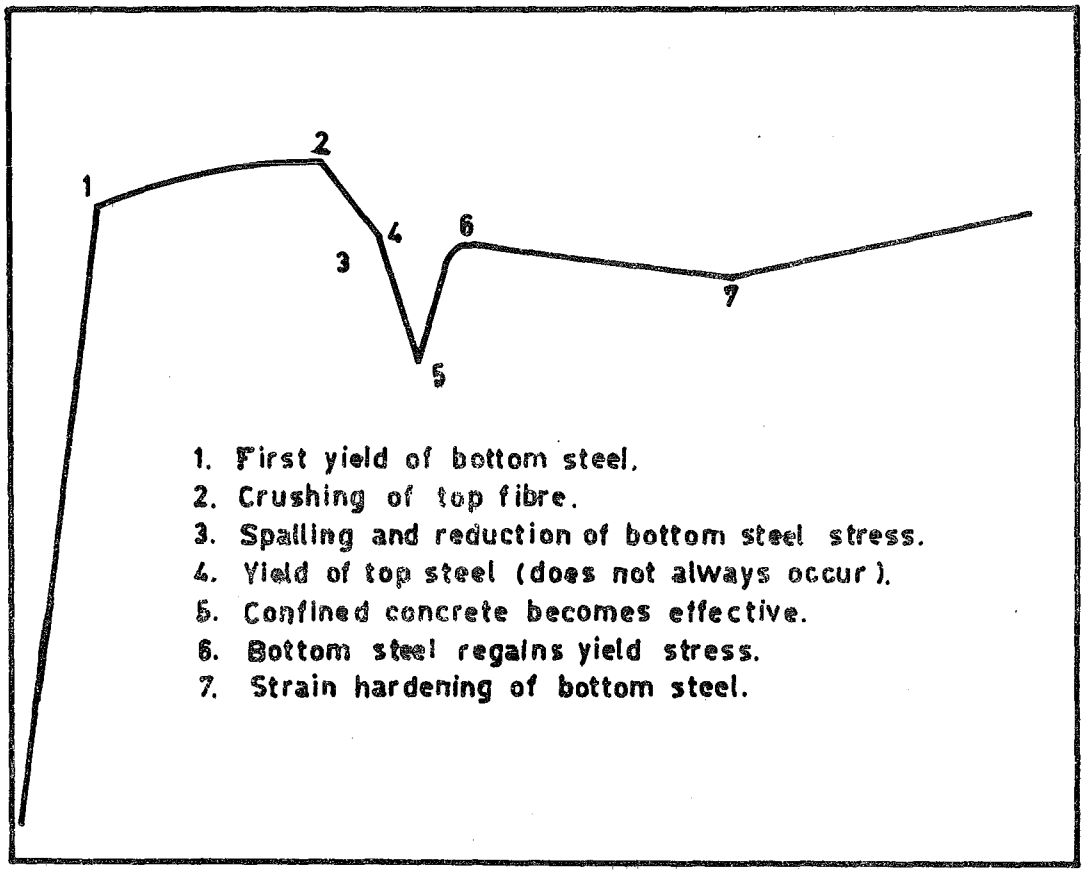

FIG.4.7 - KEY TO SIGNIFICANT POINTS ON THE GENERAL MOMENT-CURVATURE PLOT

crushing curvature to yield curvature was constructed and is illustrated in Figure 4.8 for a section with $f_y = f'_y = 40$ K.s.i., $E_s = 30 \times 10^6$ p.s.i., $\epsilon_{sh} = 16\epsilon_y$ and compression steel depth 10 per cent of effective depth.

It is to be expected that the extent of lateral reinforcement has little effect on the crushing curvature and indeed, the nomogram shows this to be the case, for the very large range in Z values has little influence on curvature ductility at crushing.

Example: Using $pf_y/f'_c = .325$, $p'/p = 0.5$ and a section laterally reinforced such that $Z = 125$, it can be seen that ϕ_{cr}/ϕ_y has a value of 6.3.

Often, it is of more use to obtain the ratio of absorbed energy at crushing to absorbed energy at yield. For an ideal elasto-plastic response, the ratio E_{cr}/E_y is:

$$\frac{E_{cr}}{E_y} = \frac{\frac{1}{2}M_y\phi_y + M_y(\phi_{cr} - \phi_y)}{\frac{1}{2}M_y\phi_y}$$

$$= 1 + \frac{2(\phi_{cr} - \phi_y)}{\phi_y}$$

$$= 2\frac{\phi_{cr}}{\phi_y} - 1 \qquad \ldots\ldots(4.42)$$

For the example above, substitution into Equation (4.42)

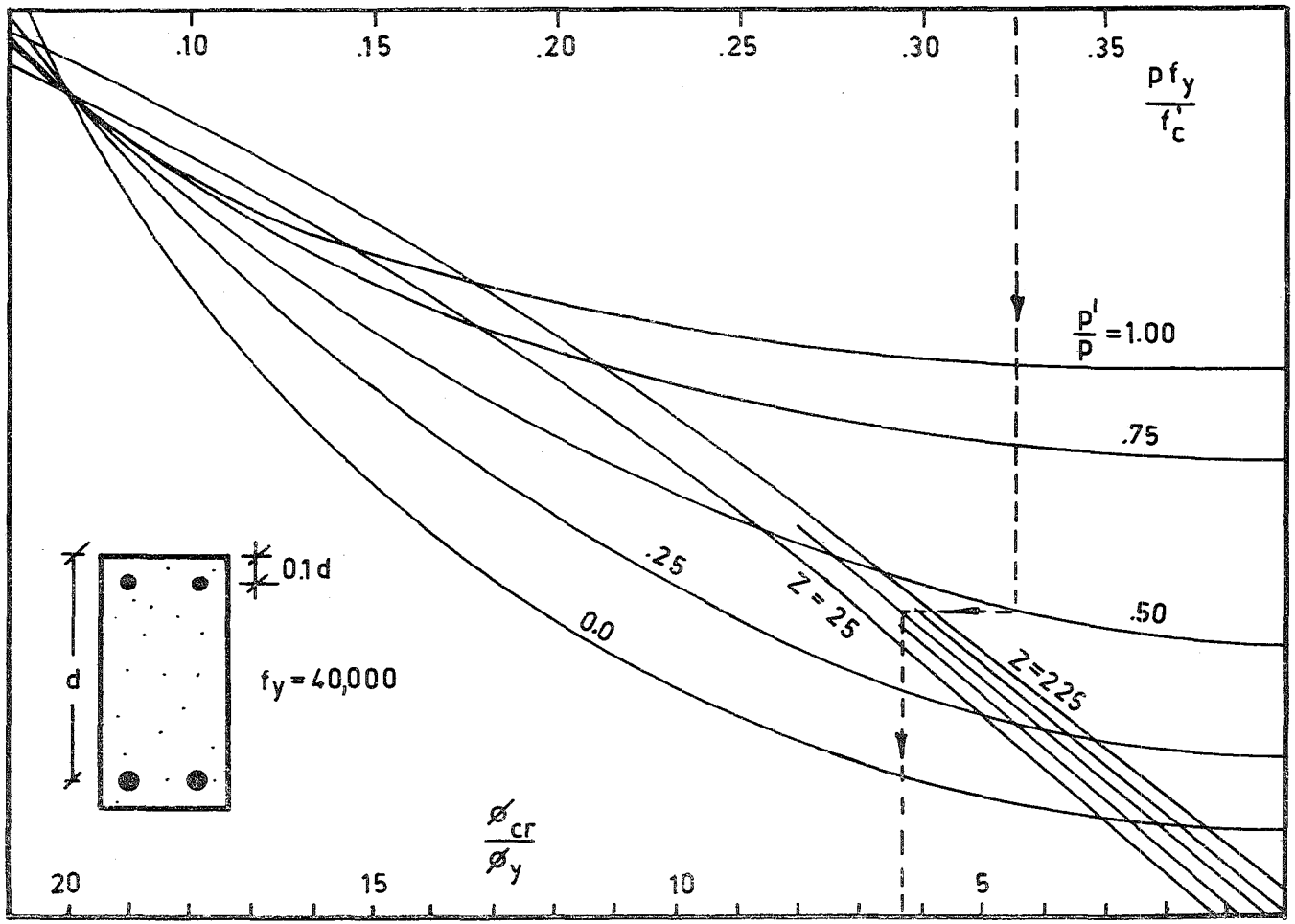

FIG.4.8 - NOMOGRAM FOR CURVATURE RATIO AT CRUSHING

would produce $E_{cr} = 11.6E_y$.

Figure 4.9 illustrates a nomogram for strain energy at crushing to strain energy at yield ratios, and using the section described in the above example, an energy absorption ratio of 13.2 is obtained. The reason for this difference in energy absorption ratios is that the reinforced concrete does not behave ideally elasto-plastically and the deviation from elasto-plastic behaviour becomes more marked with increased tension steel content, as illustrated in Figure 4.6.

Nomograms such as those illustrated in Figures 4.8 and 4.9 may be used for designing structures in which it is undesirable to have spalling of concrete during post-elastic deformation.

4.10 MAXIMUM AND ULTIMATE MOMENTS AND CURVATURES:

Tables 4.5 to 4.12 show the essential details for moment-curvature responses of reinforced concrete rectangular sections for a variety of concrete strengths, Z values, and rinforcement ratios. In all cases, constant quantities are f_y = 40 K.s.i., f_u = 68 K.s.i., $E_s = 30 \times 10^6$ p.s.i., $\epsilon_{sh} = 16\,\epsilon_y$, $\epsilon_u = \epsilon_{sh} + .14$ and ratio of core width to section width, b" = 0.8. Depth from top of section to compression steel, when present, is 10 per cent of effective depth.

Dimensionless (ϕd) and ($M/f'_c bd^2$) values are tabulated

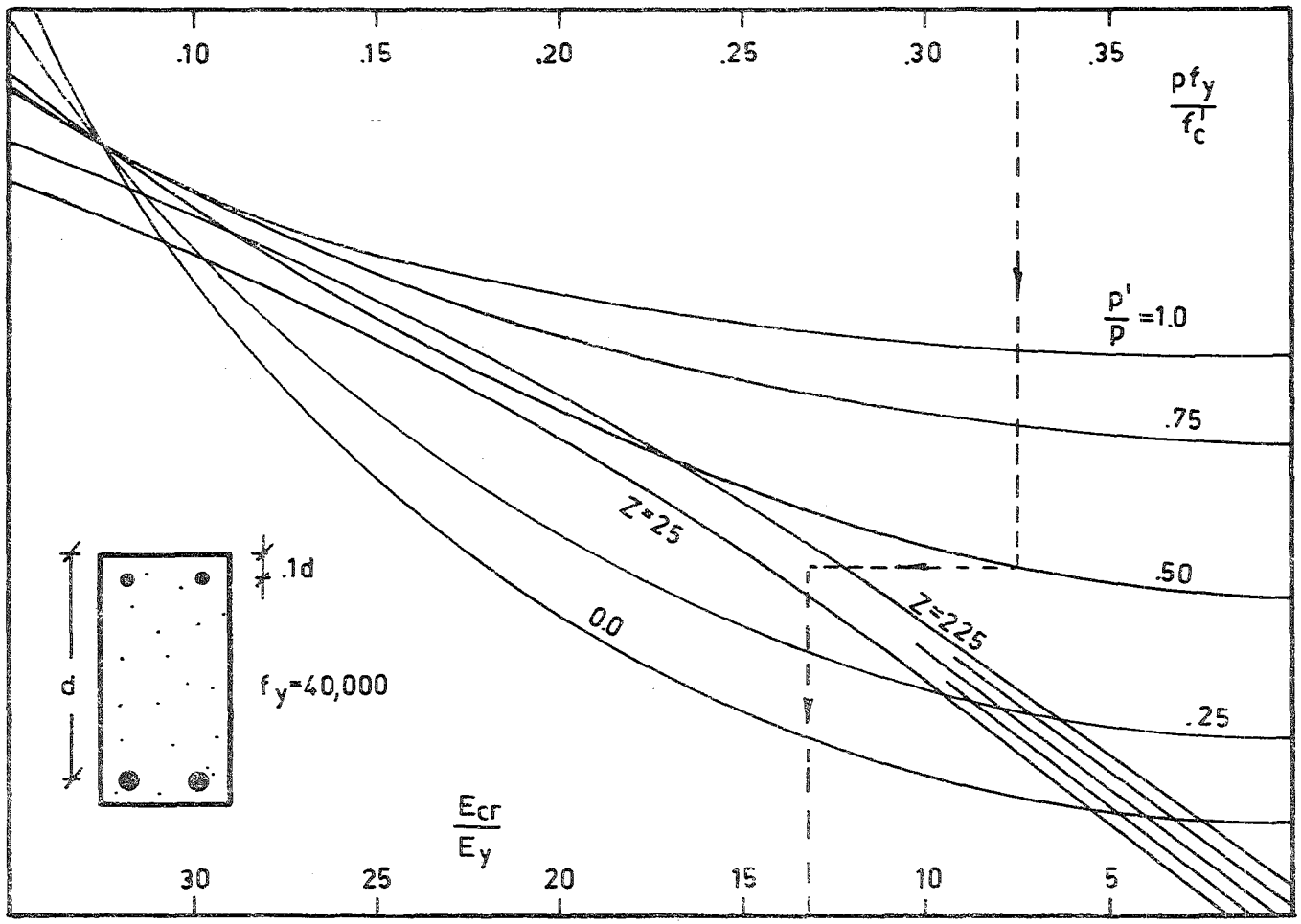

FIG.4.9 - NOMOGRAM FOR ENERGY ABSORPTION AT CRUSHING

TABLE 4.5

POST-ELASTIC BEAM BEHAVIOUR, $pf_y/f'_c = 0.05$

p'/p	$\frac{M_y}{f'_c bd^2}$	$\phi_y d$	z	$\frac{M_{cr}}{M_y}$	$\frac{M_m}{M_y}$	$\frac{M_u}{M_y}$	$\frac{\phi_{cr}}{\phi_y}$	$\frac{\phi_m}{\phi_y}$	$\frac{\phi_u}{\phi_y}$
0	.0458	.001794	25	1.468	1.520	*	26.1	84.9	*
			75	1.446	**	1.170	25.6	**	52.5
			125	1.433	**	1.133	25.0	**	38.6
			175	1.421	**	1.120	24.4	**	32.4
			225	1.403	**	1.081	23.8	**	29.0
0.5	.0459	.001781	25	1.431	1.605	*	24.6	102.0	*
			75	1.421	1.541	1.210	24.2	63.0	72.7
			125	1.411	1.487	1.161	23.9	47.7	53.2
			175	1.400	1.455	1.165	23.6	32.2	44.7
			225	1.388	1.447	1.041	23.2	31.9	40.3
1.0	.0460	.001751	25	1.420	1.649	*	24.4	105.9	*
			75	1.410	1.639	*	24.1	99.2	*
			125	1.400	1.623	1.321	23.9	79.0	85.4
			175	1.390	1.603	1.290	23.6	66.5	71.1
			225	1.380	1.585	1.223	23.4	59.8	63.6

* Fails by tension steel fracture;
** Spalling is maximum moment.

TABLE 4.6

POST-ELASTIC BEAM BEHAVIOUR, $pf_y/f'_c = 0.10$

p'/p	$\frac{M_y}{f'_c bd^2}$	$\phi_y d$	z	$\frac{M_{cr}}{M_y}$	$\frac{M_m}{M_y}$	$\frac{M_u}{M_y}$	$\frac{\phi_{cr}}{\phi_y}$	$\frac{\phi_m}{\phi_y}$	$\frac{\phi_u}{\phi_y}$
0	.0886	.002049	25	1.182	1.317	1.050	14.4	42.0	67.7
			75	1.164	**	.934	14.1	**	28.2
			125	1.149	**	.917	13.8	**	21.1
			175	1.130	**	.900	13.6	**	18.0
			225	1.110	**	.900	13.3	**	16.2
0.25	.0890	.001973	25	1.234	1.430	1.146	16.2	57.5	263.0
			75	1.222	1.257	.998	15.9	29.5	34.1
			125	1.211	**	.974	15.7	**	26.0
			175	1.199	**	.955	15.5	**	22.2
			225	1.182	**	.936	15.2	**	19.9
0.5	.0895	.002001	25	1.263	1.545	*	16.7	78.5	*
			75	1.252	1.369	1.129	16.5	33.0	39.3
			125	1.240	1.304	1.034	16.4	26.6	30.3
			175	1.233	1.280	1.010	16.2	18.5	26.0
			225	1.222	1.270	.966	16.0	18.3	23.7
0.75	.0899	.002017	25	1.274	1.630	*	17.2	111.0	*
			75	1.270	1.480	1.178	17.0	40.3	48.1
			125	1.260	1.412	1.160	16.8	31.9	36.2
			175	1.250	1.372	1.110	16.7	28.4	31.4
			225	1.242	1.345	1.038	16.6	21.8	28.6
1.0	.0902	.002023	25	1.280	1.650	*	17.4	111.1	*
			75	1.280	1.570	1.270	17.3	52.0	62.0
			125	1.270	1.530	1.210	17.2	40.6	46.0
			175	1.260	1.490	1.180	17.1	36.2	39.6
			225	1.250	1.470	1.160	17.0	32.9	35.9

* Fails by tension steel fracture;
** Spalling is maximum moment.

TABLE 4.7

POST-ELASTIC BEAM BEHAVIOUR, $pf_y/f'_c = 0.15$

p'/p	$\frac{M_y}{f'_c bd^2}$	$\phi_y d$	z	$\frac{M_{cr}}{M_y}$	$\frac{M_m}{M_y}$	$\frac{M_u}{M_y}$	$\frac{\phi_{cr}}{\phi_y}$	$\frac{\phi_m}{\phi_y}$	$\frac{\phi_u}{\phi_y}$
0	.1295	.002295	25	1.07	1.13	.90	9.55	27.8	41.6
			75	1.06	**	.88	9.27	**	18.6
			125	1.06	**	.85	8.95	**	14.0
			175	1.05	**	.84	8.67	**	11.6
			225	1.05	**	.80	8.40	**	10.5
0.5	.1321	.002170	25	1.17	1.44	1.15	13.50	53.6	380.0
			75	1.16	1.24	.976	13.40	23.4	29.4
			125	1.15	1.17	.915	13.25	19.0	22.9
			175	1.14	**	.915	13.12	**	19.7
			225	1.13	**	.888	13.00	**	18.0
1.0	.1337	.002129	25	1.230	1.678	*	15.25	104.6	*
			75	1.225	1.508	1.204	15.16	38.6	47.6
			125	1.220	1.456	1.185	15.07	31.3	35.5
			175	1.212	1.420	1.125	14.98	27.4	31.3
			225	1.207	1.400	1.045	14.89	25.8	29.0

* Fails by tension steel fracture;
** Spalling is maximum moment.

TABLE 4.8

POST-ELASTIC BEAM BEHAVIOUR, $pf_y/f'_c = 0.20$

p'/p	$\frac{M_y}{f'_c bd^2}$	$\phi_y d$	z	$\frac{M_{cr}}{M_y}$	$\frac{M_m}{M_y}$	$\frac{M_u}{M_y}$	$\frac{\phi_{cr}}{\phi_y}$	$\frac{\phi_m}{\phi_y}$	$\frac{\phi_u}{\phi_y}$
0	.1687	.002470	25	1.065	**	.850	6.65	**	29.60
			75	1.059	**	.841	6.45	**	13.00
			125	1.050	**	.812	6.25	**	9.74
			175	1.042	**	.809	6.05	**	8.05
			225	1.035	**	.777	5.85	**	7.43
0.25	.1719	.002387	25	1.064	1.146	.919	8.85	29.80	66.40
			75	1.060	**	.846	8.60	**	18.80
			125	1.058	**	.839	8.32	**	14.27
			175	1.050	**	.822	8.06	**	11.91
			225	1.048	**	.805	7.80	**	10.28
0.50	.1742	.002324	25	1.110	1.345	1.072	11.61	41.50	306.00
			75	1.101	1.139	.902	11.53	18.60	24.05
			125	1.092	1.075	.871	11.40	15.76	18.80
			175	1.080	**	.815	11.22	**	16.58
			225	1.065	**	.794	11.07	**	15.20
0.75	.1755	.002197	25	1.162	1.630	*	13.32	144.2	*
			75	1.158	1.300	1.030	13.23	24.65	31.60
			125	1.150	1.238	.972	13.17	20.40	24.50
			175	1.142	1.201	.950	13.09	18.30	21.50
			225	1.137	1.180	.908	13.00	17.18	19.85
1.00	.1767	.002124	25	1.192	1.690	*	14.50	114.70	*
			75	1.190	1.450	1.170	14.42	32.50	42.60
			125	1.185	1.398	1.115	14.36	27.20	31.90
			175	1.179	1.362	1.090	14.31	24.70	28.30
			225	1.175	1.341	1.071	14.23	22.60	26.00

* Fails by tension steel fracture;
** Spalling is maximum moment.

TABLE 4.9

POST-ELASTIC BEAM BEHAVIOUR, $pf_y/f'_c = 0.25$

p'/p	$\frac{M_y}{f'_c bd^2}$	$\phi_y d$	z	$\frac{M_{cr}}{M_y}$	$\frac{M_m}{M_y}$	$\frac{M_u}{M_y}$	$\frac{\phi_{cr}}{\phi_y}$	$\frac{\phi_m}{\phi_y}$	$\frac{\phi_u}{\phi_y}$
0	.2063	.002647	25	1.052	**	.845	4.96	**	20.50
			75	1.047	**	.840	4.81	**	8.65
			125	1.039	**	.821	4.66	**	6.79
			175	1.028	**	.785	4.51	**	6.00
			225	1.016	**	.773	4.36	**	5.46
0.5	.2159	.002438	25	1.061	1.268	1.010	9.84	35.60	282.00
			75	1.059	1.069	.862	9.55	16.36	21.00
			125	1.057	**	.850	9.24	**	16.31
			175	1.052	**	.815	8.91	**	14.40
			225	1.050	**	.805	8.60	**	12.44
1.0	.2199	.002206	25	1.171	1.701	*	13.55	112.5	*
			75	1.169	1.405	1.115	13.49	28.00	38.60
			125	1.167	1.352	1.080	13.43	23.70	28.65
			175	1.160	1.328	1.058	13.38	21.60	25.55
			225	1.157	1.305	1.042	13.30	20.45	23.45

* Fails by tension steel fracture;
** Spalling is maximum moment.

TABLE 4.10

POST-ELASTIC BEAM BEHAVIOUR, $pf_y/f'_c = 0.30$

p'/p	$\frac{M_y}{f'_c bd^2}$	$\phi_y d$	z	$\frac{M_{cr}}{M_y}$	$\frac{M_m}{M_y}$	$\frac{M_u}{M_y}$	$\frac{\phi_{cr}}{\phi_y}$	$\frac{\phi_m}{\phi_y}$	$\frac{\phi_u}{\phi_y}$
0	.2427	.002875	25	1.043	**	.836	3.81	**	11.30
			75	1.033	**	.817	3.70	**	6.38
			125	1.021	1.033	.808	3.57	2.64	4.99
			175	1.010	1.030	.790	3.46	2.60	4.48
			225	.997	1.028	.780	3.34	1.54	4.00
0.25	.2518	.002673	25	1.056	**	.842	5.29	**	34.50
			75	1.049	1.050	.838	5.13	3.69	11.55
			125	1.040	1.049	.836	4.96	3.65	8.12
			175	1.038	1.049	.834	4.81	3.62	6.70
			225	1.029	1.048	.832	4.66	2.15	6.12
0.50	.2572	.002503	25	1.059	1.201	.961	7.94	49.40	278.00
			75	1.058	1.059	.845	7.70	5.57	18.90
			125	1.056	1.058	.844	7.47	5.51	14.32
			175	1.050	1.057	.828	7.24	5.45	11.76
			225	1.048	1.056	.825	7.00	5.39	10.10
0.75	.2608	.002371	25	1.109	1.587	1.270	11.50	118.20	336.50
			75	1.105	1.189	.947	11.42	19.10	26.45
			125	1.100	1.138	.892	11.37	15.99	20.15
			175	1.096	1.109	.885	11.32	14.40	17.61
			225	1.090	**	.872	11.27	**	16.24
1.00	.2637	.002347	25	1.150	1.700	*	12.41	107.80	*
			75	1.145	1.730	*	12.39	121.10	*
			125	1.142	1.312	1.053	12.34	21.00	25.65
			175	1.140	1.287	1.010	12.30	19.27	22.95
			225	1.135	1.269	.955	12.25	18.21	21.50

* Fails by tension steel fracture;
** Spalling is maximum moment.

TABLE 4.11

POST-ELASTIC BEAM BEHAVIOUR, $pf_y/f'_c = 0.35$

p'/p	$\frac{M_y}{f'_c bd^2}$	$\phi_y d$	z	$\frac{M_{cr}}{M_y}$	$\frac{M_m}{M_y}$	$\frac{M_u}{M_y}$	$\frac{\phi_{cr}}{\phi_y}$	$\frac{\phi_m}{\phi_y}$	$\frac{\phi_u}{\phi_y}$
0	.2770	.003073	25	1.035	**	.830	3.05	**	7.39
			75	1.022	1.028	.825	2.96	2.14	4.44
			125	1.010	1.024	.820	2.87	2.11	3.50
			175	.996	1.019	.812	2.77	2.09	3.06
			225	.980	1.017	.797	2.68	1.24	2.97
0.50	.2988	.002602	25	1.052	1.159	.925	6.55	55.50	266.00
			75	1.050	1.052	.849	6.36	4.59	16.76
			125	1.049	1.050	.842	6.17	4.54	11.89
			175	1.042	1.050	.838	6.00	4.48	9.64
			225	1.040	1.049	.829	5.81	2.64	8.25
1.0	.3059	.002310	25	1.140	1.711	*	12.41	112.20	*
			75	1.139	-	*	12.38	-	*
			125	1.132	1.290	1.041	12.34	19.52	25.20
			175	1.130	1.265	1.008	12.30	18.77	22.60
			225	1.129	1.249	.956	12.27	17.37	21.15

* Fails by tension steel fracture;
** Spalling is maximum moment.

TABLE 4.12

POST-ELASTIC BEAM BEHAVIOUR, $pf_y/f'_c = 0.40$

p'/p	$\frac{M_y}{f'_c bd^2}$	$\phi_y d$	z	$\frac{M_{cr}}{M_y}$	$\frac{M_m}{M_y}$	$\frac{M_u}{M_y}$	$\frac{\phi_{cr}}{\phi_y}$	$\frac{\phi_m}{\phi_y}$	$\frac{\phi_u}{\phi_y}$
0	.3100	.003333	25	1.021	**	.818	2.46	**	5.25
			75	1.006	1.015	.815	2.39	1.72	3.28
			125	.992	1.011	.812	2.31	1.70	2.58
			175	.975	1.006	.794	2.24	1.68	2.50
			225	.960	1.001	.773	2.16	1.00	2.42
0.25	.3304	.002905	25	1.031	**	.822	3.65	**	20.90
			75	1.023	1.025	.820	3.54	2.55	7.41
			125	1.017	1.024	.815	3.43	2.52	5.60
			175	1.007	1.021	.805	3.33	2.50	4.69
			225	.995	1.019	.800	3.22	1.48	4.22
0.50	.3392	.002650	25	1.051	1.131	.904	5.64	58.00	261.00
			75	1.050	1.051	.841	5.49	3.94	14.75
			125	1.043	1.050	.834	5.34	3.90	10.39
			175	1.041	1.049	.830	5.16	3.86	8.41
			225	1.037	1.048	.820	5.01	2.31	7.34
0.75	.3463	.002506	25	1.056	1.535	1.227	10.15	99.20	298.00
			75	1.050	1.115	.884	9.92	16.06	24.45
			125	1.049	1.072	.855	9.55	13.97	17.88
			175	1.048	1.060	.841	9.20	12.67	15.80
			225	1.045	1.050	.815	8.89	6.73	14.70
1.0	.3504	.002406	25	1.125	1.711	*	11.77	107.30	*
			75	1.122	-	*	11.72	-	*
			125	1.120	1.263	.996	11.70	18.51	23.80
			175	1.118	1.240	.959	11.65	16.98	21.50
			225	1.114	1.224	.952	11.61	16.17	19.83

* Fails by tension steel fracture;
** Spalling is maximum moment.

for yield and ratios of M/M_y and ϕ/ϕ_y shown for conditions corresponding to crushing, maximum and ultimate moments.

It should be reiterated that no allowance has been made for compression steel buckling and that some of the higher cruvatures in these tables could not be reached in real beams because of it.

4.11 EFFECT OF AXIAL LOAD ON DUCTILITY

To make an assessment of the effect of axial compression stress on moment-curvature characteristics of reinforced concrete sections, the analysis was performed on the column section shown in Figure 4.10 for two total steel contents, $p_t f_y/f'_c = 0.3$ and $p_t f_y/f'_c = 0.6$; and for two Z values, Z = 10 and Z = 100. All other variables had the same values as for the beam in Figure 4.6. Table 2.3 gives an indication of what these Z values mean. For example, Z = 100 could refer to an unconfined section using 2000 p.s.i. concrete. Z = 10 could refer to a 2500 p.s.i. concrete with 6 per cent binding ratio and tie spacing equal to minimum core dimension.

The interaction diagrams in Figure 4.11 show that binder ratios have little effect on the load-moment relationship, particularly in the middle range of axial load levels.

What is of more significance is the curvature

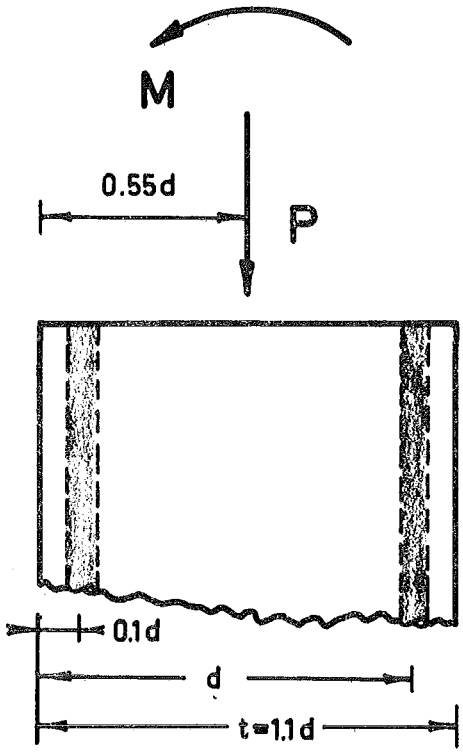

FIG.4.10 - CONCENTRICALLY-LOADED COLUMN

FIG. 4.11 - INTERACTION & DUCTILITY DIAGRAMS FOR COLUMNS

profiles illustrated in Figure 4.11, in which curvatures corresponding to maximum and ultimate moments are compared with axial load level.

The axial load, $P = 0.12 f'_c bt$, is the value recommended by the SEAOC code[31] as being the limit above which the sum of the ultimate moments of the column sections above and below the beam joints should be greater than the sum of the ultimate moments of the adjoining beams. Figure 4.11 shows that the SEAOC axial load level closely corresponds to the optimum amount of ductility available from any section under combined axial and bending loads, and these peaks occur at curvature ductility factors of approximately 100.

The reason for this is that at axial load levels increasing toward the peak curvature value, the onset of yield and fracture in the "tension" steel is retarded and so greater curvatures result. As this peak is reached and passed, failure is caused at increasingly lower curvatures by the "compression" steel reaching ultimate strain. Hence the very rapid drop off of curvatures at axial loads just higher than that at the peak curvature value. This drop-off is in turn retarded by better confinement since the concrete is better able to relieve the "compression" steel of load, and at such high strains, the difference in concrete stress between a $Z = 100$ core and a $Z = 10$ core is considerable.

Also it can be seen from Figure 4.11, that an increase in binding efficiency from Z = 100 to Z = 10, doubles the axial load range over which significant ductility is available.

In comparing the effects of Z on the moment-load interaction diagrams it can be seen that for a Z value of 10, maximum and crushing moments are nearly coincident above the balance point (so nearly coincident that the difference cannot be plotted). This is not so for the Z = 100 columns. In these columns, the maximum moment occurs before crushing and this is explained by the faster drop-off of load-carrying capacity of the Z = 100 core after maximum stress is passed. For the Z = 10 core, the concrete stress at crushing is 98 per cent of that at maximum stress; while for the Z = 100 core, the concrete stress has fallen to 80 per cent of the maximum value.

It is of interest to consider this Z value by means of two examples. By A.C.I. code requirements, a 19" square column must have a core size of no more than 16" square. This being the case, the requirements of A.C.I.[38] clause 913 and S.E.A.O.C. clause 2630(e)4c, give a minimum binding steel ratio, p" = .0369. $\frac{3}{4}$" dia. hoops at 3" centres satisfy this condition and, for a 4000 p.s.i. concrete, leads to a Z value of 25. It can be seen from Figure 4.11 that such a value for Z will place the peak

curvature even closer to the S.E.A.O.C. value of $P = 0.12 f'_c bt$.

A 15" square column, satisfying exactly the same requirements with $\frac{5}{8}$" dia. hoops at 2" centres, produces $Z = 5$. This substantial increase in ductility required for smaller columns is the subject of much controversy. The problems stem from A.C.I. Equation (9.1), which when modified for rectangular ties and the notation used in this thesis, has the form:

$$p'' = 0.9 \frac{f'_c}{f_y} \left(\frac{A_g}{A_c} - 1\right) \qquad \ldots\ldots(4.43)$$

Since the cover to the steel is fixed, then as the columns become smaller the A_g/A_c term increases exponentially. For example, a 24" square column with $1\frac{1}{2}$" cover to ties has $A_g/A_c = 1.31$. A 12" square column has $A_g/A_c = 1.78$. This discrepancy is not immediately significant but a "difference of comparatively large numbers" effect occurs when unity is subtracted from A_g/A_c in Equation (4.43) and thus p" for the 12" square column is more than twice that required for the 24" column.

The philosophy adopted in the use of Equation (4.43) is that the strength of an axially-loaded column after spalling of the cover concrete should be at least equal to that just before spalling. There is an anomaly here when this equation is applied to eccentrically-loaded columns,

in that provision for strength rather than adequate ductility is required.

4.12 COMPUTER PROGRAMS

Two computer programs were written for work described in this chapter. The first for producing stress-block parameters α and γ, and the second for moment-curvature responses of reinforced concrete T or rectangular sections with or without axial load. Listings of these programs appear in Appendix B.

Program 4.1 ("GAMMATAB"): Production of tables for stress-block parameters α and γ using equations derived in Section 4.3.

Program 4.2 ("TBEAMS"): Moment-curvature responses for T and rectangular sections with or without axial load are produced. To obtain theoretical moments and curvatures, the value of the strain in the top concrete fibre is incremented by a fixed amount. For each increment, the neutral axis is found using an iterative technique and force compatibility and thus moments and curvatures may be computed. This type of approach is discussed more fully in Chapter 5.

4.13 CONCLUSIONS

It has been shown that the analysis developed in this

chapter can predict moments and curvatures that correspond with reasonable accuracy to experimental results.

The effects on ductility of top and bottom steel contents, parameter Z, and axial load have been studied.

In the case of beams, the most significant contribution to ductility is obtained by increasing p'/p or decreasing p or both. Parameter Z, describing the confinement of the core concrete, has a comparatively small effect, particularly at low tension steel percentages.

Columns tend to reflect the dependence on good binding more definitely. As with beams, Z has negligible effects on load carrying capacity, but has beneficial effects on the capacity for energy absorption and the range of axial load levels over which a column can be considered as ductile.

CHAPTER 5

MOMENT-CURVATURE RESPONSES FOR CYCLICALLY-LOADED REINFORCED CONCRETE SECTIONS

SUMMARY

Previously used idealised moment-curvature responses for reinforced concrete sections are discussed. An "exact" moment-curvature analysis for such sections is developed in accordance with the theory presented in Chapters 2 and 3, and tested against nine experimental moment-curvature responses for beam sections.

5.1 INTRODUCTION

Most previous researches into ductility, plastic hinging and other post-elastic characteristics of reinforced concrete sections have consisted of applying monotonically increasing loads to test specimens until failure. Under most circumstances, particularly in the case of seismic loading, the likelihood of a building being loaded to failure in this fashion is slight. What has not been considered fully is the effect that cyclic loading has on concrete sections and the structural deterioration

that results.

In this chapter, a method is derived for predicting the flexural behaviour of concrete sections under earthquake-type loading, more specifically, the deformation properties and energy-absorbing capacity. The analysis is compared with experimental moment-curvature responses obtained from beams tested specifically for this purpose.

5.2 IDEALISED MOMENT-CURVATURE RESPONSES

To date, two idealised moment-curvature (or load-deflection) responses, have been used by investigators in studying post-elastic cyclic behaviour of structures.

The first, and still most common idealisation, is the elasto-plastic response shown in Figure 5.1. Such a system returns to its original stiffness during all intervals when it is not actually yielding and behaves exactly like an undamaged section during such intervals. This expression errs on the unsafe side for analysing both structural steel and concrete sections. In the case of structural steel, the phenomenon known as the Bauschinger Effect allows considerably less stiffness on reversal than is represented by an elasto-plastic response. The opening and closing of cracks in concrete sections, and again the Bauschinger Effect, generally produce moment-curvature responses that are difficult to idealise at all, and assumed elasto-plastic behaviour would predict greater

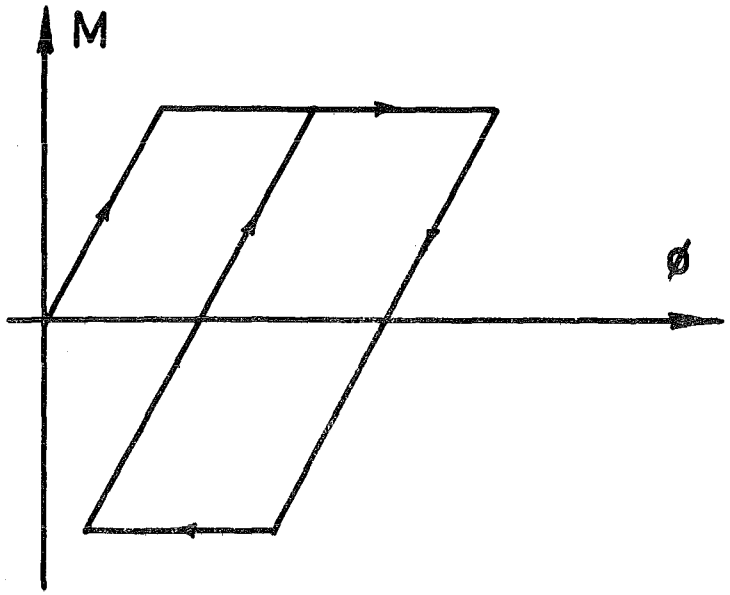

FIG.5.1 - ELASTO-PLASTIC PROPERTY

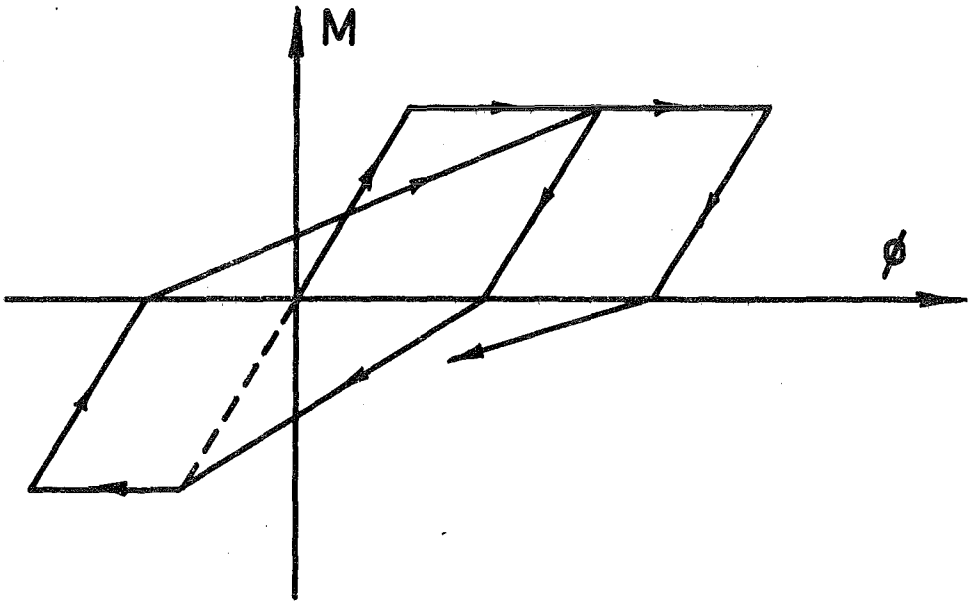

FIG.5.2 - DEGRADING STIFFNESS PROPERTY

stiffnesses than would occur in the real structure.

The second, and probably more realistic idealisation, is the "degrading stiffness" response proposed by Clough[58] as a load-deflection plot. Figure 5.2 illustrates the degrading stiffness property, and shows that it is much less resistant to deformation after it has undergone yield deformation, and thus responds to later phases of cyclic loading in a fashion completely different from its initial response behaviour. This degrading stiffness property is more typical of reinforced concrete and would generally prove to be conservative for structural steel framed structures. Clough's approximation is based on test results.

It is uneconomic to design for seismicity such that the maximum expected load lies within the elastic range of all structural components. The current ACI code, in common with most other building codes, recommends that the "reserve energy" brought about by post-elastic deformations, at critical sections, be utilised for earthquake resistance. Consequently, the properties after elastic behaviour of buildings which have been designed to this philosophy need to be studied.

Clough has applied a series of earthquake accelerograms to a simple single degree of freedom system and compared the ductility requirements of the elasto-plastic

and degrading stiffness responses. The results show that ductility requirements vary most markedly with the period of vibration. Taking the worst case considered by Clough, an undamped single degree of freedom system with an elasto-plastic response requires a deflection ductility factor of about 9 for a 0.3 second period, and less than 3 for a 2.7 second period. If the same accelerogram is applied to a similar system with a degrading stiffness response, the ductility requirement for the low period has become 24. The more flexible structure is unaffected, but Clough suggests that the higher mode behaviour of larger period buildings may be somewhat similar to the response of short period structures, in which case the degrading stiffness property could have a detrimental effect on the performance of such structures.

It is therefore evident that a more accurate prediction of post-elastic response is necessary.

Aoyama[44] studied the moment-curvature characteristics of rectangular reinforced concrete members subjected to axial load and reversal of bending. While not an idealised moment-curvature response in the direct sense, Aoyama's analysis was based on elasto-plastic reinforcing steel response and elasto-plastic concrete response with tension neglected. His conclusion to the effect that "the amount of plastic deformation under previous loading made drastic changes" illustrated the necessity for a description

of the Bauschinger Effect.

5.3 "EXACT" MOMENT-CURVATURE RESPONSES

The term "exact", in the context of this chapter, refers to moment-curvature responses that are not idealised but that are derived from assumed material properties with known loading histories. The term is not intended to imply that the results of the "exact" analysis are absolutely correct.

The analysis developed in this section draws largely from the theories presented in Chapters 2 and 3 and is for use with either cyclically- or monotonically-loaded T sections (of which rectangular sections are a special case), either with or without axial compression. (It is possible to consider axial tension but no consideration of shear capacity is included in this analysis.)

The analysis has been programmed for computer use.

5.3.1 Cyclically-loaded Concrete

The assumed behaviour of concrete when loaded cyclically has been presented in Section 2.7 and is illustrated in Figure 2.14. It was shown in Chapter 4 that for monotonic loading using the proposed concrete stress-strain response, there are twelve general cases for the compression stress block. It is not known how many such cases would be needed for cyclic loading but

a simple elasto-plastic response as used by Aoyama, giving only two general stress blocks for monotonic loading, requires eighteen such general stress blocks for cyclic loading. It is therefore clear that some other algorithm is required to mathematically describe the stress-strain behaviour of cyclically-loaded concrete and this is confirmed by the situation represented in Figure 5.3.

Figure 5.3(i) is the general concrete stress-strain curve assumed for this thesis. Figure 5.3(ii) shows stress and strain profiles resulting from the confined concrete being loaded monotonically, such that the strain in the extreme fibre reaches ϵ_{cx} (where $\epsilon_{cx} > \epsilon_{20}$). The concrete can then be unloaded and the strain in the extreme fibre reduced by a small amount $\Delta\epsilon_{cx}$ such that the stress in the top fibre becomes zero. Hence at the point corresponding to a strain of $0.75\epsilon_{cx}$ before unloading, the strain reduction must be $0.75\Delta\epsilon_{cx}$ (assuming that plane sections remain plane and for simplicity, that the neutral axis does not move). Similarly for the points originally corresponding to $0.50\epsilon_{cx}$ and $0.25\epsilon_{cx}$. Therefore, although the strain distribution after unloading (Figure 5.3(iii)) is little different from that prior to unloading, the stress distribution is markedly altered.

The above example is not complicated by a shift in the neutral axis position.

To solve this problem, the approach adopted in this

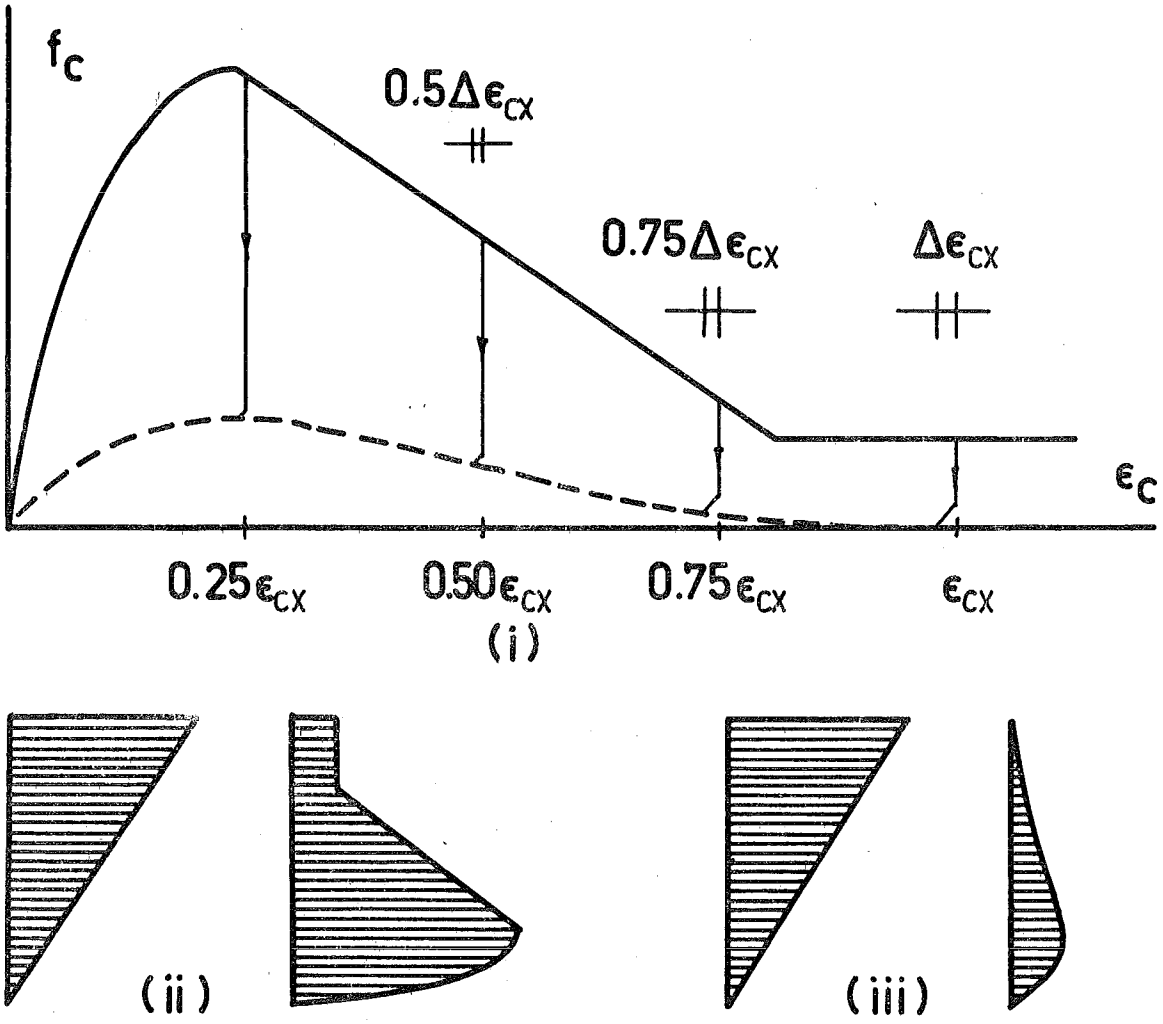

FIG.5.3 - UNLOADING OF CONCRETE

analysis is to consider the concrete section as being composed of NEL discrete horizontal elements each of depth hd/NEL and of equal width to the section at the same depth. Figure 5.4 illustrates the arrangement for the general T shape.

By simple geometry it can be shown that there are:

$\frac{d_F}{h}$ x NEL elements in the flange of the beam;

that the top steel resides in element $\frac{d'}{h}$ x NEL ; and that the bottom steel resides in element (NEL/h). If the strain in the top concrete fibre is ϵ_{cm} and the neutral axis depth is kd (k may be negative), then the average strain in concrete element, i, is given as:

$$\epsilon_{ci} = \epsilon_{cm} \quad \frac{\frac{(NEL \times k)}{h} - i + 0.5}{\frac{(NEL \times k)}{h}} \qquad \ldots\ldots(5.1)$$

This discrete element technique has the disadvantage of being comparatively slow, for given the strain in the top concrete fibre, the neutral axis depth is found by an iterative method. Further it is necessary to store for each element the parameters that record the progress along the stress-strain path.

The technique does, however, have the advantage of coping with unusual stress distributions and it is a

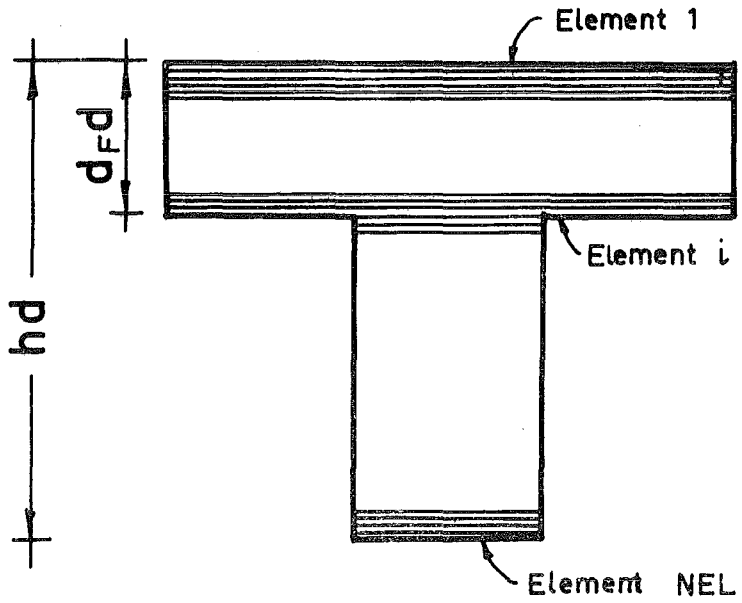

FIG.5.4. - DISCRETE ELEMENTS FOR T-SECTIONS

simple matter to alter the element force for area reductions due to spalling and to record which elements have cracked. Tension capacity is considered in accordance with Equation (2.15).

In this analysis, and in that for monotonic loading developed in Chapter 4, the unconfined concrete has been allowed to follow the same stress-strain response as for the confined core concrete up to crushing. There are two reasons for this simplification. Firstly, as shown later in this chapter, the role of concrete in the cyclic behaviour of reinforced concrete sections, is primarly to provide lateral support for the reinforcing steel. There are considerable stretches of the moment-curvature plot that during cyclic loading, rely solely on the steel couple for energy absorption. Therefore, the complication of allowing two different concrete stress-strain curves is felt to be not warranted. The complication that arises is illustrated in Figure 5.5. Figure 5.5(i) shows a reinforced concrete section with element i shaded. The compressive strain in this element is ϵ_{ci1}. The section may then be unloaded such that the strain in element i is reduced to ϵ_{ci2} as shown in Figure 5.5(ii). This extent of unloading results in tension stress in the unconfined cover concrete and a residual compression stress in the confined core concrete. Thus a shear stress develops between the core and cover concrete as shown in

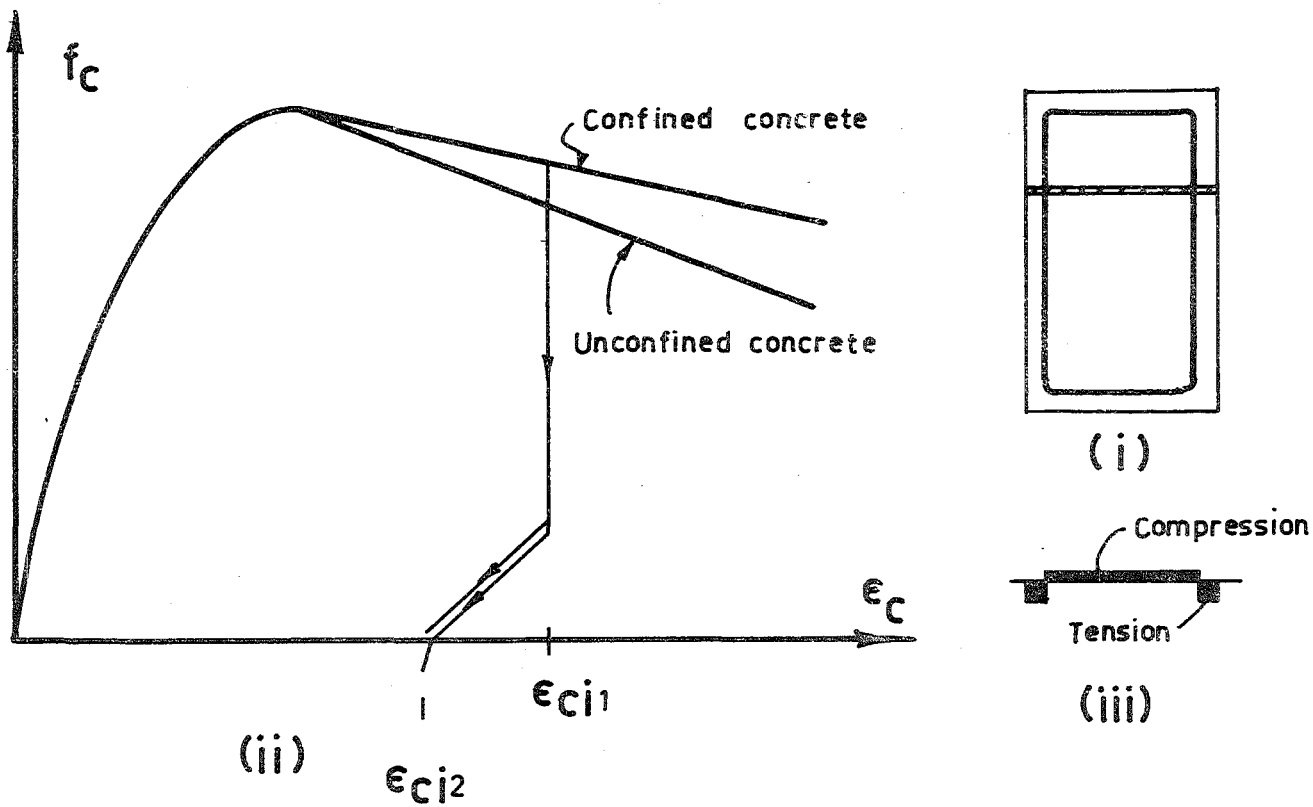

FIG.5.5 - DUAL STRESS-STRAIN BEHAVIOUR FOR CONCRETE

Figure 5.5(iii). Note that it is not necessary for the core concrete to be in tension for a shear stress to develop between core and cover concretes, nor is it even necessary to unload the concrete at all. This situation may well arise in reality but its inclusion in this analysis is considered to be a refinement beyond the accuracy of the present concrete stress-strain representation. Further, the unconfined concrete is assumed to be ineffective at strains exceeding $\epsilon_{cr} = 0.004$, at which strain, deviations in stress between confined and unconfined concretes are not generally large.

5.3.2 Cyclically-loaded Reinforcing Steel

The expression for Bauschinger Effect in reinforcing steel, proposed in Section 3.9, is incorporated in this analysis.

5.4 ALGORITHMS FOR COMPUTER PROGRAMS

Two computer programs were developed for this analysis. The first computes bending moments, curvatures and energy absorptions for cylically-loaded reinforced concrete T or rectangular sections, with or without constant axial compression stress, and considers the Bauschinger Effect expressions advanced in Chapter 3. The programs operate within stipulated curvature cycles. The second program was almost identical to the first, the only difference being that the stress-strain behaviour of the reinforcing steel

was allowed to be elasto-plastic. The algebra of the analysis appears in the program listings in Appendix B.

In order to keep the analysis general, the dimensions b and d are eliminated by using the dimensionless parameters d_F, W_F, d', b" and h as illustrated previously in Figure 4.3. Other input requirements are: steel properties (f_u, f_y, p, ϵ_{sh}, E_s) for top and bottom steels; concrete properties (ϵ_o, ϵ_{cr}, Z, f'_c); and the number of elements, NEL. Axial load in the form (P/bd) p.s.i. can be read in conjunction with e_p (where $e_p d$ is the distance from the top of the section to the point of action of the axial load) if axial compression is required. Finally, dimensionless curvature readings, Ød, representing points of curvature reversal are required.

From this input, various other properties are established, including the strain hardening parameters discussed in Chapter 3, and arrays are initialised.

5.4.1 Iteration and Compatibility

The iterative technique used is based on adjusting the strain, ϵ_{cm}, in the top concrete fibre by a fixed positive or negative amount, depending on whether it is desired to increase or decrease the curvature respectively. Having established ϵ_{cm}, k is chosen as -20000 and all concrete and steel strains, and hence stresses, are computed for this neutral axis depth. From a force compatibility test it is then established whether or not the actual

neutral axis depth is positive or negative. If it is found to be positive, k is set equal to 100 and the concrete and steel stresses and strains recomputed. Subsequently, if the neutral axis is found to be too high, k is incremented by g (where initially g is +20000 for negative neutral axis depth, and is +100 for positive neutral axis depth). If k is too large, it is reduced by g; g is then halved, and the new g added to k. If $|k| \leq 0.001$, it is considered as being too large and is reduced by g. In this way, neutral axis depths within the range - 20000d to +15000d are allowed. If the neutral axis depth is not within these limits, the analysis proceeds to the next value for ϵ_{cm}. In any case, a maximum of 150 trial values for k is permitted for each ϵ_{cm} value. If compatibility is not obtained to within (bd/3)1b before 150 k values have been studied, the k value giving the least force compatibility error is chosen. Using the sign convention, compression positive, the criterion for determining whether k is to be increased or decreased depends on whether ϵ_{cm} x ($\sum$ compression forces - $\sum$ tension forces - axial force) is negative or positive respectively.

Having obtained compatibility the bending moment and curvature are computed. If, at this stage, the computed curvature is found to exceed the input value for curvature for the cycle being considered, an assumed linear relation between ϵ_{cm} and computed curvature values of the previous increment, and the ϵ_{cm} and computed curvature values of the

current increment, is used to obtain an ϵ_{cm} value that will produce the required curvature value. In all cases studied, this technique resulted in calculated curvatures that coincided with input curvature values for the extremities of the cycles.

Algorithms for obtaining concrete and steel stresses from the computed strains were found to be considerably more complex.

5.4.2 Concrete Behaviour

In the case of the concrete, the first check for each element is to establish whether or not the strain is greater than that previously experienced by the element. If it is a maximum value, the stress is computed from Equations (2.19) or (2.20) or (2.23). If however, the strain value is less than a previous maximum value, the concrete could be in one of four states. Either it is being unloaded, or it is in tension, or it is being reloaded, or the strain may be such that no stress exists at all. In all four cases, a necessary parameter is the stress in the element at the maximum strain value. Also, in the case of the unloading and reloading states, the values for concrete strain in the previous increment and at the next zero stress are required to determine whether the concrete element is being unloaded or reloaded. If the strain indicates tension stress, a check is made to establish whether the element can sustain this stress, i.e. whether f_r is exceeded or whether the element has cracked previously.

Finally, adjustments for stress reductions due to spalling are made if necessary and the summation of bending moment and force contributions for each element are computed.

When compatibility of the whole section has been obtained, the counters and parameters for each element are recorded or adjusted if necessary.

5.4.3 Algorithm for Steel Behaviour Considering Bauschinger Effect

The difficulties experienced with this algorithm have been mentioned previously and are discussed in Chapter 3.

5.4.4 Algorithm for Elasto-Plastic Steel Behaviour

Algorithims for elasto-plastic steel behaviour are comparatively straightforward. The approach used in this program takes advantage of the sign conventions, in that an algebraic increase in strain will always produce an algebraic increase in stress, unless the steel is yielding. The values for stress and strain in the previous increment, f_{sl} and ϵ_{sl} are used to give stress as:

$$f_s = f_{sl} - E_s(\epsilon_{sl} - \epsilon_s) \qquad \ldots\ldots(5.2)$$

Checks are then made to establish whether $|f_s| \geqslant f_y$ and, if so, whether $|\epsilon_s| > \epsilon_{sh}$. Adjustments to f_s are made if necessary.

A further steel test, to check whether $|\epsilon_s| > \epsilon_{su}$, is

performed following each successful force compatibility equilibrium.

5.4.5 Operation of the Programs

Using the analysis described here, computer time required for the production of moment-curvature responses for each beam with 14 or 15 loading cycles, was of the order of 60 minutes for 100 elements and an ϵ_{cm} increment of 10^{-4}. Some comparisons using 200 elements indicated no difference in any computed values, and comparisons using 50 elements indicated very small differences compared with the 100-element analysis. All neutral axis depths fell within the range allowed by the program.

5.5 EXPERIMENTAL MOMENT-CURVATURE RESPONSES

Very little experimental effort has been directed at the study of cyclically-loaded reinforced concrete sections and it was therefore necessary to conduct a test series to assess the accuracy of this analysis. Full details of this investigation and of the derivation of moment-curvature responses appear in Chapter 7 and in Appendix D.

Of the eleven beams tested, nine were considered to give acceptable results.

Each beam was 10' - 0" long and was simply supported over 9' - 0" by means of an axle at beam mid-depth. The central part of the beam simulated a column stub, to which the point loads were applied. All beams were of 4 15/16"x8"

section with 2 - $\frac{1}{2}$" dia. deformed bars top steel and $\frac{1}{4}$" dia. plain bar stirrups. Cover to all main steel was 1". Stirrup spacings considered were 2", 4" and 6" and the first digit of the beam number indicates this spacing. The second digit of the beam number specifies the nominal diameter in $\frac{1}{8}$" of the two deformed bars at the bottom of the beam, i.e. Beam 27 has 2" stirrup spacing and $\frac{7}{8}$" dia. bottom steel.

Figures 5.6 to 5.14 illustrate experimental moment-average curvature responses for the critical sections of the nine beams, compared with the theoretical behaviour predicted by the analysis presented in this chapter. In all cases, the experimental curvatures at load reversal points were given, and the moments computed at these points and at intervals between successive points. The sign conventions adopted are as follows: positive bending moment arises from a downward load being applied to the beam; positive curvature corresponds to tension on the bottom of the beam. Dead load bending moment at critical sections was approximately 6 K.in. for all beams as shown.

Figures 5.15 and 5.16 show experimental moment-curvature responses for two of the beams compared with a theoretical analysis using an elasto-plastic reinforcing steel response.

Lines, rather than points, illustrate the experimental

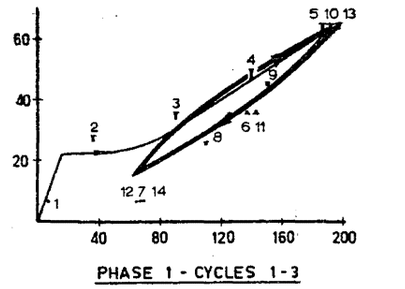

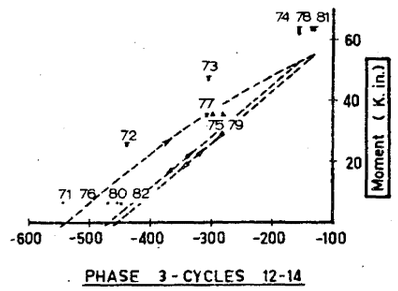

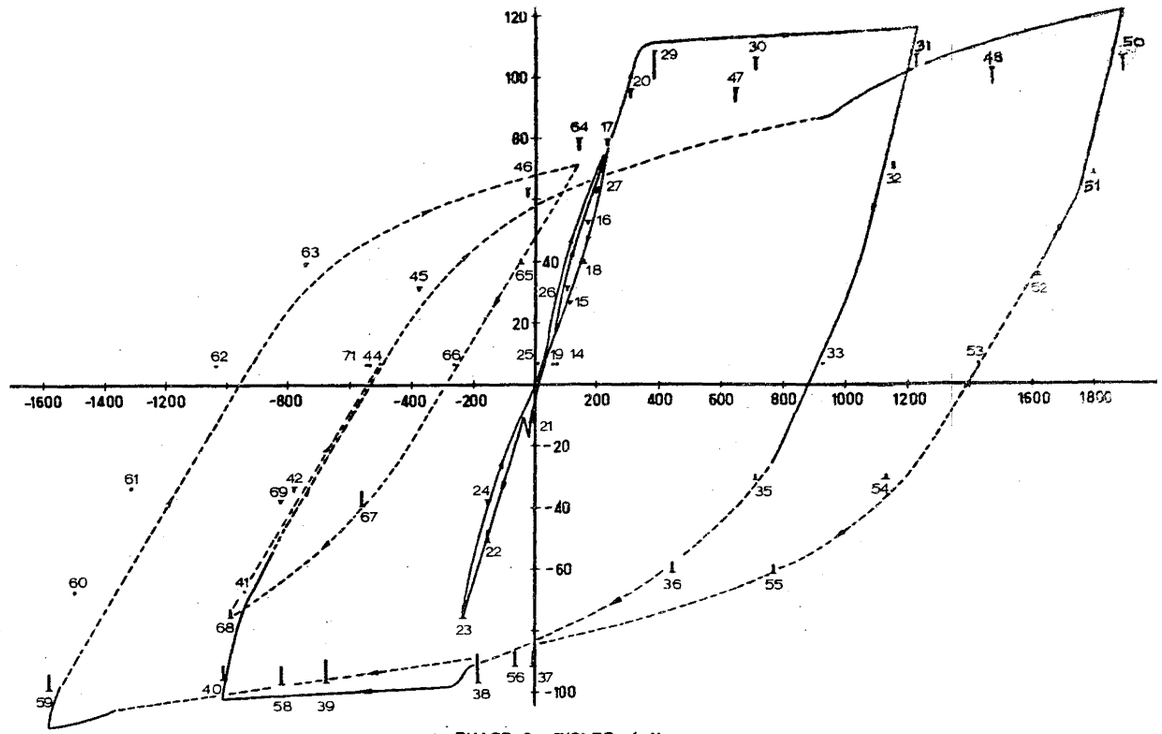

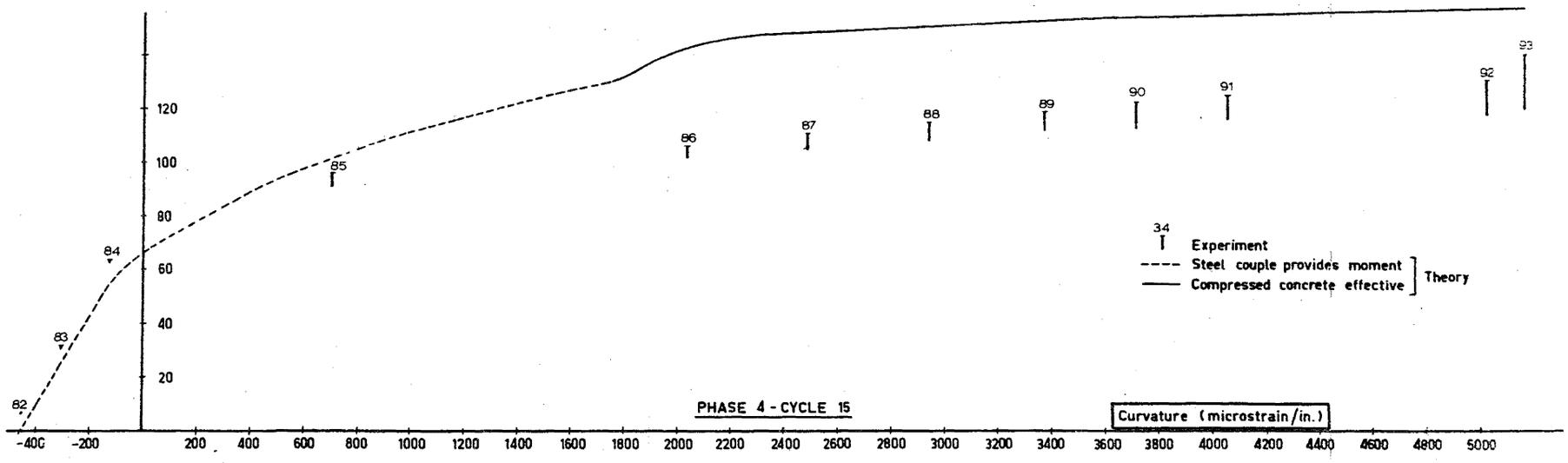

FIG.5.6 - MOMENT-CURVATURE FOR BEAM 24 PLASTIC HINGE

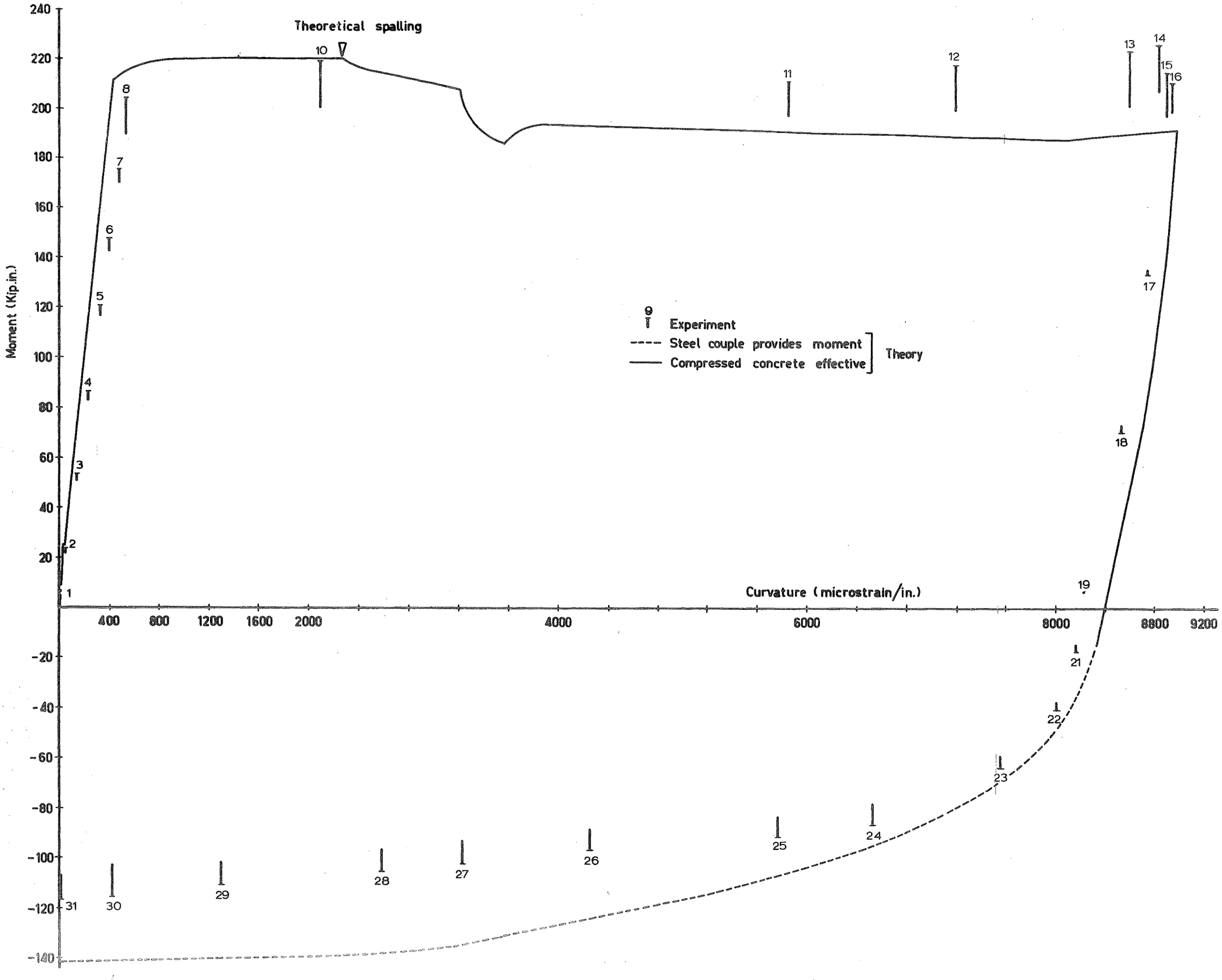

FIG.5.7 - MOMENT-CURVATURE FOR BEAM 26 PLASTIC HINGE

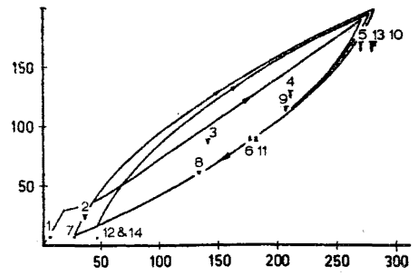

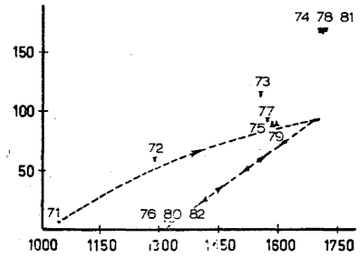

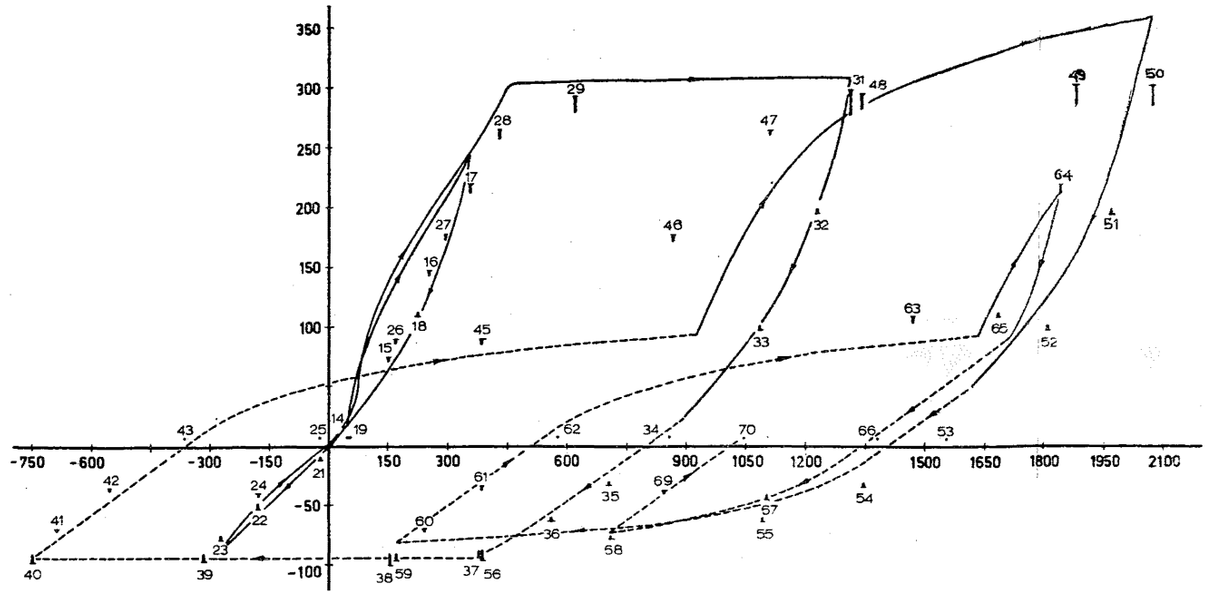

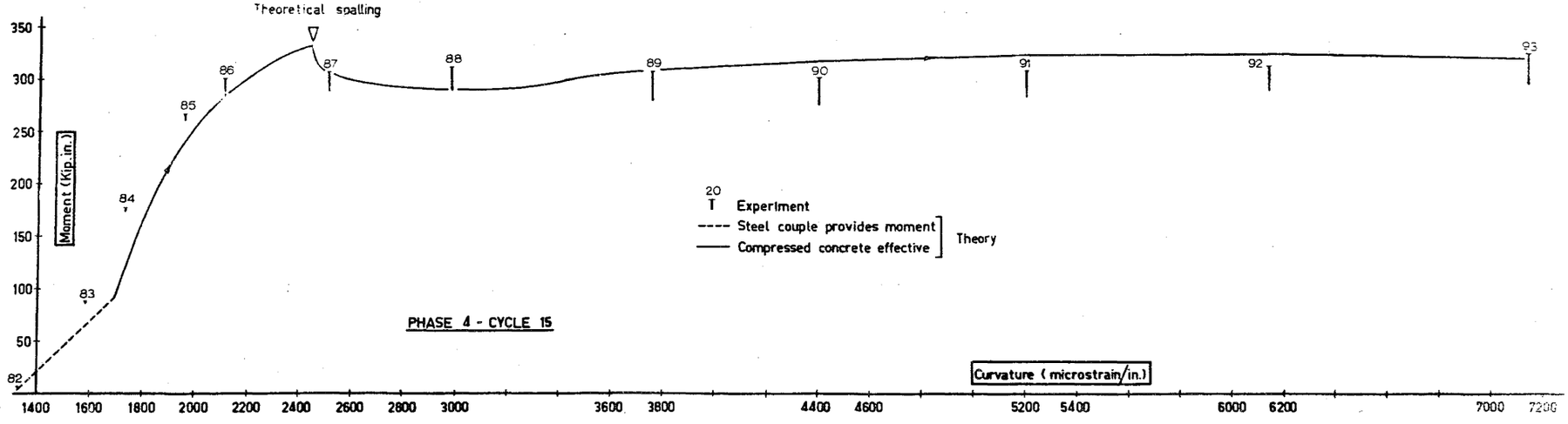

FIG.5.8 - MOMENT-CURVATURE FOR BEAM 27 PLASTIC HINGE

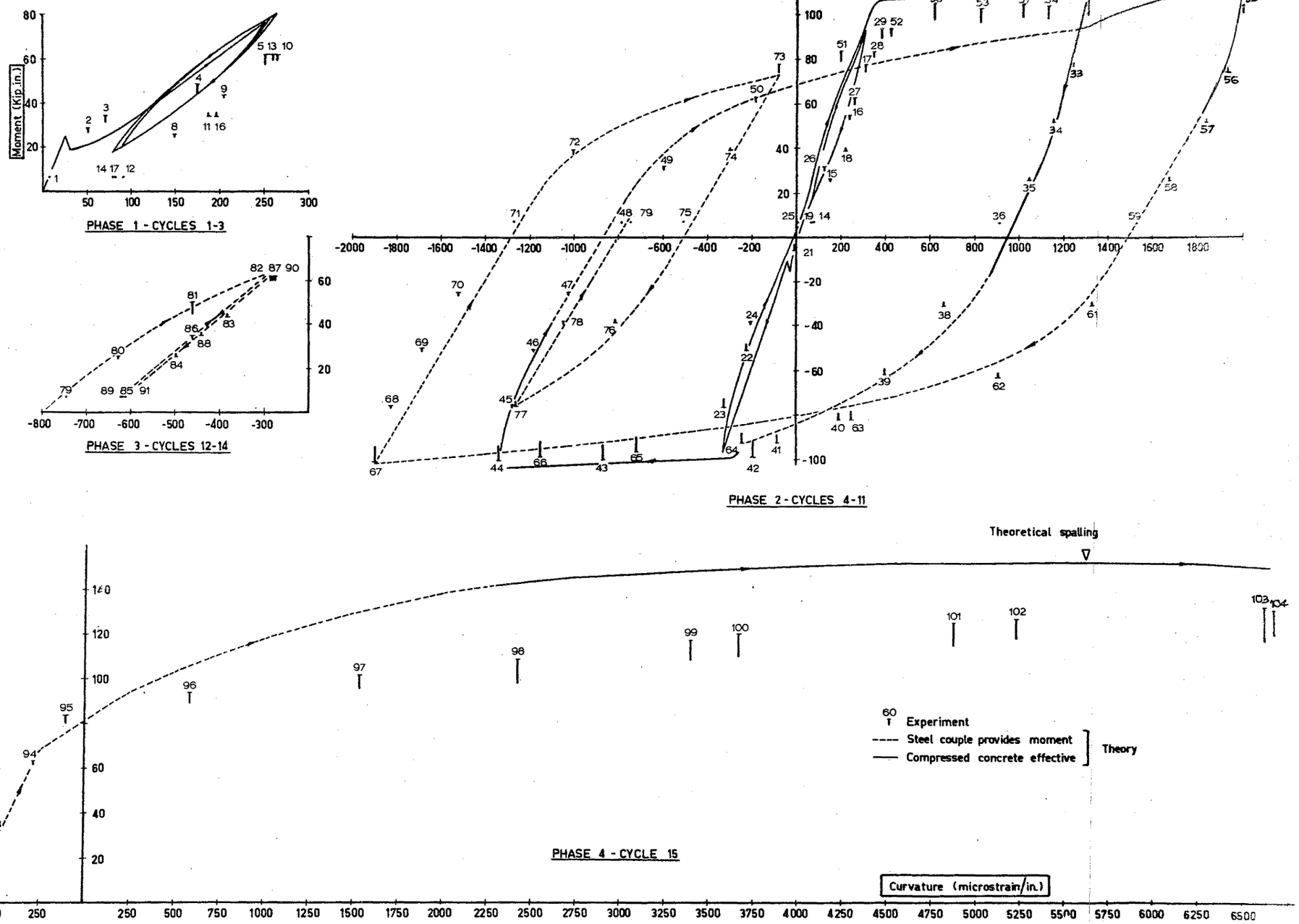

FIG.5.9 - MOMENT-CURVATURE FOR BEAM 44 PLASTIC HINGE

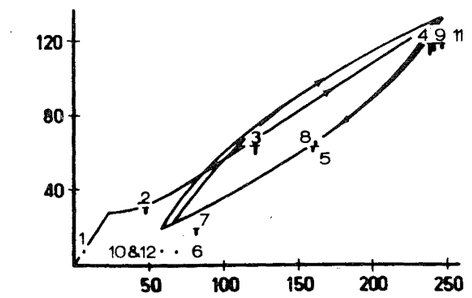

PHASE 1 - CYCLES 1-3

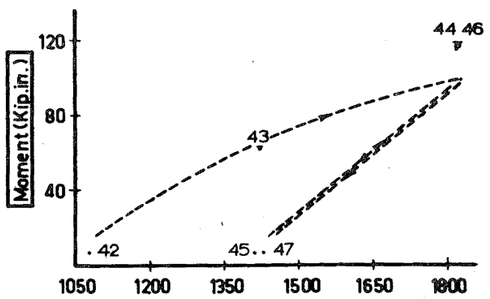

PHASE 3 - CYCLES 12-13

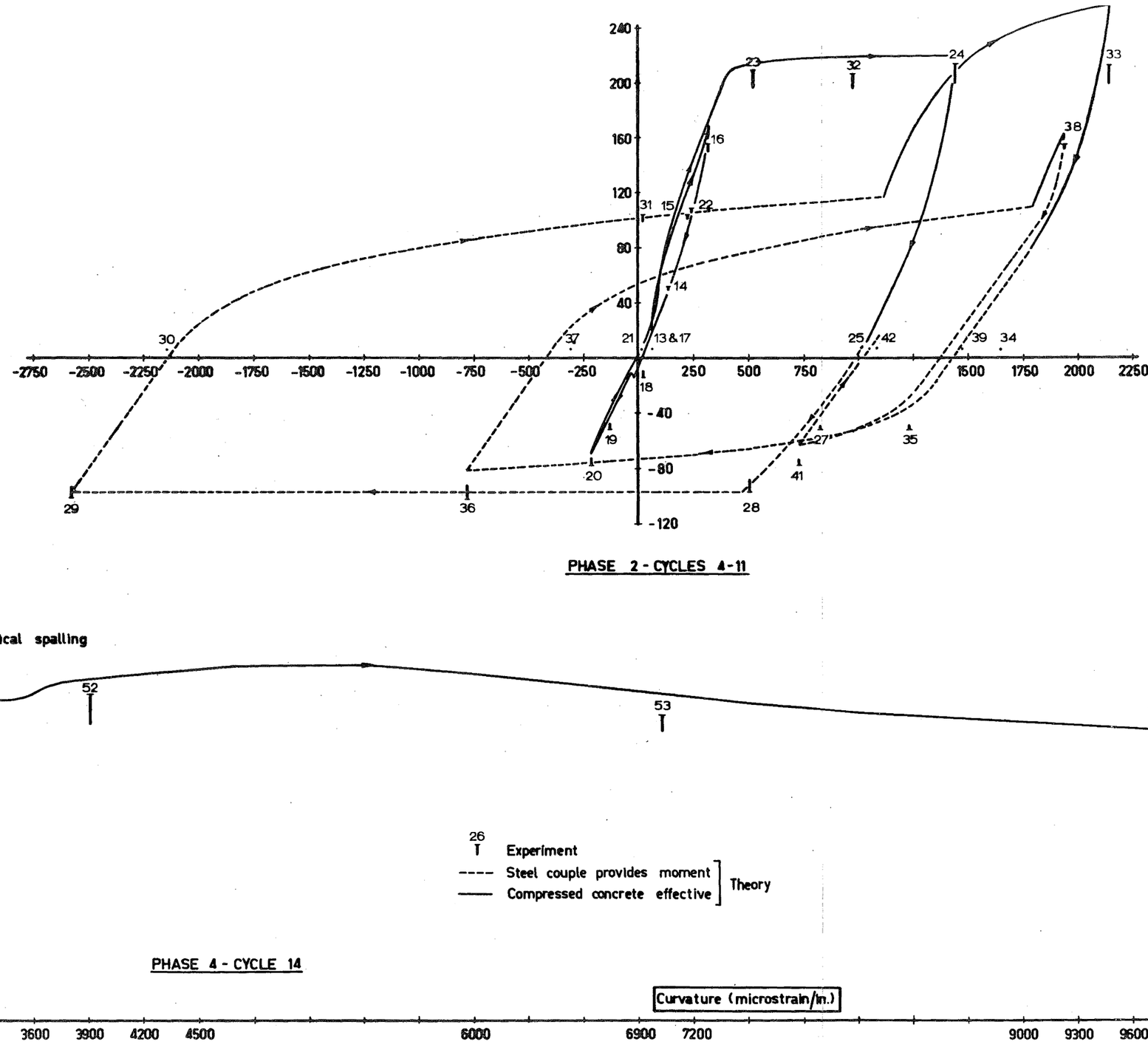

PHASE 2 - CYCLES 4-11

PHASE 4 - CYCLE 14

FIG.5.10 - MOMENT-CURVATURE FOR BEAM 46 PLASTIC HINGE

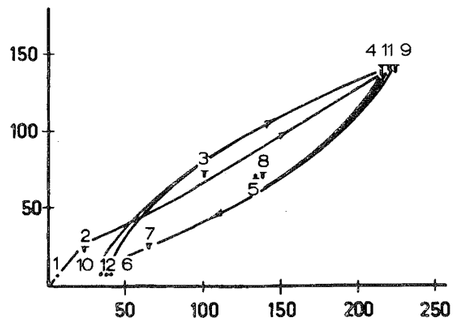

PHASE 1 - CYCLES 1-3

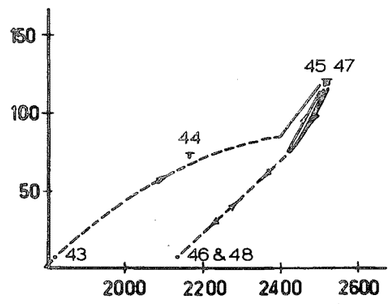

PHASE 3 - CYCLES 12-13

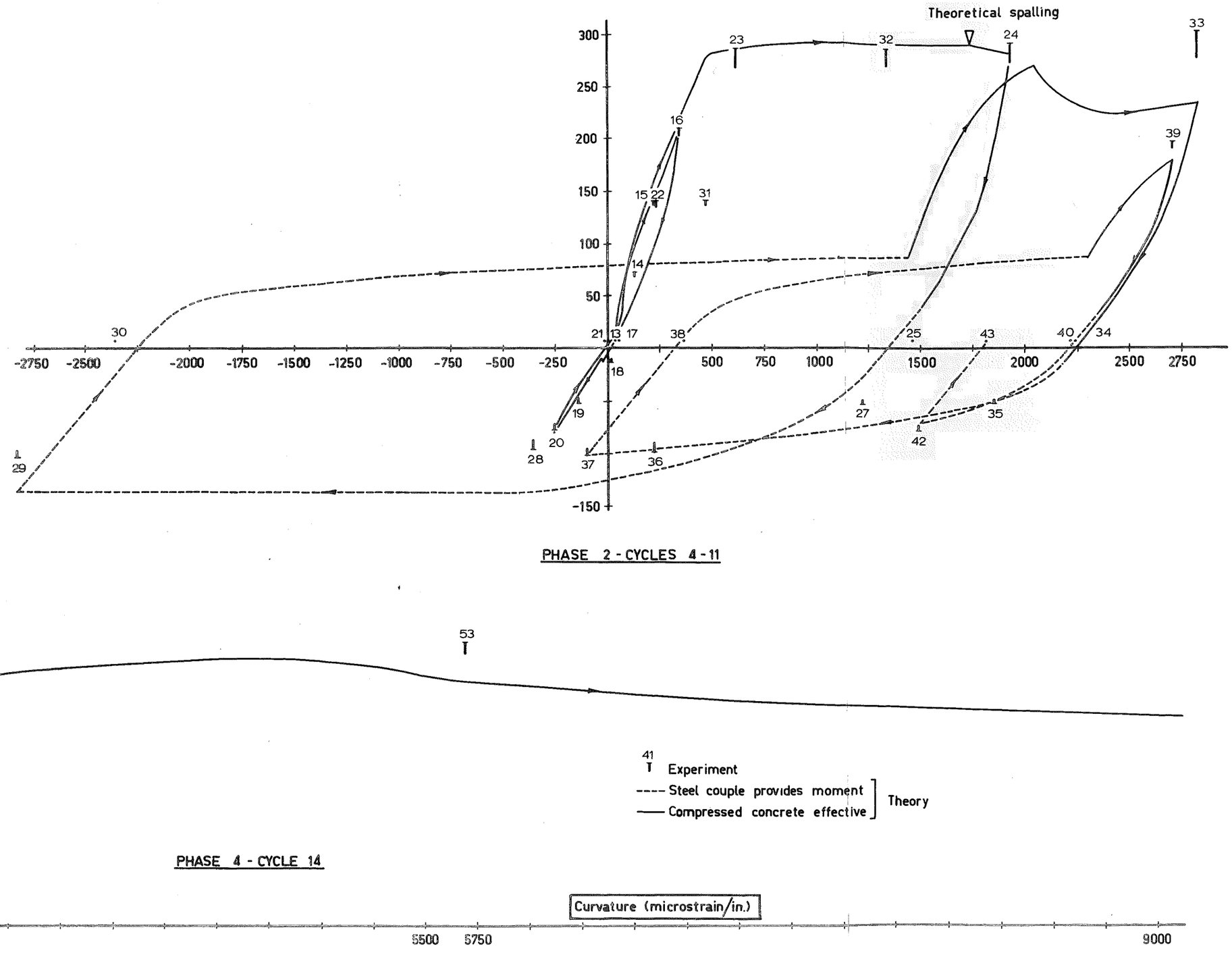

FIG.5.11 - MOMENT-CURVATURE FOR BEAM 47 PLASTIC HINGE

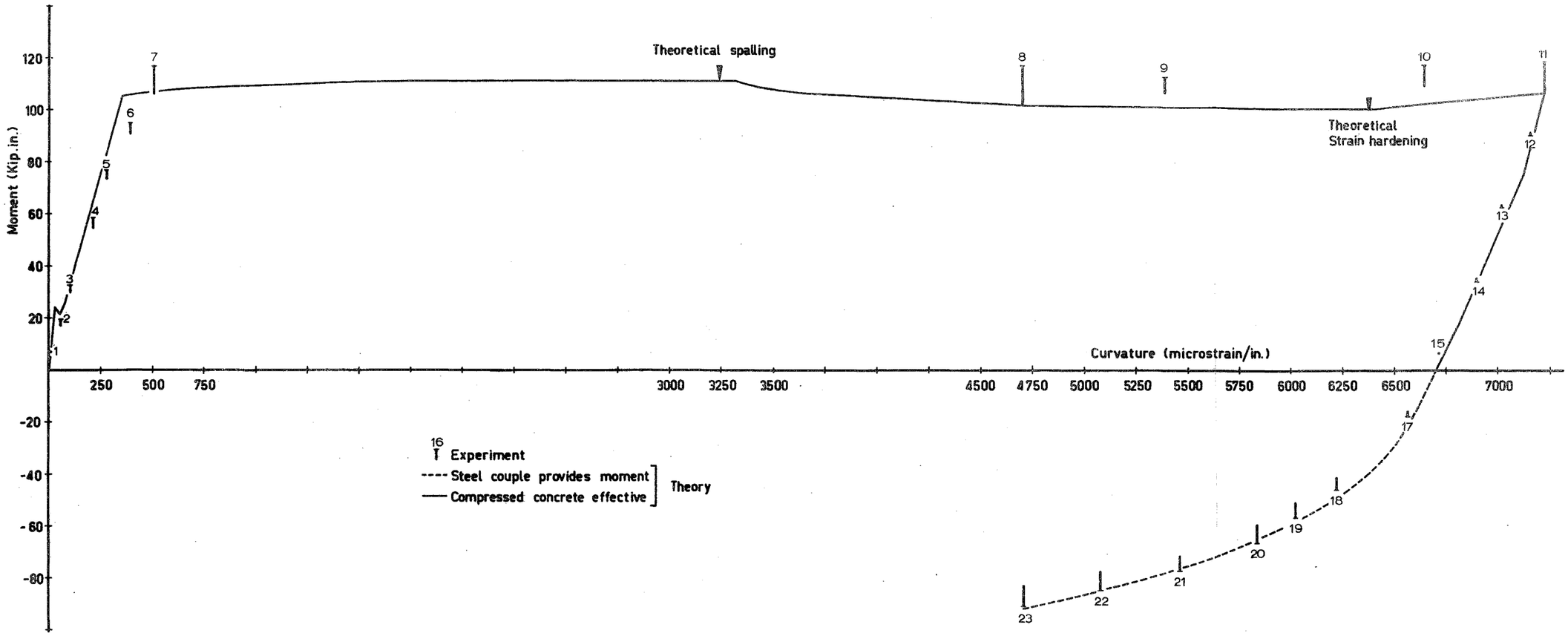

FIG.5.12 - MOMENT-CURVATURE FOR BEAM 64 PLASTIC HINGE

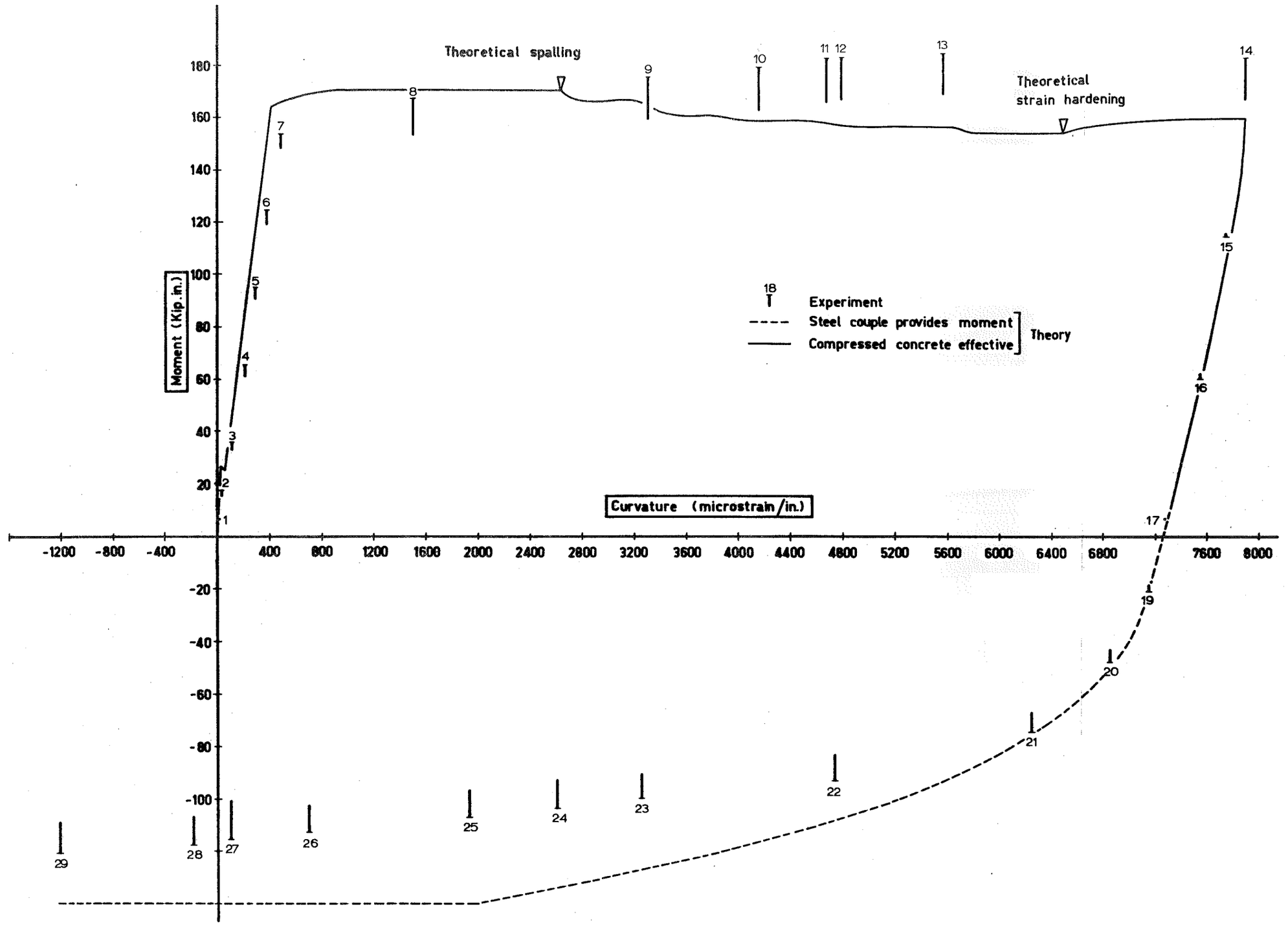

FIG.5.13 - MOMENT-CURVATURE FOR BEAM 65 PLASTIC HINGE

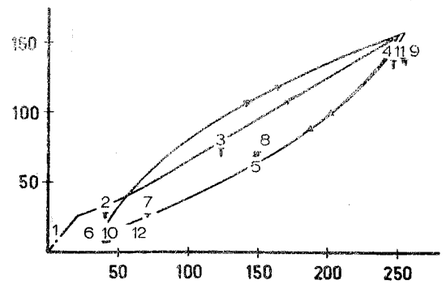

PHASE 1 - CYCLES 1-3

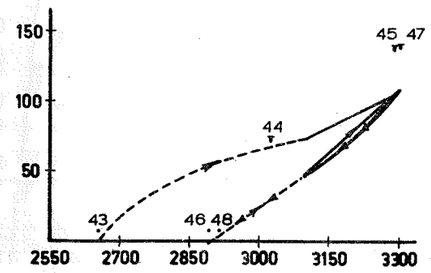

PHASE 3 - CYCLES 12-13

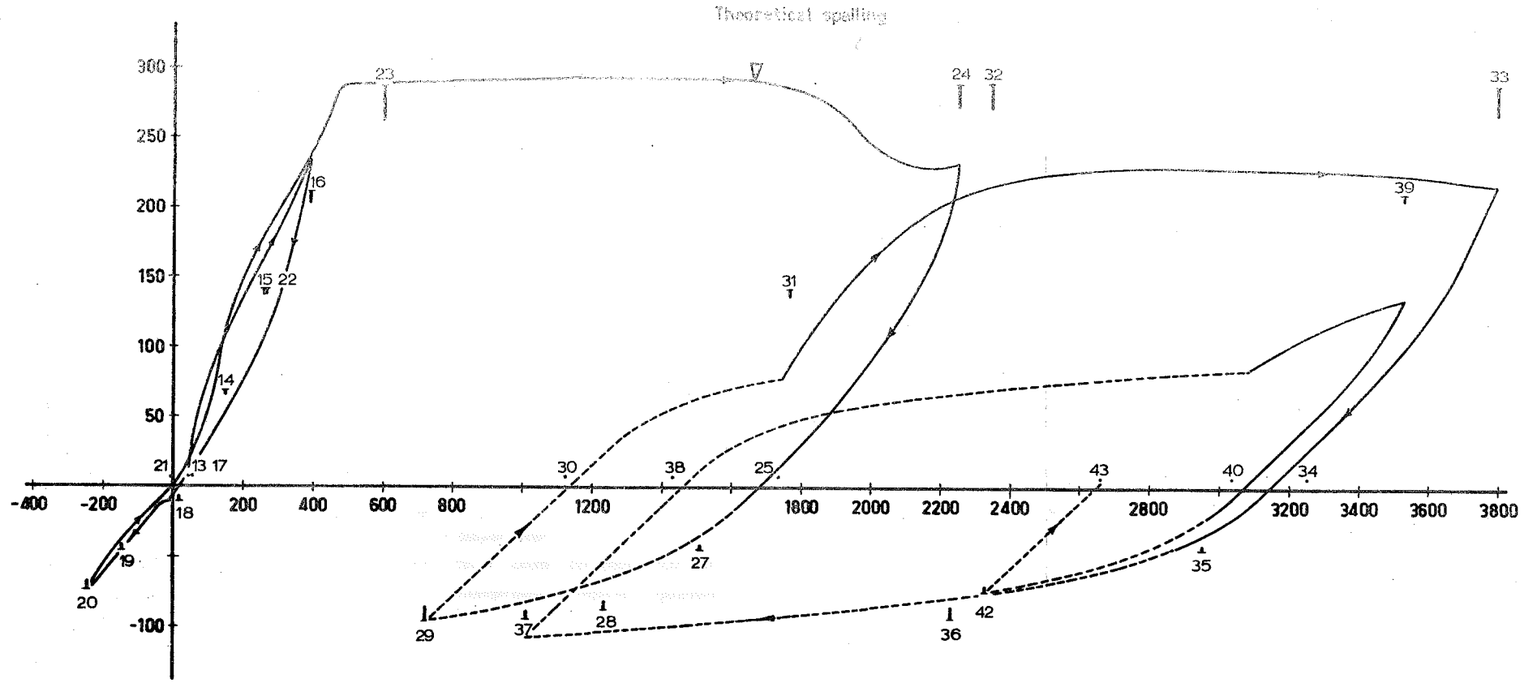

PHASE 2 - CYCLES 4-11

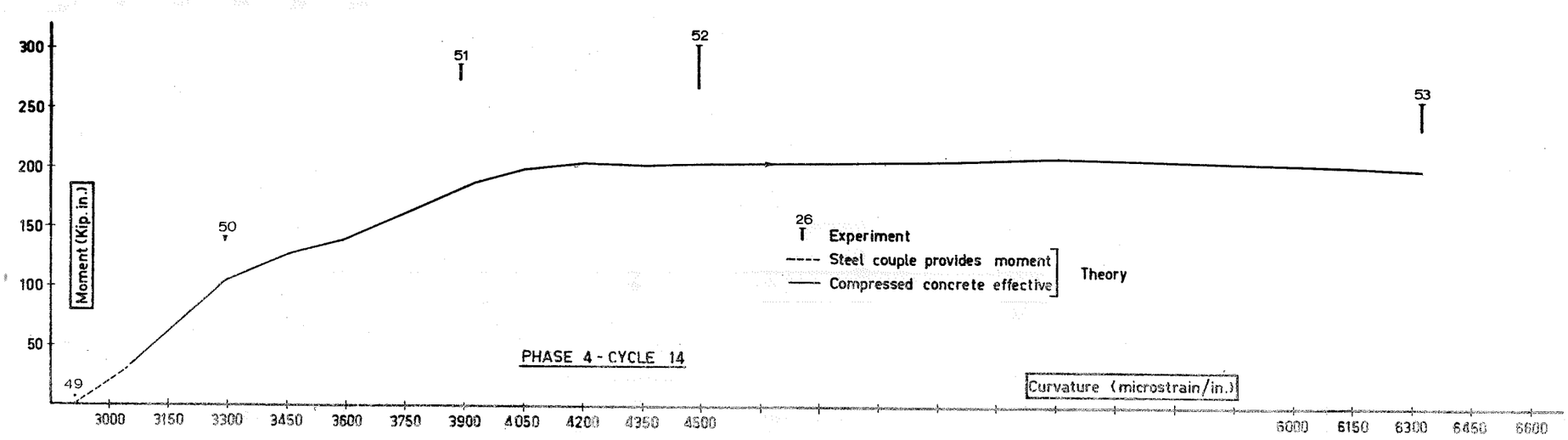

PHASE 4 - CYCLE 14

FIG.5.14 - MOMENT-CURVATURE FOR BEAM 67 PLASTIC HINGE

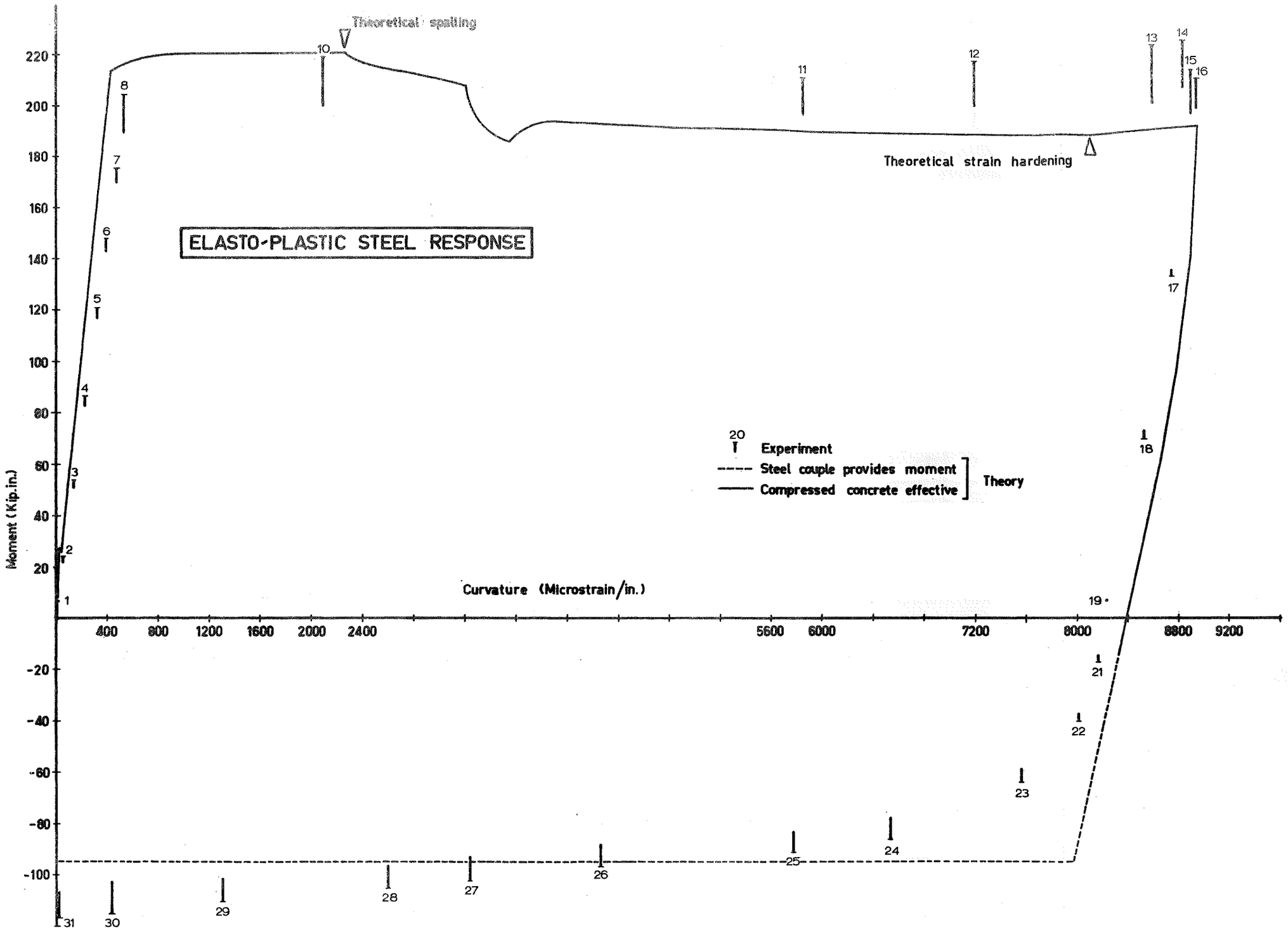

FIG.5.15 - MOMENT-CURVATURE FOR BEAM 26 PLASTIC HINGE

ELASTO PLASTIC STEEL RESPONSE

Cycles 1-6 (Load Stages 1-25) give results the same as those shown in Fig. 5.10

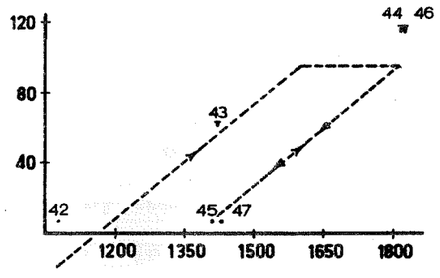

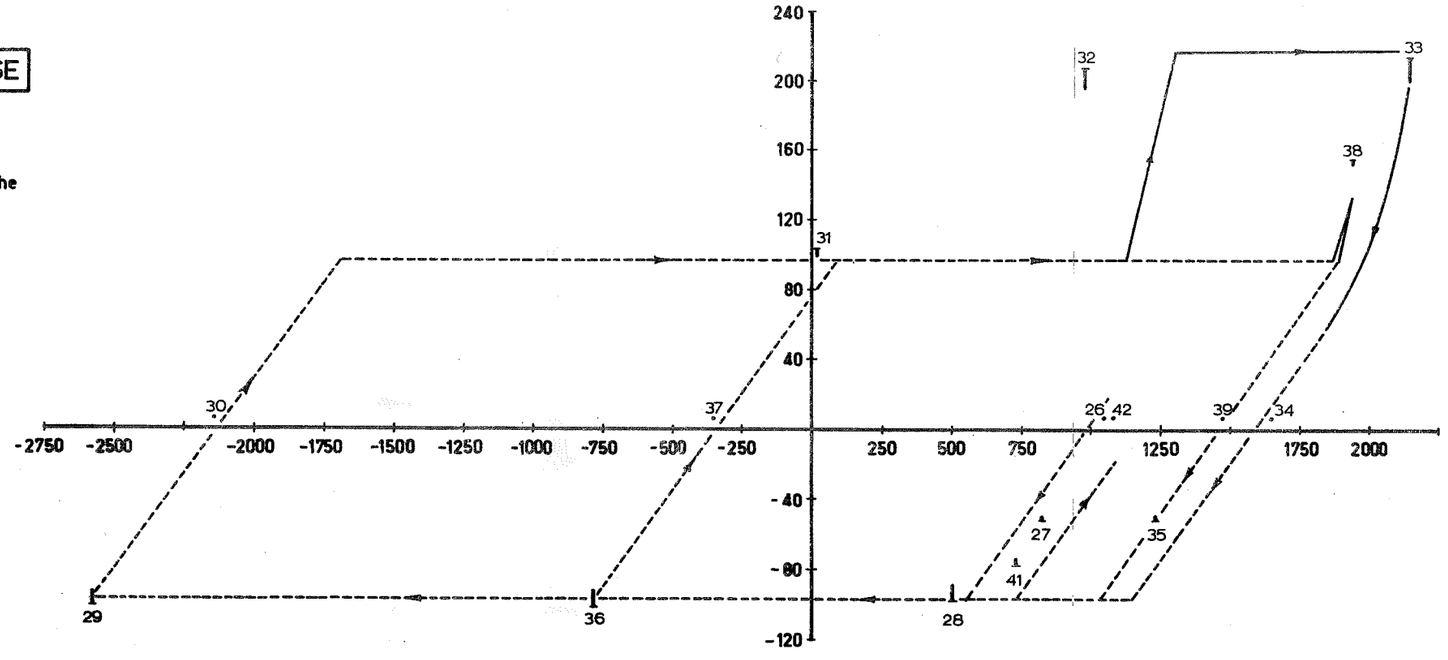

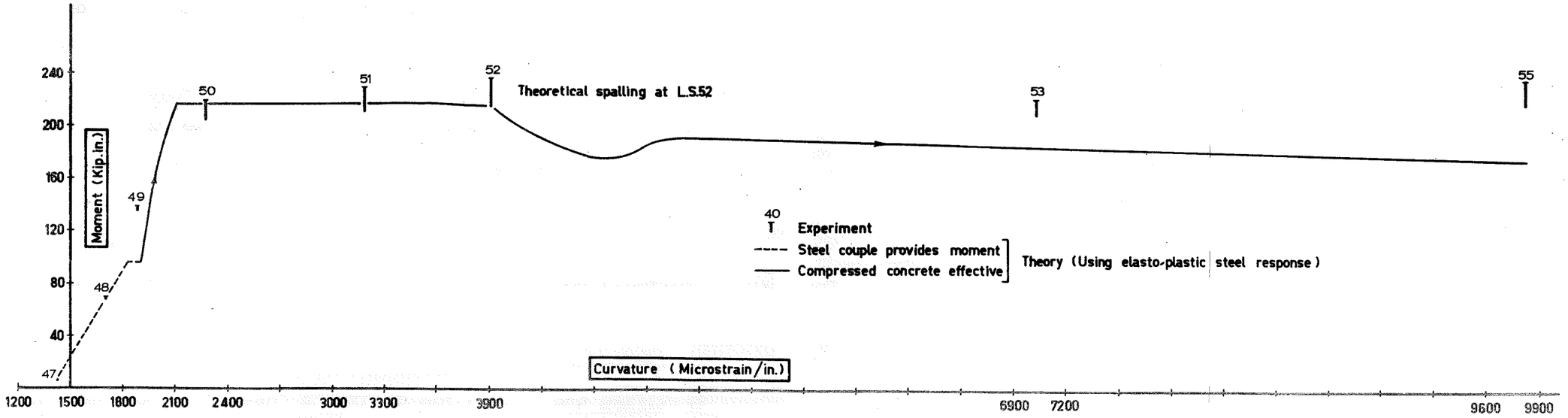

FIG.5.16 -MOMENT-CURVATURE FOR BEAM 46 PLASTIC HINGE

values in Figures 5.6 to 5.16. This reflects the creep that occurs between the termination of load application and the termination of readings. The moment reading nearest the load stage number corresponds to the bending moment before creep.

5.6 DISCUSSION OF EXPERIMENTAL AND ANALYTICAL RESULTS

A study of Figures 5.6 to 5.14 indicates two main areas of deviation of analytical from experimental responses.

The first of these is concerned with the transfer of response from purely steel couple action to that brought about by compressed concrete contribution. During initial yielding in each direction, large cracks open up due to the very large extensions taking place in the tension steel. On moment reversal, these large steel extensions must be reversed before the cracks close and the concrete sustains compressive stress again. That this occurs is quite well known and is experimentally illustrated in Figure 5.11 with load stages 30, 31, 32, 33. This phenomenon is accounted for in the theory but the concrete contribution is rather more sudden and produces a much greater stiffness than occurs in practice. Further, this concrete contribution tends to occur rather earlier in practice than in theory. The explanation for this discrepancy appears to be that in the real beam, "clean" cracks do not exist, and particles of concrete that flake off during cracking fill the cracks

and so the cracks effectively close more quickly. Also, because these particles do not comprise the full surface area of the cracked section, their contribution to stiffness is initially rather less and so a more "gentle" increase in stiffness than is represented by the theory takes place.

The second deviation of theory from practice is illustrated for Phase 4 of Beams 24, 27, 44, 46, 47 and 67. This last loading phase is a downward push to failure. Beams 27 and 46 show good agreement of theory and experiment for this phase but bending moment predictions for Beams 24 and 44 are rather high while for Beams 47 and 67 the prediction is low. In the case of Beams 24 and 44, both lightly reinforced with equal steel areas top and bottom, the cause of this deviation is derived from the limitation on the Bauschinger Effect expression described in Section 3.9.1. In these beams, the tension steel is highly strained and the theoretical stress corresponds to ultimate stress. This is due to the fact that the Ramberg-Osgood function it not assymptotic to a given limiting stress, and for the parameters used for this steel, the theoretical stress rises to an imposed limiting stress (ultimate) at comparatively low strains.

The case for Beams 47 and 67 is rather different. In these beams it is the inability to sustain additional

compression stress which results in the low bending moment predictions. Both are comparatively poorly confined with 4" and 6" stirrup spacing, and the concrete is highly strained, and the neutral axis rather low. Therefore, in theory, most of the unconfined concrete on the side of the section is ineffective, and with a low core width to total width ratio of 0.66, this unconfined concrete amounts to a large proportion of concrete area. With higher and more realistic ratios of core width to total section width, this discrepancy will become negligible.

The good agreement between theory and experiment exhibited in Phase 4 of Beams 27 and 46 is probably a result of the two effects described above cancelling each other.

Other aspects of the theoretical and experimental moment-curvature responses indicate very good agreement.

It is of interest to note the theoretical moment-curvatures produced by assuming elasto-plastic steel response. Figures 5.15 and 5.16 illustrate two such responses and may be compared with Figures 5.7 and 5.10 respectively. Because concrete stress plays such a minor role in the cyclic behaviour of sections, the moment-curvature inter-relationship follows the steel behaviour very closely. Consequently, an elasto-plastic steel gives an elasto-plastic moment-curvature relationship when the concrete is ineffective. The consequences of this

similarity are discussed more fully in Chapter 8.

5.7 COMPUTER PROGRAMS

Two computer programs were written for this section of the work and listings appear in Appendix B.

Program 5.1 ("CYCBAUS"): Cyclic loading of reinforced concrete T sections with or without axial compression, using up to 500 discrete elements for concrete force, and using the Bauschinger Effect representation for reinforcing steel developed in Chapter 3.

Program 5.2 ("CYCBMS"): As for Program 5.1 but using an elasto-plastic reinforcing steel response.

5.8 CONCLUSIONS

It has been shown that the theories for concrete and steel behaviour developed in Chapters 2 and 3 can be applied to cyclically-loaded reinforced concrete sections. Further, that this application results in moment-curvature responses that, with some exceptions, show good agreement with experimentally-obtained behaviour. These exceptions are: that the Ramberg-Osgood function for Bauschinger Effect limits the absolute steel strains (considering the strain at which stress was last zero as origin) for good theoretical predictions; and that the assumption of a limiting concrete strain above which the concrete is considered to be

ineffective requires the ratio of bound concrete width to total section width, to be reasonably high for low p'/p ratios.

Figures 5.15 and 5.16 comparing experimental moment-curvature responses with theory using an elasto-plastic reinforcing steel stress-strain relationship, illustrate the necessity for a consideration of the Bauschinger Effect.

The computer programs currently use curvature readings as input for determining the point at which moment reversal is to take place. This has proved the most successful method of testing the analysis against the available test data. It may well be that in using the programs for prediction of deformations, required energy-absorptions would be a more useful input. The modifications to the programs required to allow for this are very minor.

CHAPTER 6

DEFLECTION ANALYSIS FOR REINFORCED CONCRETE MEMBERS

SUMMARY

The theory advanced in Chapter 5 is extended to predict the deflection behaviour of reinforced concrete members and is compared with experimental load-deflection plots. Clough's idealised degrading stiffness model is confirmed as a reasonable design approximation.

6.1 INTRODUCTION

Building on theory developed in earlier chapters, the analysis has been extended beyond the consideration of concrete sections to members composed of a number of such sections. This chapter is concerned with deflection profiles for a cyclically-loaded simple cantilever. Some generality is obtained by considering a cantilever as half of a simply-supported beam, such that the fixed end of the cantilever coincides with the centre of the beam span.

A computer program is developed for the determination of loads and bending moments for given deflections.

The general T shape is retained but no provision is made for axial load. Constant section properties throughout the length of the beam are assumed and point loading at the cantilever free end, or uniformly distributed loading, are permitted.

A further computer program utilises Clough's "Degrading Stiffness" property as a moment-curvature model and is used to produce comparison load-deflection profiles.

An elasto-plastic load-deflection plot illustrates the inadequacy of this idealisation.

6.2 BENDING MOMENT DISTRIBUTION

Figure 6.1 illustrates a point-loaded cantilever and the resulting bending moment diagram. The cantilever is considered as comprising N_s sections of equal length such that their combined length is ($l_c d$) inches. The point load is (Pbd) lb., i.e. P is in stress units.

Section numbering starts at the cantilever fixed end. Each of these sections is described by NEL discrete horizontal elements so that each is analysed in the same way as were the cyclically-loaded sections in the previous chapter.

The average bending moment in any section, i, of the point-loaded cantilever is given by:

$$M_{P_i} = (Pbd)(l_c d)(1 - \frac{2i - 1}{2N_s}) \qquad \ldots\ldots(6.1)$$

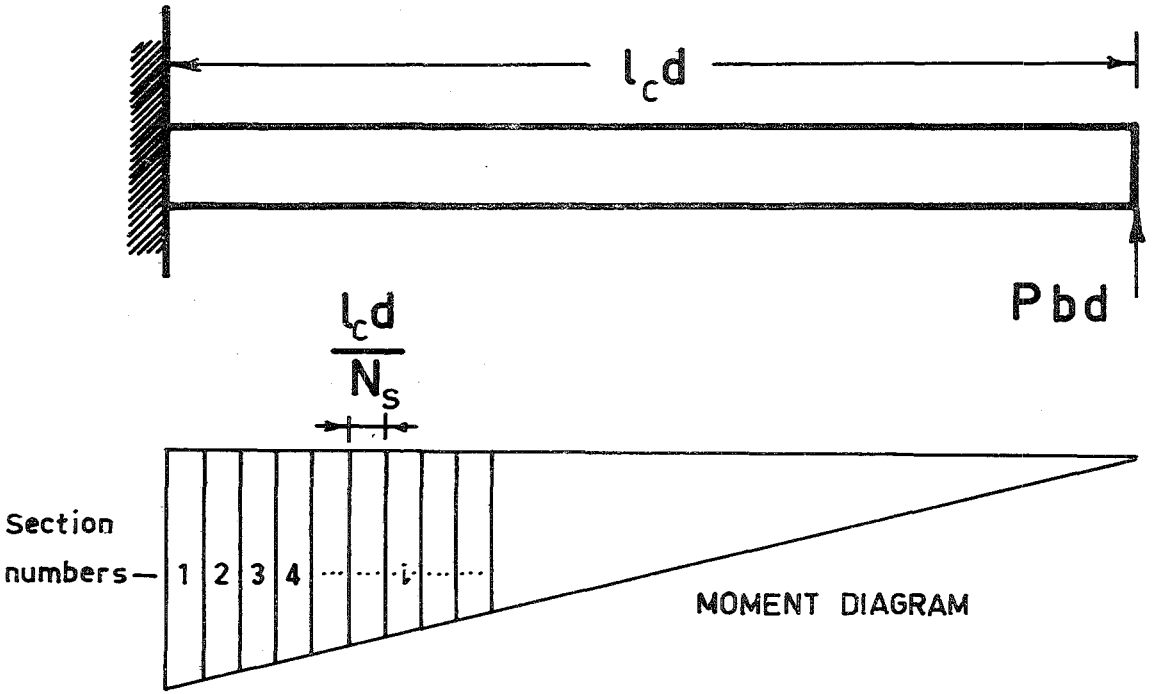

FIG.6.1 - POINT-LOADED CANTILEVER

or more generally,

$$\frac{M_{P_i}}{bd^2} = Pl_c\left(1 - \frac{2i - 1}{2N_s}\right) \qquad \ldots\ldots(6.2)$$

If the cantilever is deformed by a uniformly-distributed load, (wb) lb./in., the bending moment in section i is represented by:

$$\frac{M_{W_i}}{bd^2} = \frac{wl_c^2}{2}\left[1 - \frac{2i - 1}{2N_s}\right]^2 \qquad \ldots\ldots(6.3)$$

The analysis developed in this chapter uses a predetermined bending moment in section 1 to establish the loading and hence bending moments in all other sections. Fuller details of this aspect of the analysis are given in Section 6.5.

6.3 DEFLECTION COMPUTATIONS - "EXACT" METHOD

Member deflections may be computed from the rotations (or curvatures) present in each section.

The "exact" method of computing deflections may be illustrated by considering Figure 6.2 which shows the configuration of beam section 1.

The curvature in section 1 is ϕ_1 radians in.$^{-1}$ and therefore the beam rotation caused by the curvature in this

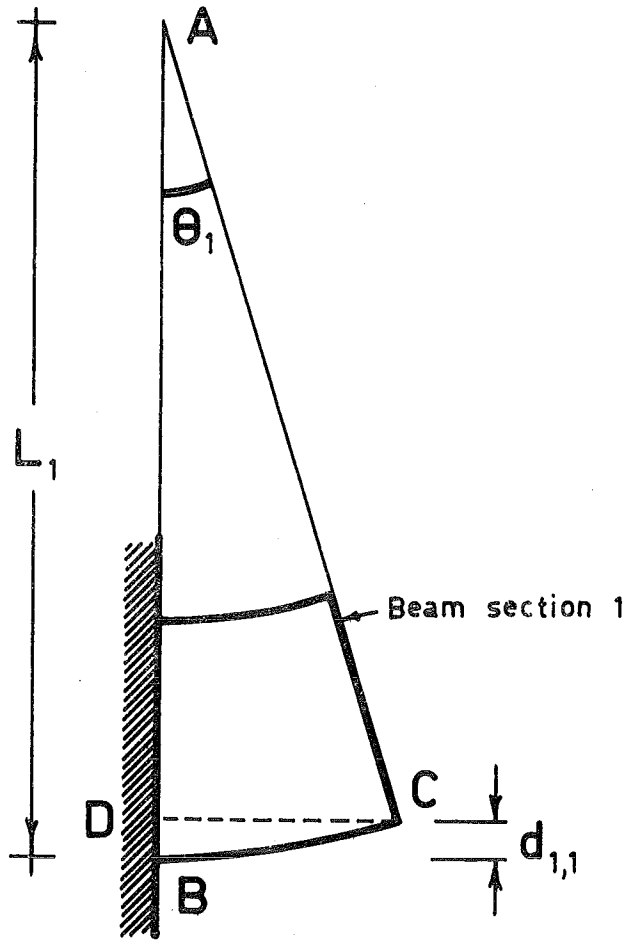

FIG.6.2 - DEFLECTION COMPUTATIONS "EXACT" METHOD

section is:

$$\theta_1 = \phi_1 \frac{l_c d}{N_s} \text{ radians} \qquad \ldots\ldots(6.4)$$

The deflection at the interface of sections 1 and 2 caused by the curvature in section 1 is represented by $d_{1,1}$ and using the Sine rule and triangle ACD of Figure 6.2 we have:

$$L_1 = \frac{L_1 - d_{1,1}}{\sin(\frac{\pi}{4} - \theta_1)} = \frac{L_1 - d_{1,1}}{\cos \theta_1}$$

hence $d_{1,1} = L_1 (1 - \cos \theta_1)$

If ϵ_{bc} is the strain along arc BC

then $\theta_1 = \frac{l_c d}{L_1 N_s} (1 + \epsilon_{bc})$

$$\therefore d_{1,1} = \frac{l_c d}{\theta_1 N_s} (1 - \cos \theta_1)(1 + \epsilon_{bc}) \qquad \ldots\ldots(6.5)$$

Equation (6.5) illustrates the difficulty of using this method for deflection computations. The term $(1 - \cos \theta_1)$ is very small and instability results from the product of this term and the large value for $(l_c d/\theta_1 N_s)$.

6.4 DEFLECTION COMPUTATIONS - "APPROXIMATE" METHOD

Prior to a discussion of the "approximate" method, it is

necessary to define the notation used.

ϕ_i = curvature (radians. in^{-1}) in section i

θ_i = rotation (radians) in section i

ψ_i = cumulative rotation at interface of sections (i - 1) and i due to rotations in section 1 to i - 1

$d_{i,1}$ = deflection contribution (inches) due to ϕ_i

$d_{i,2}$ = deflection contribution (inches) due to ψ_i

$d_i = d_{i,1} + d_{i,2}$ = deflection contribution (inches) of section i

D_i = cumulative deflection contributions (inches) of sections 1 to i. Hence D_i is the deflection (with respect to the fixed end) at the interface of sections i and (i + 1).

Figure 6.3 shows sections 1 and 3 of a deflected cantilever. By referring to Figure 6.3(i) it can be seen that for section 1:

$$\psi_1 = 0$$

$$d_{1,1} = \frac{l_c d}{N_s} \frac{\theta_1}{2} = \left(\frac{l_c d}{N_s}\right)^2 \frac{\phi_1}{2} \qquad \ldots\ldots(6.6)$$

The approximation used in this method, then, is that

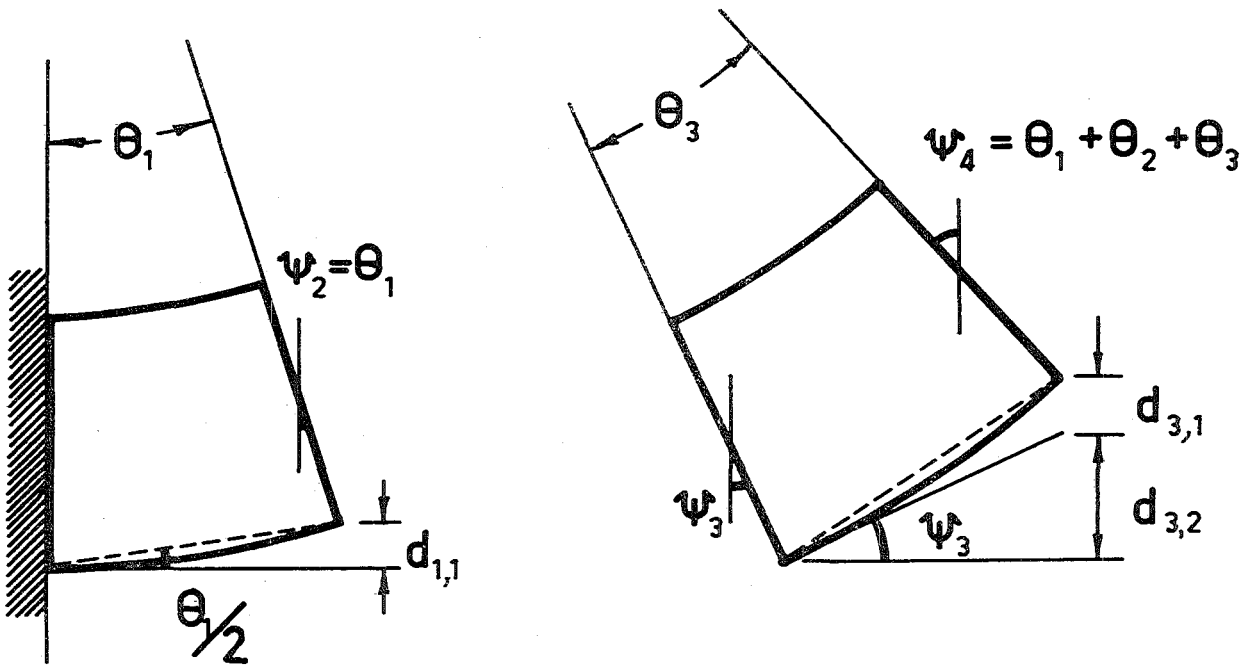

FIG.6.3 - DEFLECTION COMPUTATIONS "APPROXIMATE" METHOD

$\sin(\Theta/2) = (\Theta/2)$ and for the small Θ values encountered, the error is not large.

Further,

$$d_{1,2} = 0$$

$$d_1 = d_{1,1} + d_{1,2} = d_{1,1}$$

$$D_1 = d_1 = d_{1,1}$$

in more general form:

$$\frac{D_1}{d} = \left(\frac{l_c}{N_s}\right)^2 \frac{(\phi_1 d)}{2} \qquad \ldots\ldots(6.7)$$

where $(\phi_1 d)$ is dimensionless curvature and (D_1/d) is dimensionless deflection.

Figure 6.3(ii) shows section 3 for a deflected cantilever and it can be seen that:

$$\psi_3 = \Theta_1 + \Theta_2$$

$$d_{3,1} = \left(\frac{l_c}{N_s}\right)^2 d \frac{(\phi_3 d)}{2}$$

$$d_{3,2} = \psi_3 \frac{l_c d}{N_s} = (\Theta_1 + \Theta_2) \frac{l_c d}{N_s}$$

$$= \left(\frac{l_c}{N_s}\right)^2 d\left[(\phi_1 d) + (\phi_2 d) + \tfrac{1}{2}(\phi_3 d)\right]$$

It can be shown that:

$$D_3 = \left(\frac{l_c}{N_s}\right)^2 d \left[\frac{(\phi_1 d) + (\phi_2 d) + (\phi_3 d)}{2} + 2(\phi_1 d) + (\phi_2 d)\right] \qquad \ldots\ldots(6.8)$$

From Equation (6.8), the trend for the general expression for deflection is:

$$D_i = \left(\frac{l_c}{N_s}\right)^2 d \left[\frac{1}{2}\sum_{m=1}^{i} (\phi_m d) + \sum_{n=1}^{i} (i-n)(\phi_n d)\right]$$

$$= \left(\frac{l_c}{N_s}\right)^2 d \left[\sum_{m=1}^{i} (\tfrac{1}{2} + i - m)(\phi_m d)\right]$$

or $$\frac{D_i}{d} = \left(\frac{l_c}{N_s}\right)^2 \sum_{m=1}^{i} (\tfrac{1}{2} + i - m)(\phi_m d) \qquad \ldots\ldots(6.9)$$

The deflection expression, then, is a series and may be rewritten as:

$$\frac{D_i}{d}\left(\frac{N_s}{l_c}\right)^2 = \frac{1}{2}(\phi_i d) + \frac{3}{2}(\phi_{i-1} d) + \frac{5}{2}(\phi_{i-2} d) + \ldots\ldots + \frac{2i-1}{2}(\phi_1 d) \qquad \ldots\ldots(6.10)$$

6.5 DEVELOPMENT OF COMPUTER PROGRAM

A computer program was written for the computation of member loads, moments and deflections. As with all previous programs, the dimensions b and d were eliminated as input parameters and the input requirements were similar to those for the program discussed in Chapter 5.

Additional input requirements were the parameters l_c and N_s. In the programs (Chapter 5) for cyclic loading of

sections computed within stipulated curvature cycles, the dimensionless curvature values corresponding to the extremities of each cycle were required. In this program, the method was similar although deflection cycles were being considered, and therefore dimensionless deflection readings were required as input to define the extremities of cycles. Finally, a code number indicating either point or uniform loading is required.

The cantilever sign convention used is compression strain, upward deflection and upward loading positive. This convention is not that generally used for cantilevers, but was the most convenient for comparison with beam experiments. For such an application, the theoretical load corresponds to the end reaction of a simply-supported beam.

Iterations within deflection cycles were performed by increasing or decreasing the concrete strain in the top concrete element, ϵ_{cm}, of section 1, depending on whether it was desired to increase or decrease the deflection of the beam. Using the same iterative technique as that discussed in Section 5.4, the neutral axis depth, bending moment and curvature were evaluated for section 1. Using either Equation (6.1) or Equation (6.3), the loading producing this bending moment in section 1 could be established and hence the bending moments in the remaining sections determined.

The procedure for each of these remaining sections was to increase or decrease the ϵ_{cm} value obtained for that

section in the previous increment, locate the neutral axis depth from force compatibility, and then compute the bending moment in the section for the given trial value of ϵ_{cm}. The computed bending moment was then compared with that required and ϵ_{cm} adjusted, and the iteration repeated, until the computed and required bending moments coincided to within 1 per cent of the required moment. If computed moments were not within this limit after twenty trial values for ϵ_{cm}, the ϵ_{cm} value giving the least bending moment error for that section was selected. In this way, bending moments and curvatures for all sections were calculated.

Having obtained curvatures for all sections, the deflection profile was calculated using Equation (6.9) and the computed deflection at the free end of the cantilever was then compared with the input value limiting the deflection in the cycle under consideration. This process continued until the computed deflection was found to exceed the input value for the cycle, when an assumed linear relation between ϵ_{cm} for section 1 and the deflection in the previous cycle, and ϵ_{cm} for section 1 and the deflection in the current cycle, was used to give a value for ϵ_{cm} in section 1, that would produce a cantilever free-end deflection that coincided with the input requirements. In most cases this linear assumption was found to be

satisfactory, though not as accurate as when applied to moment-curvature behaviour (q.v. Section 5.4).

6.6 COMPARISON OF THEORY WITH EXPERIMENT

The experimental load-deflection plots for two beams were used to test the validity of the theory developed in this chapter. The measured deflection readings at beam midspan were corrected to "Equivalent Central Deflections" and this step is discussed fully in Chapter 7.

Figures 6.4 and 6.5 illustrate the experimental and theoretical load-central deflection plots for Beams 24 and 46 respectively.

Prior to a discussion of theoretical and experimental comparisons, it is of interest to note one aspect of the theoretical behaviour. The load-deflection response of the beam is greatly influenced by the moment-curvature behaviour at the critical section (c.f. Figures 5.6 and 5.10). Although it is obvious that this must be the case, the actual extent of this influence is very marked. This effect is probably accentuated by the fact that each beam shank (cantilever) was comprised of only 9 sections, and each section of only 10 discrete horizontal elements, owing to limitations in the core store of the computer at the time. The errors induced by having only 10 elements per section would be of the order of 10 per cent at most, but it is difficult to assess the effect that the number of

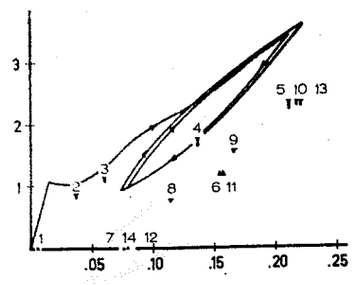

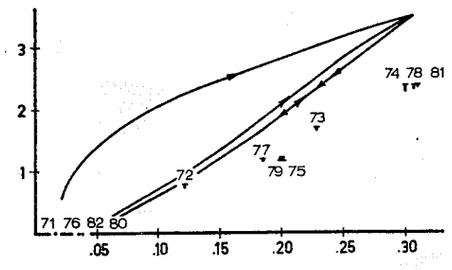

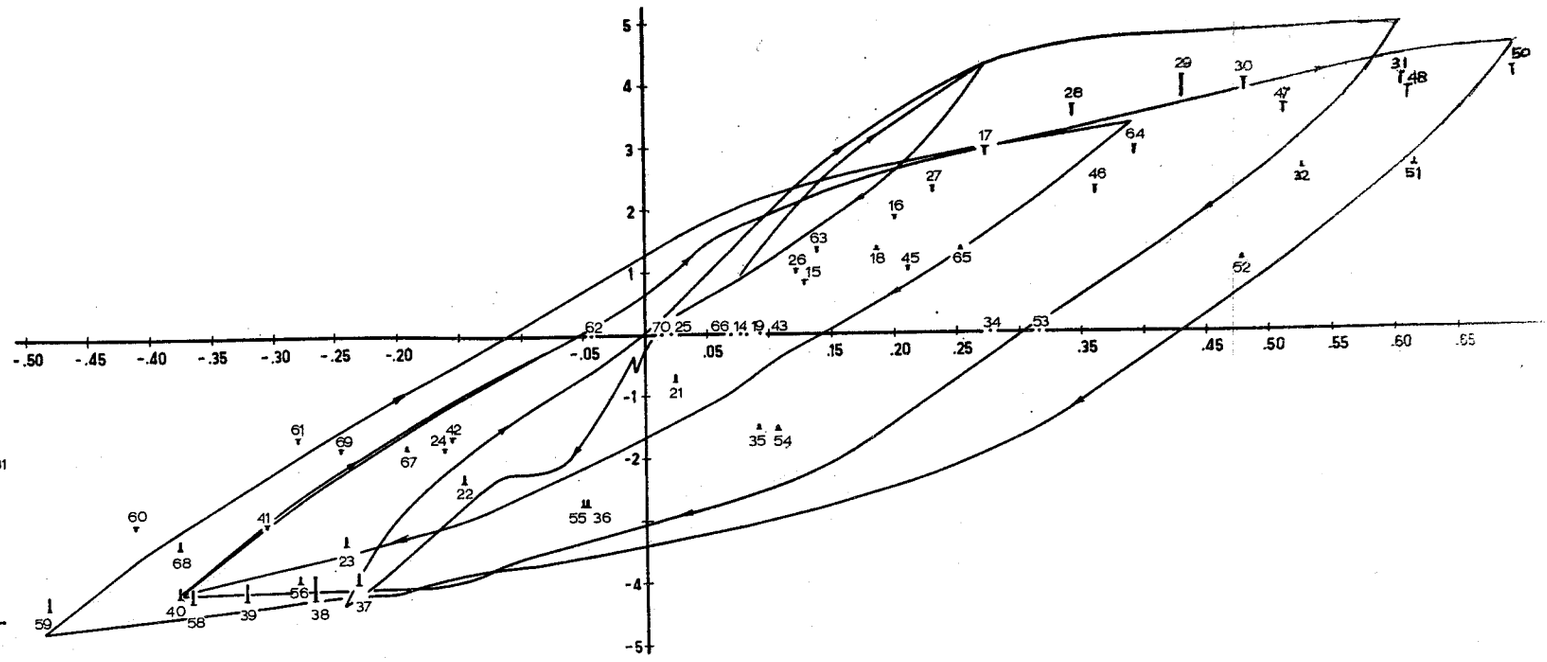

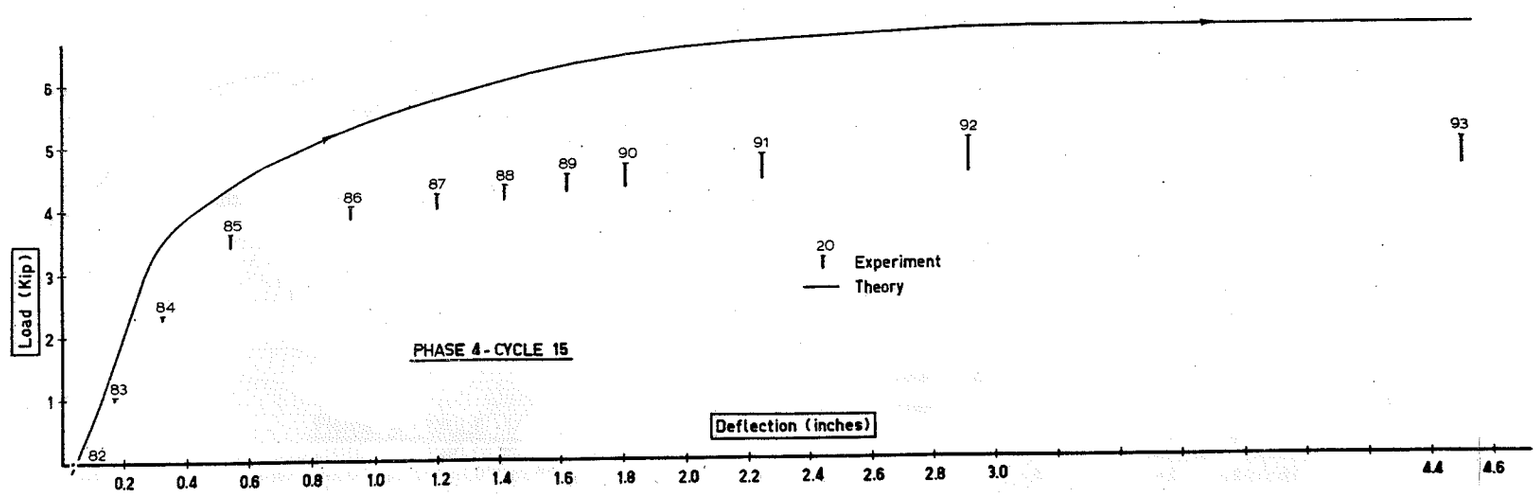

FIG.6.4 - LOAD vs EQUIVALENT CENTRAL DEFLECTION FOR BEAM 24

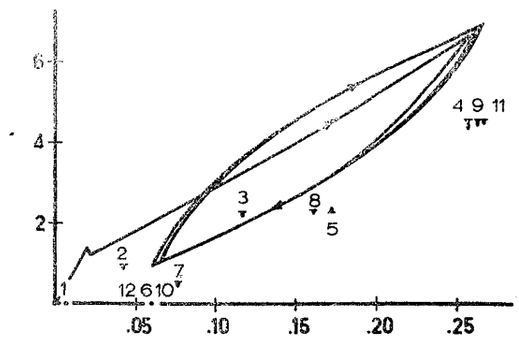

PHASE 1 - CYCLES 1-3

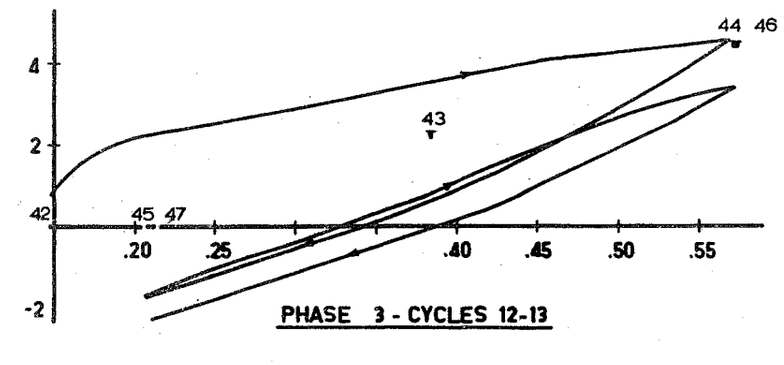

PHASE 3 - CYCLES 12-13

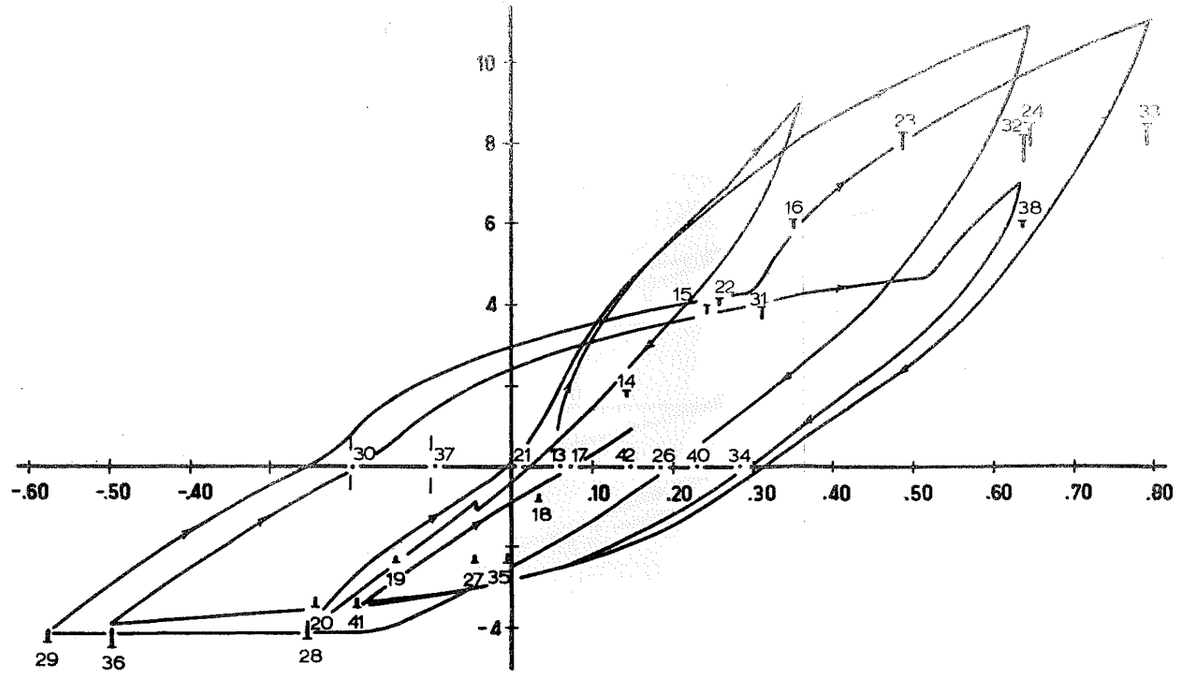

PHASE 2 - CYCLES 4-11

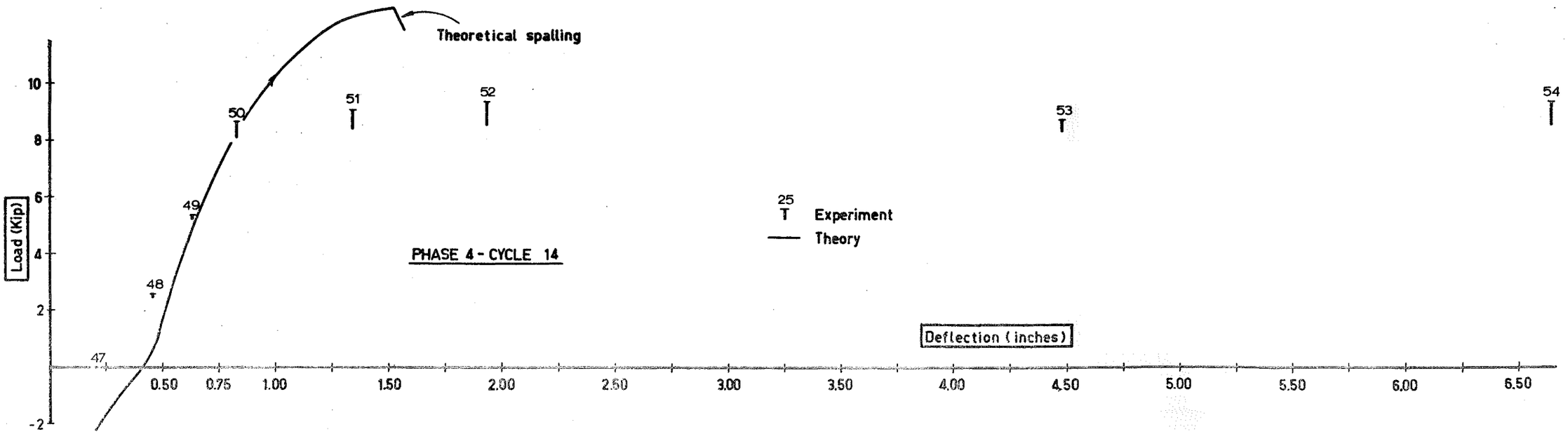

FIG.6.5 - LOAD vs EQUIVALENT CENTRAL DEFLECTION FOR BEAM 46

sections has on the accuracy. The choice of number of sections effectively stipulates the plastic hinge length (i.e. plastic hinge length = integer x section length), and in this case each section was (50/9) inches long. Despite the low accuracy (9 sections of 10 elements) chosen for the theoretical load-deflection analyses, computer time required was 3 hours and 4 hours respectively for Beams 24 and 46.

In comparing the theoretical and experimental responses, it can be seen that for given deflection values, the theoretical loads are generally higher than the observed loads. This difference in load value can be reduced slightly by using more sections to represent the cantilever length, as shown later in this chapter.

That the closing of cracks at the critical section increases the beam stiffness as a whole is illustrated in Figure 6.5. This behaviour is supported experimentally by load stages 30, 31, 32 and 33. In Phase 4 (on Figure 6.5) the theoretical analysis broke down when crushing occurred in section 1. The reduction in moment caused a reduction in load and moments in all other sections, and resulted in a smaller deflection immediately after crushing than at the point of crushing, and so the run was terminated.

Higher theoretical loads (compared with observed loads at the same deflection) was a phenomenon that was contrary

to the behaviour that had been expected initially, as the analysis described here takes no account of the increased stiffness between cracks in a reinforced concrete beam. Priestley[53] has developed a theory for assessing the increased stiffness between cracks in Prestressed Concrete beams and found this to produce very good predictions of beam deflection.

On further investigation, an apparent anomaly emerges which makes a study of this feature very difficult for cyclic loading. Also, the findings of ACI Committee 435[54] seem to indicate that the effect of increased stiffness between cracks is negligible for highly-loaded reinforced concrete beams. The following equation has been recommended by ACI Committee 435 for determining the effective design stiffness of cracked sections:

$$I_{eff} = \left(\frac{M_{crk}}{M_{max}}\right)^3 I_g + \left[1 - \left(\frac{M_{crk}}{M_{max}}\right)^3\right] I_{crk} \qquad ....(6.11)$$

where M_{crk} = cracking moment,

M_{max} = maximum moment,

I_g = moment of inertia of gross section, neglecting the steel,

I_{crk} = moment of inertia of cracked transformed section,

I_{eff} = effective moment of inertia.

In most highly-loaded concrete beams, the ratio

(M_{crk}/M_{max}) is quite small (approximately 0.2 for the beams in this investigation), thus the cube becomes negligible and $I_{eff} \rightarrow I_{crk}$.

For prestressed concrete beams, the M_{crk}/M_{max} ratio is significantly higher.

The theory advanced by Priestley is based on monotonically-loaded prestressed concrete beams, and utilises the bond stress distribution to obtain tension steel stress at any point between cracks, by reducing this stress below that at the crack. In its present form, the theory cannot be extended to consider cyclically-loaded reinforced concrete beams since the Bauschinger Effect complicates the stress distribution. This is illustrated in Figure 6.6 which shows a "tension" steel stress-strain history at a cracked section. To simplify the following explanation, it has been assumed that the bottom steel stress midway between cracks is 90 per cent of that at the crack. It will be seen that the exact percentage, which will be variable anyway, is not relevant to this discussion.

In cycle 0, (Figure 6.6(i)), the bottom steel has yielded to a strain of 0.01 at the crack and thus the steel midway between cracks remains elastic at a stress of 0.9 f_y.

In cycle 1, (Figure 6.6(ii)), the bottom steel is subjected to compression stress and so the bond behaviour is unimportant. However, a Bauschinger response has been initiated.

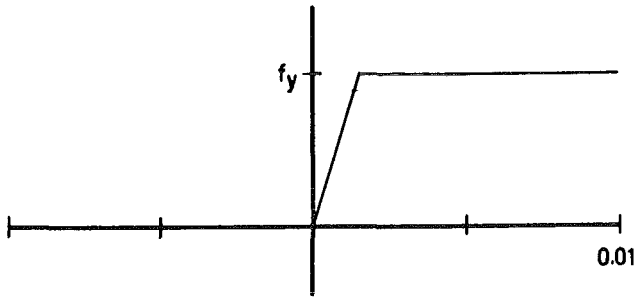

(i) CYCLE 0

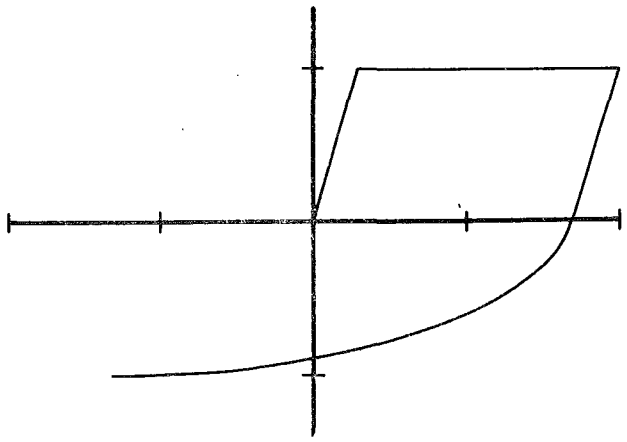

(ii) CYCLE 1

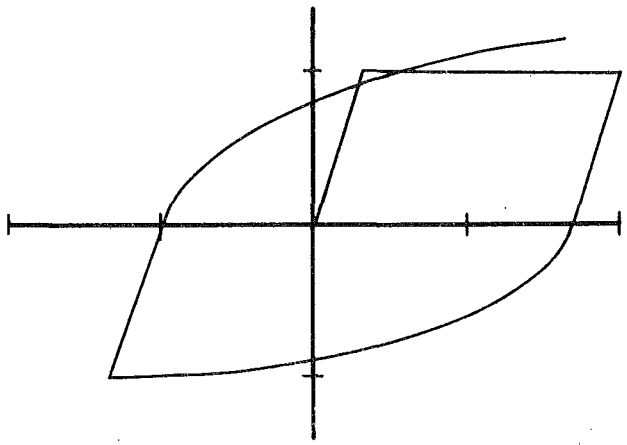

(iii) CYCLE 2

FIG.6.6 - THE BOND STRESS ANOMALY

In the final cycle shown (Figure 6.6(iii)), the bottom steel stress at the crack has risen to 1.20 f_y at a tension strain of 0.008. The assumed 10 per cent stress reduction for steel between cracks requires a stress of 1.08 f_y. Therefore this section of the steel, which has remained elastic up until this point, is strain hardening at a strain of the order of three times that at the crack. This is clearly impossible.

An event has been excluded from the discussion of cycle 1 which explains why this anomaly is only "apparent". In cycle 0, the concrete at the bottom of the beam will crack. In cycle 1, the concrete at the top of the beam will crack and a fully-cracked section develops. Therefore, whether or not bond stress is effective in increasing stiffness is irrelevant, as the beam now becomes sections of concrete joined with reinforcing steel.

As with moment-curvature behaviour then, the main benefit derived from the concrete after cyclic loading, is that it prevents steel from buckling and maintains the lever arm. Further, it would appear that resistance to shear must rely almost entirely on dowel action, and perhaps to a lesser and irregular extent, on aggregate interlock.

6.7 LOAD-DEFLECTION RESPONSES USING IDEALISED MOMENT-CURVATURE MODELS

The view that Moment-Curvature responses are difficult to idealise accurately has already been expressed. It is obvious, however, that some simplification is necessary as considerable computer time is required to produce load-deflection plots using the theory developed in this thesis.

As Clough's "Degrading Stiffness" approximation is intuitively better than the elasto-plastic assumption, and has been shown in Chapter 5 to be more accurate, it was decided to apply this property (in the form of a moment-curvature response) to a cantilever subjected to point loading.

A computer program (Program 6.2) was written for this purpose and provision was made for differing initial (and unloading) stiffnesses for both positive and negative moments.

The experimental deflection cycles of Beam 24 were used as data to test this idealisation and analyses were performed with 10 and 100 beams sections. The results are shown in Figure 6.7.

It will be appreciated that since the bending moment in section 1 must be greater than that in all other sections, then all other sections must remain elastic. This results in a theoretical load-deflection plot that is

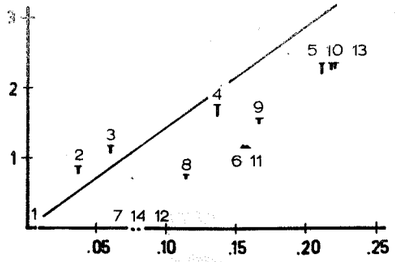

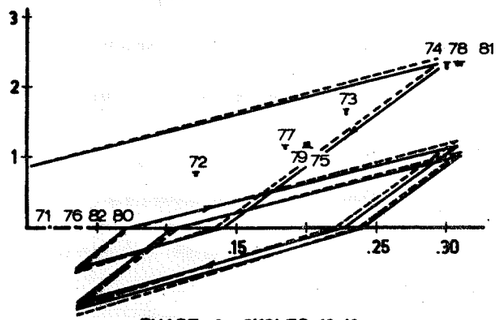

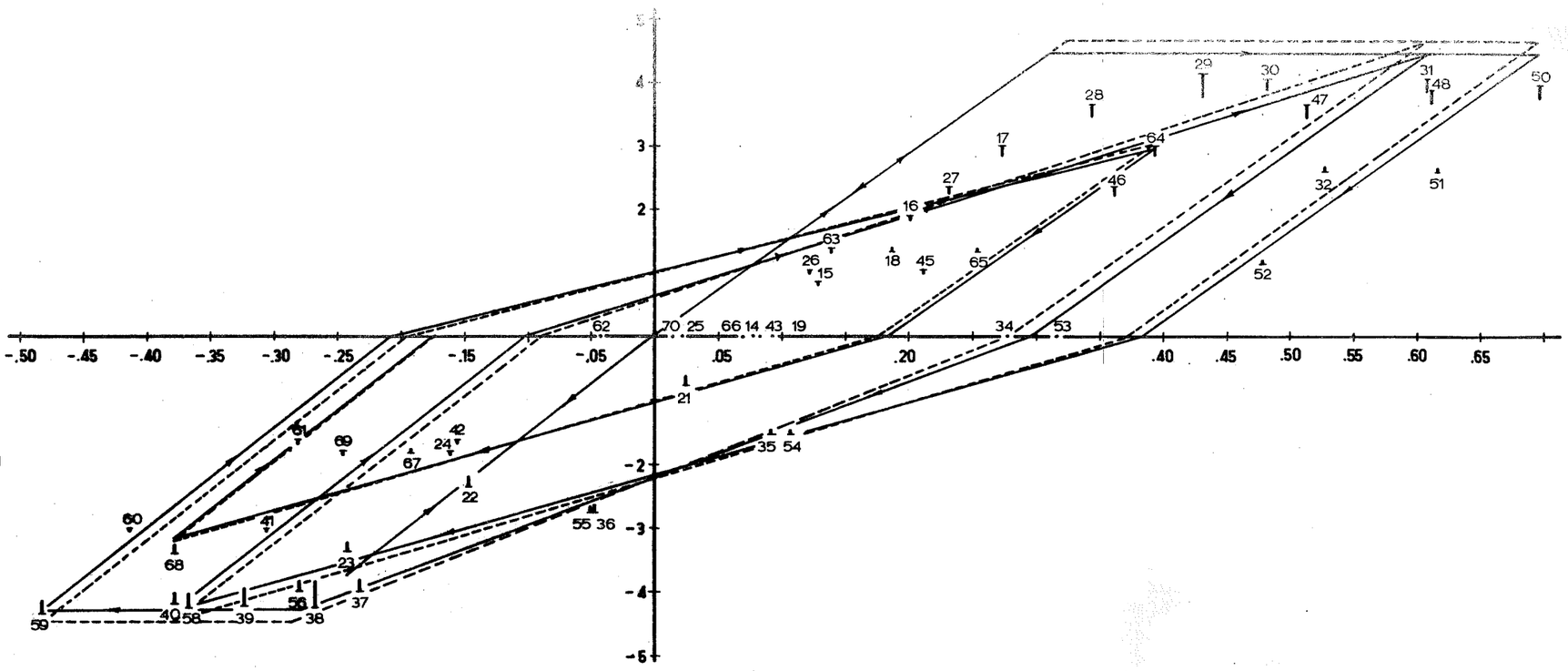

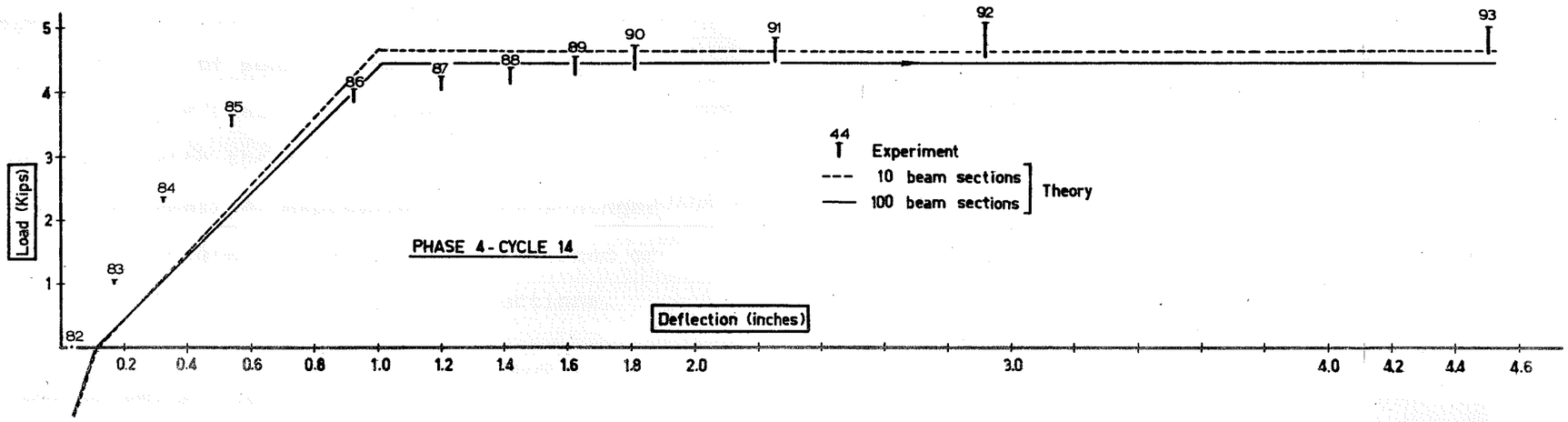

FIG.6.7 - LOAD vs EQUIVALENT CENTRAL DEFLECTION FOR BEAM 24 - DEGRADING STIFFNESS RESPONSE

almost entirely dependent on the moment-curvature behaviour at the critical section. The implications of this feature are discussed in Chapter 8.

Figure 6.8 shows the experimental load-deflection plot of the earthquake simulation cycle for Beam 46 compared with the traditional elasto-plastic model.

6.8 COMPUTER PROGRAMS

Two computer programs were developed to solve load-deflection responses of Reinforced Concrete cantilevers.

Program 6.1 ("BEAMDEFS"): Described in Section 6.5.

Program 6.2 ("CLOUGH"): Described in Section 6.7.

Listings of both programs and details for their use appear in Appendix B.

6.9 CONCLUSIONS

It has been shown that the theoretical cyclic behaviour of reinforced concrete sections can be extended to predict load-deflection responses of members comprising a number of such sections. That these analytical curves do not correspond particularly well with the two experimental plots is due to the inexact mathematical expression for Bauschinger Effect, and to a lesser degree, to the behaviour forced on the model by the choice of the number of beam sections.

The impracticability of using this analysis as a design tool has been emphasised by the considerable computer time

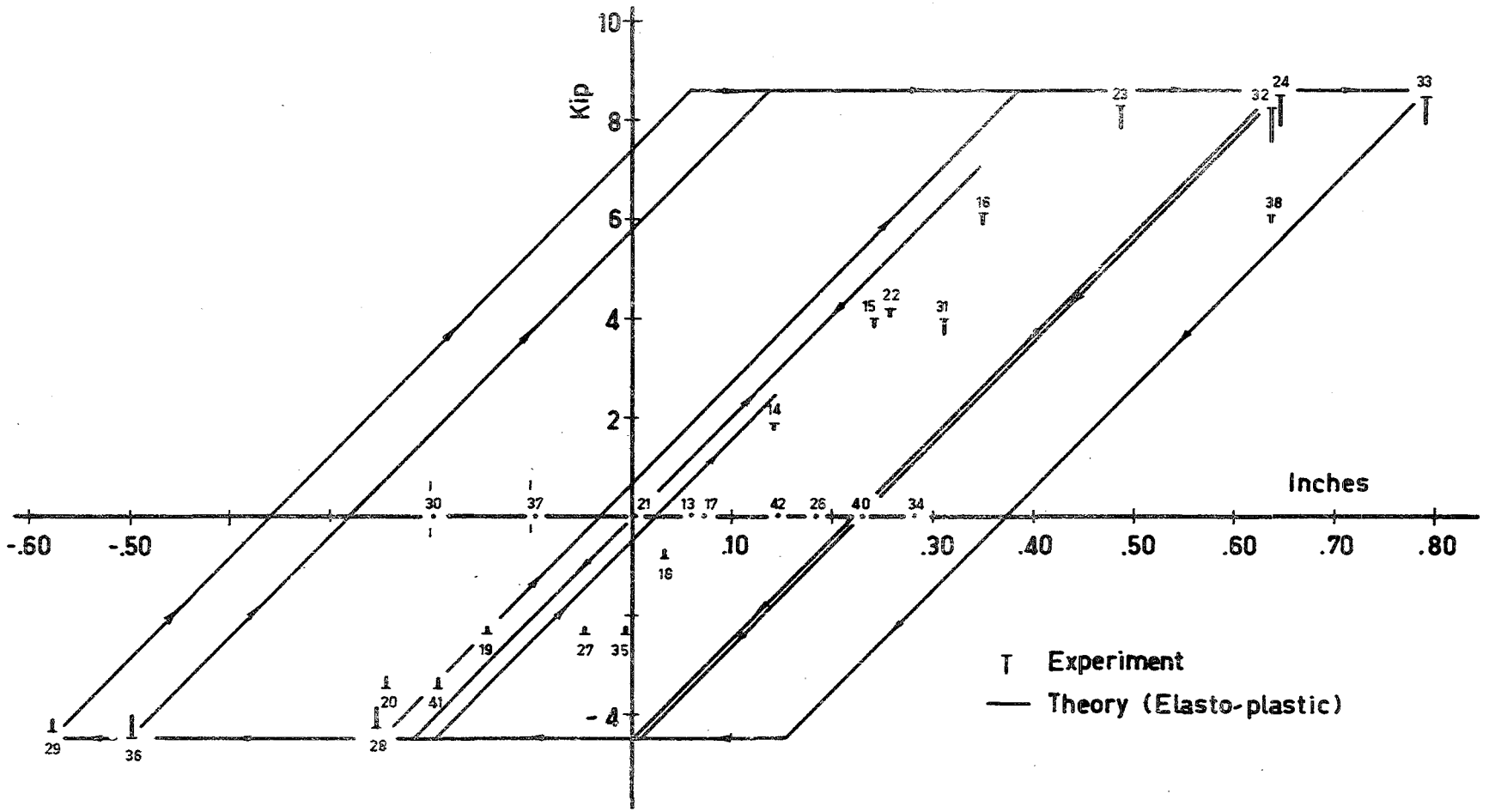

FIG.6.8 - LOAD vs EQUIVALENT CENTRAL DEFLECTION FOR BEAM 46

required to obtain load-deflection profiles for even a simple cantilever. However, given a more exact representation of the Bauschinger Effect, the analysis could be used to produce "exact" load-deflection profiles that could be systematically idealised to give realistic load-deflection models for design purposes.

Clough's Degrading Stiffness model is generally conservative both when applied as a moment-curvature and as a load-deflection response.

Conversely, the elasto-plastic model has been shown to predict considerably more energy absorption than is in fact available.

CHAPTER 7

EXPERIMENTAL RESULTS FROM REINFORCED CONCRETE BEAMS

SUMMARY

Eleven reinforced concrete beams were tested to obtain experimental comparison with the theories developed in this thesis. Of particular significance was the moment-curvature responses of the plastic hinges and load-deflection behaviour of these beams, which have been compared with theory in previous chapters. This chapter discusses the aims, limitations and results of this experimental programme, and also compares the measured lengths of plastic hinges with some design expressions proposed by other investigators.

7.1 INTRODUCTION

The tests on beams described in this thesis were conducted with the aim of comparing the results so obtained with the theories of the previous chapters.

A large number of readings and measurements were taken to ensure that all aspects of behaviour could be studied.

The principal purpose of the experimental programme was

to obtain moment-curvature and load-deflection responses of reinforced concrete beams to cyclic loading, and these responses have been discussed fully in Chapters 5 and 6. Therefore this chapter deals only briefly with the derivation of these responses and with the properties of the beams. The effect of cyclic loading on plastic hinge length is discussed by comparing two pairs of comparison beams, and the design recommendations for plastic hinge lengths proposed by Baker and Amarakone[43] and by Corley[55], are compared with experimental evidence.

Of the eleven beams tested, two will not be discussed in this thesis. One of these was a pilot test and showed the column stub as being poorly shaped for obtaining strain readings adjacent to the column; insufficient readings were recorded for the other.

A detailed description of the materials, equipment, and testing procedure used in these experiments appears in Appendix D.

7.2 RANGE OF VARIABLES STUDIED

Principal vaiables for this investigation were: tension steel ratio, p; binding ratio, p", and effect of rectangular lateral binding steel; and the ratio of compression steel to tension steel, p'/p. It was not intended that concrete cylinder strength be a significant

variable in this programme but a large range of values for this parameter was obtained. It is well known, however, and has been illustrated in Chapter 4, that the influence of concrete strength on the ductility of under-reinforced beams is not marked.

The main properties of the beams in this series are summarised in Table 7.1.

7.3 SELECTION OF SPECIMEN SHAPE

In a typical, multi-storey all-frame structure, seismic lateral loads produce points of contraflexure in beams at approximately mid-span. Also, the cyclic nature of this type of loading induces bending moments in the beams that increase in magnitude to a maximum at the column face and these moments change sign each time the earthquake changes direction. It therefore seemed that a convenient test specimen shape would be that represented by a length of beam spanning between two adjacent points of contraflexure and having a column stub midway between these points (Figure 7.1 illustrates the selected specimen shape and its derivation). Further, by simply-supporting the specimen at its ends, and by applying upward and downward point loads to the column stub, the triangular bending moment diagram and moment sign changes will occur as in the real structure.

There is one major inconsistency, however, between

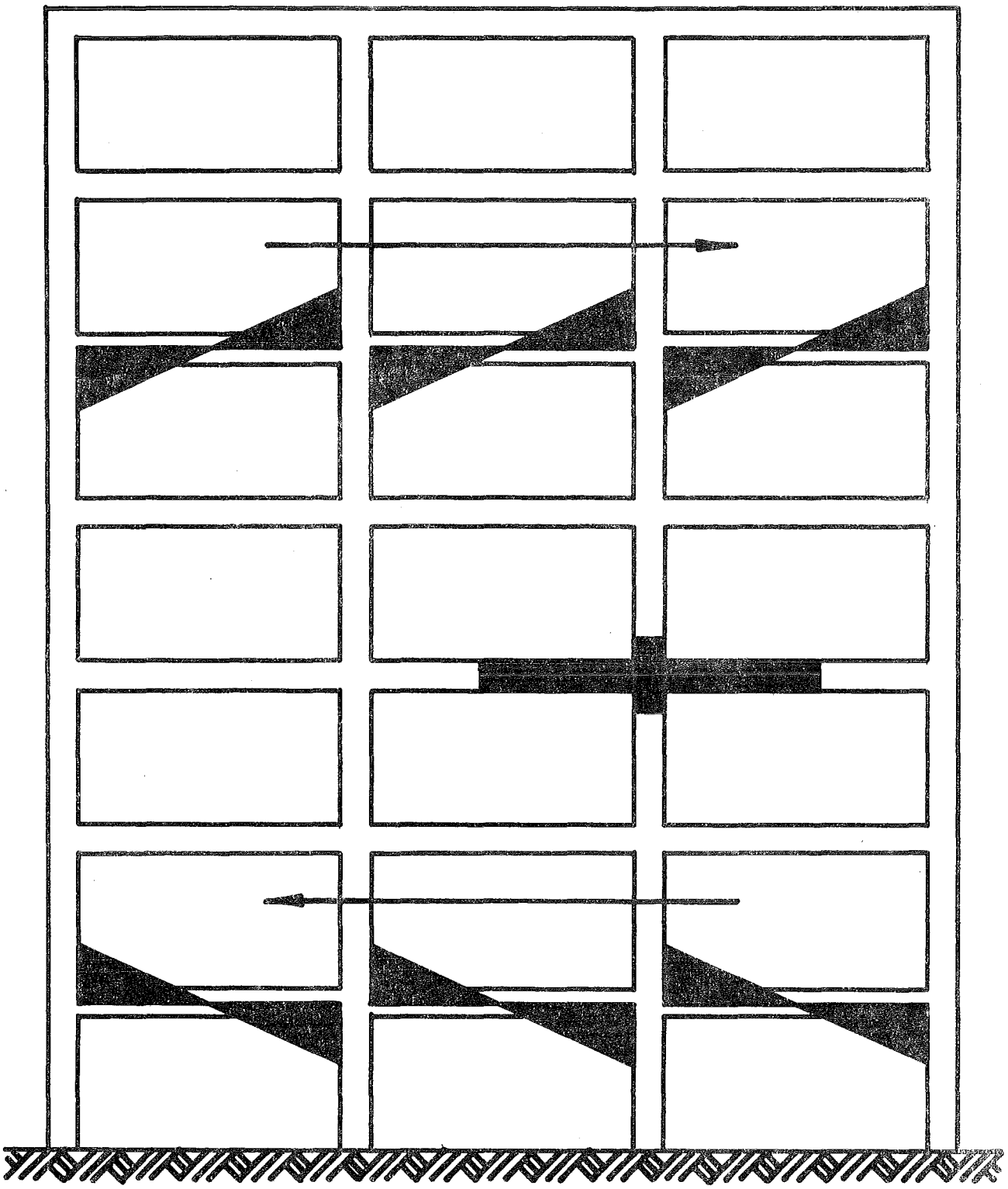

FIG.7.1 - SPECIMEN SHAPE

the real case and that represented in the specimen. In the real case, beam bending moments on either side of the column are of different sign, yet in the specimen, moments in the beam will be of the same sign. In the real structure, then, considerable bond stress between the steel and the column concrete must be developed. At any stage following yield, the bond force to be transferred in the real structure is twice the yield force of the bar, since yeilding of opposite signs will occur on each side of the column. Transfer lengths calculated using normal Code of Practice allowable bond stress would indicate a much longer length than the column dimension for practically all structures of this type. However, the bond transfer is helped considerably by compression in the column. The importance of this difference is difficult to assess. The effect of this variable was not included in this test programme.

7.4 LOADING SEQUENCE

Two loading sequences were used in this investigation. The first was simply a downward push to failure followed by an upward push to failure; its purpose being to assess the influence on moment-curvature behaviour of the Bauschinger Effect when very large initial plastic strains were involved. Three beams, 26, 64, 65, each having different

tension steel ratios were tested in this fashion.

The remaining six beams were subjected to a series of load reversals. The loading sequence used to represent earthquake loading is similar to that used in the Portland Cement Association's tests on reinforced concrete beams meeting an external column[60,62]. The derivation of this simulation is not clear but the loading sequence and extent is not of major significance, there obviously being an infinite number of responses to a real earthquake and no advance warning. What was considered important was that some post-elastic loading history be generated in the beam specimens so that comparison could be made with theory. Chapter 8 discusses a possible avenue of research given a reasonably accurate mathematical model for this behaviour.

The loading sequence used in this series deviated from that used by the Portland Cement Association[60,62] in three ways. Firstly, the ductility factors used in the P.C.A. tests were derived from beam rotations near the column face which were measured by means of transducers mounted on a frame surrounding and attached to the beam. In this series Demec strain gauges were used to measure tension steel strains where the plastic hinge was thought to be. This technique was rather crude and there was little possibility of achieving predetermined ductility factors exactly. This was not considered to be disadvantageous however, as mentioned above.

The second derivation from the P.C.A. loading sequence involved a reduction in the number of cycles from two earthquake simulations to only one. This alteration was an expedient used in order to reduce the testing duration.

Thirdly, it was considered desirable to precede and follow the earthquake simulation with several cycles from zero to design load to assess the effect that the cyclic loading has on the subsequent performance of the structure. Also, the initial cycles to design load settled the system to the sort of condition it could be expected to be in when an earthquake occurs. Three initial cycles to working load were used. It was found that two cycles were sufficient to obtain reproducible behaviour and the third cycle confirmed this. Following the cyclic loading in the inelastic range, two, and in some cases three, cycles to design load, indicated a considerable loss in stiffness of the beam (q.v. Chapter 5).

The loading sequence used for these beams is illustrated schematically in Figure 7.2.

7.5 RATE OF LOADING

Tests using the earthquake representation as a loading sequence were of four to six days duration and therefore the loading rate was appreciably slower than that associated with seismic behaviour. However, several references

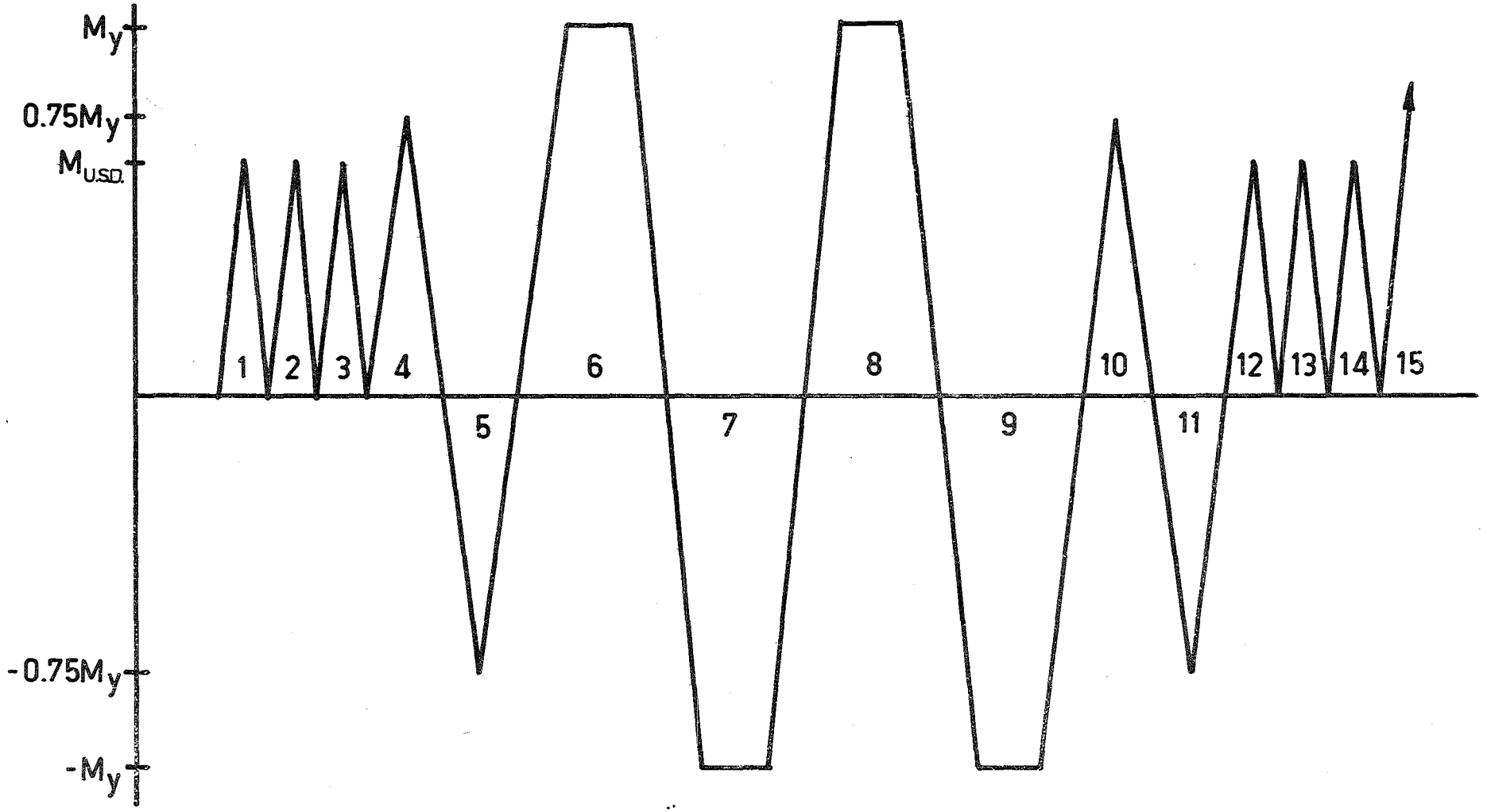

FIG.7.2 - EARTHQUAKE SIMULATION

discussed by Blume, Newmark and Corning[29] and research by others[20,63], indicate that strength and energy absorption characteristics of reinforced concrete members are increased with increased speed of loading. Consequently it appears conservative to use slow loading as a basis for testing seismic specimens. Further, the work of Rüsch[28] on loading rates of concrete, shows that the rate of loading has an exponential effect on the deviation of behaviour from that occurring at an instantaneous rate. By comparison with some of Rüsch's tests, the loading rate used for these beams was quite fast and therefore the deviation of behaviour from that occurring at very fast loading rates may not be very great (see Figure 7.3).

More recently, A.C.I. Committee 439[68] has summarised a range of load-rate test data on both concrete and steel. It is shown that at an average strain rate of 10 in. per in. per sec., concrete exhibits an 83 - 84 per cent increase in strength. These results stem from experiments on low and high strength concretes. Steel is influenced to a lesser extent for the same strain rate, but a 118 per cent increase in yield stress has been reported for a 40 K.s.i. "static" yield stress steel, loaded at 225 in. per in. per sec.

7.6 DERIVATION OF MOMENT-CURVATURE RESPONSES

It is well known that in reinforced concrete beams subjected to overload, the portion of the beam where the

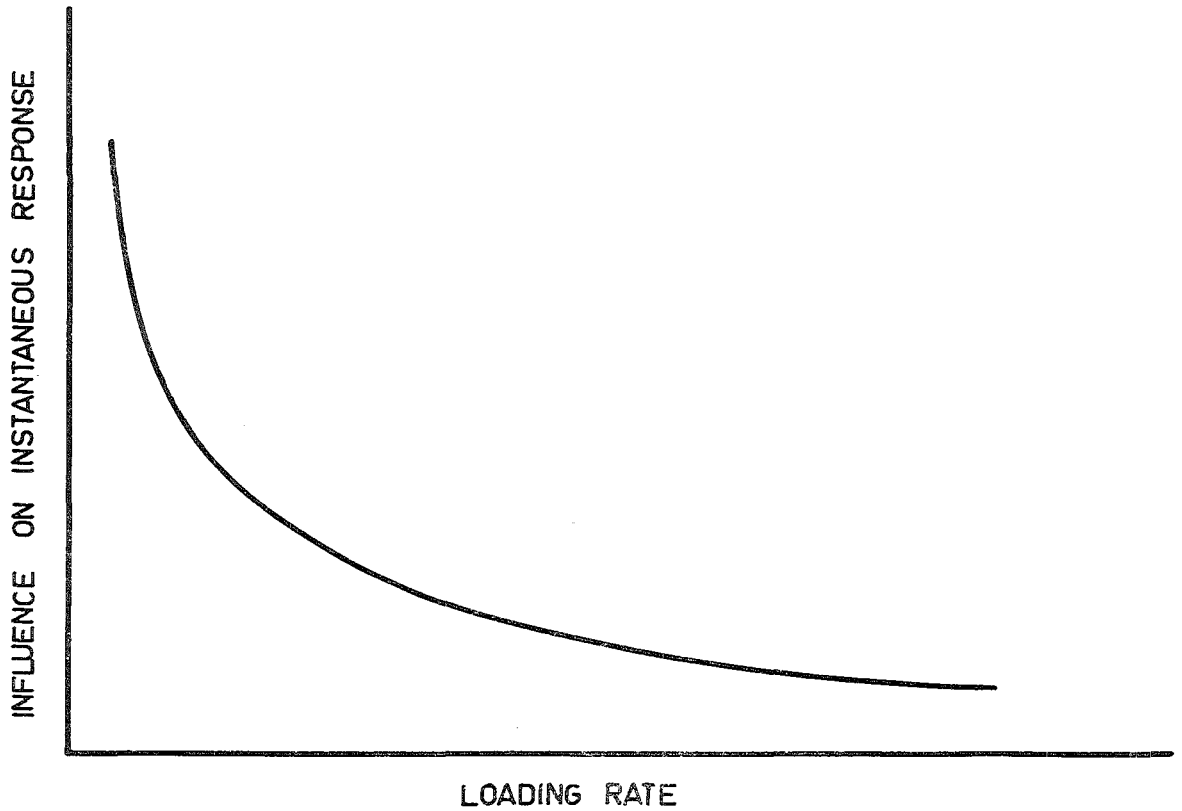

FIG.7.3 - INFLUENCE OF LOADING RATE

tension steel yields will deform inelastically.

The beam cannot sustain a load that is significantly larger than the yield load, and because it undergoes a considerable reduction in stiffness in the region of yielding, this portion will deform considerably while others about it undergo relatively little change in moment or curvature. This phenomenon is known as "plastic hinging" and the extent over which it occurs is termed the "plastic hinge length". It has been illustrated in Chapter 6 that the load-deformation response of a beam after yielding is determined almost entirely by the properties of the plastic hinge and it is on this behaviour that the energy absorption requirements of seismic design relies.

The experimental moment-curvature curves illustrated in Chapter 5 are those corresponding to the critical 2" gauge lengths adjacent to the column stubs in the beams. It has already been explained in Chapter 5 that the concrete strain readings obtained from these experiments were considered to be unsuitable for curvature determination because of the crack formation down the whole depth of the member. Therefore the standard method of obtaining curvature, based on the strain distribution in the compressed concrete, could not be used. Instead, the assumption was made that plane sections remain plane, and the strains in the tension and compression steels were used to obtain curvature.

Because two strains at least are required to compute curvature, and since only two values were available, great care was taken when measuring these strains.

7.7 DERIVATION OF LOAD-DEFLECTION RESPONSES

Since concrete is a non-uniform material and fabrication methods are not perfect, the properties of the beam sections on either side of the column stub were not identical. Therefore plastic hinging did not occur to the same extent on both sides of the stub but favoured the weaker section, and so the beams deflected asymmetrically. Had the sections on both sides of the stub been identical, the central deflection of the beam would have been greater. In order that theoretical and experimental load-deflection behaviour could be compared, it was necessary to modify the observed central deflections and to compute the "equivalent central deflections" which would occur if the beam had deflected symmetrically with two equally-weak sections. This process is illustrated in Figure 7.4. The rotation of the column stub, θ, was found from the average of the inclinometer readings at the top and bottom of the stub.

The initial loads and equivalent central deflections at the cycle extremities of the seven beams for which load-deflection curves are not plotted, are shown in Table 7.2. The load-deflection information for the other beams is shown plotted in Figures 6.4 and 6.5.

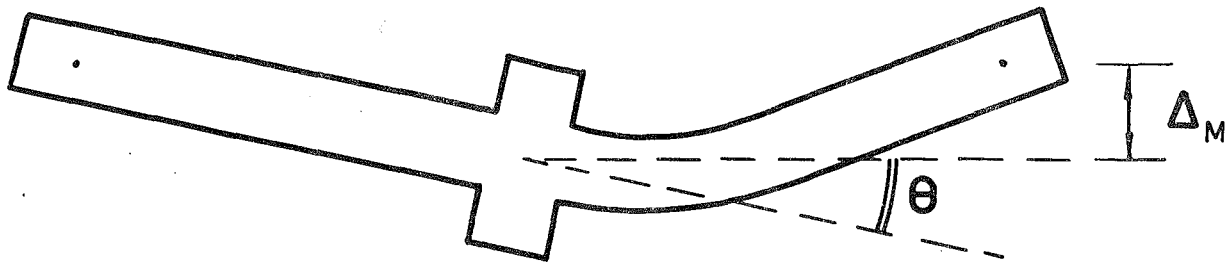

(i) Asymmetrical deflection

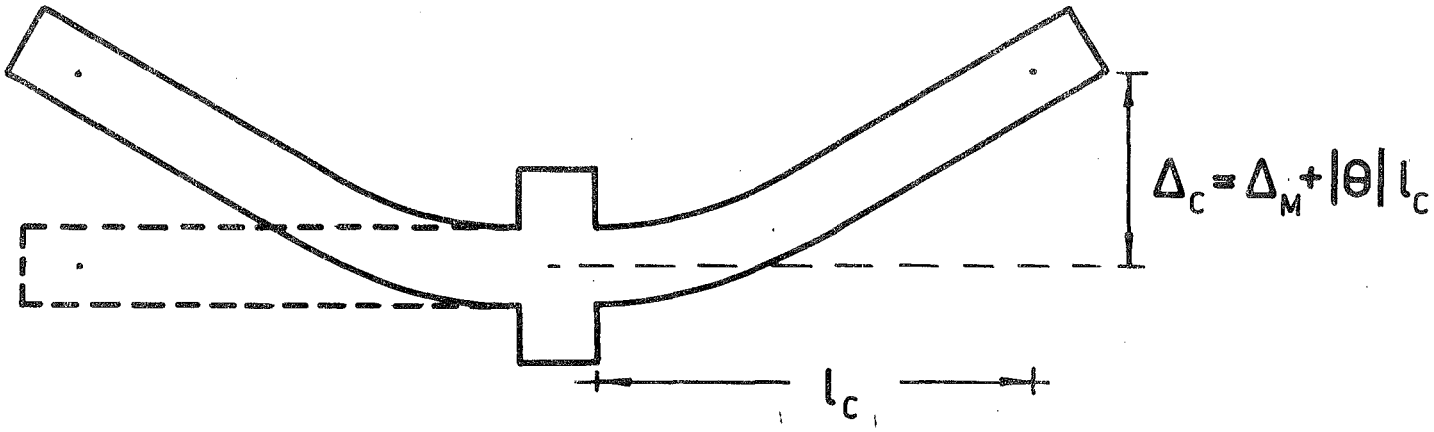

(ii) Symmetrical deflection

FIG.7.4 - EQUIVALENT CENTRAL DEFLECTION

TABLE 7.2

LOAD-DEFLECTION CYCLES FOR BEAMS

Beam	26		27		44		47		64		65		67	
Reversal	Load (lb)	Defln. (in)	Load (lb)	Defln. (in)	Load (lb)	Defln. (in)	Load (lb)	Defln. (in)	Load (lb)	Defln. (in)	Load (lb)	Defln. (in)	Load (lb)	Defln. (in)
1	8680	4.7684	6516	0.3265	2246	0.2137	5479	0.2756	4802	3.3122	7210	4.0047	5427	0.2749
2	-5218	-1.9963	0	0.0705	0	0.0707	0	0.0542	-4466	0.1264	-5433	-3.5693	0	0.0555
3			6516	0.3279	2246	0.2265	5479	0.2852					5415	0.2858
4			0	0.0640	0	0.0722	0	0.0656					0	0.0568
5			6540	0.3313	2246	0.2297	5479	0.2911					5431	0.2900
6			0	0.0639	0	0.0713	0	0.0615					0	0.0532
7			8542	0.4201	2905	0.2912	8300	0.4278					8340	0.4376
8			-3412	-0.2455	-3400	-0.2759	-3460	-0.2137					-3190	-0.2327
9			11666	0.7383	4078	0.4881	11680	0.8096					11500	0.6446
10			-4156	-0.3143	-4409	-0.4184	-4536	-0.4980					-4167	-0.0833
11			11874	0.9353	4026	0.6492	12091	1.1002					11500	1.4148
12			-4126	-0.2630	-4429	-0.6431	-4512	-0.4537					-4100	0.0490
13			8542	0.7959	2905	0.2884	8300	0.9315					8340	1.2524
14			-3412	-0.1142	-3400	-0.5128	-3460	-0.0193					-3284	0.3204
15			6516	0.6928	2246	0.2095	5479	0.7819					5415	1.0885
16			0	0.2739	0	-0.0901	0	0.3994					0	0.7022
17			6516	0.6911	2246	0.2048	5479	0.7850					5507	1.0959
18			0	0.2739	0	-0.0892	0	0.3984					0	0.7029
19			6516	0.6954	2246	0.2134	12245	1.3789					12075	1.7874
20			0	0.2727	0	-0.0820	10880	4.7866					4784	4.1080
21			13042	5.5910	5123	5.8216								

Notes: 1. Loads shown are those at the termination of load application.

2. Deflections are Equivalent Central Deflections except for Beam 67 which are measured central deflections.

7.8 PLASTIC HINGE LENGTHS

The average curvature plots for two pairs of reasonably similar beams are shown in Figures 7.5 - 7.8. The average curvatures for the gauge lengths of these beams have been plotted at the midpoints of the gauge lengths. (Strain gauge locations are illustrated in Figure D.2, Appendix D). The results from these four beams are typical of those from the test series.

The first pair of beams (Beams 26 and 46), have $\frac{3}{4}$" dia. bottom steel, and 2" and 4" stirrup spacing respectively. Cylinder and cube strengths for the concrete are similar. Beams 44 and 64 comprised the second pair with $\frac{1}{2}$" dia. bottom steel, and 4" and 6" stirrup spacing respectively. Again concrete properties were similar. One beam from each pair had been loaded in two directions to failure (26 and 64), the other had been subjected to multi-cyclic loading.

7.8.1 Design Recommendations for Plastic Hinge Length

In this thesis, deformations of members have been derived using moment-curvature relationships. An alternative approach for calculating the ultimate deformation of members is to use equations proposed for the plastic rotation which can occur at the hinge regions. This alternative approach has a disadvantage in that

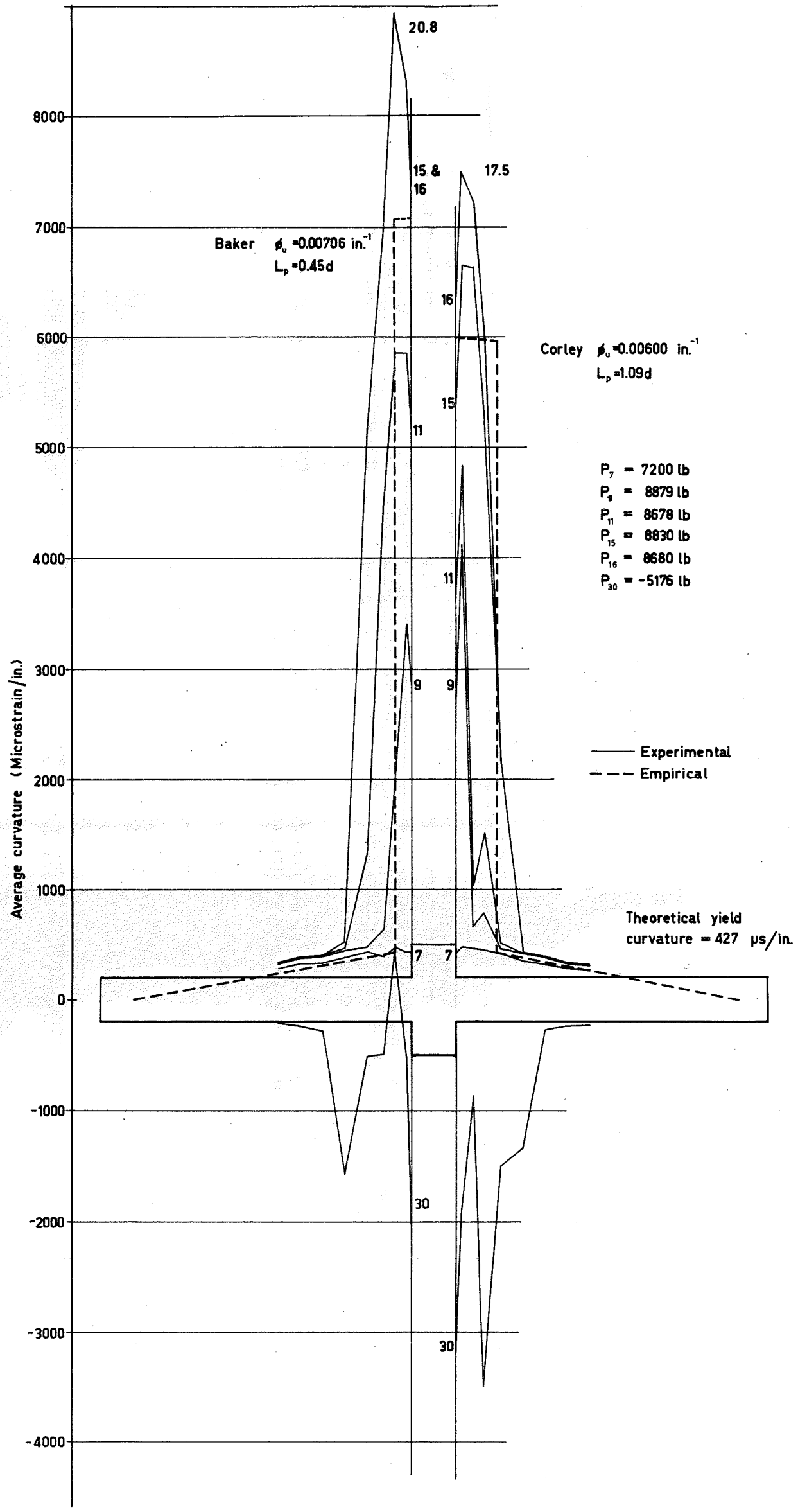

FIG.7.5 - AVERAGE CURVATURE PROFILE FOR BEAM 26

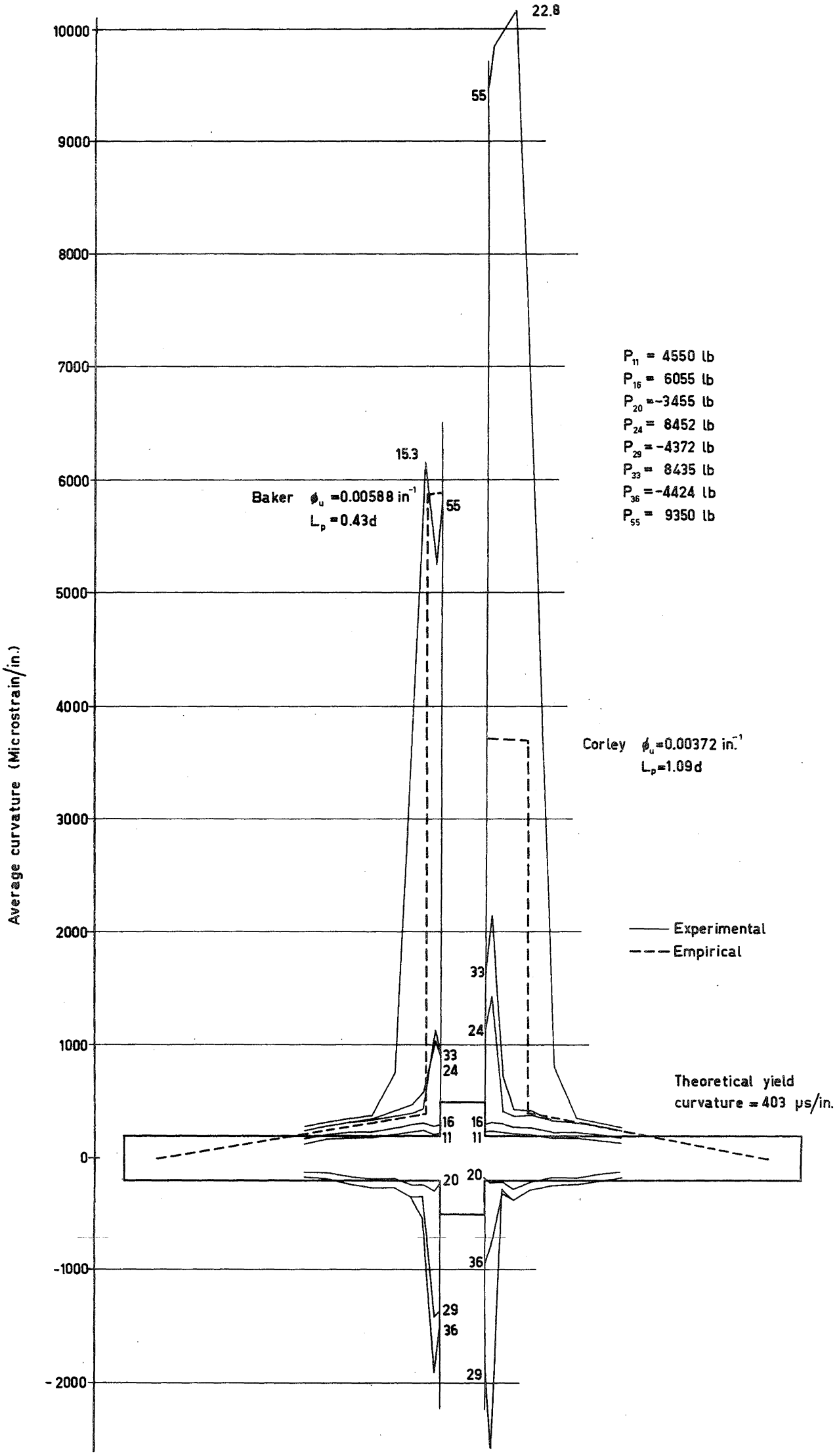

FIG.7.6 - AVERAGE CURVATURE PROFILE FOR BEAM 46

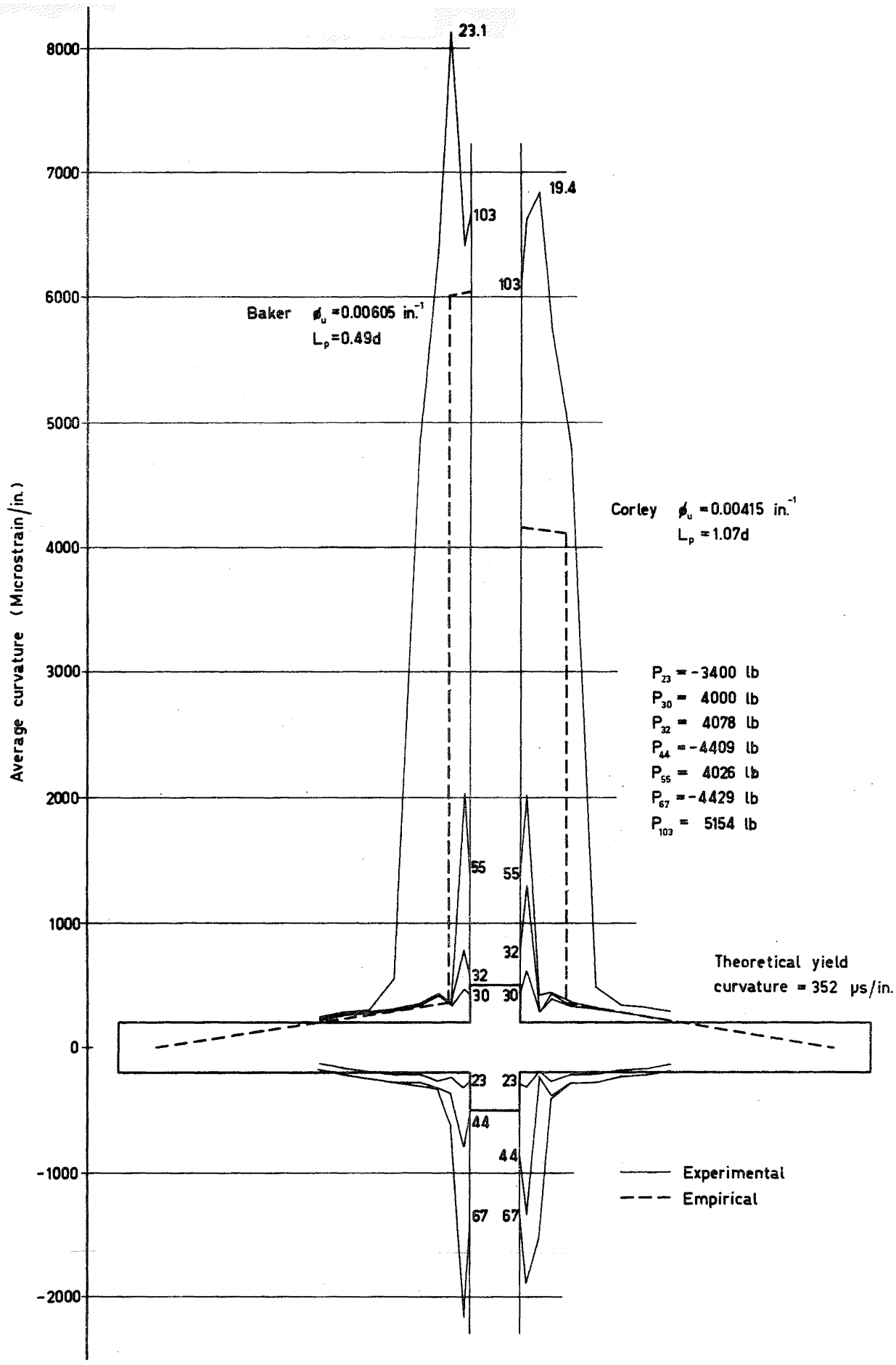

FIG. 7.7 - AVERAGE CURVATURE PROFILE FOR BEAM 44

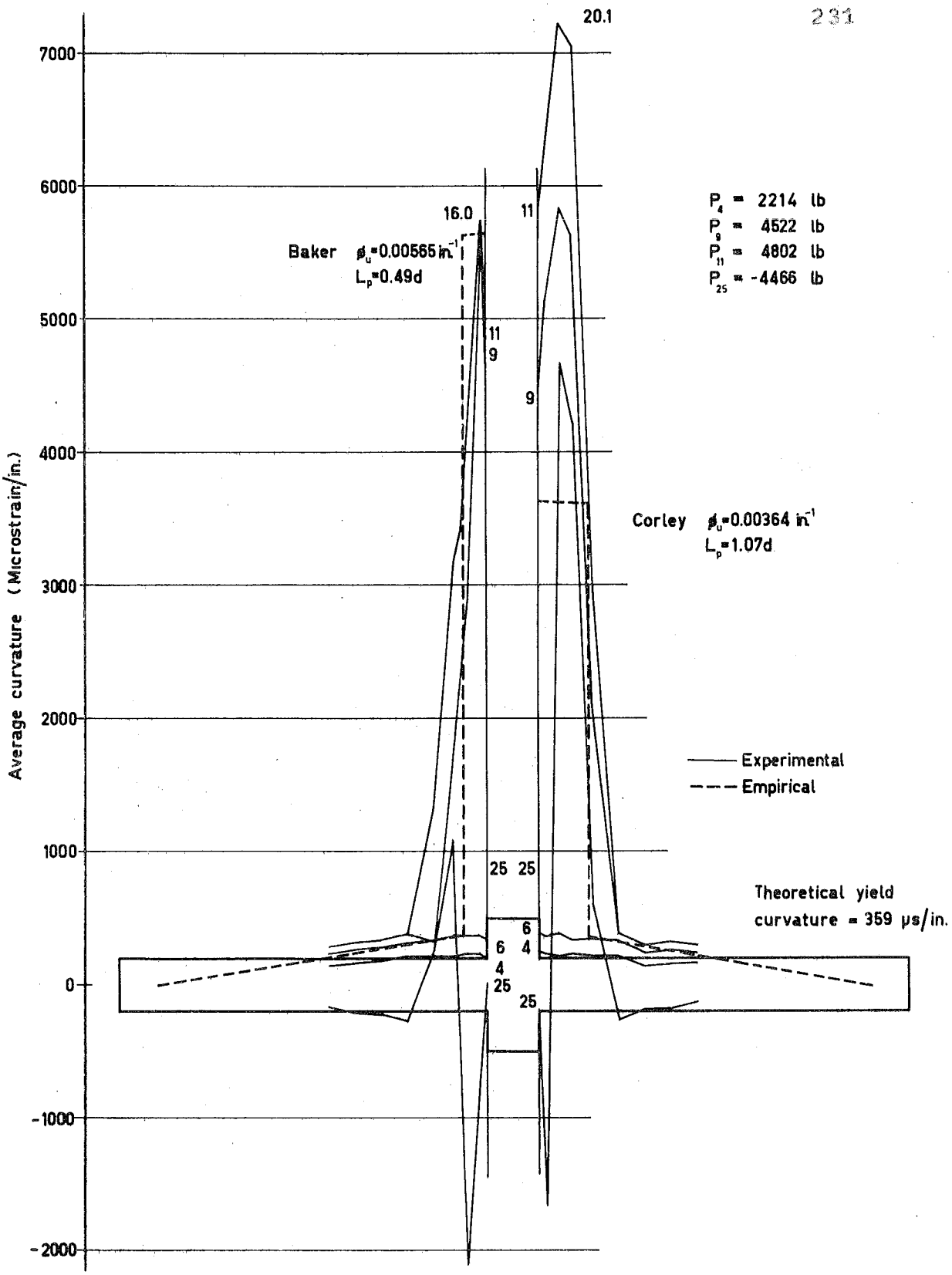

FIG.7.8 - AVERAGE CURVATURE PROFILE FOR BEAM 64

deformations between yield and ultimate cannot be determined. A number of investigators have made design recommendations for equivalent plastic hinge length. The equivalent plastic hinge length may be defined as that length which when multiplied by the difference between ultimate and yield curvature, results in the same plastic rotation as actually occurs in the member, i.e. the actual distribution of plastic curvature is replaced by a rectangle of identical area and maximum curvature.

Only two of these proposals will be discussed here: the first is that presented by Baker and Amarakone[43], since this is representative of recent European work; the second, by Corley[55], is representative of research at the Portland Cement Association Laboratories.

In both cases, these recommendations are based on experiments with monotonically-loaded beams, and it is of interest to compare them with plastic hinge lengths of beams subjected to cyclic load.

(a) Baker and Amarakone[43]

The necessary equations advanced by Baker and Amarakone for computing plastic hinge lengths and rotations are: (The notation has been changed to avoid confusion with other well-known parameters)

$$L_p = 0.8\, b_1 b_3 \frac{z}{d}\, c \qquad \ldots\ldots(7.1)$$

$$\epsilon_{cu} = 0.0015(1 + 150p'' + (0.7 - 10p'')\frac{d}{c}) \leqslant 0.01 \quad \ldots\ldots(7.2)$$

where L_p = equivalent length of plastic hinge

b_1 = 0.7 for mild steel

= 0.9 for cold-worked steel

$$b_3 = \frac{0.3}{4000}\,(14000 - C_u)$$

C_u = cube strength

z = distance of critical section to the point of contraflexure

c = neutral axis depth at ultimate

ϵ_{cu} = limiting concrete strain

For the beams of this investigation, z was constant with a value of fifty inches. Also, for all of the beams in this sample, it was found that c = 0.2d approximately. Other section properties are shown in Table 7.1

(b) Corley[55]

Corley's equations are:

$$L_p = 0.5d + 0.2\sqrt{d}\,\frac{z}{d} \quad \ldots\ldots(7.3)$$

$$\epsilon_{cu} = 0.003 + 0.02\,\frac{b}{z} + \left(\frac{p''f''_y}{20}\right)^2 \quad \ldots\ldots(7.4)$$

where f''_y = yield stress (K.s.i.) of stirrups.

Plastic Rotation

For both methods, by definition, the plastic rotation is given by:

$$\theta_p = \frac{\epsilon_{cu} - \epsilon_{ce}}{c} \cdot L_p \qquad \ldots\ldots(7.5)$$

where ϵ_{ce} is the concrete strain in the extreme fibre at yield.

Therefore, the average ultimate curvature is:

$$\phi_u = \phi_y + \frac{\theta_p}{L_p} \qquad \ldots\ldots(7.6)$$

Values for ϵ_{ce} for these beams were obtained from theoretical analyses such as those described in Chapter 4. These strains had values of the order of 0.00077 for Beams 44 and 64, and 0.00121 for Beams 26 and 46.

The results from the methods of Baker and Amarakone and of Corley are shown in Figures 7.5 - 7.8 and it can be seen that both methods produce safe and reasonable results. It should be noted that the experimental curvatures increased beyond those plotted and that insufficient range for the Demec gauges terminated strain measurement.

It has been shown in Chapter 4 that the most significant contribution to beam ductility results from the provision of compression steel, and that lateral reinforcement has only a minor influence. Both of the plastic hinge

expressions here consider compression steel indirectly with the inclusion of the c term; in addition, Corley includes the compression steel content in the p" term. In the writer's opinion, however, both expressions are unrealistically sensitive to changes in p".

7.8.2 Influence of Shear on Plastic Hinging

The action of shear at a plastic hinge has a beneficial effect on ductility, providing shear failure can be prevented, since diagonal tension cracking increases the length of the tension steel at yield, and therefore increases the extent of the plastic hinge region. The free body diagram of Figure 7.9 illustrates this behaviour.

Figure 7.9 also indicates that stirrups retard the extension of the plastic hinge length. If moments are taken about the centroid of concrete compression, and if no stirrups are present and dowel forces are ignored, it is evident that the tension at B is due to the external bending moment at A, thus spreading the region of steel yield. If stirrups are present, it can be seen that they partly resist the external moment and will reduce the force in the tension steel at B. It appears that this effect is responsible for the slightly smaller plastic hinge length of Beam 26 as compared with that of Beam 46. The stirrup spacings in the Beams 44 and 64 pair are more similar and so this influence cannot be seen.

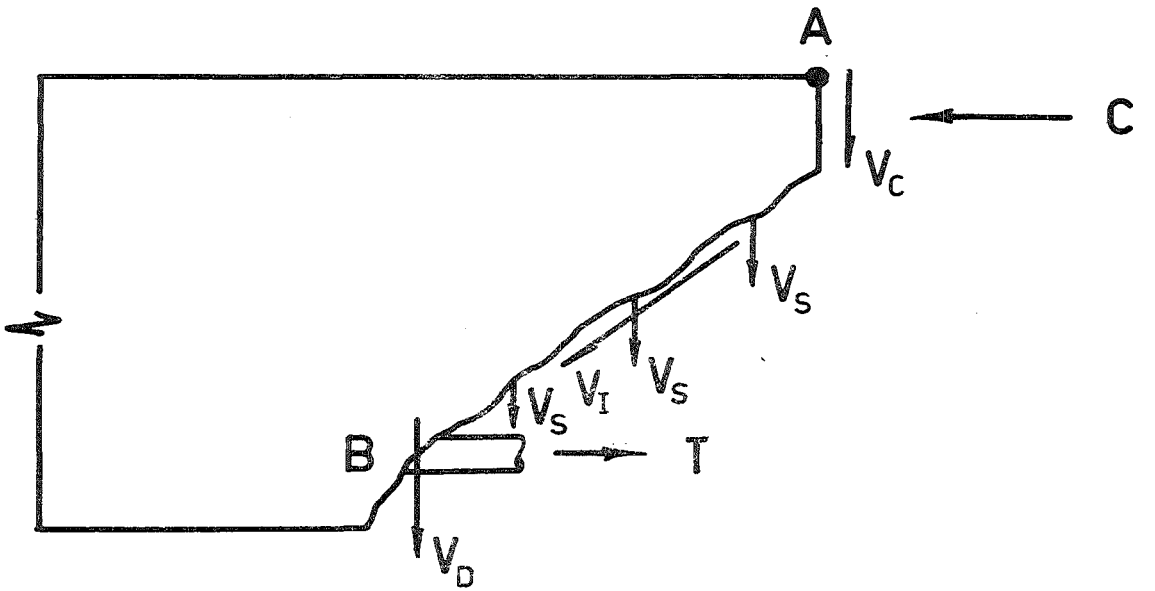

FIG.7.9 - DIAGONAL CRACKING

A number of empirical expressions[69] for plastic hinge length include a term to allow for the spread of plasticity due to diagonal tension cracks. The analyses of Chapters 4, 5 and 6 take no account of this behaviour and should therefore be conservative.

Nominal shear stresses in these beams at ultimate load were in the range 120 p.s.i. for beams with $\frac{1}{2}$" dia. tension steel to 350 p.s.i. for beams with $\frac{7}{8}$" dia. tension steel. Dowel stresses (shear stress in reinforcing bars) were of the order of 2,600 p.s.i. during intervals of purely steel couple moment resistance in cyclically-loaded beams.

Plates 7.1 - 7.3 illustrate the crack patterns for Beams 26, 44 and 64. It is evident that diagonal cracking was not extensive in these test beams.

7.8.3 Influence of Cyclic Loading on Plastic Hinge Length

A study of the average curvature plots of Figures 7.5-7.8 for the beam pairs 26 and 46, and 44 and 64, indicates no increase or decrease in plastic hinge length at ultimate for the cyclically-loaded beams (44 and 46). In these beams, the cycles resulting from upward loading have smaller plastic hinge lengths than do Beams 26 and 64 because unloading had been initiated at comparatively low ductility factors and therefore the plastic hinge had not developed to its full extent. Beams 44 and 46 were yielded twice in each direction before the final failure cycle and concrete

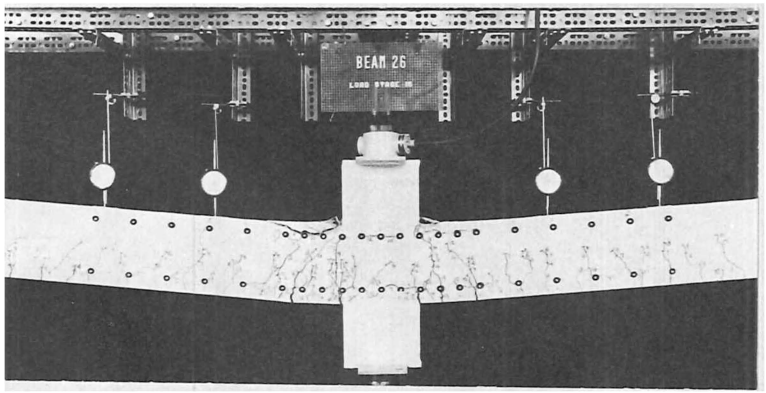

PLATE 7.1 - BEAM 26

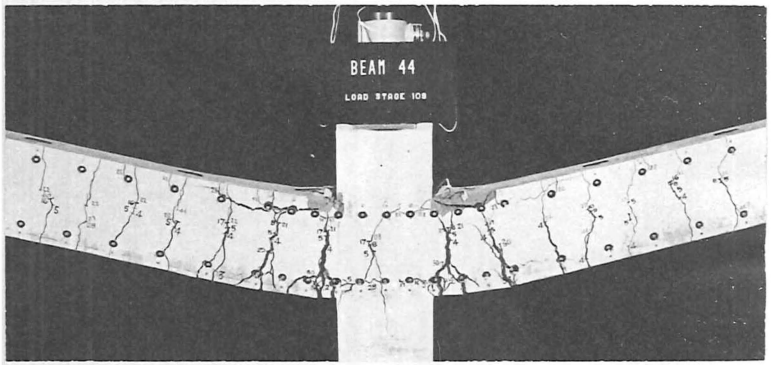

PLATE 7.2 - BEAM 44

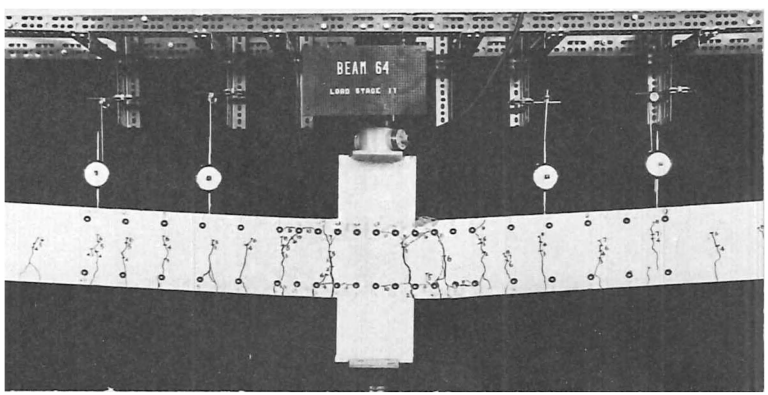

CRACK PATTERNS

PLATE 7.3 - BEAM 64

spalling did not occur in either beam during the cyclic loading phase.

7.9 COMPUTER PROGRAMS

As there were on average twelve thousand readings and measurements for each of the beams in this series, computer programs were written to reduce this data to the required form.

The purpose of the principal program (Program 7.2 - "BEAMTEST") was to accept loads, Demec and dial gauge readings, and temperature corrections, and to produce bending moments, strains, curvatures and deflections for each load stage. Also, the "zero" readings were measured when the beam was subjected to self weight and by providing the concrete density and beam weight, the zero readings could be redefined and computed as those at which the beam was under no load. Provision was also made for including shrinkage effects when re-defining the zeros, but as some difficulty was encountered in measuring shrinkage strain (q.v. Appendix D) this feature was not used and was eventually removed from the program.

The order in which the beam data was collected and punched on to cards was not immediately suitable for processing with "BEAMTEST" and so the cards were each punched with reference numbers and then resorted. As some

40 minutes was required to process the data with the main program, a smaller program (Program 7.1 - "DATATEST") was used to check the new data sequence. This program also indicated omissions from the punched data.

A third program (Program 7.3 - "INCLINO") was written to output angles, both in radians and degrees, from the inclinometer readings.

The final program (Program 7.4 - "DATALIST") simply listed the input data and provided a convenient means of checking for obvious errors in the measurement or recording of results.

Listings of these programs appear in Appendix B.

CHAPTER 8

CONCLUSIONS AND SUGGESTED FUTURE RESEARCH

8.1 GENERAL

A theory has been developed to predict the flexural response of reinforced concrete T or rectangular members when subjected to monotonic or cyclic load, and either with or without axial compression.

The conclusions reached have already appeared at the end of the relevant chapters or as discussion in the text. These are summarised below and are followed by suggestions for future research in this field.

8.2 SUMMARY OF CONCLUSIONS

An investigation into the influence of conventional rectangular binding steel on concrete stress-strain properties was carried out. A theory was evolved for predicting moment-curvature response to monotonic load in beams and columns and compared with published experimental evidence. Using this theory, the effect of lateral reinforcement on the ductility and load carrying capacity of monotonically-loaded beam and column sections

was studied. It is concluded that the most significant contribution to the ductility of under reinforced beams arises from increased p'/p ratios and reduced tension steel content, and that lateral binding of compression concrete has only a negligible effect on ductility. However, it was found that lateral reinforcement has a very beneficial effect on the energy absorbing capacity for columns. The theory indicates negligible enhancement in load-carrying capacity due to confinement for both beams and columns.

The Bauschinger Effect in structural grade reinforcing steel was investigated experimentally and using the method of least squares; a mathematical model for this behaviour is advanced. The model is compared with, and shown to be generally more accurate than, the only other known model - that postulated by Singh, Gerstle and Tulin[49]. The expression described herein takes account of the three variables that most influence the Bauschinger property, viz., the virgin properties of the steel, the plastic strain in the previous cycle, and the number of prior cycles. The proposed expression is therefore more complex than that advanced by Singh et al. but it is felt that this is justified in view of the complicated nature of the Bauschinger Effect.

By combining the above theories, moment-curvature responses of cyclically-loaded reinforced concrete sections are obtained theoretically and compared with test responses

from beams. The theoretical predictions are shown to compare very well with experiment and consider such features as opening and closing of concrete cracks. The large reaches of the theoretical moment-curvature plots for these beams indicate that after load reversal from initial yield, moment resistance is provided by purely steel couple action. It is concluded that the primary role of concrete during cyclic loading is to prevent buckling of the reinforcing steel.

Further comparison is made between experimental moment-curvature behaviour and theory by using an elastic-perfectly plastic reinforcing steel response. These comparisons are plotted and show the elasto-plastic idealisation to predict more energy-absorption than is available.

Extension of the moment-curvature theory enables the prediction of load-deflection response to be made. Again, experimental and theoretical comparisons are drawn for load versus equivalent central deflection for two of the beams tested in this series. As considerable computer time is required for the prediction of load-deflection responses, a study was made of two idealised load-deflection models. The first, and most commonly used, the elasto-plastic model, over-estimates the available energy absorption even more than when used as a moment-curvature

response. This model does not allow for purely steel couple moment-resistance and large inaccuracies are incurred because of this. The second model, which is shown to be generally conservative, is that proposed by Clough[58] and takes into account the stiffness degradation that results from cyclic loading.

The influence of cyclic loading, shear, and stirrup spacing on plastic hinge length is discussed. Design recommendations for plastic hinge lengths as proposed by Baker and Amarakone[43] and by Corley[55], are compared with experimental results from four beams in this investigation, and shown to predict safe and reasonable values. Also, it was found that cyclic loading had a negligible influence on the length of the plastic hinge at failure for these beams.

8.3 SUGGESTED FUTURE RESEARCH

On the basis of the analysis presented in this thesis, it may be possible to avoid the considerable computer time required to predict moment-curvature and load-deflection behaviour, by evolving envelope curves for these responses. This would enable immediate assessment of energy absorption potential to be made for different sections and would not require computer access. In view of the complex nature of steel and concrete response to cyclic load, the feasibility of this may be doubtful, but it would prove of considerable use in design.

The most obvious need for further research is for a more accurate Bauschinger Effect model. In Chapter 5 it was shown that an elasto-plastic steel stress-strain response produced, with the exception of the closing of concrete cracks, an elasto-plastic moment-curvature property. Further, in Chapter 6 an elasto-plastic moment-curvature idealisation resulted in elasto-plastic load-deflection behaviour. This sequence of behaviour pattern from steel stress-strain to load-deflection is extremely significant and implies that, given an accurate model for the steel cyclic stress-strain curve, then a realistic load-deflection idealisation can be derived. This would remove the need for the lengthy calculations at present required to obtain moment-curvature relationships from essentially steel stress-strain expressions and load-deflection responses from moment-curvature behaviour. Therefore, although the stress-strain expression for Bauschinger Effect described in this thesis is reasonably accurate, and has a stress standard deviation of $0.05f_y$ to $0.10f_y$ for the specimens tested, it is felt that a more thorough and systematic study is required to evolve load-deflection idealisations.

The difficulty of obtaining a suitable idealisation for moment-curvature responses under cyclic load suggests that sensitivity studies similar to the comparison

performed by Clough[58], could be carried out using different idealisations to determine the effect of seismic motions on the response of reinforced concrete structures.

The order of enhanced bond strength available when bars are subjected to lateral compression stress is not well known. It can be shown that, using current Code of Practice formulae, practically all columns are of insufficient width to transfer the steel stress in the beam from negative yield at one column face, to positive yield at the other. The deterioration of such bond strength under repeated cyclic loading may have a considerable influence on the ductility and strength of the beam adjacent to the joint.

APPENDIX A

BIBLIOGRAPHY

1. RICHART, F.E., BRANDTZAEG, A., and BROWN, R.L., "A Study of the Failure of Concrete under Combined Compressive Stresses". University of Illinois Engineering Experiment Station, Bulletin No. 185, Nov. 1928.

2. ————————,————————,————————. "The Failure of Plain and Spirally Reinforced Concrete in Comparison". University of Illinois Engineering Experiment Station, Bulletin No. 190, Apr. 1929.

3. WHITNEY, C.S., "Design of Reinforced Concrete Members Under Flexure or Combined Flexure and Direct Compression". Proceedings A.C.I. Journal, Vol. 33, Mar. - Apr. 1937.

4. WHITNEY, C.S., "Plastic Theory of Reinforced Concrete Design". Proceedings A.S.C.E. Journal, Vol. 66, No. 10, Dec. 1940, pp. 1749-1780.

5. JENSEN, V.P., "The Plasticity Ratio of Concrete and its Effect on the Ultimate Strength of Beams". Proceedings A.C.I. Journal, Vol. 39, June 1943.

6. BLANKS, R.F., and McHENRY, D., "Plastic Flow of Concrete Relieves High-Load Stress Concentrations". Civil Engineering,Vol. 19, No. 5, May 1949, pp. 320-322.

7. BALMER, G.G., "Shearing Strength of Concrete Under High Triaxial Stress - Computation of Mohr's Envelope as a Curve". U.S. Bureau of Reclamation, Structural Research Laboratory, Report No. SP-23, Oct. 1949.

8. HERR, L.A., and VANDEGRIFT, L.E., "Studies of Compressive Stress Distribution in Simply Reinforced Concrete Near the Point of Failure". Proceedings, Highway Research Board, Vol. 30, 1950, pp. 114-125.

9. BAKER, A.L.L., "Recent Research in Reinforced Concrete and its Application to Design". Journal of the Institute of Civil Engineers, Vol. 35, No. 4, Feb. 1951, pp. 262-298.

10. HOGNESTAD, E., "A Study of Combined Bending and Axial load in Reinforced Concrete Members". The Reinforced Concrete Research Council of the Engineers Foundation, Bulletin No. 1, June 1951.

11. PARME, A.L., A discussion of "Review of Research of Ultimate Strength of Reinforced Concrete Members" by C.P. Seiss. Proceedings A.C.I. Journal, Vol. 48, No. 10, June 1952.

12. HOGNESTAD, E., "Inelastic Behaviour in Tests of Eccentrically-Loaded Short Reinforced Concrete Columns". The Reinforced Concrete Research Council of the

Engineers Foundation, Bulletin No. 2, Oct. 1952.

13. BAKER, A.L.L., "Further Research in Reinforced Concrete and its Application to Ultimate Load Design". Proceedings of the Institution of Civil Engineers, Part III, Vol. 2, Aug. 1953, pp. 269-310.

14. MORICE, P.B., and BASE, G.D., "The Design and Use of a Demountable Mechanical Strain Gauge for Concrete Structures". Magazine of Concrete Research, Vol. 5, No. 13, Aug. 1953, pp. 37-42.

15. LEE, L.H.N., "Inelastic Behaviour of Reinforced Concrete Members Subjected to Short-time Static Loads". Proceedings A.S.C.E. Journal, Vol. 79, Separate No. 286, Sept. 1953.

16. SMITH, G.M., and YOUNG, L.E., "Ultimate Theory in Flexure by Exponential Function". Proceedings A.C.I. Journal, Vol. 52, No. 3, Nov. 1955, pp. 349-360.

17. CHAN, W.W.L., "The Ultimate Strength and Deformation of Plastic Hinges in Reinforced Concrete Frameworks". Magazine of Concrete Research, Vol. 7, No. 21, Nov. 1955.

18. HOGNESTAD, E., HANSON, N.W., and McHENRY, D., "Concrete Stress Distribution in Ultimate Strength Design". Proceedings A.C.I. Journal, Vol. 53, No. 4, Dec. 1955, pp. 455-479.

19. BAKER, A.L.L., "The Ultimate Load Theory Applied to

the Design of Reinforced and Prestressed Concrete Frames". Concrete Publications Limited, London, 1956.

20. McHENRY, D., and SHIDELER, J.J. "Review of Data on Effect of Speed of Testing of Concrete". Portland Cement Association, Research and Development Laboratories, Bulletin D9, 1956.

21. MATTOCK, A.H., "The Strength of Singly-Reinforced Beams in Bending". Cement and Concrete Association. Proceedings of a symposium on "The Strength of Concrete Structures". London, 1956.

22. KHAN, N.M., and MATTOCK, A.H., "An Experimental Investigation of the Influence of a Plastic Hinge on the Shear Strength of a Singly Reinforced Concrete Beam". Magazine of Concrete Research, Vol. 8, No. 24, Nov. 1956.

23. SMITH, G.M., and YOUNG, L.E., "Ultimate Flexural Analysis Based on Stress-Strain Curves of Cylinders". Proceedings A.C.I. Journal, Vol. 53, No. 6, Dec. 1956, pp. 597-610.

24. HOGNESTAD, E., "Confirmation of Inelastic Stress Distribution in Concrete". Proceedings A.S.C.E. Journal, Vol. 83, No. ST2, Mar. 1957.

25. ERNST, G.C., "Plastic Hinging at the Intersection of Beams and Columns". Proceedings A.C.I. Journal, Vol. 53, No. 12, June 1957, pp. 1119-1144.

26. VELETOS, A.S., and NEWMARK, N.M., "Effect of Inelastic Behaviour on the Response of Simple Systems to

Earthquake Motions". Proceedings Second International Conference of Earthquake Engineering, Tokyo, Vol. II, 1960.

27. KRIZ, L.B. and LEE, S.L., "Ultimate Strength of Over-Reinforced Beams". Proceedings A.S.C.E., Vol. 86, No. EM3, June 1960.

28. RÜSCH, H., "Researches Towards a General Flexural Theory for Structural Concrete". Proceedings A.C.I. Journal, Vol. 57, No. 1, July 1960.

29. BLUME, J.A., NEWMARK, N.M., and CORNING, L.H. "Design of Multistorey Reinforced Concrete Buildings for Earthquake Motions". Portland Cement Association, 1961.

30. BRESLER, B., and GILBERT, P.H., "Tie Requirements for Reinforced Concrete Columns". Proceedings A.C.I. Journal, Vol. 58, No. 5, Nov. 1961, pp. 555-570.

31. Seismology Committee, Structural Engineers Association of California, "Recommended Lateral Force Requirements and Commentary". 1967, 90 pp.

32. BURNS, N.H., and SEISS, C.P., "Load-Deformation Characteristics of Beam-Column Connections in Reinforced Concrete". Civil Engineering Studies, Structural Research Series No. 234, University of Illinois, Jan. 1962.

33. BROCK, G., "Concrete : Complete Stress-Strain Curves". Engineering, Vol. 193, May 1962, pp. 606-607.

34. LIEBENBERG, A.C., "A Stress-strain Function for Concrete Subjected to Short-Term Loading". Magazine of Concrete Research, Vol. 14, No. 41, July 1962.

35. CHAN, W.W.L., "The Rotation of Reinforced Concrete Plastic Hinges at Ultimate Load". Magazine of Concrete Research, Vol. 14, No. 41, July 1962.

36. YAMASHIRO, R., and SEISS, C.P., "Moment-Rotation Characteristics of Reinforced Concrete Members Subjected to Bending, Shear and Axial Load". Civil Engineering Studies, Structural Research Series No. 260, University of Illinois, Dec. 1962.

37. RÜSCH, H., and STÖCKL, S., "Der Einflub von Bügeln und Druckstäben auf das Verhalten der Biegedruckzone von Stahlbetonbalken". Heft. 148. Berlin, 1963.

38. A.C.I. Standard Building Code Requirements for Reinforced Concrete, (A.C.I. 318-63).

39. SINHA, B.P., GERSTLE, K.H., and TULIN, L.G., "Stress-Strain Relations for Concrete Under Cyclic Loading". Proceedings A.C.I. Journal, Vol. 61, No. 2, Feb. 1964.

40. DESAYI, P., and KRISHNAN, S., "Equation for the Stress-Strain Curve of Concrete". Proceedings A.C.I. Journal, Vol. 61, No. 3, Mar. 1964, pp. 345-350.

41. SINHA, B.P., GERSTLE, K.H., and TULIN, L.G., "Response of Singly Reinforced Beams to Cyclic Loading". Proceedings A.C.I. Journal, Vol. 61, No. 8, Aug. 1964.

42. MATTOCK, A.H., "Rotational Capacity of Hinging Regions

in Reinforced Concrete Beams". Flexural Mechanics of Reinforced Concrete, Proceedings of the International Symposium, Miami, Fla., 1964.

43. BAKER, A.L.L., and AMARAKONE, A.M.N., "Inelastic Hyperstatic Frames Analysis". Flexural Mechanics of Reinforced Concrete, Proceedings of the International Symposium, Miami, Fla., 1964.

44. AOYAMA, H., "Moment-Curvature Characteristics of Reinforced Concrete Members Subjected to Axial Load and Reversal of Bending". Flexural Mechanics of Reinforced Concrete. Proceedings of the International Symposium, Miami, Fla., 1964.

45. ROY, H.E.H., and SOZEN, M.A., "Ductility of Concrete". Flexural Mechanics of Reinforced Concrete. Proceedings of the International Symposium, Miami, Fla., 1964.

46. BERTERO, V.V., and FELIPPA, C., Discussion to reference 45.

47. BARNARD, P.R., "Researches into the Complete Stress-Strain Curve for Concrete". Magazine of Concrete Research, Vol. 16, No. 49, Dec. 1964.

48. FOX, L., "An Introduction to Numerical Linear Algebra". Oxford University Press, 1965.

49. SINGH, A., GERSTLE, K.H., and TULIN, L.G., "The Behaviour of Reinforcing Steel Under Reversed Loading". Journal A.S.T.M., Matierals Research and Standards, Vol. 5, No. 1, Jan. 1965.

50. AGRAWAL, G.L., TULIN, L.G., and GERSTLE, K.H., "Response of Doubly-Reinforced Concrete Beams to Cyclic Loading". Proceedings A.C.I. Journal, Vol. 62, No. 7, July 1965. pp. 823-836.

51. STURMAN, G.M., SHAH, S.P., and WINTER, G., "Effects of Flexural Strain Gradients on Microcracking and Stress-Strain Behaviour of Concrete". Proceedings A.C.I. Journal, Vol. 62, No. 7, July 1965.

52. BASE, G.D., and READ, J.B., "Effectiveness of Helical Binding in the Compression Zone of Concrete Beams". Proceedings A.C.I. Journal, Vol. 62, No. 7, July 1965.

53. PRIESTLEY, M.J.N., "Moment Redistribution in Pre-stressed Concrete Continuous Beams". Ph. D. Thesis, University of Canterbury, Christchurch, New Zealand, 1966.

54. A.C.I. COMMITTEE 435, "Deflections of Reinforced Concrete Flexural Members". Proceedings A.C.I. Journal, Vol. 63, No. 6, June 1966, pp. 637-674.

55. CORLEY, W.G., "Rotational Capacity of Reinforced Concrete Beams". Journal of the Structural Division, A.S.C.E., Vol. 92, No. ST5, Oct. 1966.

56. BURNS, N.H., and SEISS, C.P., "Repeated and Reversed Loading in Reinforced Concrete". Journal of the Structural Division, A.S.C.E., Vol. 92, No. ST5, Oct. 1966.

57. ————————, and ————————., "Plastic Hinging in

Reinforced Concrete", Journal of the Structural Division, A.S.C.E., Vol. 92, No. ST5, Oct. 1966.

58. CLOUGH, R.W., "Effect of Stiffness Degradation on Earthquake Ductility Requirements". Report No. 66-16, Structural Engineering Laboratory, University of California. Oct. 1966.

59. WARWARUK, J., "Strength in Flexure of Bonded and Unbonded Prestressed Concrete Beams". Civil Engineering Studies, Structural Research Series No. 138, University of Illinois, Aug. 1967.

60. BENNETT, W.B., PARME, A.L., HANSON, N.W., and SBAROUNIS, J.A., "Laboratory Investigation of Reinforced Concrete Beam-Column Connections under Lateral Loads". Adaptation of a film script - detailed report still being prepared. 1967.

61. KALDJIAN, M.J., "Moment-Curvature of Beams as Ramberg-Osgood Function". Journal of the Structural Division, A.S.C.E. Vol. 93, No. ST5, Oct. 1967.

62. HANSON, N.W., and CONNER, H.W., "Seismic Resistance of Reinforced Concrete Beam-Column Joints". Journal of the Structural Division, A.S.C.E., Vol. 93, No. ST5, Oct. 1967. pp. 533-560.

63. ATCHLEY, W.L., and FURR, H.L., "Strength and Energy Absorption Capabilities of Plain Concrete under Dynamic and Static Loadings". Proceedings A.C.I. Journal, Vol. 64, No. 11, Nov. 1967.

64. SOLIMAN, M.T.M., and YU, C.W., "The Flexural Stress-Strain Relationship of Concrete Confined by Rectangular Transverse Reinforcement". Magazine of Concrete Research, Vol. 19, No. 61, Dec. 1967. pp. 223-238. (Also, Private Communication).

65. SHERBOURNE, A.N., and PARAMESWAR, H.C., "Limit Analysis of Continuous Prestressed Beams". Journal of the Structural Division, A.S.C.E., Vol. 94, No. ST1, Jan. 1968. pp. 19-40.

66. NAWY, E.G., DANESI, R.F., and GROSKO, J.J., "Rectangular Spiral Binders Effect on Plastic Hinge Rotation Capacity in Reinforced Concrete Beams". Proceedings ACI Journal, Vol. 65, No. 12, Dec. 1968, pp. 1001-1010.

67. BERTERO, V., and BRESLER, B., "Seismic Behaviour of Reinforced Concrete Framed Structures". Paper presented at the Fourth World Conference on Earthquake Engineering, Chile, 1969.

68. A.C.I. COMMITTEE 439, "Effect of Steel Strength and of Reinforcement Ratio on the Mode of Failure and Strain Energy Capacity of Reinforced Concrete Beams". Proceedings A.C.I. Journal, Vol. 66, No. 3, March 1969, pp. 165-173.

69. A.C.I. - A.S.C.E. Committee 428, "Progress Report on Code Clauses for Limit Design". Proceedings A.C.I. Journal, Vol. 65, No. 9, Sept. 1968, pp. 713-719.

APPENDIX B

COMPUTER PROGRAMS

Listings of programs developed for this thesis are presented in this appendix. Output from all of these programs is self-explanatory. Input requirements are shown below.

Program 2.1 - "CORE"

Input: E50B = Value for ϵ_{50b}

PDD(1) = Product of p" and fourth root of B/S

PDD(2) = Product of p" and cube root of B/S

PDD(3) = Product of p" and square root of B/S

PDD(4) = Value for p"

Program 2.2 - "ZTABLE"

No input

Program 3.1 - "FCHANDR"

Input: EZEROL = Strain at which stress was last zero

NCYC = Cycle number

EIPL = Plastic strain in previous cycle

YM = Young's Modulus (p.s.i.)

FU = Ultimate stress (p.s.i.)

FY = Yield stress (p.s.i.)

D = Bar diameter (in.)

ESH = Strain hardening strain

WH = Weight of hanger (lb)

WLC = Weight of load cell (lb)

EZERO = Initial extensometer reading

F1L = Gauge Factor for Load

F2L = Initial load reading

NSPEC = Specimen number

LR = Load reading

SR = Strain reading

Program 3.2 - "FCOR"

Input: RATIO = Characteristic ratio

EIPL = Plastic strain in previous cycle

SD = Standard deviation of stress (p.s.i.)

(All input obtained from Program 3.1)

Program 3.3 - "FINDR"

Input: As for Program 3.1

Program 3.4 - "STEEL"

YM = Young's Modulus (p.s.i.)

FU = Ultimate stress (p.s.i.)

FY = Yield stress (p.s.i.)

D = Bar diameter (in.)

NR = Number of readings

ESH = Strain hardening strain

HW = Hanger weight (lb)

WLC = Weight of load cell (lb)

EZERO = Initial extensometer reading

F1L = Gauge factor for load

F2L = Initial load reading

NSPEC = Specimen number

LR = Load reading

SR = Strain reading

Program 4.1 - "GAMMATAB"

Input: ZVAL = Z values (up to 18 permitted)

Program 4.2 - "TBEAMS"

Input: FU(1) = Ultimate stress (p.s.i.) for top steel

FY(1) = Yield stress (p.s.i.) for top steel

ESH(1) = Strain hardening strain for top steel

P(1) = Top steel ratio

YM(1) = Young's Modulus (p.s.i.) for top steel

(Subscript (2) for above input refers to bottom steel)

EO = Concrete strain, ϵ_o

ECR = Unconfined concrete crushing strain

Z = Confined concrete parameter Z

FCD = Concrete cylinder strength, f'_c (p.s.i.)

DD = Ratio of compression steel depth to effective depth

H = Ratio of section depth to effective depth

BDD = Ratio of confined core width to web width

WF = Ratio of flange width to web width

DF = Ratio of flange thickness to effective depth

KODE = 1 for axial load considered

= 0 for axial load not considered

EP = Ratio of distance of centroid of axial load from top of section, to effective depth

POB(1) = Effective depth (in.)

POB(2) = Inverse of product of web width and square of effective depth ($in.^{-3}$)

Note: POB(1) and POB(2) need only be used when web width and effective depth are known.

Program 5.1 - "CYCBAUS"

Input: As for Program 4.2 with the following additions:

NEL = Number of discrete horizontal concrete elements per section (up to 500)

CR = Curvature readings at extremities of cycles (dimensionless)

NCR = Number of curvature readings

BIGP = Axial stress (p.s.i.)

Program 5.2 - "CYCBMS"

Input: As for Program 5.1

Program 6.1 - "BEAMDEFS"

Input: As for Program 5.1 with the following additions:

DR = Deflection readings at extremities of cycles (dimensionless)

NDR = Number of deflection readings

NSECT = Number of beam sections, N_s

BEAML = Ratio of cantilever length to effective depth, l_c

LTYPE = 2 for uniformly-distributed load; otherwise point load

Program 6.2 - "CLOUGH"

Input: PYM = Positive yield moment

PYC = Positive yield curvature

NYM = Negative yield moment

NYC = Negative yield curvature

(Choice of units for the above parameters)

NSECT = Number of beam sections, N_s

DR = Deflection readings at extremities of cycles (dimensionless)

NR = Number of deflection readings

BEAML = Ratio of cantilever length to effective depth, l_c

Program 7.1 - "DATATEST"

Program 7.2 - "BEAMTEST"

Program 7.3 - "INCLINO"

Program 7.4 - "DATALIST"

As these programs were written for the test beams of the experimental programme, instructions for their use have not been included.

```
C     ******************************************************************
C
C     E50B  VS.  PDD*(B/S)**N  FOR CONFINED CONCRETE
C
C     APRIL 1969
C
C     ******************************************************************
      REAL NUM
      DIMENSION E50B(100),PDD(100,4),X(100,2),Z(100),PHI(2,2),PROD(2),AL
     1PH(2)
C     READ IN DATA
    1 DO 3 I=1,100
      READ(5,100,END=99)E50B(I),(PDD(I,J),J=1,4)
      IF(E50B(I)) 4,4,2
    2 NR=I
    3 CONTINUE
C     VARIETY OF N VALUES  1/4,1/3,1/2,&0
    4 KLOB=1
   45 DO 24 J=1,4
      GO TO (5,6,7,8),J
    5 WRITE(6,101)
  100 FORMAT(F6.5,4F8.5)
  101 FORMAT('1'/'1N=.25'/'1')
      GO TO 9
    6 WRITE(6,102)
  102 FORMAT('1'/'1N=.33'/'1')
      GO TO 9
    7 WRITE(6,103)
  103 FORMAT('1'/'1N=.50'/'1')
      GO TO 9
    8 WRITE(6,104)
  104 FORMAT('1'/'1N=0.0'/'1')
    9 RN=NR
      KOUNT=1
      SDSUM=0.
      DO 22 N=1,8
      A=N-1
      A=A/2000.
C     ESTABLISH MATRIX X(NR,2)
      DO 10 I=1,NR
      X(I,1)=1.
   10 X(I,2)=ALOG(PDD(I,J))
C     ESTABLISH VECTOR Z(NR)
      DO 11 I=1,NR
   11 Z(I)=ALOG(E50B(I)-A)
C     ESTABLISH PRODUCT MATRIX PHI(2,2)=SUM OF X(NR,2).X(2,NR)
      DO 12 I=1,2
      DO 12 K=1,2
      PHI(I,K)=0.
      DO 12 L=1,NR
   12 PHI(I,K)=PHI(I,K)+X(L,I)*X(L,K)
C     INVERT PHI(2,2)
      DO 16 I=1,2
      T=PHI(I,I)
      PHI(I,I)=1.
      DO 13 M=1,2
   13 PHI(I,M)=PHI(I,M)/T
      DO 16 K=1,2
      IF(K-I) 14,16,14
   14 T=PHI(K,I)
      PHI(K,I)=0.
      DO 15 M=1,2
   15 PHI(K,M)=PHI(K,M)-T*PHI(I,M)
   16 CONTINUE
C     ESTABLISH PRODUCT VECTOR PROD(2)
      DO 17 I=1,2
      PROD(I)=0.
      DO 17 M=1,NR
   17 PROD(I)=PROD(I)+X(M,I)*Z(M)
C     SOLVE FOR B AND C
      DO 18 I=1,2
      ALPH(I)=0.
      DO 18 M=1,2
   18 ALPH(I)=ALPH(I)+PHI(I,M)*PROD(M)
      B=EXP(ALPH(1))
      C=ALPH(2)
   19 WRITE(6,105)
  105 FORMAT(' '///////' ',14X,'A',14X,'B',14X,'C',7X,'STD DEVN'///)
C     COMPUTE STANDARD DEVIATIONS
      DO 20 I=1,NR
      E=A+B*PDD(I,J)**C
   20 SDSUM=SDSUM+(E-E50B(I))**2
      SD=SQRT(SDSUM/RN)
      SDSUM=0.
      WRITE(6,106) A,B,C,SD
  106 FORMAT(' ',4F15.7//////' ',8X,'PDD*(B/S)**N',16X,'E50B',5X,'ANALYT
     1ICAL E50B',11X,'DEVIATION'//)
      DO 21 I=1,NR
      E=A+B*PDD(I,J)**C
      DEV=E50B(I)-E
      WRITE(6,107) PDD(I,J),E50B(I),E,DEV
   21 CONTINUE
  107 FORMAT(' ',4F20.5)
      GO TO (22,24),KOUNT
   22 CONTINUE
      KOUNT=2
      NUM=0.
      DENOM=0.
      DO 23 I=1,NR
      NUM=NUM+PDD(I,J)*E50B(I)
   23 DENOM=DENOM+PDD(I,J)**2
      B=NUM/DENOM
      A=0.
      C=1.
      GO TO 19
   24 CONTINUE
      GO TO (25,1),KLOB
   25 KLOB=2
```

PROGRAM 2.1

```
      NR=NR-1
      GO TO 45
   99 CONTINUE
      END
```

CONTINUED(2)

PROGRAM 2.2 'ZTABLE'

```
C     ******************************************************************
C
C     TABLE FOR Z
C
C     MAY 1969
C
C     ******************************************************************
      DIMENSION M(11)
      WRITE(6,100)
  100 FORMAT('1',56X,'TABLE OF Z-VALUES'///' ',7X,'B/S',7X,'PDD',42X,'FC
     1D'//' ',26X,  '2500',6X,'3000',6X,'3500',6X,'4000',6X,'4500',6X,'5
     2000',6X,'5500',6X,'6000',6X,'6500',6X,'7000',6X,'7500'/)
      DO2I=50,200,25
      BS=I
      BS=BS/100.
      WRITE(6,101)BS
  101 FORMAT(' ',F10.2)
      DO2J=1,1001,100
      PDD=J-1
      PDD=.0001*PDD
      E50B=.75*PDD*SQRT(BS)
      DO1K=1,11
      L=2000+500*K
      FCD=L
      E50C=(3.+.002*FCD)/(FCD-1000.)
      E50T=E50B+E50C
      Z=.5/(E50T-.002)+.5
      M(K)=Z
    1 CONTINUE
      WRITE(6,102)PDD,(M(K),K=1,11)
  102 FORMAT('+',F20.4,11I10/)
    2 CONTINUE
      END
```

```
C     ***********************************************************************
C
C     BAUSCHINGER FORMULA
C
C     RAMBERG-OSGOOD FUNCTION
C
C     FCH  AND  R  FOUND BY THE METHOD OF LEAST SQUARES
C
C     FEB 1969
C
C     ***********************************************************************
      DIMENSION FA(1500),EA(1500),C(1500),A(1500,2),PHI(2,2),PROD(2),
     1FACT(40),IT(40)
      PI=3.14159
    1 READ(5,100)EZEROL,NCYC,EIPL
  100 FORMAT(F8.6,I3,F8.6)
      READ(5,101)YM,FU,FY,D,I,ESH,WH,WLC,EZERO,F1L,F2L,NSPEC
  101 FORMAT(F9.0,2F8.0,F8.3,I5,F7.4,F6.0,F5.0,F9.6,F5.1,F8.0,I4)
      WRITE(6,102)NSPEC,NCYC,EIPL
  102 FORMAT('1SPECIMEN',I3,' CYCLE',I2,10X,' LAST PLASTIC STRAIN =',F8.
     16////)
      DO51I=1,1000
   14 READ(5,103)LR,SR
      RL=LR
      IF(LR)2,15,3
   15 IF(SR)2,6,2
    2 P=F1L*(RL+F2L)-WH-WLC
      GO TO 4
    3 P=F1L*(RL-F2L)-WH-WLC
    4 FA(I)=4.*P/(PI*D*D)
      EA(I)=(SR-EZERO)/(1.+EZERO)-4.*WH/(PI*D*D*YM)
      IF(ABS(EA(I)-EZEROL)*YM-ABS(FA(I)))14,14,16
   16 NR=I
    5 CONTINUE
    6 IF(FA(1))7,99,9
    7 DO8I=1,NR
      FA(I)=-FA(I)
      ES=EA(I)
      EA(I)=EZEROL-ES
    8 CONTINUE
      GO TO 11
    9 DO10I=1,NR
      EA(I)=EA(I)-EZEROL
   10 CONTINUE
   11 WRITE(6,104)
  103 FORMAT(I6,F9.6)
  104 FORMAT(1H ,5X,'CHARACTERISTIC STRESS',5X,'CHARACTERISTIC STRAIN',
     115X,'PARAMETER R',17X,'MEAN DEVN',18X,'STD DEVN'/////)
      NROLD=NR
C     WEIGHTING ROUTINE
      DO60I=1,NROLD
      WEIGHT=.5+10000.*EA(I)
      K=WEIGHT
      IF(K-1)60,60,58
```



```
   58 K=K-1
      DO59J=1,K
      EA(J+NR)=EA(I)
   59 FA(J+NR)=FA(I)
      NR=NR+K
   60 CONTINUE
      RN=NROLD
C     ESTABLISH VECTOR  C(NR)
      DO40I=1,NR
   40 C(I)=ALOG(EA(I)*YM-FA(I))
      UV=4.
      KOUNT=1
C     ESTABLISH MATRIX  A(NR,2)
   41 DO42I=1,NR
      A(I,1)=1.-UV
   42 A(I,2)=ALOG(FA(I))
C     ESTABLISH MATRIX  PHI(2,2)
      DO43I=1,2
      DO43J=1,2
      PHI(I,J)=0.
      DO43K=1,NR
   43 PHI(I,J)=PHI(I,J)+A(K,I)*A(K,J)
C     ESTABLISH VECTOR  PROD(2)
      DO44I=1,2
      PROD(I)=0.
      DO44J=1,NR
   44 PROD(I)=PROD(I)+A(J,I)*C(J)
C     INVERT  PHI(2,2)
      DO48I=1,2
      T=PHI(I,I)
      PHI(I,I)=1.
      DO45J=1,2
   45 PHI(I,J)=PHI(I,J)/T
      DO48K=1,2
      IF(K-I)46,48,46
   46 T=PHI(K,I)
      PHI(K,I)=0.
      DO47J=1,2
   47 PHI(K,J)=PHI(K,J)-T*PHI(I,J)
   48 CONTINUE
C     FIND  FCH  AND  R
      DO49I=1,2
      C(I)=0.
      DO49J=1,2
   49 C(I)=C(I)+PHI(I,J)*PROD(J)
      R=C(2)
      IF(ABS(R-UV)-.05)51,51,50
   50 KOUNT=KOUNT+1
      UV=.5*(R+UV)
      IF(KOUNT-1500)41,41,1
   51 FCH=EXP(C(1))
      ECH=FCH/YM
      RATIO=FCH/FY
C     MEAN AND STANDARD DEVIATIONS
```

PROGRAM 3.1 CONTINUED(2)

```
      AVENUM=0.
      SDSUM=0.
      DO12L=1,NROLD
      ES=EA(L)
      ALPHA=ES/ECH
      GAMMA=ALPHA
      IT(L)=1
   65 BETA=ALPHA-(ALPHA+ALPHA**R-GAMMA)/(1.+R*ALPHA**(R-1.))
      IF(ABS(ALPHA-BETA)-10./FCH)67,67,66
   66 ALPHA=BETA
      IT(L)=IT(L)+1
      GO TO 65
   67 FS=FCH*BETA
      FACT(L)=FS
      AVENUM=AVENUM+FS-FA(L)
      SDSUM=SDSUM+(FS-FA(L))**2
   12 CONTINUE
      AVE=AVENUM/RN
      SD=SQRT(SDSUM/RN)
      WRITE(6,105)FCH,RATIO,ECH,R,AVE,SD
  105 FORMAT(1H ,F13.0,' = ',F5.3,' * FY',2F26.6,2F26.0)
      WRITE(6,111)
  111 FORMAT(1H ///////)
C     OUTPUT THEORETICAL STRESSES
      WRITE(6,108)
  108 FORMAT(1H ,14X,'STRAIN',8X,'EXPTL STRESS',8X,'THEOR STRESS',11X,
     1'DEVIATION',10X,'NUMBER OF ITERATIONS'////)
      DO22I=1,NROLD
      ES=EA(I)
      FS=FACT(I)
      DEV=FA(I)-FS
      WRITE(6,110)ES,FA(I),FS,DEV,IT(I)
   22 CONTINUE
  110 FORMAT(1H F20.6,3F20.0,20X,I10)
      GO TO 1
   99 CONTINUE
      END
```

PROGRAM 3.2 'FCOR'

```
C     ******************************************************************
C
C     PROGRAM TO CORELATE FCH AND EIPL
C
C     MARCH 1969
C
C     ******************************************************************
      DIMENSION RATIO(1600),EIPL(1600),SD(60),E(1600,3),PROD(3),PHI(3,3)
     1,GREEK(3)
C     INPUT ROUTINE
   98 DO 2 I=1,600
      READ(5,100) RATIO(I),EIPL(I),SD(I)
      IF(RATIO(I)) 99,3,1
    1 NR=I
    2 CONTINUE
    3 NROLD=NR
  100 FORMAT(F5.3,F9.6,F8.0)
C     WEIGHTING ROUTINE
      A=4.E+7
   35 DO6I=1,NROLD
      WEIGHT=.5+A*EIPL(I)/SD(I)
      K=WEIGHT
      IF(K-1) 6,6,4
    4 K=K-1
      IF(NR+K-1600)45,45,44
   44 A=A/2.
      NR=NROLD
      GO TO 35
   45 DO5J=1,K
      RATIO(J+NR)=RATIO(I)
    5 EIPL(J+NR)=EIPL(I)
      NR=NR+K
    6 CONTINUE
C     SET OUT HEADING
      WRITE(6,101)
  101 FORMAT('1',25X,'ALPHA',26X,'BETA',25X,'GAMMA'////)
C     ESTABLISH STRAIN VECTOR  E(NR,3)
      DO 7 I=1,NR
      E(I,1)=1./ALOG(1.+1000.*EIPL(I))
      E(I,2)=1./(EXP(1000.*EIPL(I))-1.)
    7 E(I,3)=1.
C     ESTABLISH PRODUCT MATRIX  PHI(3,3) = E(3,NR) . E(NR,3)
      DO8I=1,3
      DO8J=1,3
      PHI(I,J)=0.
      DO 8 K=1,NR
    8 PHI(I,J)=PHI(I,J)+E(K,I)*E(K,J)
C     ESTABLISH PRODUCT VECTOR  PROD(3) = E(NR,3) . RATIO(NR)
      DO9I=1,3
      PROD(I)=0.
      DO 9 J=1,NR
    9 PROD(I)=PROD(I)+E(J,I)*RATIO(J)
C     INVERT  PHI(3,3)  BY JORDANIAN ELIMINATION
      DO13I=1,3
```

PROGRAM 3.2 CONTINUED(1)

```
      T=PHI(I,I)
      PHI(I,I)=1.
      DO10J=1,3
   10 PHI(I,J)=PHI(I,J)/T
      DO13K=1,3
      IF(K-I) 11,13,11
   11 T=PHI(K,I)
      PHI(K,I)=0.
      DO12J=1,3
   12 PHI(K,J)=PHI(K,J)-T*PHI(I,J)
   13 CONTINUE
C     SOLVE FOR ALPHA, BETA AND GAMMA
      DO14I=1,3
      GREEK(I)=0.
      DO14J=1,3
   14 GREEK(I)=GREEK(I)+PHI(I,J)*PROD(J)
      ALPHA=GREEK(1)
      BETA=GREEK(2)
      GAMMA=GREEK(3)
      WRITE(6,102)(GREEK(I),I=1,3)
  102 FORMAT(1H ,4F30.6////)
C     OUTPUT FOR CURVE
      WRITE(6,103)
  103 FORMAT(1H ,9X,'STRAIN',10X,'RATIO'///)
      DO15I=1,23
      J=I-1
      X=J/1000.
      IF(I-1)99,141,142
  141 X=.0001
  142 Y=ALPHA/ALOG(1.+1000.*X)+BETA/(EXP(1000.*X)-1.)+GAMMA
      WRITE(6,104) X,Y
   15 CONTINUE
  104 FORMAT(1H ,2F15.6)
      WRITE(6,105)
  105 FORMAT('1')
      GO TO 98
   99 CONTINUE
      END
```

PROGRAM 3.3 'FINDR'

```
C     ***************************************************************
C
C     BAUSCHINGER FORMULA
C
C     KNOWING  FCH  ,  FIND  R
C
C      MARCH 1969
C
C     ***************************************************************
      DIMENSION FA(1950),EA(1950),FE(1950),STR(1950),FACT(50)
      PI=3.14159
    1 READ(5,100)EZEROL,NCYC,EIPL
  100 FORMAT(F8.6,I3,F9.6)
      READ(5,101)YM,FU,FY,D,I,ESH,WH,WLC,EZERO,F1L,F2L,NSPEC
  101 FORMAT(F9.0,2F8.0,F6.3,I5,F7.4,F6.0,F5.0,F9.6,F5.1,F8.0,I4)
      WRITE(6,102)NSPEC,NCYC,EIPL
  102 FORMAT('1SPECIMEN',I3,' CYCLE',I2,10X,'LAST PLASTIC STRAIN =',F8.6
     1////)
      DO5I=1,1000
   14 READ(5,103)LR,SR
      RL=LR
      IF(LR)2,15,2
   15 IF(SR)2,6,2
    2 P=F1L*(RL+F2L)-WH-WLC
      GO TO 4
    3 P=F1L*(RL-F2L)-WH-WLC
    4 FA(I)=4.*P/(PI*D*D)
      EA(I)=(SR-EZERO)/(1.+EZERO)-4.*WH/(PI*D*D*YM)
      IF(ABS(EA(I)-EZEROL)*YM-ABS(FA(I)))14,14,45
   45 NR=I
    5 CONTINUE
    6 IF(FA(1))7,99,9
    7 DO8I=1,NR
      FA(I)=-FA(I)
      ES=EA(1)
      EA(I)=EZEROL-ES
    8 CONTINUE
      GO TO 11
    9 DO10I=1,NR
      EA(I)=EA(I)-EZEROL
   10 CONTINUE
   11 WRITE(6,104)
  103 FORMAT(I6,F9.6)
  104 FORMAT(1H ,5X,'CHARACTERISTIC STRESS',5X,'CHARACTERISTIC STRAIN',
     115X,'PARAMETER R',17X,'MEAN DEVN',16X,'STD DEVN'/////)
C     FITTING ROUTINE
      NROLD=NR
      RN=NROLD
      FCH=FY*(.744/ALOG(1.+1000.*EIPL)+.071/(EXP(1000.*EIPL)-1.)+.241)
      IF(FCH-FY)57,57,56
   56 FCH=FY
   57 RATIO=FCH/FY
      ECH=FCH/YM
C     WEIGHTING ROUTINE
```

```
      DO60I=1,NROLD
      WEIGHT=.5+10000.*EA(I)
      K=WEIGHT
      IF(K-1)60,60,58
   58 K=K-1
      DO59J=1,K
      EA(J+NR)=EA(I)
   59 FA(J+NR)=FA(I)
      NR=NR+K
   60 CONTINUE
C     ESTABLISH STRESS VECTOR   STR(NR)
      DO61I=1,NR
   61 STR(I)=ALOG(FA(I)/FCH)
C     ESTABLISH PRODUCT SCALAR  PHI = SUM OF  STR(NR) . STR(NR)
      PHI=0.
      DO62I=1,NR
   62 PHI=PHI+STR(I)**2
C     ESTABLISH STRESS AND STRAIN VECTOR  FE(NR)
      DO63I=1,NR
   63 FE(I)=ALOG((EA(I)*YM-FA(I))/FCH)
C     FIND  R
      R=0.
      DO64I=1,NR
   64 R=R+FE(I)*STR(I)
      R=R/PHI
C     FIND MEAN AND STANDARD DEVIATIONS
      AVENUM=0.
      SDSUM=0.
      DO12L=1,NROLD
      ES=EA(L)
      ALPHA=ES/ECH
      GAMMA=ALPHA
   65 BETA=ALPHA-(ALPHA+ALPHA**R-GAMMA)/(1.+R*ALPHA**(R-1.))
      IF(ABS(ALPHA-BETA)-10./FCH)67,67,66
   66 ALPHA=BETA
      GO TO 65
   67 FS=FCH*BETA
      FACT(L)=FS
      AVENUM=AVENUM+FS-FA(L)
      SDSUM=SDSUM+(FS-FA(L))**2
   12 CONTINUE
      AVE=AVENUM/RN
      SD=SQRT(SDSUM/RN)
      WRITE(6,105)FCH,RATIO,ECH,R,AVE,SD
  105 FORMAT(1H ,F13.0,' =',F6.3,' * FY',2F26.6,2F26.0)
      WRITE(6,111)
  111 FORMAT(1H //////)
C     OUTPUT
      WRITE(6,108)
  108 FORMAT(1H ,14X,'STRAIN',8X,'EXPTL STRESS',8X,'THEOR STRESS',11X,
     1'DEVIATION',////)
      DO22I=1,NROLD
      ES=EA(I)
      FS=FACT(I)
```



```
      DEV=FA(I)-FS
      WRITE(6,110)ES,FA(I),FS,DEV
   22 CONTINUE
  110 FORMAT(1H ,F20.6,3F20.0)
      GO TO 1
   99 CONTINUE
      END
```

```
C     ********************************************************************
C
C      BAUSCHINGER EFFECT  -  A COMPARISON
C                          -  EXPERIMENTAL
C                          -  SINGH , TULIN & GERSTLE
C                          -  MODIFIED RAMSBERG-OSGOOD
C
C      MARCH 1969
C
C     ********************************************************************
      DIMENSIONFS(2),EZERON(2),EZEROL(2),SENSE(2),KBAUS(2),EDIFF(2),EIPL
     1(2),FA(600),EA(600),AVENUM(2),SDSUM(2),FSL(2),ESL(2),FT(2)
     2,NCYC(2),RVAL(40)
      PI=3.14159
    1 READ(5,101)YM,FU,FY,D,NR,ESH,HW,WLC,EZERO,F1L,F2L,NSPEC
  101 FORMAT(F9.0,2F8.0,F6.3,I5,F7.4,F6.0,F5.0,F9.6,F5.1,F8.0,I4)
      WRITE(6,102)NSPEC
  102 FORMAT('1SPECIMEN',I3//////)
      WRITE(6,103)
  103 FORMAT(' ',24X,'STRAIN',18X,'EXPTL STRESS',16X,'S,T & G STRESS',7X
     1,'MODIFIED RAMBERG-OSGOOD'////)
      DO 6 I=1,NR
      READ(5,104) LR,SR
      RL=LR
      IF(LR) 2,3,4
    2 P=F1L*(RL+F2L)-HW-WLC
      GO TO 5
    3 P=-HW
      GO TO 5
    4 P=F1L*(RL-F2L)-HW-WLC
    5 FA(I)=4.*P/(PI*D*D)
      EA(I)=(SR-EZERO)/(1.+EZERO)-4.*HW/(PI*D*D*YM)
    6 CONTINUE
  104 FORMAT(I6,F9.6)
C     INITIALISE
      DO 7 I=1,2
      ESL(I)=0.
      FSL(I)=0.
      EZERON(I)=0.
      EZEROL(I)=0.
      KBAUS(I)=0
      NCYC(I)=0
      SENSE(I)=0.
      EDIFF(I)=0.
      EIPL(I)=0.
      AVENUM(I)=0.
    7 SDSUM(I)=0.
      ONE=1.
      RN=NR
C     SET UP R VALUES ARRAY
      DO75I=1,39,2
      G=I
   75 RVAL(I)=4.489/ALOG(1.+G)-6.026/(EXP(G)-1.)+.297
      DO76I=2,40,2
```



```
      G=I
   76 RVAL(I)=2.197/ALOG(1.+G)-.469/(EXP(G)-1.)+3.043
C     TRANSITION STRESS FOR A,G&T EXPRESSION
      ET=.0001
      G=.0001
    8 LHS=YM*ET
      RHS=64500.-52700.*.838**(1000.*ET)
      IF(LHS-RHS)9,11,10
    9 ET=ET+G
      GO TO 8
   10 ET=ET-G
      G=.1*G
      IF(G-1.E-8)11,11,9
   11 FT(1)=ET*YM
C     TRANSITION STRESS FOR MODIFIED RAMBERG-OSGOOD
      FT(2)=.15*FY
C     MODIFIED BURNS & SEISS PARAMETERS FOR STRAIN HARDENING
      WC=FU/FY
      WB=.14
      WH=(WC*(30.*WB+1.)**2-60.*WB-1.)/(15.*WB**2)
      ESU=ESH+WB
      WA=(WH*WB+2.)/(60.*WB+2.)
C     COMPUTE THEORETICAL STRESSES
      DO 60 I=1,NR
      ES=EA(I)
      DO405J=1,2
      FS(J)=YM*(ES-EZERON(J))
      KAD=KBAUS(J)
      GO TO (12,27),KAD
C     ELASTO PLASTIC SYSTEM
   12 IF(FS(J)*SENSE(J))19,13,13
   13 IF(ABS(FS(J))-FY)40,40,14
   14 IF(ABS(ES)-ESH)15,15,16
   15 FS(J)=SIGN(FY,ES)
      GO TO 40
   16 TEMP=1.
      IF(ES)17,99,18
   17 TEMP=-1.
   18 DELTA=ABS(ESH-ABS(ES))
      FS(J)=TEMP*FY*((WH*DELTA+2.)/(60.*DELTA+2.)+DELTA*(WC-WA)/WB)
      GO TO 40
   19 IF(ABS(FS(J))-FT(J))40,40,20
C     ITERATION ROUTINE
   20 DELTA=ABS(EZERON(J)-ES)
      GO TO (21,22),J
   21 FS(J)=-SENSE(J)*(64500.-52700.*.838**(1000.*DELTA))
      GO TO 40
   22 PLAST=ABS(EZERON(J)-EZEROL(J))
      R=RVAL(NCYC(J)+1)
      FCH=FY*(.744/ALOG(1.+1000.*PLAST)+.071/(EXP(1000.*PLAST)-1.)+.241)
      IF(FCH-FY)225,225,224
  224 FCH=FY
  225 ECH=FCH/YM
      ALPHA=DELTA/ECH
```

```
      GAMMA=ALPHA
   23 BETA=ALPHA-(ALPHA+ALPHA**R-GAMMA)/(1.+R*ALPHA**(R-1.))
      IF(ABS(ALPHA-BETA)-10./FCH) 25,25,24
   24 ALPHA=BETA
      GO TO 23
   25 GO TO(26,38,39),KAD
   26 FS(J)=-FCH*BETA*SENSE(J)
      GO TO 40
C     BAUSCHINGER SYSTEM
   27 IF(ABS(FS(J))-FT(J))40,40,28
   28 IF(FS(J)*FSL(J))29,99,30
   29 KAD=3
      IF(ABS(FSL(J))-FT(J))32,32,315
   30 IF(ABS(FSL(J))-FT(J)) 31,31,32
   31 IF(ABS(ESL(J)-EZEROL(J))-ABS(EZERON(J)-EZEROL(J)))315,99,32
  315 DELTA=ABS(EZERON(J)-ES)
      GO TO (34,22),J
   32 IF(ABS(EZEROL(J)-ES)-EDIFF(J))325,325,33
  325 IF((EZERON(J)-EZEROL(J))*(ES-EZERON(J)))315,40,40
   33 DELTA=ABS(EZEROL(J)-ES)
      GO TO (34,37),J
   34 FS(J)=64500.-52700.*.838**(1000.*DELTA)
      GO TO (99,35,36),KAD
   35 FS(J)=FS(J)*SIGN(ONE,FSL(J))
      GO TO 40
   36 FS(J)=-FS(J)*SIGN(ONE,FSL(J))
      GO TO 40
   37 R=RVAL(NCYC(J))
      FCH=FY*(.744/ALOG(1.+1000.*EIPL(J))+.071/(EXP(1000.*EIPL(J))-1.)+.
     1241)
      IF(FCH-FY)375,375,374
  374 FCH=FY
  375 ECH=FCH/YM
      ALPHA=DELTA/ECH
      GAMMA=ALPHA
      GO TO 23
   38 FS(J)=FCH*BETA*SIGN(ONE,FSL(J))
      GO TO 40
   39 FS(J)=-FCH*BETA*SIGN(ONE,FSL(J))
   40 IF(ABS(FS(J))-FU)405,405,404
  404 FS(J)=SIGN(FU,FS(J))
  405 CONTINUE
      WRITE(6,105)ES,FA(I),FS(1),FS(2)
  105 FORMAT(1H ,F30.6,3F30.0)
      DO 41 J=1,2
      AVENUM(J)=AVENUM(J)+FA(I)-FS(J)
   41 SDSUM(J)=SDSUM(J)+(FA(I)-FS(J))**2
C     UPDATE ROUTINE
      DO 59 J=1,2
      KAD=KBAUS(J)
      GO TO(42,48),KAD
C     ELASTO-PLASTIC SYSTEM
   42 IF(SENSE(J)) 45,43,45
   43 IF(ABS(ES)-FY/YM)58,58,44
```



```
   44 SENSE(J)=SIGN(ONE,ES)
      GO TO 57
   45 IF(SENSE(J)*FS(J)) 46,57,57
   46 IF(ABS(FS(J))-FT(J))57,57,47
   47 KBAUS(J)=2
      GO TO 55
C     BAUSHINGER SYSTEM
   48 IF(ABS(FS(J))-FT(J))58,58,49
   49 IF(FS(J)*FSL(J))50,99,54
   50 IF(ABS(FSL(J))-FT(J))51,51,53
   51 IF(ABS(EZEROL(J)-ES)-EDIFF(J))515,515,52
  515 IF((EZERON(J)-EZEROL(J))*(ES-EZERON(J)))53,57,57
   52 EDIFF(J)=ABS(EZEROL(J)-ES)
      GO TO 57
   53 EDIFF(J)=ABS(EZERON(J)-ES)
      GO TO 56
   54 IF(ABS(FSL(J))-FT(J)) 55,55,51
   55 IF(ABS(ESL(J)-EZEROL(J))-ABS(EZERON(J)-EZEROL(J)))53,99,51
   56 EIPL(J)=ABS(EZERON(J)-EZEROL(J))
      EZEROL(J)=EZERON(J)
      NCYC(J)=NCYC(J)+1
   57 EZERON(J)=ES-FS(J)/YM
   58 ESL(J)=ES
   59 FSL(J)=FS(J)
   60 CONTINUE
C     MEAN AND STANDARD DEVIATIONS
      DO 61 I=1,2
      AVENUM(I)=AVENUM(I)/RN
   61 SDSUM(I)=SQRT(SDSUM(I)/RN)
      WRITE(6,106)(AVENUM(I),I=1,2)
  106 FORMAT(1H ////// MEAN DEVIATIONS',45X,2F30.0//)
      WRITE(6,107)(SDSUM(I),I=1,2)
  107 FORMAT(' STANDARD DEVIATIONS',41X,2F30.0//)
      WRITE(6,108)(FT(I),I=1,2)
  108 FORMAT(' TRANSITION STRESSES',41X,2F30.0)
      WRITE(6,109)
  109 FORMAT('1')
      GO TO 1
   99 CONTINUE
      END
```

```
C     ****************************************************************
C
C     TABLES FOR STRESS BLOCK PARAMETERS ALPHA AND GAMMA
C
C     MAY 1969 , MODIFIED JULY 1969
C
C     ****************************************************************
      INTEGER ZVAL
      DIMENSION ZVAL(18),VALZ(18),E20(18),ALPHA(18),GAMMA(18)
C     READ Z-VALUES
      READ(5,100)ZVAL
  100 FORMAT(18I4)
C     ALPHA VALUES
      WRITE(6,101)
  101 FORMAT('1',55X,'TABLE OF ALPHA VALUES'//////)
      WRITE(6,102) ZVAL
  102 FORMAT('  ',1X,'EC',59X,'Z-VALUES'/'0 ',3X,18I7/)
      DO 1 I=1,18
      VALZ(I)=ZVAL(I)
    1 E20(I)=.002+.8/VALZ(I)
      F1=2./3.
      F3=.2
      DO 5 I=20,150,2
      EC=I
      EC=.0001*EC
      DO 4 J=1,18
      IF(EC-E20(J)) 2,2,3
    2 F2=1.-.5*VALZ(J)*(EC-.002)
      ALPHA(J)=(.002*F1+(EC-.002)*F2)/EC
      GO TO 4
    3 F2=1.-.5*VALZ(J)*(E20(J)-.002)
      ALPHA(J)=(.002*F1+(E20(J)-.002)*F2+F3*(EC-E20(J)))/EC
    4 CONTINUE
      WRITE(6,103) EC,ALPHA
  103 FORMAT(' ',F5.4,18F7.3)
    5 CONTINUE
C     GAMMA VALUES
      WRITE(6,104)
  104 FORMAT('1',55X,'TABLE OF GAMMA VALUES'//////)
      WRITE(6,102) ZVAL
      DO 9 I=20,150,2
      EC=I
      EC=.0001*EC
      F1=.004/(3.*EC)
      DO 8 J=1,18
      IF(EC-E20(J))  6,6,7
    6 F2=(1.-.5*VALZ(J)*(EC-.002))*(EC-.002)/EC
      EB2=.002+(EC-.002)*(3.-2.*VALZ(J)*(EC-.002))/(6.-3.*VALZ(J)*(EC-.0
     102))
      EBAR=(F1*.625*.002+F2*EB2)/(EC*(F1+F2))
      GAMMA(J)=1.-EBAR
      GO TO 8
    7 F2=(1.-.5*VALZ(J)*(E20(J)-.002))*(E20(J)-.002)/EC
      EB2=.002+(E20(J)-.002)*(3.-2.*VALZ(J)*(E20(J)-.002))/(6.-3.*VALZ(J
     1)*(E20(J)-.002))
      F3=.2*(EC-E20(J))/EC
      EB3=.5*(EC+E20(J))
      EBAR=(F1*.625*.002+F2*EB2+F3*EB3)/(EC*(F1+F2+F3))
      GAMMA(J)=1.-EBAR
    8 CONTINUE
      WRITE(6,103) EC,GAMMA
    9 CONTINUE
C     E20 VALUES
      WRITE(6,105) E20
  105 FORMAT('1VALUES FOR E20'//'  ',3X,18F7.4)
      END
```

```
C     ***********************************************************************
C
C     MOMENT CURVATURE RELATIONSHIPS T-BEAMS
C
C     APRIL 1968 - MODIFIED JULY 1968 , MAY 1969
C
C     ***********************************************************************
      DIMENSION FU(2),FY(2),ESH(2),P(2),YM(2),WA(2),WB(2),WC(2),WH(2),ES
     1L(2),FSL(2),FS(2),ESU(2),ES(2)
      DIMENSION POB(2),FSM(2)
C     READ STEEL PROPERTIES
    1 READ(5,100,END=99)((FU(I),FY(I),ESH(I),P(I),YM(I)),I=1,2)
  100 FORMAT(F6.0,F8.0,2F7.4,F11.0,2F8.0,2F7.4,F11.0)
C     READ CONCRETE PROPERTIES
      READ(5,101) EO,ECR,Z,FCD
  101 FORMAT(F5.4,F7.4,F6.0,F7.0)
      ER=500.*EO/(FCD+4000.)
      YMC=2.*FCD/EO
      E20=EO+.8/Z
C     READ BEAM GEOMETRY
      READ(5,102) DD,H,BDD,WF,DF,KODE
  102 FORMAT(F4.3,F7.3,F6.3,F6.2,F7.3,9X,I3)
C     READ AXIAL LOAD ECCENTRICITY AND CORRECTION FACTORS
      READ(5,103)EP,POB(1),POB(2)
  103 FORMAT(6X,F7.3,F8.3,F8.0)
      IF(POB(1).EQ.0.0)POB(1)=1.
      IF(POB(2).EQ.0.0)POB(2)=1.
C     CHECK THAT COMPRESSION STEEL IS WITHIN FLANGE
      IF(DD) 99,3,2
    2 IF(DD-DF) 3,3,99
C     HEADINGS AND INPUT RECORD
    3 WRITE(6,104)
  104 FORMAT('1'/'1MOMENT-CURVATURE RELATIONS FOR T-BEAMS'//////)
      WRITE(6,105)
  105 FORMAT(' TOP STEEL PROPERTIES',10X,'BOTTOM STEEL PROPERTIES',7X,'C
     1ONCRETE PROPERTIES',11X,'BEAM GEOMETRY'////)
      WRITE(6,106) FU(1),FU(2),FCD,DD
  106 FORMAT(' ',2('ULTIMATE STRESS =',F7.0,6X),'CYLINDER STRENGTH =',F6
     1.0,5X,'DEPTH COMPRESSION STEEL =',F5.3,'D')
      WRITE(6,107) FY(1),FY(2),Z,H
  107 FORMAT(' ',2('YIELD STRESS =',F7.0,9X),'PARAMETER Z =',F5.0,12X,'T
     1OTAL SECTION DEPTH =',F6.3,'D')
      WRITE(6,108) ESH(1),ESH(2),EO,BDD
  108 FORMAT(' ',2('STRAIN HARDENING =',F8.4,4X),'STRAIN AT MAX STRESS =
     1',F6.4,2X,'BOUND WIDTH =',F5.3,'B')
      ESU(1)=100.*P(1)
      ESU(2)=100.*P(2)
      WRITE(6,109) ESU(1),ESU(2),ECR,DF
  109 FORMAT(' ',2('STEEL PERCENTAGE =',F6.3,6X),'SPALLING STRAIN =',F6.
     14,7X,'FLANGE DEPTH =',F6.3,'D')
      WRITE(6,110) YM(1),YM(2),YMC,WF
  110 FORMAT(' ',3('YOUNGS MODULUS =',F10.0,4X),'FLANGE WIDTH =',F6.3,'B
     1')
      IF(KODE) 5,5,4
```



```
    4 WRITE(6,111) EP
  111 FORMAT(' '//' ECCENTRICITY OF AXIAL LOAD =',F6.3,'D'////////)
C     STRAIN HARDENING
    5 DO 6 I=1,2
      WC(I)=FU(I)/FY(I)
      WB(I)=.14
      ESU(I)=ESH(I)+WB(I)
      WH(I)=(WC(I)*(30.*WB(I)+1.)**2-60.*WB(I)-1.)/(15.*WB(I)**2)
    6 WA(I)=(WH(I)*WB(I)+2.)/(60.*WB(I)+2.)
      PMAX=FCD*H
      DIV=PMAX/10.
      AXP=-DIV
      DO 63 JJ=1,8
      AXP=AXP+DIV
      IF(KODE) 7,7,8
    7 IF(JJ-1) 8,8,63
    8 DO 9 I=1,2
      ESL(I)=0.
      FSM(I)=0.
    9 FSL(I)=0.
      PSI=0.
      BMAX=0.
      PSIL=0.
      BML=0.
      AK=.5
      ENERGY=0.
      EC=0.
      CHANGE=.0001
      WRITE(6,112)
  112 FORMAT('1',2X,'EC',11X,'K',11X,'CC',12X,'CS',13X,'T',13X,'P',11X,'
     1MOMENT',8X,'CURVATURE',5X,'CASE',5X,'ENERGY'//////)
   10 EC=EC+CHANGE
      IF(AK.GT.10.0)AK=.5
      G=AK
      EB=0.
   11 CC=0.
      BMCC=0.
      ES(1)=EC*(1.-DD/AK)
      ES(2)=EC*(1.-1./AK)
C     COMPRESSION STEEL REDUCTION
      IF(AK-DD) 27,27,12
   12 IF(ES(1)-EO) 13,13,14
   13 CSR=P(1)*FCD*(2.*ES(1)/EO-(ES(1)/EO)**2)
      GO TO 16
   14 IF(ES(1)-ECR) 15,17,17
   15 CSR=P(1)*FCD*(1.-Z*(ES(1)-EO))
   16 QSR=AK-DD
      CC=-CSR
      BMCC=-CSR*QSR
C     TENSION STEEL REDUCTION
   17 IF(AK-1.) 27,27,18
   18 IF(ES(2)-EO) 19,19,20
   19 TSR=P(2)*FCD*(2.*ES(2)*EO-(ES(2)/EO)**2)
      GO TO 215
```

```
   20 IF(ES(2)-ECR) 21,22,22
   21 TSR=P(2)*FCD*(1.-Z*(ES(2)-EO))
  215 CC=CC-TSR
      QSR=AK-1.
      BMCC=BMCC-TSR*QSR
C     NEUTRAL AXIS OUTSIDE SECTION
   22 IF(AK-H) 27,27,23
   23 EB=EC*(1.-H/AK)
      IF(EB-EO) 24,24,25
   24 CCM=(AK-H)*FCD*EB*(EO-EB/3.)/EO**2
      CC=CC-CCM
      EBAR=(8.*EB*EO-3.*EB**2)/(12.*EO-4.*EB)
      QCM=AK*EBAR/EC
      BMCC=BMCC-CCM*QCM
      GO TO 27
   25 IF(EB-ECR) 26,27,27
   26 FAB=2.*FCD/3.
      EBAR=.625*EO
      QCB=AK*EBAR/EC
      CCB=FAB*AK*EO/EC
      CC=CC-CCB
      BMCC=BMCC-CCB*QCB
      FAT=FCD*(1.-.5*Z*(EB-EO))
      EBAR=EO+(EB-EO)*(3.-2.*Z*(EB-EO))/(6.-3.*Z*(EB-EO))
      CCT=FAT*AK*(EB-EO)/EC
      QCT=EBAR*AK/EC
      CC=CC-CCT
      BMCC=BMCC-CCT*QCT
C     ESTABLISH CASE
   27 IF(EC-EO) 28,28,32
   28 IF(DF) 99,30,29
   29 IF(AK-DF) 30,30,31
C  CASE 1
   30 FA=FCD*EC*(EO-EC/3.)/EO**2
      KASE=1
      CCC=FA*WF*AK
      EBAR=(8.*EC*EO-3.*EC**2)/(12.*EO-4.*EC)
      QCC=AK*EBAR/EC
      CC=CC+CCC
      BMCC=BMCC+CCC*QCC
      GO TO 52
C  CASE 2
   31 EB=EC*(1.-DF/AK)
      KASE=2
      FAF=FCD*(EO*(EC**2-EB**2)-(EC**3-EB**3)/3.)/(EO**2*(EC-EB))
      CCF=FAF*WF*DF
      EBAR=(8.*EO*EC**3-3.*EC**4-8.*EO*EB**3+3.*EB**4)/(12.*EO*EC**2-4.*
     1EC**3-12.*EO*EB**2+4.*EB**3)
      QCF=AK*EBAR/EC
      FAW=FCD*EB*(EO-EB/3.)/EO**2
      CCW=FAW*(AK-DF)
      EBAR=(8.*EB*EO-3.*EB**2)/(12.*EO-4.*EB)
      QCW=AK*EBAR/EC
      BMCC=BMCC+CCF*QCF+CCW*QCW
      CC=CC+CCF+CCW
      GO TO 52
C  CASES 3 TO 12
   32 IF(EC-ECR) 33,33,39
   33 IF(DF) 99,35,34
   34 IF(AK-DF) 35,35,36
C  CASE 3
   35 FAT=FCD*(1.-.5*Z*(EC-EO))
      KASE=3
      CCT=FAT*WF*AK*(1.-EO/EC)
      EBAR=EO+(EC-EO)*(3.-2.*Z*(EC-EO))/(6.-3.*Z*(EC-EO))
      QCT=AK*EBAR/EC
      FAB=2.*FCD/3.
      CCB=FAB*WF*AK*EO/EC
      QCB=AK*.625*EO/EC
      CC=CC+CCT+CCB
      BMCC=BMCC+CCT*QCT+CCB*QCB
      GO TO 52
C  CASES 4 AND 5
   36 EB=EC*(1.-DF/AK)
      KASE=4
      IF(EO-EB) 38,37,37
   37 FAFT=FCD*(1.-.5*Z*(EC-EO))
      CCFT=FAFT*WF*AK*(1.-EO/EC)
      EBAR=EO+(EC-EO)*(3.-2.*Z*(EC-EO))/(6.-3.*Z*(EC-EO))
      QCFT=AK*EBAR/EC
      FAFB=FCD*(2.*EO**3/3.-EO*EB**2+EB**3/3.)/(EO**2*(EO-EB))
      CCFB=FAFB*WF*AK*(EO-EB)/EC
      EBAR=(5.*EO**4-8.*EO*EB**3+3.*EB**4)/(8.*EO**3-12.*EO*EB**2+4.*EB*
     1*3)
      QCFB=AK*EBAR/EC
      FAW=FCD*EB*(EO-EB/3.)/EO**2
      CCW=FAW*(AK-DF)
      EBAR=(8.*EB*EO-3.*EB**2)/(12.*EO-4.*EB)
      QCW=EBAR*AK/EC
      CC=CC+CCFT+CCFB+CCW
      BMCC=BMCC+CCFT*QCFT+CCFB*QCFB+CCW*QCW
      GO TO 52
   38 FAF=FCD*(1.-.5*Z*(EC+EB-2.*EO))
      KASE=5
      CCF=FAF*WF*DF
      EBAR=EB+(EC-EB)*(3.+3.*Z*EO-2.*Z*EC-Z*EB)/(6.*(1.+Z*EO)-3.*Z*(EB+E
     1C))
      QCF=AK*EBAR/EC
      FAWT=FCD*(1.-.5*Z*(EB-EO))
      CCWT=FAWT*AK*(EB-EO)/EC
      EBAR=EO+(EB-EO)*(3.-2.*Z*(EB-EO))/(6.-3.*Z*(EB-EO))
      QCWT=AK*EBAR/EC
      FAWB=2.*FCD/3.
      CCWB=FAWB*AK*EO/EC
      QCWB=AK*.625*EO/EC
      BMCC=BMCC+CCWT*QCWT+CCWB*QCWB+CCF*QCF
      CC=CC+CCWT+CCWB+CCF
      GO TO 52
```

```
C  CASES 6 TO 12
   39 EB=EC*(1.-DF/AK)
      IF(DF) 99,44,40
   40 IF(AK-DF) 44,44,41
   41 IF(ES(1)-ECR) 43,42,42
   42 IF(EO-EB) 48,48,49
   43 IF(EO-EB) 50,50,51
C  CASES 6 TO 8
   44 FAFT=FCD*(1.-.5*Z*(ECR-EO))
      KASE=6
      CCFT=FAFT*AK*WF*(ECR-EO)/EC
      EBAR=EO+(ECR-EO)*(3.-2.*Z*(ECR-EO))/(6.-3.*Z*(ECR-EO))
      QCFT=AK*EBAR/EC
      FAFB=2.*FCD/3.
      EBAR=.625*EO
      QCFB=AK*EBAR/EC
      CCFB=FAFB*WF*AK*EO/EC
      BMCC=BMCC+CCFT*QCFT+CCFB*QCFB
      CC=CC+CCFT+CCFB
      IF(ES(1)-ECR) 52,52,45
C  CASES 7 AND 8
   45 KASE=7
      IF(ES(1)-E20) 46,46,47
   46 FAB=FCD*(1.-.5*Z*(ECR+ES(1)-2.*EO))
      CCB=FAB*BDD*AK*(ES(1)-ECR)/EC
      EBAR=ECR+(ES(1)-ECR)*(3.+3.*Z*EO-2.*Z*ES(1)-Z*ECR)/(6.*(1.+Z*EO)-3
     1.*Z*(ES(1)+ECR))
      QCB=AK*EBAR/EC
      BMCC=BMCC+CCB*QCB
      CC=CC+CCB
      GO TO 52
   47 FA=FCD*(1.-.5*Z*(ECR+E20-2.*EO))
      KASE=8
      CCB1=FA*BDD*AK*(E20-ECR)/EC
      EBAR=ECR+(E20-ECR)*(3.+3.*Z*EO-2.*Z*E20-Z*ECR)/(6.*(1.+Z*EO)-3.*Z*
     1(E20+ECR))
      QCB1=AK*EBAR/EC
      FA=.2*FCD
      CCB2=FA*BDD*AK*(ES(1)-E20)/EC
      EBAR=.5*(ES(1)+E20)
      QCB2=AK*EBAR/EC
      BMCC=BMCC+CCB1*QCB1+CCB2*QCB2
      CC=CC+CCB1+CCB2
      GO TO 52
C  CASE 9
   48 FAF=FCD*(1.-.5*Z*(EB+ECR-2.*EO))
      KASE=9
      CCF=FAF*WF*AK*(ECR-EB)/EC
      EBAR=EB+(ECR-EB)*(3.+3.*Z*EO-2.*Z*ECR-Z*EB)/(6.*(1.+Z*EO)-3.*Z*(EC
     1R+EB))
      QCF=AK*EBAR/EC
      IF(E20-ES(1))485,485,486
  485 FAB=.2*FCD
      CCB=FAB*BDD*AK*(ES(1)-E20)/EC
```



```
      EBAR=.5*(ES(1)+E20)
      CC=CC+CCB
      BMCC=BMCC+CCB*AK*EBAR/EC
      FAB=FCD*(1.-.5*Z*(E20+ECR-2.*EO))
      CCB=FAB*BDD*AK*(E20-ECR)/EC
      EBAR=ECR+(E20-ECR)*(3.*(1.+Z*EO)-Z*(ECR+2.*E20))/(6.*(1.+Z*EO)-3.*
     1Z*(ECR+E20))
      QCB=AK*EBAR/EC
      IF(KASE-9)99,487,496
  486 FAB=FCD*(1.-.5*Z*(ES(1)+ECR-2.*EO))
      CCB=FAB*BDD*AK*(ES(1)-ECR)/EC
      EBAR=ECR+(ES(1)-ECR)*(3.+3.*Z*EO-2.*Z*ES(1)-Z*ECR)/(6.*(1.+Z*EO)-3
     1.*Z*(ECR+ES(1)))
      QCB=AK*EBAR/EC
  487 FAWT=FCD*(1.-.5*Z*(EB-EO))
      CCWT=FAWT*AK*(EB-EO)/EC
      EBAR=EO+(EB-EO)*(3.-2.*Z*(EB-EO))/(6.-3.*Z*(EB-EO))
      QCWT=AK*EBAR/EC
      FAWB=2.*FCD/3.
      CCWB=FAWB*AK*EO/EC
      EBAR=.625*EO
      QCWB=AK*EBAR/EC
      CC=CC+CCF+CCB+CCWT+CCWB
      BMCC=BMCC+CCF*QCF+CCB*QCB+CCWT*QCWT+CCWB*QCWB
      GO TO 52
C  CASE 10
   49 FAFT=FCD*(1.-.5*Z*(ECR-EO))
      KASE=10
      CCFT=FAFT*WF*AK*(ECR-EO)/EC
      EBAR=EO+(ECR-EO)*(3.-2.*Z*(ECR-EO))/(6.-3.*Z*(ECR-EO))
      QCFT=AK*EBAR/EC
      FAFB=FCD*(2.*EO**3/3.-EO*EB**2+EB**3/3.)/(EO**2*(EO-EB))
      CCFB=FAFB*WF*AK*(EO-EB)/EC
      EBAR=(5.*EO**4-8.*EO*EB**3+3.*EB**4)/(8.*EO**3-12.*EO*EB**2+4.*EB*
     1*3)
      QCFB=AK*EBAR/EC
      IF(E20-ES(1))485,485,495
  495 FAB=FCD*(1.-.5*Z*(ES(1)+ECR-2.*EO))
      CCB=FAB*BDD*AK*(ES(1)-ECR)/EC
      EBAR=ECR+(ES(1)-ECR)*(3.+3.*Z*EO-2.*Z*ES(1)-Z*ECR)/(6.*(1.+Z*EO)-3
     1.*Z*(ECR+ES(1)))
      QCB=AK*EBAR/EC
  496 FAW=FCD*EB*(EO-EB/3.)/EO**2
      CCW=FAW*AK*EB/EC
      EBAR=(8.*EB*EO-3.*EB**2)/(12.*EO-4.*EB)
      QCW=AK*EBAR/EC
      CC=CC+CCFT+CCFB+CCB+CCW
      BMCC=BMCC+CCFT*QCFT+CCFB*QCFB+CCB*QCB+CCW*QCW
      GO TO 52
C  CASE 11
   50 FAF=FCD*(1.-.5*Z*(ECR+EB-2.*EO))
      KASE=11
      CCF=FAF*WF*AK*(ECR-EB)/EC
      EBAR=EB+(ECR-EB)*(3.*(1.+Z*EO)-Z*(2.*ECR+EB))/(6.*(1.+Z*EO)-3.*Z*(
```

```
     1ECR+EB))
      QCF=AK*EBAR/EC
      FAWT=FCD*(1.-.5*Z*(EB-EO))
      CCWT=FAWT*AK*(EB-EO)/EC
      EBAR=EO+(EB-EO)*(3.-2.*Z*(EB-EO))/(6.-3.*Z*(EB-EO))
      QCWT=AK*EBAR/EC
      FAWB=2.*FCD/3.
      EBAR=.625*EO
      CCWB=FAWB*AK*EO/EC
      QCWB=AK*EBAR/EC
      CC=CC+CCF+CCWT+CCWB
      BMCC=BMCC+CCF*QCF+CCWT*QCWT+CCWB*QCWB
      GO TO 52
C  CASE 12
   51 FAFT=FCD*(1.-.5*Z*(ECR-EO))
      KASE=12
      CCFT=FAFT*WF*AK*(ECR-EO)/EC
      EBAR=EO+(ECR-EO)*(3.-2.*Z*(ECR-EO))/(6.-3.*Z*(ECR-EO))
      QCFT=AK*EBAR/EC
      FAFB=FCD*(2.*EO**3/3.-EO*EB**2+EB**3/3.)/(EO**2*(EO-EB))
      CCFB=FAFB*WF*AK*(EO-EB)/EC
      EBAR=(5.*EO**4-8.*EO*EB**3+3.*EB**4)/(8.*EO**3-12.*EO*EB**2+4.*EB*
     1*3)
      QCFB=AK*EBAR/EC
      FAW=FCD*EB*(EO-EB/3.)/EO**2
      CCW=FAW*AK*EB/EC
      EBAR=(9.*EB*EO-3.*EB**2)/(12.*EO-4.*EB)
      QCW=AK*EBAR/EC
      CC=CC+CCFT+CCFB+CCW
      BMCC=BMCC+CCFT*QCFT+CCFB*QCFB+CCW*QCW
C  STEEL
   52 DO 58 I=1,2
      FS(I)=FSL(I)-YM(I)*(ESL(I)-ES(I))
      IF(ABS(ES(I)).GT.ESU(I)) GO TO 55
      IF(FS(I)*FSM(I).GT.0.0.AND.ABS(FS(I)).LT.ABS(FSM(I)).OR.FS(I)*FSM(
     1I).LT.0.0)GO TO 58
      IF(ABS(FS(I))-FY(I)) 58,58,53
   53 IF(ABS(ES(I))-ESH(I)) 54,54,55
   54 FS(I)=SIGN(FY(I),FS(I))
      GO TO 58
   55 TEMP=1.
      IF(ES(I)) 56,99,57
   56 TEMP=-1.
      ES(I)=-ES(I)
   57 DELTA=ABS(ESH(I)-ES(I))
      FS(I)=TEMP*FY(I)*((WH(I)*DELTA+2.)/(60.*DELTA+2.)+DELTA*(WC(I)-WA(
     1I))/WB(I))
      ES(I)=ES(I)*TEMP
   58 CONTINUE
      CS=P(1)*FS(1)
      T=P(2)*FS(2)
      BMCS=CS*(AK-DD)
      BMT=T*(AK-1.)
C  AXIAL LOAD
```



```
      BMAXP=AXP*(EP-AK)
C  EQUILIBRIUM
      IF(T+CC+CS-AXP)59,61,60
   59 AK=AK+G
      IF(AK-2000.) 11,11,10
   60 AK=AK-G
      G=.1*G
      IF(G-.00001) 61,59,59
   61 BMTOT=BMCC+BMCS+BMT+BMAXP
      PSI=EC-ES(2)
      ENERGY=ENERGY+.5*(BMTOT+BML)*(PSI-PSIL)
      PSI=PSI/POB(1)
      BMTOT=BMTOT/POB(2)
      WRITE(6,113)EC,AK,CC,CS,T,AXP,BMTOT,PSI,KASE,ENERGY
  113 FORMAT(' ',F6.4,F12.3,4F14.0,F16.3,F15.6,I8,F12.4)
      PSI=PSI*POB(1)
      IF(BMTOT-BMAX)615,616,614
  614 BMAX=BMTOT
      GO TO 616
  615 IF(EC.LT.4.*ECR)GO TO 616
      IF(BMTOT-.8*BMAX)63,63,616
  616 DO62I=1,2
      ESL(I)=ES(I)
      IF(ABS(FS(I)).GT.ABS(FSM(I)))FSM(I)=FS(I)
   62 FSL(I)=FS(I)
      PSIL=PSI
      BML=BMTOT
      IF(EC.GE.ECR) CHANGE=.001
      IF(ES(2)+ESU(2).GE.0.0) GO TO 10
   63 CONTINUE
      GO TO 1
   99 CONTINUE
      END
```

```
C     ********************************************************************
C
C     MOMENT-CURVATURE RELATIONS FOR REINFORCED CONCRETE
C     T-BEAMS SUBJECTED TO CYCLIC FLEXURAL LOADING
C
C     JULY 1968
C
C     MODIFIED MARCH 1969
C
C     RAMBERG-OSGOOD FUNCTION FOR BAUSCHINGER EFFECT
C
C     ********************************************************************
      DIMENSION WH(2),WA(2),WB(2),WC(2),EDIFF(2),EIPL(2)
      DIMENSION ELAST(500),FMAX(500),FCRACK(500)
      DIMENSION EMAX(500),EZERO(500),CR(50),E(500),F(500),FW(500),ESL(2)
     1,FSL(2),EZERON(2),EZEROL(2),SENSE(2),KBAUS(2),FU(2),FY(2),ESH(2),P
     2(2),YM(2),ESU(2),SR(2),QSR(2),FS(2),ES(2),NCYC(2),RVAL(40)
      DIMENSION FT(2)
C     READ STEEL PROPERTIES
      ONE=1.
    1 READ(5,100,END=99)((FU(I),FY(I),ESH(I),P(I),YM(I)),I=1,2)
  100 FORMAT(F6.0,F8.0,2F7.4,F11.0,2F8.0,2F7.4,F11.0)
C     READ CONCRETE PROPERTIES
      READ(5,101) EO,ECR,Z,FCD
  101 FORMAT(F5.4,F7.4,F6.0,F7.0)
      ER=500.*EO/(FCD+4000.)
      YMC=2.*FCD/EO
      IF(Z) 2,2,3
    2 E20=1.
      GO TO 4
    3 E20=EO+.8/Z
C     READ BEAM GEOMETRY AND NUMBERS OF ELEMENTS AND READINGS
    4 READ(5,102) DD,H,BDD,WF,DF,NEL,NCR
  102 FORMAT(F4.3,F7.3,F6.3,F6.2,F7.3,I5,I4)
C     READ AXIAL LOAD AND ECCENTRICITY
      READ(5,103) BIGP,EP
  103 FORMAT(F6.0,F7.3)
C
C     HEADINGS AND LIST OF INPUT DATA
C
      WRITE(6,104)
  104 FORMAT(1H1,10X,'REINFORCED CONCRETE T-BEAMS SUBJECTED TO CYCLIC
     1LOADING WITH CONSIDERATION OF THE BAUSCHINGER EFFECT'////////////
     2//)
      WRITE(6,105)
  105 FORMAT(1H ,'TOP STEEL PROPERTIES',10X,'BOTTOM STEEL PROPERTIES',
     17X,'CONCRETE PROPERTIES',11X,'BEAM GEOMETRY  ETC.'//////)
      WRITE(6,106) FU(1),FU(2),FCD,DD
  106 FORMAT(1H ,2('ULTIMATE STRESS = ',F6.0,6X),'CYLINDER STRENGTH =',
     1F6.0,5X,'DEPTH COMPRESSION STEEL = ',F4.3,'D')
      WRITE(6,107) FY(1),FY(2),Z,H
  107 FORMAT(1H ,2('YIELD STRESS = ',F6.0,9X),'PARAMETER Z = ', F5.0,11X
     1,'TOTAL SECTION DEPTH = ',F5.3,'D')
      WRITE(6,108) ESH(1),ESH(2),EO,BDD
```



```
  108 FORMAT(1H ,2('STRAIN HARDENING = ',F7.4,4X),'STRAIN AT MAX STRESS
     1= ',F5.4,2X,'BOUND WIDTH = ',F4.3,'B')
      PD100=100.*P(1)
      P100=100.*P(2)
      WRITE(6,109) PD100,P100,ECR,DF
  109 FORMAT(1H ,2('STEEL PERCENTAGE = ',F5.3,6X),'CRUSHING STRAIN = ',
     1F5.4,7X,'FLANGE DEPTH = ',F5.3,'D')
      WRITE(6,110) YM(1),YM(2),YMC,WF
  110 FORMAT(1H ,3('YOUNGS MODULUS = ',F9.0,4X),'FLANGE WIDTH = ',F5.3,
     1'B')
      FT(1)=.15*FY(1)
      FT(2)=.15*FY(2)
      WRITE(6,111)FT(1),FT(2),NEL,NCR
  111 FORMAT(1H ,2('TRANSITION STRESS = ',F6.0,4X),'NUMBER OF ELEMENTS =
     1 ',I3,6X,'NUMBER OF READINGS = ',I2////////////////)
      WRITE(6,112) BIGP,EP
  112 FORMAT(1H ,'AXIAL STRESS IS ',F5.0,' PSI AT ',F5.2,'D ECCENTRICITY
     1'/////////////////)
      WRITE(6,113)
  113 FORMAT(1H ,2X,'EC',9X,'K',9X,'CC',10X,'ESD',10X,'CS',10X,'ES',11X,
     1'T',7X,'MOMENT',7X,'CURVATURE',5X,'KODE',9X,'ENERGY'////)
  114 FORMAT(' ',F7.5,F9.3,2(F12.0,F12.6),2F12.0,F14.6,I8,F15.6)
C     WIDTH FACTORS INITIALISATION
      DO 5 I=1,NEL
    5 FW(I)=1.
      EL=NEL
      TEMP=DF*EL/H
      J=TEMP
      DO 6 I=1,J
    6 FW(I)=WF
C     STEEL 'COUNTERS' INITIALISATION
      DO 7 I=1,2
      ESL(I)=0.
      FSL(I)=0.
      EZERON(I)=0.
      EZEROL(I)=0.
      NCYC(I)=0
      WC(I)=FU(I)/FY(I)
      WB(I)=.14
      WH(I)=(WC(I)*(30.*WB(I)+1.)**2-60.*WB(I)-1.)/(15.*WB(I)**2)
      WA(I)=(WH(I)*WB(I)+2.)/(60.*WB(I)+2.)
      EDIFF(I)=0.
      EIPL(I)=0.
      ESU(I)=ESH(I)+WB(I)
      SENSE(I)=0.
      KBAUS(I)=1
    7 CONTINUE
      DO700I=1,39,2
      G=I
  700 RVAL(I)=4.489/ALOG(1.+G)-6.026/(EXP(G)-1.)+.297
      DO701I=2,40,2
      G=I
  701 RVAL(I)=2.197/ALOG(1.+G)-.469/(EXP(G)-1.)+3.043
C     DETERMINATION OF STEEL RESIDENT ELEMENTS
```

```
      TEMP=EL*DD/H
      IT=TEMP
      TEMP=EL/H
      IB=TEMP
C     CONCRETE AND BEAM 'COUNTERS' INITIALISATION
      PSI=0.
      KONZ=1
      BML=0.
      PSIL=0.
      ENERGY=0.
      DO 8 I=1,NEL
      FCRACK(I)=1.
      EMAX(I)=0.
    8 EZERO(I)=0.
C     READ CURVATURE REQUIREMENTS
      DO 9 I=1,NCR
    9 READ(5,115) CR(I)
  115 FORMAT(F9.6)
C
C     COMPUTATION PHASE BEGINS
C
      CHANGE=.00005
      DO 98 I=1,NCR
      DIV=0.
      KDIV=0
      IF(I-1) 1,10,11
   10 EC=0.
      IF(CR(I)) 12,98,13
   11 IF(CR(I)-CR(I-1)) 12,98,13
   12 KODE=2
      EC=EC-CHANGE
      IF(PSI-CR(I)) 98,98,14
   13 KODE=1
      EC=EC+CHANGE
      IF(PSI-CR(I)) 14,98,98
   14 AK=-20000.
      CLAGMN=1000.
      KING=0
      KROG=1
      KFV=1
      G=20000.
      IF(EC*EC-.000000001) 97,15,15
   15 ES(1)=EC*(1.-DD/AK)
      ES(2)=EC*(1.-1./AK)
      IF(AK.GT.0.0.AND.G.GT.101.01G=100.
      SN=EL*AK/H
      NS=SN
      SR(1)=0.
      QSR(1)=0.
      SR(2)=0.
      QSR(2)=0.
      CC=0.
      BMCC=0.
      IF(EC-.0002e) 155,155,154
```



```
  154 CHANGE=.0001
C     EVALUATION OF ELEMENTAL CONCRETE STRESSES
  155 DO 24 J=1,NEL
      AB=J
      E(J)=EC*(SN-AB+.5)/SN
      IF(E(J)-EMAX(J)) 16,16,18
   16 IF(E(J)-EZERO(J)) 20,20,17
   17 IF(E(J)-ELAST(J)) 172,172,171
  171 F(J)=.25*(3.*FMAX(J)*YMC*(E(J)-EZERO(J)))
      GO TO 24
  172 F(J)=.25*YMC*(E(J)-EZERO(J))
      GO TO 24
   18 IF(E(J)-EO) 19,19,21
   19 F(J)=FCD*(2.*E(J)/EO-E(J)*E(J)/(EO*EO))
      IF(F(J))20,24,24
   20 IF(FCRACK(J)-.5) 201,201,202
  201 F(J)=0.
      GO TO 24
  202 IF(E(J)-EZERO(J)*ER) 201,203,203
  203 F(J)=YMC*(E(J)-EZERO(J))
      GO TO 24
   21 IF(E(J)-E20) 22,22,23
   22 F(J)=FCD*(1.-2*(E(J)-EO))
      GO TO 24
   23 F(J)=FCD/5.
   24 CONTINUE
C     STEEL AREA REDUCTION
      SR(1)=P(1)*F(IT)
      QSR(1)=AK-DD
      SR(2)=P(2)*F(IB)
      QSR(2)=AK-1.
      CC=CC-SR(1)-SR(2)
      BMCC=BMCC-SR(1)*QSR(1)-SR(2)*QSR(2)
C     WIDTH FACTOR CORRECTIONS (TEMPORARY)
      DO 31 K=1,NEL
      AB=K
      IF(E(K)-ECR) 25,25,26
   25 F(K)=F(K)*FW(K)
      GO TO 30
   26 IF(K-IT) 27,28,28
   27 F(K)=0.
      GO TO 30
   28 IF(K-IB) 29,27,27
   29 F(K)=F(K)*BDD
   30 CC=CC+F(K)/EL
   31 BMCC=BMCC+F(K)*AK*(SN-AB+.5)/(EL*SN)
C     STEEL FORCES
      DO565J=1,2
      FS(J)=YM(J)*(ES(J)-EZERON(J))
      KAD=KRAUS(J)
      GO TO (32,45,45),KAD
C     ELASTO-PLASTIC SYSTEM
   32 IF(FS(J)*SENSE(J)) 33,33,33
   33 IF(ABS(FS(J))-FY(J)) 56,56,34
```

```
   34 IF(ABS(ES(J))-ESH(J)) 35,35,36
   35 FS(J)=SIGN(FY(J),ES(J))
      GO TO 56
   36 TEMP=1.
      IF(ES(J)) 37,99,38
   37 TEMP=-1.
   38 DELTA=ABS(ESH(J)-ABS(ES(J)))
      FS(J)=TEMP*FY(J)*((WH(J)*DELTA+2.)/(60.*DELTA+2.)+DELTA*(WC(J)-WA(
     1J))/WB(J))
      GO TO 56
   39 IF(ABS(FS(J))-FT(J)) 56,56,40
C     ITERATION ROUTINE FOR BAUSCHINGER STRESS
   40 DELTA=ABS(EZERON(J)-ES(J))
   41 PLAST=ABS(EZERON(J)-EZEROL(J))
      FCH=FY(J)*(.744/ALOG(1.+1000.*PLAST)+.071/(EXP(1000.*PLAST)-1.)+.2
     141)
      IF(FCH-FY(J))415,415,414
  414 FCH=FY(J)
  415 R=RVAL(NCYC(J)+1)
      ECH=FCH/YM(J)
      ALPHA=DELTA/ECH
      GAMMA=ALPHA
   42 BETA=ALPHA-(ALPHA+ALPHA**R-GAMMA)/(1.+R*ALPHA**(R-1.))
      IF(ABS(ALPHA-BETA)-10./FCH) 44,44,43
   43 ALPHA=BETA
      GO TO 42
   44 GO TO (445,50,55),KAD
  445 FS(J)=-FCH*BETA*SENSE(J)
      GO TO 56
C     BAUSCHINGER SYSTEM
   45 IF(ABS(FS(J))-FT(J)) 56,56,46
   46 IF(FS(J)*FSL(J)) 464,99,465
  464 KAD=3
      IF(ABS(FSL(J))-FT(J)) 47,47,40
  465 IF(ABS(FSL(J))-FT(J)) 466,466,47
  466 IF(ABS(ESL(J)-EZEROL(J))-ABS(EZERON(J)-EZEROL(J))) 40,99,47
   47 IF(ABS(EZEROL(J)-ES(J))-EDIFF(J))475,475,48
  475 IF((EZERON(J)-EZEROL(J))*(ES(J)-EZERON(J)))40,56,56
   48 R=RVAL(NCYC(J))
      FCH=FY(J)*(.744/ALOG(1.+1000.*EIPL(J))+.071/(EXP(1000.*EIPL(J))-1.
     1)+.241)
      IF(FCH-FY(J))49,49,485
  485 FCH=FY(J)
   49 ECH=FCH/YM(J)
      ALPHA=ABS(EZEROL(J)-ES(J))/ECH
      GAMMA=ALPHA
      GO TO 42
   50 FS(J)=FCH*BETA*SIGN(ONE,FSL(J))
      GO TO 56
   55 FS(J)=-FCH*BETA*SIGN(ONE,FSL(J))
   56 IF(ABS(FS(J))-FU(J))565,565,564
  564 FS(J)=SIGN(FU(J),FS(J))
  565 CONTINUE
      CS=P(1)*FS(1)
```



```
      BMCS=CS*(AK-DD)
      T=P(2)*FS(2)
      BMT=T*(AK-1.)
C     AXIAL LOAD MOMENT
      BMP=BIGP*EP
C     EQUILIBRIUM CHECK.
      CLAG=T+CC+CS-BIGP
      IF(KROG.EQ.2)GO TO 61
      IF(CLAGMN.LE.ABS(CLAG))GO TO 566
      CLAGMN=ABS(CLAG)
      AKBEST=AK
  566 KING=KING+1
      IF(KFV.EQ.2)GO TO 58
      KFV=2
      IF(EC*CLAG)59,61,57
   57 AK=100.
      GO TO 15
   58 IF(ABS(CLAG).LT.0.33) GO TO 61
      IF(EC*CLAG)59,61,60
   59 AK=AK+G
      IF(AK.GT.20000.0) GO TO 97
      IF(ABS(AK)-0.00001)60,60,15
   60 AK=AK-G
      G=.5*G
      IF(KING.GT.150)GO TO 61
      IF(G.GT.0.000001)GO TO 59
   61 BMTOT=BMCC+BMCS+BMT+BMP
      IF(KROG.EQ.2.OR.ABS(CLAG).LT.1.0)GO TO 62
      AK=AKBEST
      KROG=2
      GO TO 15
   62 IF(ES(1)**2.LE.ESU(1)**2)GO TO 63
      WRITE(6,116)
  116 FORMAT(1H ,'TOP STEEL FRACTURED'/////)
      GO TO 1
   63 IF(ES(2)*ES(2)-ESU(2)*ESU(2)) 65,65,64
   64 WRITE(6,117)
  117 FORMAT(1H ,'BOTTOM STEEL FRACTURED'/////)
      GO TO 1
   65 IF(KDIV)70,66,70
   66 GO TO (67,68),KODE
   67 IF(EC-ES(2)-CR(I)) 70,69,69
   68 IF(EC-ES(2)-CR(I)) 69,69,70
   69 DIV=CHANGE*(EC-ES(2)-CR(I))/(EC-ES(2)-PSI)
      TEMP=KODE
      DIV=DIV*(4.-3.*TEMP)/TEMP
      KDIV=1
      EC=EC-DIV
      GO TO 14
   70 PSI=EC-ES(2)
      ENERGY=ENERGY+.5*(BML+BMTOT)*(PSI-PSIL)
      WRITE(6,114) EC,AK,CC,ES(1),CS,ES(2),T,BMTOT,PSI,KODE,ENERGY
      AKL=AK
      IF(ABS(CLAG).GT.1.0)WRITE(6,1155)
```

```
 1155 FORMAT('+',130X,'*')
      PSIL=PSI
      EC=EC+DIV
      BML=BMTOT
C     UPDATE CONCRETE 'COUNTERS'
      DO 72 K=1,NEL
      ELAST(K)=E(K)
      IF(E(K)-EMAX(K)) 72,72,71
   71 EMAX(K)=E(K)
      FMAX(K)=F(K)
      EZERO(K)=EMAX(K)-F(K)/YMC
   72 CONTINUE
      DO 77 K=1,NEL
      IF(E(K)-ECR) 77,77,73
   73 IF(K-IT) 74,75,75
   74 FW(K)=0.
      GO TO 77
   75 IF(K-IB) 76,74,74
   76 FW(K)=BDD
   77 CONTINUE
      DO 775 J=1,NEL
      IF(E(J)-EZERO(J)+ER) 774,775,775
  774 FCRACK(J)=0.
  775 CONTINUE
      IF(KONZ.EQ.2)GO TO 777
      DO776J=1,NEL
      IF(FCRACK(J).EQ.1.0)GO TO 777
  776 CONTINUE
      KONZ=2
      WRITE(6,118)
  118 FORMAT(' SECTION CRACKED THROUGHOUT')
C     UPDATE STEEL 'COUNTERS'
  777 DO96J=1,2
      KAD=KBAUS(J)
      GO TO (78,84),KAD
C     ELASTO-PLASTIC SYSTEM
   78 IF(SENSE(J)) 81,79,81
   79 IF(ABS(ES(J))-FY(J)/YM(J)) 95,95,80
   80 SENSE(J)=SIGN(ONE,ES(J))
      GO TO 94
   81 IF(SENSE(J)*FS(J)) 82,94,94
   82 IF(ABS(FS(J))-FT(J)) 94,94,83
   83 KBAUS(J)=2
      GO TO 90
C     BAUSCHINGER SYSTEM
   84 IF(ABS(FS(J))-FT(J)) 95,95,85
   85 IF(FS(J)*FSL(J)) 86,99,91
   86 IF(ABS(FSL(J))-FT(J)) 87,87,90
   87 IF(ABS(EZEROL(J)-ES(J))-EDIFF(J))875,875,89
  875 IF((EZERON(J)-EZEROL(J))*(ES(J)-EZERON(J)))90,94,94
   89 EDIFF(J)=ABS(EZEROL(J)-ES(J))
      GO TO 94
   90 EDIFF(J)=ABS(EZERON(J)-ES(J))
      GO TO 93
```



```
   91 IF(ABS(FSL(J))-FT(J)) 92,92,87
   92 IF(ABS(ESL(J)-EZEROL(J))-ABS(EZERON(J)-EZEROL(J)))90,99,87
   93 EIPL(J)=ABS(EZERON(J)-EZEROL(J))
      EZEROL(J)=EZERON(J)
      NCYC(J)=NCYC(J)+1
   94 EZERON(J)=ES(J)-FS(J)/YM(J)
   95 ESL(J)=ES(J)
   96 FSL(J)=FS(J)
      IF(KDIV)98,97,98
   97 GO TO (13,12),KODE
   98 CONTINUE
      GO TO 1
   99 CONTINUE
      END
```

```
C     ******************************************************************
C
C     MOMENT-CURVATURE RELATIONS FOR RECTANGULAR REINFORCED CONCRETE
C     BEAMS SUBJECTED TO CYCLIC FLEXURAL LOADING
C
C     JULY 1968
C
C     BAUSCHINGER EFFECT IN THE REINFORCING STEEL IS IGNORED
C
C     ******************************************************************
      DIMENSION FCRACK(500)
      DIMENSION ELAST(500),FMAX(500)
      DIMENSION EMAX(500),EZERO(500),CR(50),E(500),F(500),FW(500),ESL(2)
     1,FSL(2),FU(2),FY(2),ESH(2),P(2),YM(2),ESU(2),SR(2),QSR(2),FS(2),ES
     Z(2),WH(2),WA(2),WB(2),WC(2)
C     READ STEEL PROPERTIES
    1 READ(5,100)((FU(I),FY(I),ESH(I),P(I),YM(I)),I=1,2)
  100 FORMAT(F6.0,F8.0,2F7.4,F11.0,2F8.0,2F7.4,F11.0)
C     READ CONCRETE PROPERTIES
      READ(5,101) EO,ECR,Z,FCD
  101 FORMAT(F5.4,F7.4,F6.0,F7.0)
      ER=500.*EO/(FCD+4000.)
      YMC=2.*FCD/EO
      IF(Z) 2,2,3
    2 E20=1.
      GO TO 4
    3 E20=EO+.8/Z
C     READ BEAM GEOMETRY AND NUMBERS OF ELEMENTS AND READINGS
    4 READ(5,102) DD,H,BDD,WF,DF,NEL,NCR
  102 FORMAT(F4.3,F7.3,F6.3,F6.2,F7.3,I5,I4)
C     READ AXIAL LOAD AND ECCENTRICITY
      READ(5,103) BIGP,EP
  103 FORMAT(F6.0,F7.3)
C
C     HEADINGS AND LIST OF INPUT DATA
C
      WRITE(6,104)
  104 FORMAT(1H ,12X,'REINFORCED CONCRETE T-BEAMS SUBJECTED TO CYCLIC
     1LOADING BUT IGNORING THE BAUSCHINGER EFFECT'////////////////)
      WRITE(6,105)
  105 FORMAT(1H ,'TOP STEEL PROPERTIES',10X,'BOTTOM STEEL PROPERTIES',
     17X,'CONCRETE PROPERTIES',11X,'BEAM GEOMETRY  ETC.'/////)
      WRITE(6,106) FU(1),FU(2),FCD,DD
  106 FORMAT(1H ,2('ULTIMATE STRESS = ',F6.0,6X),'CYLINDER STRENGTH =',F
     16.0,5X,'DEPTH COMPRESSION STEEL = ',F4.3,'D')
      WRITE(6,107) FY(1),FY(2),Z,H
  107 FORMAT(1H ,2('YIELD STRESS = ',F6.0,9X),'PARAMETER Z = ',F5.0,11X,
     1'TOTAL SECTION DEPTH = ',F5.3,'D')
      WRITE(6,108) ESH(1),ESH(2),EO,BDD
  108 FORMAT(1H ,2('STRAIN HARDENING = ',F7.4,4X),'STRAIN AT MAX STRESS
     1= ',F5.4,2X,'BOUND WIDTH = ',F4.3,'B')
      PD100=100.*P(1)
      P100=100.*P(2)
      WRITE(6,109) PD100,P100,ECR,DF
```



```
  109 FORMAT(1H ,2('STEEL PERCENTAGE = ',F5.3,6X),'CRUSHING STRAIN =',F5
     1.4,8X,'FLANGE DEPTH = ',F5.3,'D')
      WRITE(6,110) YM(1),YM(2),YMC,WF
  110 FORMAT(1H ,3('YOUNGS MODULUS = ',F9.0,4X),'FLANGE WIDTH = ',F5.3,'
     1B')
      WRITE(6,111) NEL,NCR
  111 FORMAT(1H ,60X,'NUMBER OF ELEMENTS = ',I3,6X,'NUMBER OF READINGS =
     1 ',I2/////////////////)
      WRITE(6,112) BIGP,EP
  112 FORMAT(1H ,'AXIAL STRESS IS ',F5.0,' PSI AT ',F5.2,'D ECCENTRICITY
     1'/////////////////)
      WRITE(6,113)
  113 FORMAT(1H ,2X,'EC',9X,'K',9X,'CC',10X,'ESD',10X,'CS',10X,'ES',11X,
     1'T',7X,'MOMENT',7X,'CURVATURE',5X,'KODE',9X,'ENERGY'////)
  114 FORMAT(' ',F7.5,F9.3,2(F12.0,F12.6),2F12.0,F14.6,I8,F15.6)
C     WIDTH FACTORS INITIALISATION
      DO 5 I=1,NEL
    5 FW(I)=1.
      EL=NEL
      TEMP=DF*EL/H
      J=TEMP
      DO 6 I=1,J
    6 FW(I)=WF
C     STEEL 'COUNTERS' INITIALISATION
      DO 7 I=1,2
      WC(I)=FU(I)/FY(I)
      WB(I)=.14
      WH(I)=(WC(I)*(30.*WB(I)+1.)**2-60.*WB(I)-1.)/(15.*WB(I)**2)
      WA(I)=(WH(I)*WB(I)+2.)/(60.*WB(I)+2.)
      ESU(I)=ESH(I)+WB(I)
      ESL(I)=0.
    7 FSL(I)=0.
C     DETERMINATION OF STEEL RESIDENT ELEMENTS
      TEMP=EL*DD/H
      IT=TEMP
      TEMP=EL/H
      IB=TEMP
C     CONCRETE AND BEAM COUNTERS INITIALISATION
      PSI=0.
      KONZ=1
      BML=0.
      PSIL=0.
      ENERGY=0.
      DO 8 I=1,NEL
      EMAX(I)=0.
    8 EZERO(I)=0.
      DO 85 I=1,NEL
   85 FCRACK(I)=1.
C     READ CURVATURE REQUIREMENTS
      DO 9 I=1,NCR
    9 READ(5,115) CR(I)
  115 FORMAT(F9.6)
C
C     COMPUTATION PHASE BEGINS
```

```
C
      CHANGE=.00005
      DO 63 I=1,NCR
      DIV=0.
      KDIV=0
      IF(I-1) 1,10,11
   10 EC=0.
      IF(CR(I)) 12,63,13
   11 IF(CR(I)-CR(I-1)) 12,63,13
   12 KODE=2
      EC=EC-CHANGE
      IF(PSI-CR(I)) 63,63,14
   13 KODE=1
      EC=EC+CHANGE
      IF(PSI-CR(I)) 14,63,63
   14 AK=-20000.
      CLAGMN=1000.
      KING=0
      KROG=1
      KFV=1
      G=20000.
      IF(EC*EC-.000000001) 62,15,15
   15 ES(1)=EC*(1.-DD/AK)
      ES(2)=EC*(1.-1./AK)
      IF(AK.GT.0.0.AND.G.GT.101.0)G=100.
      SN=EL*AK/H
      NS=SN
      SR(1)=0.
      SR(2)=0.
      QSR(1)=0.
      QSR(2)=0.
      CC=0.
      BMCC=0.
      IF(EC-.00026)155,155,154
  154 CHANGE=.0001
C     EVALUATION OF ELEMENTAL CONCRETE STRESSES
  155 DO 24 J=1,NEL
      AB=J
      E(J)=EC*(SN-AB+.5)/SN
      IF(E(J)-EMAX(J))16,18,18
   16 IF(E(J)-EZERO(J)) 20,20,17
   17 IF(E(J)-ELAST(J))172,172,171
  171 F(J)=.25*(3.*FMAX(J)+YMC*(E(J)-EZERO(J)))
      GO TO 24
  172 F(J)=.25*YMC*(E(J)-EZERO(J))
      GO TO 24
   18 IF(E(J)-E0) 19,19,21
   19 F(J)=FCD*(2.*E(J)/E0-E(J)*E(J)/(E0*E0))
      IF(F(J)) 20,24,24
   20 IF(FCRACK(J)-0.5)201,201,202
  201 F(J)=0.
      GO TO 24
  202 IF(E(J)-EZERO(J)+ER)201,203,203
  203 F(J)=YMC*(E(J)-EZERO(J))
      GO TO 24
   21 IF(E(J)-E20) 22,22,23
   22 F(J)=FCD*(1.-Z*(E(J)-E0))
      GO TO 24
   23 F(J)=FCD/5.
   24 CONTINUE
C     STEEL AREA REDUCTION
      SR(1)=P(1)*F(IT)
      QSR(1)=AK-DD
      SR(2)=P(2)*F(IB)
      QSR(2)=AK-1.
      CC=CC-SR(1)-SR(2)
      BMCC=BMCC-SR(1)*QSR(1)-SR(2)*QSR(2)
C     WIDTH FACTOR CORRECTIONS (TEMPORARY)
      DO 31 K=1,NEL
      AB=K
      IF(E(K)-ECR) 25,25,26
   25 F(K)=F(K)*FW(K)
      GO TO 30
   26 IF(K-IT) 27,28,28
   27 F(K)=0.
      GO TO 30
   28 IF(K-IB) 29,27,27
   29 F(K)=F(K)*BDD
   30 CC=CC+F(K)/EL
   31 BMCC=BMCC+F(K)*AK*(SN-AB+.5)/(EL*SN)
C     STEEL FORCES
      DO 39 J=1,2
      FS(J)=FSL(J)-YM(J)*(ESL(J)-ES(J))
      IF(FS(J)*FS(J)-FY(J)*FY(J)) 39,39,32
   32 IF(ES(J)*ES(J)-ESH(J)*ESH(J)) 33,33,36
   33 IF(FS(J)) 34,1,35
   34 FS(J)=-FY(J)
      GO TO 39
   35 FS(J)=FY(J)
      GO TO 39
   36 TEMP=1.
      IF(ES(J)) 37,1,38
   37 TEMP=-1.
      ES(J)=-ES(J)
   38 DELTA=ABS(ESH(J)-ABS(ES(J)))
      FS(J)=TEMP*FY(J)*((WH(J)*DELTA*2.)/(60.*DELTA*2.)+DELTA*(WC(J)-WA(
     1J))/WB(J))
      ES(J)=ES(J)*TEMP
   39 CONTINUE
      CS=P(1)*FS(1)
      BMCS=CS*(AK-DD)
      T=P(2)*FS(2)
      BMT=T*(AK-1.)
C     AXIAL LOAD MOMENT
      BMP=BIGP*EP
C     EQUILIBRIUM CHECK
      CLAG=T+CC+CS-BIGP
      IF(KROG.EQ.2)GO TO 44
```

```
      IF(CLAGMN.LE.ABS(CLAG))GO TO 40
      CLAGMN=ABS(CLAG)
      AKBEST=AK
   40 KING=KING+1
      IF(KFV.EQ.2) GO TO 41
      KFV=2
      IF(EC*CLAG)42,44,405
  405 AK=100.
      GO TO 15
   41 IF(ABS(CLAG).LT.0.33) GO TO 44
      IF(EC*CLAG)42,44,43
   42 AK=AK+G
      IF(AK.GT.20000.0) GO TO 62
      IF(ABS(AK).GT.0.001)GO TO 15
   43 AK=AK-G
      G=G/2.
      IF(KING.GT.150)GO TO 44
      IF(G.GT.0.000001) GO TO 42
   44 BMTOT=BMCC+BMCS+BMT+BMP
      IF(KROG.EQ.2.OR.ABS(CLAG).LT.1.0) GO TO 445
      AK=AKBEST
      KROG=2
      GO TO 15
  445 IF(ES(1)**2-ESU(1)**2)46,46,45
   45 WRITE(6,116)
  116 FORMAT(1H ,'TOP STEEL FRACTURED'/////)
      GO TO 1
   46 IF(ES(2)*ES(2)-ESU(2)*ESU(2)) 48,48,47
   47 WRITE(6,117)
  117 FORMAT(1H ,'BOTTOM STEEL FRACTURED'/////)
      GO TO 1
   48 IF(KDIV)53,49,53
   49 GO TO (50,51),KODE
   50 IF(EC-ES(2)-CR(I)) 53,52,52
   51 IF(EC-ES(2)-CR(I)) 52,52,53
   52 DIV=.0001*(EC-ES(2)-CR(I))/(EC-ES(2)-PSI)
      TEMP=KODE
      DIV=DIV*(4.-3.*TEMP)/TEMP
      KDIV=1
      EC=EC-DIV
      GO TO 14
   53 PSI=EC-ES(2)
      ENERGY=ENERGY+.5*(BML+BMTOT)*(PSI-PSIL)
      WRITE(6,114)EC,AK,CC,ES(1),CS,ES(2),T,BMTOT,PSI,KODE,ENERGY
      IF(ABS(CLAG).GT.1.0)WRITE(6,1155)
 1155 FORMAT('+',130X,'*')
      PSIL=PSI
      BML=BMTOT
      EC=EC+DIV
C     UPDATE CONCRETE COUNTERS
      DO 55 K=1,NEL
      ELAST(K)=E(K)
      IF(E(K)-EMAX(K)) 55,55,54
   54 EMAX(K)=E(K)
      FMAX(K)=F(K)
      EZERO(K)=EMAX(K)-F(K)/YMC
   55 CONTINUE
      DO 60 K=1,NEL
      IF(E(K)-ECR) 60,60,56
   56 IF(K-IT) 57,58,58
   57 FW(K)=0.
      GO TO 60
   58 IF(K-IB) 59,57,57
   59 FW(K)=GOD
   60 CONTINUE
      DO 605 J=1,NEL
      IF(E(J)-EZERO(J)+ER)604,605,605
  604 FCRACK(J)=0.
  605 CONTINUE
C     UPDATE STEEL 'COUNTERS'
      DO 61 K=1,2
      ESL(K)=ES(K)
   61 FSL(K)=FS(K)
      IF(KDIV)63,62,63
   62 GO TO (13,12),KODE
   63 CONTINUE
      GO TO 1
      END
```

```
C     ******************************************************************
C
C     DEFLECTION ANALYSIS FOR CANTILEVERS AND SIMPLY-SUPPORTED BEAMS
C
C     SINGLE POINT LOAD AT FREE END OF CANTILEVER OR AT CENTRE POINT OF
C     SIMPLY SUPPORTED BEAM   -   OR ,  UNIFORMLY DISTRIBUTED LOAD
C
C     CYCLIC LOADING IS PERMITTED
C
C     BAUSCHINGER EFFECT IS INCORPORTED
C
C     DEFLECTIONS FORM INPUT
C
C     AUGUST 1969
C
C     ******************************************************************
      DIMENSION WH(2),WA(2),WB(2),WC(2),DR(50),FU(2),FY(2),ESH(2),P(2),
     1YM(2),ESU(2),SR(2),QSR(2),FT(2),RVAL(40),GUFF(2),GA(2)
      DIMENSION EDIFF(9,2),EIPL(9,2),FS(9,2),ES(9,2),NCYC(9,2),ESL(9,2),
     1FSL(9,2),EZERON(9,2),EZEROL(9,2),SENSE(9,2),KBAUS(9,2),PSI(9),BIGD
     2EL(9),ETOP(9),ETOPL(9),BMREQD(9)
      DIMENSION ELAST(9,10),FMAX(9,10),FCRACK(9,10),EMAX(9,10),EZERO(9,
     110),E(9,10),F(9,10),FW(9,10)
      DATA GA/'YES ','NO  '/
      PAUSE 'CANCEL JOB IF PRINTER IS IDLE FOR MORE THAN 5 MINUTES'
      ONE=1.
C     READ STEEL PROPERTIES
    1 READ(5,200,END= 99)((FU(I),FY(I),ESH(I),P(I),YM(I)),I=1,2)
  200 FORMAT(F6.0,F8.0,2F7.4,F11.0,2F8.0,2F7.4,F11.0)
      FT(1)=.15*FY(1)
      FT(2)=.15*FY(2)
C     READ CONCRETE PROPERTIES
      READ(5,201) EO,ECR,Z,FCD
  201 FORMAT(F5.4,F7.4,F6.0,F7.0)
      ER=500.*EO/(FCD+4000.)
      YMC=2.*FCD/EO
      E20=1.
      IF(Z.GT.0.0) E20=EO+.8/Z
C     READ BEAM GEOMETRY AND NUMBERS OF ELEMENTS , READINGS AND SECTIONS
      READ(5,202)DD,H,BDD,WF,DF,NEL,NDR,NSECT
  202 FORMAT(F4.3,F7.3,F6.3,F6.2,F7.3,I5,2I4)
      IF(NSECT.LE.5.OR.NSECT.GT.9)NSECT=9
      IF(NEL.LE.5.OR.NEL.GT.10)NEL=10
C     READ AXIAL LOAD , ECCENTRICITY , BEAM LENGTH AND LOADING TYPE
      READ(5,203)BIGP,EP,BEAML,LTYPE
  203 FORMAT(F6.0,2F7.3,I1)
C
C     HEADINGS AND LISTS OF INPUT DATA
C
      WRITE(6,204)
  204 FORMAT('1DEFLECTION ANALYSIS FOR CYCLICALLY- AND AXIALLY-LOADED T-
     1BEAMS'//////)
      WRITE(6,205)NSECT,BEAML
  205 FORMAT(' BEAMS WITH ',I3,' SECTIONS AND BEAM LENGTH = ',F7.3,'D'//
```



```
     1/)
      IF(LTYPE.EQ.2) GO TO 2
      LTYPE=1
      WRITE(6,206)
  206 FORMAT(' POINT LOAD'////)
      GO TO 3
    2 WRITE(6,207)
  207 FORMAT(' UNIFORMLY DISTRIBUTED LOAD'////)
    3 WRITE(6,208)
  208 FORMAT(' TOP STEEL PROPERTIES',10X,'BOTTOM STEEL PROPERTIES',7X,'C
     1ONCRETE PROPERTIES',11X,'SECTION PROPERTIES'/////)
      WRITE(6,209) FU,FCD,DD
  209 FORMAT(' ',2('ULTIMATE STRESS = ',F6.0,6X),'CYLINDER STRENGTH =',F
     16.0,5X,'COMPRESSION STEEL DEPTH =',F5.3,'D')
      WRITE(6,210) FY,Z,H
  210 FORMAT(' ',2('YIELD STRESS = ',F6.0,9X),'PARAMETER Z = ',F5.0,11X,
     1'TOTAL SECTION DEPTH = ',F5.3,'D')
      WRITE(6,211)ESH,EO,BDD
  211 FORMAT(' ',2('STRAIN HARDENING =',F8.4,4X),'STRAIN AT MAX STRESS =
     1',F6.4,2X,'BOUND WIDTH =',F5.3,'B')
      EL=100.*P(1)
      G=100.*P(2)
      WRITE(6,212)EL,G,ECR,DF
  212 FORMAT(' ',2('STEEL PERCENTAGE =',F6.3,6X),'CRUSHING STRAIN =',F6.
     14,7X,'FLANGE DEPTH =',F6.3,'D')
      WRITE(6,213) YM,YMC,WF
  213 FORMAT(' ',3('YOUNGS MODULUS =',F10.0,4X),'FLANGE WIDTH =',F6.3,'B
     1')
      WRITE(6,214) FT,NEL,NDR
  214 FORMAT(' ',2('TRANSITION STRESS = ',F6.0,4X),'NUMBER OF ELEMENTS =
     1',I4,6X,'NUMBER OF READINGS =',I3////////)
      WRITE(6,215) BIGP,EP
  215 FORMAT(' AXIAL STRESS IS',F6.0,'PSI AT',F6.2,'D ECCENTRICITY'/'1')
C
C     INITIALISATION
C
      SECTN=NSECT
      EL=NEL
      TEMP=DF*EL/H+.5
      K=TEMP
      IF(K.GT.NEL) K=NEL
      L=K+1
C     WIDTH FACTORS
      DO 6 I=1,NSECT
      DO 4 J=1,K
    4 FW(I,J)=WF
      IF(L.GT.NEL) GO TO 6
      DO 5 J=L,NEL
    5 FW(I,J)=1.
    6 CONTINUE
C     STEEL COUNTERS
      DO 7 J=1,2
      WC(J)=FU(J)/FY(J)
      WB(J)=0.14
```

```
      WH(J)=(WC(J)*(30.*WB(J)+1.)**2-60.*WB(J)-1.)/(15.*WB(J)**2)
      WA(J)=(WH(J)*WB(J)+2.)/(60.*WB(J)+2.)
      ESU(J)=ESH(J)+WB(J)
      DO 7 I=1,NSECT
      ESL(I,J)=0.
      FSL(I,J)=0.
      EZERON(I,J)=0.
      EZEROL(I,J)=0.
      NCYC(I,J)=0
      EDIFF(I,J)=0.
      EIPL(I,J)=0.
      SENSE(I,J)=0.
      KBAUS(I,J)=1
    7 CONTINUE
      DO 8 J=1,39,2
      G=J
    8 RVAL(J)=4.489/ALOG(1.+G)-6.026/(EXP(G)-1.)+.297
      DO 9 J=2,40,2
      G=J
    9 RVAL(J)=2.197/ALOG(1.+G)-0.469/(EXP(G)-1.)+3.043
C     DETERMINATION OF STEEL-RESIDENT ELEMENTS
      TEMP=EL*DD/H+.5
      IT=TEMP
      TEMP=EL/H+.5
      IB=TEMP
C     CONCRETE AND BEAM 'COUNTERS' INITIALISATION
      DO 10 J=1,NSECT
      PSI(J)=0.
      ETOPL(J)=0.
   10 BIGDEL(J)=0.
      DO 11 I=1,NSECT
      DO 11 J=1,NEL
      FCRACK(I,J)=1.
      EMAX(I,J)=0.
      EZERO(I,J)=0.
      ELAST(I,J)=0.
   11 FMAX(I,J)=0.
C
C     READ IN DEFLECTION VALUES
C
      DO 12 I=1,NDR
   12 READ(5,216) DR(I)
  216 FORMAT(F9.6)
C
C     COMPUTATION  SEGMENT
C
      DO 87 N=1,NDR
      DIV=0.
      KDIV=0
      IF(N.EQ.1) CHANGE=.00005
      IF(N.GT.1) GO TO 13
      ETOP(1)=0.
      IF(DR(N)) 14,87,15
   13 IF(DR(N)-DR(N-1))14,87,15
```



```
   14 KODE=2
      ETOP(1)=ETOP(1)-CHANGE
      IF(BIGDEL(NSECT).GT.DR(N)) GO TO 16
      GO TO 87
   15 KODE=1
      ETOP(1)=ETOP(1)+CHANGE
      IF(BIGDEL(NSECT).GE.DR(N)) GO TO 87
   16 IF(ABS(ETOP(1)).GT.0.00097)CHANGE=0.0005
C     SECTION COMPATIBILITY FOR SECTION 1
      I=1
      IF(ABS(ETOP(1)).LT.0.00001) GO TO (15,14),KODE
   17 AK=-20000.
      CLAGMN=1000.
      KING=0
      KROG=1
      G=20000.
      EC=ETOP(I)
   18 ES(I,1)=EC*(1.-DD/AK)
      ES(I,2)=EC*(1.-1./AK)
      SN=EL*AK/H
      DO 19 J=1,2
      SR(J)=0.
   19 QSR(J)=0.
      CC=0.
      BMCC=0.
C     EVALUATE ELEMENTAL CONCRETE STRESSES
      DO 27 J=1,NEL
      AB=J
      E(I,J)=EC*(SN-AB+.5)/SN
      IF(E(1,J).GT.EMAX(I,J)) GO TO 21
      IF(E(I,J).LE.EZERO(I,J)) GO TO 22
      IF(E(I,J).LE.ELAST(I,J)) GO TO 20
      F(I,J)=.25*(3.*FMAX(I,J)+YMC*(E(I,J)-EZERO(I,J)))
      GO TO 27
   20 F(I,J)=.25*YMC*(E(I,J)-EZERO(I,J))
      GO TO 27
   21 IF(E(I,J).GT.E0) GO TO 25
      F(I,J)=FCD*(2.*E(I,J)/E0-(E(I,J)/E0)**2)
      IF(F(I,J).GT.0.0) GO TO 27
   22 IF(FCRACK(I,J).GT.0.5) GO TO 24
   23 F(I,J)=0.
      GO TO 27
   24 IF(E(I,J)-EZERO(I,J)+ER.LT.0.0) GO TO 23
      F(I,J)=YMC*(E(I,J)-EZERO(I,J))
      GO TO 27
   25 IF(E(I,J).GT.E20) GO TO 26
      F(I,J)=FCD*(1.-Z*(E(I,J)-E0))
      GO TO 27
   26 F(I,J)=FCD/5.
   27 CONTINUE
C     STEEL AREA REDUCTION
      SR(1)=P(1)*F(I,IT)
      QSR(1)=AK-DD
      SR(2)=P(2)*F(I,IB)
```

```
      QSR(2)=AK-1.
      CC=CC-SR(1)-SR(2)
      BMCC=BMCC-SR(1)*QSR(1)-SR(2)-QSR(2)
C     TEMPORARY WIDTH FACTOR CORRECTIONS
      DO 31 J=1,NEL
      AB=J
      IF(E(I,J).GT.ECR) GO TO 28
      F(I,J)=F(I,J)*FW(I,J)
      GO TO 30
   28 IF(J.LT.IT.OR.J.GT.IB)F(I,J)=0.
      F(I,J)=F(I,J)*BDD
   30 CC=CC+F(I,J)/EL
   31 BMCC=BMCC+F(I,J)*AK*(SN-AB+.5)/(EL*SN)
C     STEEL FORCES
      DO 45 J=1,2
      FS(I,J)=YM(J)*(ES(I,J)-EZERON(I,J))
      KAD=KBAUS(I,J)
      IF(KAD.GT.1) GO TO 35
C     ELASTO-PLASTIC SYSTEM
      IF(FS(I,J)*SENSE(I,J).LT.0.0) GO TO 33
      IF(ABS(FS(I,J)).LE.FY(J)) GO TO 44
      IF(ABS(ES(I,J)).GT.ESH(J)) GO TO 32
      FS(I,J)=SIGN(FY(J),ES(I,J))
      GO TO 44
   32 TEMP=1.
      IF(ES(I,J).LT.0.0)TEMP=-1.
      DELTA=ABS(ESH(J)-ABS(ES(I,J)))
      FS(I,J)=TEMP*FY(J)*((WH(J)*DELTA+2.)/(60.*DELTA+2.)
     1+DELTA*(WC(J)-WA(J))/WB(J))
      GO TO 44
   33 IF(ABS(FS(I,J)).LE.FT(J)) GO TO 44
C     ITERATION ROUTINE FOR BAUSHINGER STRESS
   34 DELTA=ABS(EZERON(I,J)-ES(I,J))
      PLAST=ABS(EZERON(I,J)-EZEROL(I,J))
      FCH=FY(J)*(.744/ALOG(1.+1000.*PLAST)+.071/(EXP(1000.
     1*PLAST)-1.)+.241)
      IF(FCH.GT.FY(J)) FCH=FY(J)
      R=RVAL(NCYC(I,J)+1)
      ECH=FCH/YM(J)
      ALPHA=DELTA/ECH
      GAMMA=ALPHA
   35 BETA=ALPHA-(ALPHA+ALPHA**R-GAMMA)/(1.+R*ALPHA**(R-1.))
      IF(ABS(ALPHA-BETA).LE.(10./FCH)) GO TO 36
      ALPHA=BETA
      GO TO 35
   36 IF(KAD-2) 37,42,43
   37 FS(I,J)=-FCH*BETA*SENSE(I,J)
      GO TO 44
C     BAUSHINGER SYSTEM
   38 IF(ABS(FS(I,J)).LE.FT(J)) GO TO 44
      IF(FS(I,J)*FSL(I,J).GT.0.0) GO TO 39
      KAD=3
      IF(ABS(FSL(I,J))-FT(J))40,40,34
   39 IF(ABS(FSL(I,J)).GT.FT(J)) GO TO 40
```



```
      IF(ABS(ESL(I,J)-EZEROL(I,J))-ABS(EZERON(I,J)-EZEROL(I,J))) 34,99,4
     10
   40 IF(ABS(EZEROL(I,J)-ES(I,J)).GT.EDIFF(I,J)) GO TO 41
      IF((EZERON(I,J)-EZEROL(I,J))*(ES(I,J)-EZERON(I,J)))34,44,44
   41 R=RVAL(NCYC(I,J))
      FCH=FY(J)*(.744/ALOG(1.+1000.*EIPL(I,J))+.071/(EXP(1000.*EIPL(I,J)
     1)-1.)+.241)
      IF(FCH.GT.FY(J))FCH=FY(J)
      ECH=FCH/YM(J)
      ALPHA=ABS(EZEROL(I,J)-ES(I,J))/ECH
      GAMMA=ALPHA
      GO TO 45
   42 FS(I,J)=FCH*BETA*SIGN(ONE,FSL(I,J))
      GO TO 44
   43 FS(I,J)=-FCH*BETA*SIGN(ONE,FSL(I,J))
   44 IF(ABS(FS(I,J)).GT.FU(J))FS(I,J)=SIGN(FU(J),FS(I,J))
   45 CONTINUE
      CS=P(1)*FS(I,1)
      BMCS=CS*(AK-DD)
      T=P(2)*FS(I,2)
      BMT=T*(AK-1.)
C     AXIAL LOAD MOMENT
      BMP=BIGP*EP
C     EQUILIBRIUM CHECK
      CLAG=T+CC+CS-BIGP
      IF(KROG.EQ.2) GO TO 51
      IF(CLAGMN.LE.ABS(CLAG)) GO TO 46
      CLAGMN=ABS(CLAG)
      AKBEST=AK
   46 KING=KING+1
      IF(KING.GT.1)GO TO 48
      IF(EC*CLAG)49,51,47
   47 AK=1000.
      G=1000.
      GO TO 18
   48 IF(ABS(CLAG).LT.0.33) GO TO 51
      IF(EC*CLAG)49,51,50
   49 AK=AK+G
      IF(AK.GT.20000.0) GO TO (15,14),KODE
      IF(KING.GT.100)GO TO 51
      IF(ABS(AK).GT.0.00001) GO TO 18
   50 AK=AK-G
      G=.5*G
      IF(KING.LE.100) GO TO 49
   51 BMTOT=BMCC+BMCS+BMT+BMP
      IF(KROG.EQ.2.OR.ABS(CLAG).LT.0.33) GO TO 52
      KROG=2
      AK=AKBEST
      GO TO 18
   52 IF(I.GT.1) GO TO 60
      KOD=1
      IF(LTYPE.EQ.2) GO TO 54
C     POINT LOAD
      PLOAD=2.*BMTOT*SECTN/(BEAML*(2.*SECTN-1.))
```

```
      IF((3.-2.*KODE)*(PLOAD-PLOADL).LT.0.0)KOD=2
      DO 53 J=1,NSECT
      G=J
   53 BMREQD(J)=PLOAD*BEAML*(1.-(2.*G-1.)/(2.*SECTN))
      GO TO 56
C     UNIFORM LOAD
   54 WLOAD=2.*BMTOT/(BEAML**2*(1.-1./(2.*SECTN))**2)
      IF((3.-2.*KODE)*(WLOAD-WLOADL).LT.0.0)KOD=2
      DO 55 J=1,NSECT
      G=J
   55 BMREQD(J)=.5*WLOAD*BEAML**2*(1.-(2.*G-1.)/(2.*SECTN))**2
   56 PSI(1)=EC-ES(1,2)
C     ESTABLISH CURVATURES IN OTHER SECTIONS
   57 DO 62 I=2,NSECT
      G=I
      KRIG=1
      KONG=0
      BMDIFF=1000.
      SINC=CHANGE*(2.*SECTN+1.-2.*G)/(2.*SECTN-1.)
      ETOP(I)=ETOPL(I)
      IF(KOD.EQ.2)ETOP(I)=ETOP(I)+(2.*KODE-3.)*SINC*.9
      GO TO (59,58),KODE
   58 ETOP(I)=ETOP(I)-SINC*2.
   59 ETOP(I)=ETOP(I)+SINC
      GO TO 17
   60 IF(ABS(BMTOT-BMREQD(I)).LT.ABS(0.01*BMREQD(I))) GO TO 61
      IF(KRIG.EQ.2)GO TO 61
      KONG=KONG+1
      IF(KONG.LT.20)GO TO 605
      ETOP(I)=ECBEST
      KRIG=2
      GO TO 17
  605 IF(ABS(BMTOT-BMREQD(I)).GT.BMDIFF)GO TO 606
      BMDIFF=ABS(BMTOT-BMREQD(I))
      ECBEST=EC
  606 IF(BMTOT-BMREQD(I).LT.0.0)GO TO 59
      ETOP(I)=ETOP(I)-SINC
      SINC=.5*SINC
      GO TO 59
   61 PSI(I)=EC-ES(I,2)
   62 CONTINUE
C     COMPUTE DEFLECTIONS
      DELTA=0.
      DO 63 J=1,NSECT
      G=J
   63 DELTA=DELTA+(G-.5)*PSI(NSECT-J+1)
      DELTA=(DELTA/G**2)*BEAML**2
      IF(KDIV.NE.0) GO TO 66
      IF(KODE.EQ.2) GO TO 64
      IF(DELTA-DR(N)) 66,65,65
   64 IF(DELTA-DR(N)) 65,65,66
   65 KDIV=1
      DIV=CHANGE*(DELTA-DR(N))/(DELTA-BIGDEL(NSECT))
      TEMP=KODE
```



```
      DIV=DIV*(4.-3.*TEMP)/TEMP
      ETOP(1)=ETOP(1)-DIV
      GO TO 16
C     COMPUTE ALL DEFLECTIONS
   66 IF(LTYPE.EQ.2) GO TO 67
      PLOAD=PLOAD/1000.
      WRITE(6,227) PLOAD
  227 FORMAT('1LOAD = ',F9.3,' *B*D  KIP'/////)
      GO TO 68
   67 WLOAD=WLOAD/1000.
      WRITE(6,228) WLOAD
  228 FORMAT('1LOAD = ',F9.3,' *B  KIP/IN'/////)
   68 WRITE(6,229)
  229 FORMAT(' SECTION',14X,'CRACKED',14X,'BENDING',13X,'CURVATURE',13X,
     1'DEFLECTION',13X,'CUMULATIVE'/' ',20X,'TOP',3X,'BOT',13X,'MOMENT',
     259X,'DEFLECTION'/'0',41X,'(KIP.IN.)',12X,'(RADS/IN)',14X,'(INCHES)
     3'/////)
      DO 71 I=1,NSECT
      GUFF(1)=GA(2)
      IF(FCRACK(I,1).LT.0.5.OR.E(I,1)-EZERO(I,1)+ER.LT.0.0)
     1GUFF(1)=GA(1)
      GUFF(2)=GA(2)
      IF(FCRACK(I,NEL).LT.0.5.OR.E(I,NEL)-EZERO(I,NEL)+ER.LT.0.0) GUFF(2
     1)=GA(1)
      BIGDEL(I)=0.
      BMREQD(I)=BMREQD(I)/1000.
      G=I
      DO 69 J=1,I
      G1=J
      BIGDEL(I)=BIGDEL(I)+(.5+G-G1)*PSI(J)
   69 CONTINUE
      BIGDEL(I)=(BIGDEL(I)/SECTN**2)*BEAML**2
      SMLDEL=BIGDEL(I)
      IF(I.EQ.1) GO TO 70
      SMLDEL=BIGDEL(I)-BIGDEL(I-1)
   70 WRITE(6,230)I,GUFF,BMREQD(I),PSI(I),SMLDEL,BIGDEL(I)
  230 FORMAT(' ',I7,13X,A4,2X,A4,F13.3,'*B*D*D',F20.6,'/D',2(F21.6,'*D*
     1)
   71 CONTINUE
C     UPDATE SEGMENT
      ETOP(1)=ETOP(1)+DIV
      PLOADL=PLOAD*1000.
      WLOADL=WLOAD*1000.
C     UPDATE CONCRETE COUNTERS
      DO 86 I=1,NSECT
      ETOPL(I)=ETOP(I)
      DO 72 J=1,NEL
      ELAST(I,J)=E(I,J)
      IF(E(I,J).LE.EMAX(I,J)) GO TO 72
      EMAX(I,J)=E(I,J)
      FMAX(I,J)=F(I,J)
      EZERO(I,J)=EMAX(I,J)-F(I,J)/YMC
   72 CONTINUE
      DO 75 J=1,NEL
```

```
      IF(E(I,J).LE.ECR) GO TO 75
      FW(I,J)=BDD
      IF(J.LT.IT.OR.J.GT.IB)FW(I,J)=0.
   75 CONTINUE
      DO 76 J=1,NEL
      IF(E(I,J)-EZERO(I,J)+ER.GE.0.0) GO TO 76
      FCRACK(I,J)=0.
   76 CONTINUE
C     UPDATE STEEL COUNTERS
      DO 86 J=1,2
      KAD=KBAUS(I,J)
      IF(KAD.EQ.2) GO TO 78
C     ELASTO-PLASTIC SYSTEM
      IF(SENSE(I,J).NE.0.0) GO TO 77
      IF(ABS(ES(I,J)).LE.FY(J)/YM(J)) GO TO 85
      SENSE(I,J)=SIGN(ONE,ES(I,J))
      GO TO 84
   77 IF(SENSE(I,J)*FS(I,J).GE.0.0) GO TO 84
      IF(ABS(FS(I,J)).LE.FT(J)) GO TO 84
      KBAUS(I,J)=2
      GO TO 81
C     BAUSHINGER SYSTEM
   78 IF(ABS(FS(I,J)).LE.FT(J)) GO TO 85
      IF(FS(I,J)*FSL(I,J).GT.0.0) GO TO 82
      IF(ABS(FSL(I,J)).GT.FT(J)) GO TO 81
   79 IF(ABS(EZEROL(I,J)-ES(I,J)).GT.EDIFF(I,J)) GO TO 80
      IF((EZERON(I,J)-EZEROL(I,J))*(ES(I,J)-EZERON(I,J)))81,84,84
   80 EDIFF(I,J)=ABS(EZEROL(I,J)-ES(I,J))
      GO TO 84
   81 EDIFF(I,J)=ABS(EZERON(I,J)-ES(I,J))
      GO TO 83
   82 IF(ABS(FSL(I,J)).GT.FT(J)) GO TO 79
      IF(ABS(ESL(I,J)-EZEROL(I,J))-ABS(EZERON(I,J)-EZEROL(I,J)))81,81,79
   83 EIPL(I,J)=ABS(EZERON(I,J)-EZEROL(I,J))
      EZEROL(I,J)=EZERON(I,J)
      NCYC(I,J)=NCYC(I,J)+1
   84 EZERON(I,J)=ES(I,J)-FS(I,J)/YM(J)
   85 ESL(I,J)=ES(I,J)
   86 FSL(I,J)=FS(I,J)
      IF(KDIV.EQ.0) GO TO (15,14),KODE
   87 CONTINUE
      GO TO 1
   99 CONTINUE
      END
```



```
C     ***************************************************************
C
C      DEFLECTION ANALYSIS
C      CANTILEVERS AND SIMPLY-SUPPORTED BEAMS
C      CLOUGH'S IDEALISED MOMENT-CURVATURE RELATION IS UTILISED
C
C      SINGLE POINT LOAD AT FREE END OF CANTILEVER OR AT CENTRE POINT OF
C      SIMPLY-SUPPORTED BEAM  -  OR , UNIFORM LOAD
C
C      CYCLIC LOADING IS PERMITTED
C
C      CLOUGH'S IDEALISATION REQUIRES ALL ELEMENTS EXCEPT THE FIRST TO RE
C      MAIN ELASTIC
C
C      DEFLECTIONS FORM INPUT
C
C      SEPTEMBER 1969
C
C     ***************************************************************
      REAL*4 NYM,NYC
      DIMENSION PSI(100),DEFL(100)
C*****READ YIELD MOMENTS AND CURVATURES FOR POSITIVE AND NEGATIVE SENSES
C      , AND NUMBERS OF SECTIONS AND READINGS
      READ(5,101) PYM,PYC,NYM,NYC,NSECT,NR,BEAML
  101 FORMAT(2(F6.0,F9.6,2X),I2,I4,F6.2)
      IF(NYM.GT.0.0) NYM=-NYM
      IF(NYC.GT.0.0) NYC=-NYC
      IF(NSECT.GT.100.OR.NSECT.LE.3) NSECT=100
      IF(BEAML.EQ.0.0) BEAML=1.
C*****HEADINGS AND LIST OF INPUT DATA
      WRITE(6,102)
  102 FORMAT('1DEFLECTION ANALYSIS FOR CYCLICALLY-LOADED BEAMS USING CLO
     1UGHS IDEALISATION'////////)
      WRITE(6,103) PYM,PYC,NYM,NYC,NSECT,NR
  103 FORMAT(' POSITIVE YIELD MOMENT =',F12.0/' POSITIVE YIELD CURVATURE
     1 ='
     1 ,F9.6/' NEGATIVE YIELD MOMENT =',F12.0/' NEGATIVE YIELD CURVATURE
     2 =',F9.6/' NUMBER OF SECTIONS =',I15/' NUMBER READINGS =',I15//1
     '3 P',11X,'M1',39X,'SECTION DEFLECTIONS',36X,'FREE-END',9X,'M2'/' ',
     409X,'DEFLECTION'///)
  104 FORMAT(' ',F7.0,F13.0,90X,F9.6,F12.0)
  105 FORMAT('+',25X,9F9.6/)
C*****INITIALISE
      SECTN=NSECT
      DRL=0.
      CURV=0.
      STIFFP=PYM/PYC
      STIFFN=NYM/NYC
      BML=0.
      FED=0.
      FEDL=0.
      CZERON=0.
      CZEROL=0.
      SLOPEP=STIFFP
```

```
      SLOPEN=STIFFN
C
C*****COMPUTATION SEGMENT
C
      DO 19 N=1,NR
      READ(5,106) DR
  106 FORMAT(F9.6)
      DIV=0.
      KDIV=0
      CHANGE=.0001
      A=DR-DRL
      DRL=DR
      IF(A) 6,19,3
C*****KODE = 1   DEFLECTION INCREASING ALGEBRAICALLY
    3 KODE=1
      CURV=CURV+CHANGE
      IF(FEDL.GE.DR) GO TO 19
    4 IF(BML.LT.0.0) GO TO 5
      BM=(CURV-CZEROL)*SLOPEP
      IF(BM.GT.(CURV-CZERON)*STIFFP)BM=(CURV-CZERON)*STIFFP
      IF(BM.GT.PYM) BM=PYM
      GO TO 9
    5 BM=(CURV-CZERON)*STIFFN
      IF(BM.GT.0.0) BM=(CURV-CZERON)*SLOPEP
      IF(BM.GT.PYM)BM=PYM
      GO TO 9
C*****KODE = 2   DEFLECTION DECREASING ALGEBRAICALLY
    6 KODE=2
      CURV=CURV-CHANGE
      IF(FEDL.LE.DR) GO TO 19
    7 IF(BML.GT.0.0) GO TO 8
      BM=(CURV-CZEROL)*SLOPEN
      IF(BM.LT.(CURV-CZERON)*STIFFN)BM=(CURV-CZERON)*STIFFN
      IF(BM.LT.NYM) BM=NYM
      GO TO 9
    8 BM=(CURV-CZERON)*STIFFP
      IF(BM.LT.0.0)BM=(CURV-CZERON)*SLOPEN
      IF(BM.LT.NYM)BM=NYM
C*****COMPUTE POINT LOAD AND REMAINING CURVATURES
    9 PSI(1)=CURV
      P=2.*BM*SECTN/(BEAML*(2.*SECTN-1.))
      DO 10 J=2,NSECT
      G=J
      A=P*BEAML*(1.-(2.*G-1.)/(2.*SECTN))
      PSI(J)=A/STIFFP
      IF(A.LT.0.0) PSI(J)=A/STIFFN
   10 CONTINUE
C*****COMPUTE FREE END DEFLECTION
      FED=0.
      DO 11 J=1,NSECT
      G=J
   11 FED=FED+(G-.5)*PSI(NSECT-J+1)
      FED=FED*(BEAML/G)**2
      IF(KDIV.NE.0) GO TO 14
```



```
      IF(KODE.EQ.2) GO TO 12
      IF(FED-DR) 14,13,13
   12 IF(FED-DR) 13,13,14
   13 KDIV=1
      DIV=CHANGE*(FED-DR)/(FED-FEDL)
      TEMP=KODE
      DIV=DIV*(4.-3.*TEMP)/TEMP
      CURV=CURV-DIV
      GO TO (4,7),KODE
C*****COMPUTE ALL DEFLECTIONS
   14 DO 16 I=1,NSECT
      DEFL(I)=0.
      G=I
      DO 15 J=1,I
      H=J
      DEFL(I)=DEFL(I)+(H-.5)*PSI(I-J+1)
   15 CONTINUE
      DEFL(I)=DEFL(I)*(BEAML/SECTN)**2
   16 CONTINUE
      WRITE(6,104)P,BM,FED,P
C*****UPDATE SEGEMENT
      IF(BM*BML.LT.0.0) CZEROL=CZERON
      IF(KODE.EQ.2) GO TO 17
      IF(BM.GT.0.0)CZERON=CURV-BM/STIFFP
      IF(CURV.LT.CMAXP) GO TO 18
      CMAXP=CURV
      IF(CZERON-CMAXN.NE.0.0)SLOPEN=-NYM/(CZERON-CMAXN)
      IF(CMAXN.GT.NYC)SLOPEN=-NYM/(CZERON-NYC)
      GO TO 18
   17 IF(BM.LT.0.0) CZERON=CURV-BM/STIFFN
      IF(CURV.GT.CMAXN) GO TO 18
      CMAXN=CURV
      IF(CZERON-CMAXP.NE.0.0)SLOPEP=PYM/(CMAXP-CZERON)
      IF(CMAXP.LT.PYC)SLOPEP=PYM/(PYC-CZERON)
   18 BML=BM
      FEDL=FED
      IF(KDIV.EQ.0) GO TO (3,6),KODE
   19 CONTINUE
      WRITE(6,105)(DEFL(I),I=1,NSECT)
      END
```

```
C     ********************************************************************
C
C     PROGRAM TO CHECK DATA SEQUENCE
C
C     ********************************************************************
      DO1K=1,3
      READ(5,100) ICT
      IF(ICT-K)2,11,2
20    WRITE(6,106)K3,K4
    2 WRITE(6,101)
      GO TO 99
   11 WRITE(6,105)ICT
    1 CONTINUE
      K3=0
      K4=0
      READ(5,102)KN,NS,NDGC,ICT
      IF(ICT-4)2,13,2
   13 WRITE(6,105)ICT
    3 KCH=NS&4&NDGC
      DO4I=1,KCH
      READ(5,100) ICT
      IF(ICT-I-4)2,14,2
   14 WRITE(6,105)ICT
    4 CONTINUE
      IF(KN-66)10,12,12
10    IF(KN-46)16,12,17
17    IF(KN-47)16,12,16
16    I=1
      DO18J=1,46
      READ(5,103)K1,K2
      IF(I-K1)20,26,20
26    IF(J-K2)20,35,20
35    K3=K1
      K4=K2
18    CONTINUE
      DO7I=2,NS
      DO8J=1,3
      READ(5,103)K1,K2
      IF(K1-I)20,27,20
27    IF(K2-J)20,28,20
28    K3=K1
      K4=K2
8     CONTINUE
      DO7J=5,45,2
      READ(5,103)K1,K2
      IF(I-K1)20,29,20
29    IF(J-K2)20,30,20
30    K3=K1
      K4=K2
7     CONTINUE
      GO TO 50
12    DO5I=1,NS
      DO5J=1,46
      READ(5,103) K1,K2
```



```
      IF(K1-I)20,6,20
6     IF(K2-J)20,15,20
15    K3=K1
      K4=K2
    5 CONTINUE
 50   CONTINUE
      WRITE(6,104)
   99 CONTINUE
  100 FORMAT(77X,I3)
  101 FORMAT(1H ,23HINPUT DATA NOT IN ORDER)
  102 FORMAT(I2,14,17X,I2,52X,I3)
  103 FORMAT(74X,2I3)
  104 FORMAT(1H ,22HINPUT DATA IS IN ORDER)
  105 FORMAT(1H ,I6)
  106 FORMAT(1H ,2I3)
      END
```

```
C     ********************************************************************
C
C     ANALYSIS OF RESULTS FOR SERIES K BEAMS
C
C     ********************************************************************
      DIMENSION GUFF1(5),GUFF2(5)
      DIMENSION ECS(6),ESS(5),ECSS(6),ESSS(5),XG(4),DEFS(9)
      DIMENSION BMS(22),CURV(22),AS(2,6,22),BM1(22),BMSW(22)
      DIMENSION DEFSW(7),CAS(2,6,22),CUR(22),AVS(6,22),TC(2,120,4)
      DIMENSION KDIFF(2,31),SD(2)
      DIMENSION CF(2,4),ICF(22),DG(2,9),DE(2,2,6,22)
      DIMENSION ZDE(2,6,22),ZDG(9)
      DIMENSION DGC(120,9),DGC1(9)
      DIMENSION KTEMP(6)
      DO176I=1,120
      DO 176 J=1,9
      DGC(I,J)=0.
  176 CONTINUE
      DENOM=528.
      DO2999J=1,2
      DO2999M=1,31
 2999 KDIFF(J,M)=0
      READ(5,762)KODE
  762 FORMAT(I1)
      READ(5,763)GUFF1
      READ(5,763)GUFF2
  763 FORMAT(5A4)
      READ(5,100)KN,NS,XG(1),XG(2),XG(3),NDGC
  100 FORMAT(I2,I4,F5.0,F5.0,F5.0,I4)
      READ(5,101) H,B,D,DD,TW,SS
  101 FORMAT(F5.3,F7.3,F7.3,F7.3,F7.3,F8.2,F4.0)
      READ(5,102) CONC,FCD,RUPT,FCDF,S
  102 FORMAT(F6.2,F7.0,F6.0,F7.0,F6.0)
      READ(5,104) FYD,FY,ESHD,ESH,YM,DT
  104 FORMAT(F6.0,2X,F6.0,2X,F7.0,2X,F7.0,2X,F9.0,2X,F4.3)
      PI=3.14159
      YMC=30000000./(6.&10000./FCD)
      RM=YM/YMC
      C1=B*H*.5*H&(RM-1.)*((PI/8.)*(H-DD)&.5*PI*DT*DT*(H-D))
      AT=B*H&(RM-1.)*(PI/8.&.5*PI*DT*DT)
      C=C1/AT
      TI1=B*H*(.5*H-C)*(.5*H-C)&(RM-1.)*.5*PI*DT*DT*(C-H&D)*(C-H&D)
      TI=TI1&B*H*H*H/12.&(RM-1.)*(PI/8.)*(H-C-DD)*(H-C-DD)
      DO1I=1,5
      ESS(I)=0.
    1 ESSS(I)=0.
      WRITE(6,103) KN
      PUNCH 300,KN,NS,FY,FYD
300   FORMAT(1H ,2I3,2F7.0)
  103 FORMAT(1H1,34X,8HBEAM NO.,I2//////)
      FR=1000./(1.&4000./FCD)
      DO162I=1,22
      BM1(I)=0.
  162 CONTINUE
```



```
      WRITE(6,764)GUFF1
      WRITE(6,765)GUFF2
  163 FORMAT(1H ,18X,16HYIELD STRAIN TOP,4X,1H=,F5.0,6H MICRO)
  164 FORMAT(1H ,18X,16HYIELD STRAIN BOT,4X,1H=,F5.0,6H MICRO/////)
      EYD=1000000.*FY/YM
      EYDD=1000000.*FYD/YM
   18 WRITE(6,105)
  105 FORMAT(1H ,29X,20HSHRINKAGE  NEGLECTED/////)
   28 WRITE(6,107) H
  107 FORMAT(1H ,4X,4HBEAM,10X,14HOVERALL HEIGHT,6X,1H=,F5.3,1X,2HIN)
      WRITE(6,108) B
  108 FORMAT(1H ,18X,5HWIDTH,15X,1H=,F5.3,1X,2HIN)
      WRITE(6,109) D
  109 FORMAT(1H ,18X,15HEFFECTIVE DEPTH,5X,1H=,F5.3,1X,2HIN)
      WRITE(6,110) DD
  110 FORMAT(1H ,18X,16HCOMP STEEL DEPTH,4X,1H=,F5.3,1X,2HIN)
      WRITE(6,111) TW
  111 FORMAT(1H ,18X,6HWEIGHT,14X,1H=,F5.1,1X,2HLB)
      WRITE(6,112) SS
  112 FORMAT(1H ,18X,15HSTIRRUP SPACING,5X,1H=,3X,F2.0,1X,2HIN//)
      WRITE(6,113) CONC
  113 FORMAT(1H ,4X,8HCONCRETE,6X,7HDENSITY,13X,1H=,F5.1,4H PCF)
      WRITE(6,114) FCD
  114 FORMAT(1H ,18X,13HCYL STR START,7X,1H=,F5.0,1X,3HPSI)
      WRITE(6,115) RUPT
  115 FORMAT(1H ,18X,13HMOD RUPT EXPT,7X,1H=,F5.0,4H PSI)
      WRITE(6,116) FR
  116 FORMAT(1H ,18X,14HMOD RUPT THEOR,6X,2H= ,F4.0,4H PSI)
      WRITE(6,117) YMC
  117 FORMAT(1H ,18X,16HYOUNGS MOD THEOR,4X,1H=,F8.0,4H PSI)
      WRITE(6,118) FCDF
  118 FORMAT(1H ,18X,13HCUBE STRENGTH,7X,1H=,F5.0,4H PSI)
      WRITE(6,119) S
  119 FORMAT(1H ,18X,16HSHRINKAGE STRAIN,4X,1H=,F4.0,6H MICRO//)
      WRITE(6,136) FYD
  136 FORMAT(1H ,4X,5HSTEEL,9X,16HYIELD STRESS TOP,4X,1H=,F6.0,4H PSI)
      WRITE(6,137) FY
  137 FORMAT(1H ,18X,16HYIELD STRESS BOT,4X,1H=,F6.0,4H PSI)
      WRITE(6,138) YM
  138 FORMAT(1H ,18X,14HYOUNGS MODULUS,6X,1H=,F9.0,4H PSI)
      WRITE(6,139) ESHD
  139 FORMAT(1H ,18X,21HSTRAIN HARDENING TOP=,F8.0,6H MICRO)
      WRITE(6,140) ESH
  140 FORMAT(1H ,18X,21HSTRAIN HARDENING BOT=,F8.0,6H MICRO)
      WRITE(6,141) DT
  141 FORMAT(1H ,18X,15HDIAM TENS REINF,5X,1H=,F4.3,3H IN)
      WRITE(6,163) EYDD
      WRITE(6,164) EYD
      DO29I=1,22
      BMS(I)=0.
      CURV(I)=0.
      DO29J=1,6
      DO29K=1,2
      AS(K,J,I)=0.
```

```
   29 CONTINUE
      DO36I=1,9
      DEFS(I)=0.
   36 CONTINUE
      WRITE(6,142)
  142 FORMAT(1H ,4X,25HPOSITIVE SIGN CONVENTIONS///)
      WRITE(6,143)
  143 FORMAT(1H ,4X,4HLOAD,21X,8HDOWNWARD)
      WRITE(6,144)
  144 FORMAT(1H ,4X,10HDEFLECTION,15X,8HDOWNWARD)
      WRITE(6,145)
  145 FORMAT(1H ,4X,6HSTRAIN,20X,7HTENSION)
      WRITE(6,146)
  146 FORMAT(1H ,4X,6HMOMENT,13X,14HTENSION BOTTOM)
      WRITE(6,147)
  147 FORMAT(1H ,4X,9HCURVATURE,10X,14HTENSION BOTTOM)
      WRITE(6,148)
  148 FORMAT(1H ,4X,21HLONGITUDINAL MOVEMENT,6X,6HINWARD////)
C     SELF WEIGHT CONSIDERATIONS
   37 VT=12.*B*H
      VS=(PI/64.)*(18.5&9.*PI/8.)*(12./SS)&PI*(1.5&6.*DT*DT)
      VC=(VT-VS)/1728.
      WC=VC*CONC
      WS=VS*.28333
      UDL=(WC&WS)/12.
      UDLS=TW/8.-14.*UDL
      DO70I=1,10
      GO TO (71,72,73,74,75,76,77,78,79,80),I
   71 XSW=32.
   69 IF(XSW-56.)68,68,67
   68 TEM1=0
      GO TO 66
   67 TEM1=.5*(UDLS-UDL)*(XSW-56.)*(XSW-56.)
   66 BMSW(I)=(-UDL*.5*XSW*XSW&.5*TW*(XSW-6.)-TEM1)/1000.
      BMSW(21-I)=BMSW(I)
      GO TO 70
   72 XSW=36.
      GO TO 69
   73 XSW=40.
      GO TO 69
   74 XSW=44.
      GO TO 69
   75 XSW=48.
      GO TO 69
   76 XSW=51.
      GO TO 69
   77 XSW=53.
      GO TO 69
   78 XSW=55.
      GO TO 69
   79 XSW=57.
      GO TO 69
   80 XSW=59.
      GO TO 69
```



```
   70 CONTINUE
      BMSW(21)=(-UDL*.5*56.*56.&.5*TW*50.)/1000.
      BMSW(22)=BMSW(21)
      XG(4)=60.
      REA=56.*UDL&4.*UDLS
      TIS=TI&2.*(B.*B*(.5*(H&6.))*(.5*(H&6.))&B*18.)
      TERMC=(UDLS-UDL)*32./3.&UDL*36000.-27.*54.*REA
      TERMA=(TI/TIS)*(.5*REA*2500.-UDL*56.*56.*56./6.&TERMC)&UDL*56.
     1*56.*56./6.-.5*REA*2500.
      TERMB=54.*UDL-6.*TERMA
      TERMD=(TIS/TI)*((REA/6.)*125000.-UDL*56.*56.*56.*56./24.&56.*
     1TERMA&TERMB)&UDL*56.*56.*56.*56./24.-REA*125000./6.-56.*TERMC
      DO81I=1,4
      IF(XG(I)-56.)170,170,171
  170 DEFSW(I)=-(REA*(XG(I)-6.)*(XG(I)-6.)*(XG(I)-6.)/6.-UDL*XG(I)*XG(
     1I)*XG(I)*XG(I)/24.&TERMA*XG(I)&TERMB)/(YMC*TI)
      GO TO 172
  171 DEFSW(I)=-(REA*(XG(I)-6.)*(XG(I)-6.)*(XG(I)-6.)/6.-UDL*XG(I)*XG(I)
     1*XG(I)*XG(I)/24.-(UDLS-UDL)*(XG(I)-56.)*(XG(I)-56.)*(XG(I)-56.)*
     2(XG(I)-56.)/24.&TERMC*XG(I)&TERMD)/(YMC*TIS)
  172 DEFSW(8-I)=DEFSW(I)
   81 CONTINUE
      DO82I=1,20
      FCT=100.
      G=100.
   86 FCC=FCT*(H-C)/C
      ECC=FCC/YMC
      ESC=ECC*(H-C-DD)/(H-C)
      FSC=ESC*YM
      ECT=FCT/YMC
      EST=ECT*(C-H&D)/C
      FST=EST*YM
      TSTM1=(PI/8.)*FSC*(H-C-DD)&B*FCC*(H-C)*(H-C)/3.
      TSTM=(TSTM1&(PI/2.)*DT*DT*FST*(C-H&D)&FCT*B*C*C/3.)/1000.
      IF(TSTM-BMSW(I))83,84,85
   83 FCT=FCT&G
      GO TO 86
   85 FCT=FCT-G
      G=.1*G
      IF(G-1.)84,83,83
   84 DO87J=1,2
      DAS(J,1,I)=-ESC*1000000.*(H-C-DD&.75)/(H-C-DD)
      DAS(J,2,I)=-ESC*1000000.
      DAS(J,3,I)=-ESC*1000000.*(H-C-DD-.75)/(H-C-DD)
      DAS(J,4,I)=EST*1000000.*(C-H&D-.75)/(C-H&D)
      DAS(J,5,I)=EST*1000000.
      DAS(J,6,I)=EST*1000000.*(C-H&D&.75)/(C-H&D)
   87 CONTINUE
      CUR(I)=(DAS(1,5,I)-DAS(1,2,I))/(1000000.*(D-DD))
   82 CONTINUE
      DO165J=1,6
      DO165K=1,2
      DAS(K,J,21)=.5*(DAS(K,J,8)&DAS(K,J,9))
      DAS(K,J,22)=.5*(DAS(K,J,12)&DAS(K,J,13))
```

```
  165 CONTINUE
      CUR(21)=(DAS(1,5,21)-DAS(1,2,21))/(1000000.*(D-DD))
      CUR(22)=(DAS(1,5,22)-DAS(1,2,22))/(1000000.*(D-DD))
C     SELF WEIGHT OUTPUT
      WRITE(6,149)
  149 FORMAT(1H ,63X,16HSELF WEIGHT ONLY/////)
      WRITE(6,121)
      WRITE(6,122)
      WRITE(6,123)
      DO39I=1,22
      DO5002K=1,6
 5002 KTEMP(K)=DAS(1,K,I)
      WRITE(6,124)I,(KTEMP(K),K=1,6)
   39 CONTINUE
      WRITE(6,125)
      WRITE(6,126)
      DO52I=1,7
      WRITE(6,127) I,BMSW(I),CUR(I),I,DEFSW(I)
   52 CONTINUE
      DO53I=1,3
      I7=I&7
      WRITE(6,128) I7,BMSW(I7),CUR(I7)
   53 CONTINUE
      I=11
      WRITE(6,129) I,BMSW(I),CUR(I)
      I=12
      WRITE(6,128) I,BMSW(I),CUR(I)
      I=13
      YECHT=0.
      WRITE(6,130) I,BMSW(I),CUR(I),YECHT
      I=14
      WRITE(6,131) I,BMSW(I),CUR(I),YECHT
      DO57I=1,3
      I14=I&14
      WRITE(6,128) I14,BMSW(I14),CUR(I14)
   57 CONTINUE
      I=18
      WRITE(6,132) I,BMSW(I),CUR(I)
      I=19
      WRITE(6,128) I,BMSW(I),CUR(I)
      I=20.
      WRITE(6,133) I,BMSW(I),CUR(I),YECHT
      I=21
      WRITE(6,134) I,BMSW(I),CUR(I),YECHT
      I=22
      WRITE(6,135) I,BMSW(I),CUR(I),YECHT
      KLUB=1
C     LOAD STAGE 1
  243 DO58I=1,22
      BMS(I)=BMS(I)&BMSW(I)
      DO58J=1,6
      DO58K=1,2
   58 AS(K,J,I)=AS(K,J,I)&DAS(K,J,I)
      DO59L=1,7
```



```
   59 DEFS(L)=DEFS(L)&DEFSW(L)
      DEFS(8)=0.
      DEFS(9)=0.
      DO60I=1,22
      CURV(I)=(AS(1,5,I)-AS(1,2,I))/(1000000.*(D-DD))
   60 CONTINUE
      DO61I=1,22
      DO61J=1,6
   61 AVS(J,I)=AS(1,J,I)
      LS=1
      PA=0.
      PS=0.
      PF=0.
      PD=0.
  246 WRITE(6,150) LS
  150 FORMAT(1H ,66X,11HLOAD STAGE ,I3/////)
      PUNCH 301,PA,AVS(2,13),AVS(5,13),LS
  301 FORMAT(1H ,F7.0,2F10.0,I3)
      WRITE(6,121)
      WRITE(6,122)
      WRITE(6,151)
  151 FORMAT(1H ,6HCOLUMN,21X,1H1,35X,1H3//)
      WRITE(6,152)
  152 FORMAT(1H ,13X,5HNORTH,7X,5HSOUTH,8X,3HAVE,8X,5HNORTH,7X,5HSOUTH,
     18X,3HAVE//)
      DO62I=1,22
      KTEMP(1)=AS(1,1,I)
      KTEMP(2)=AS(2,1,I)
      KTEMP(3)=AVS(1,I)
      KTEMP(4)=AS(1,3,I)
      KTEMP(5)=AS(2,3,I)
      KTEMP(6)=AVS(3,I)
      WRITE(6,124)I,(KTEMP(K),K=1,6)
   62 CONTINUE
      WRITE(6,153)
  153 FORMAT(1H ,///34X,10HROW NUMBER//)
      WRITE(6,154)
  154 FORMAT(1H ,6HCOLUMN,21X,1H2,35X,1H5//)
      WRITE(6,152)
      DO63I=1,22
      KTEMP(1)=AS(1,2,I)
      KTEMP(2)=AS(2,2,I)
      KTEMP(3)=AVS(2,I)
      KTEMP(4)=AS(1,5,I)
      KTEMP(5)=AS(2,5,I)
      KTEMP(6)=AVS(5,I)
      WRITE(6,124)I,(KTEMP(K),K=1,6)
   63 CONTINUE
      WRITE(6,153)
      WRITE(6,155)
  155 FORMAT(1H ,6HCOLUMN,21X,1H4,35X,1H6//)
      WRITE(6,152)
      DO 64I=1,22
      KTEMP(1)=AS(1,4,I)
```

```
      KTEMP(2)=AS(2,4,I)
      KTEMP(3)=AVS(4,I)
      KTEMP(4)=AS(1,6,I)
      KTEMP(5)=AS(2,6,I)
      KTEMP(6)=AVS(6,I)
      WRITE(6,124)I,(KTEMP(K),K=1,6)
   64 CONTINUE
      WRITE(6,125)
      WRITE(6,126)
      DO88I=1,7
      WRITE(6,127) I,BMS(I),CURV(I),I,DEFS(I)
   88 CONTINUE
      DO89I=1,3
      I7=I&7
      WRITE(6,128) I7,BMS(I7),CURV(I7)
   89 CONTINUE
      I=11
      WRITE(6,129) I,BMS(I),CURV(I)
      I=12
      WRITE(6,128) I,BMS(I),CURV(I)
      I=13
      WRITE(6,130) I,BMS(I),CURV(I),DEFS(8)
      I=14
      WRITE(6,131) I,BMS(I),CURV(I),DEFS(9)
      DO90I=1,3
      I14=I&14
      WRITE(6,128) I14,BMS(I14),CURV(I14)
   90 CONTINUE
      I=18
      WRITE(6,132) I,BMS(I),CURV(I)
      I=19
      WRITE(6,128) I,BMS(I),CURV(I)
      I=20
      WRITE(6,133) I,BMS(I),CURV(I),PS
      I=21
      WRITE(6,134) I,BMS(I),CURV(I),PF
      I=22
      WRITE(6,135) I,BMS(I),CURV(I),PD
      GO TO (244,245),KLUB
  244 KLUB=2
C     READ IN DATA SUBROUTINE (CONSTANT DATA)
      DO91I=1,NS
      READ(5,156)LS,TC(1,I,2),TC(2,I,2),TC(1,I,4),TC(2,I,4)
      IF(I-100)700,701,701
  701 LS=LS&100
  700 IF(I-LS)157,91,157
   91 CONTINUE
  156 FORMAT(I2,4(4X,F4.0))
      GO TO 92
  157 WRITE(6,158)
  158 FORMAT(1H ,33HTEMP CORRECTION DATA OUT OF ORDER)
      GO TO 99
   92 DO93I=1,NS
      TC(1,I,1)=0.
      TC(2,I,1)=0.
      TC(1,I,3)=0.
   93 TC(2,I,3)=0.
      CF(1,1)=0.
      CF(2,1)=0.
      CF(1,3)=0.
      CF(2,3)=0.
      READ(5,159) (CF(J,2),J=1,2),(CF(J,4),J=1,2)
  159 FORMAT(F5.3,3(4X,F5.3))
      DO205I=1,22
      IF(I-6)206,207,208
  206 ICF(I)=4
      GO TO 205
  207 ICF(I)=2
      GO TO 205
  208 IF(I-16)207,206,206
  205 CONTINUE
      IF(NDGC)177,178,177
  177 LS2=0
      DO179I=1,NDGC
      READ(5,180)LS1,DGC1(8),(DGC1(J),J=1,7),DGC1(9)
      IF(LS1-LS2)702,703,703
  702 LS1=LS1&100
  703 LS2=LS1
      DO 179 K=1,NS
      IF(K-LS1)179,181,181
  181 DO 182 L=1,9
      DGC(K,L)=DGC(K,L)&DGC1(L)
  182 CONTINUE
  179 CONTINUE
  180 FORMAT(I2,1X,9F7.0)
  178 DO98N=1,NS
      READ(5,249) LS,PS,DG(1,8),(DG(1,J),J=1,7),DG(1,9)
      READ(5,249) ICHT,PF,DG(2,8),(DG(2,J),J=1,7),DG(2,9)
  249 FORMAT(I2,1X,F6.0,9F7.0)
      IF(N-100)704,705,705
  705 LS=LS&100
  704 IF(N-1)99,251,254
  254 IF(KN-66)250,251,251
  250 IF(KN-46)252,251,253
  253 IF(KN-47)252,251,252
  252 DO255J=1,5
  255 READ(5,160)((DE(1,L,M,J),L=1,2),M=1,6)
      DO256J=21,22
  256 READ(5,160)((DE(1,L,M,J),L=1,2),M=1,6)
      DO257J=16,20
  257 READ(5,160)((DE(1,L,M,J),L=1,2),M=1,6)
      DO258J=6,15
  258 READ(5,160)((DE(1,L,M,J),L=1,2),M=1,6)
      IF(N-2)202,259,203
  259 DO260J=1,22
      DO260L=1,2
      DO260M=1,6
  260 DE(2,L,M,J)=0.
```

```
      DENOM=352.
      GO TO 203
  251 DO94J=1,5
      DO94K=1,2
      READ(5,160) ((DE(K,L,M,J),L=1,2),M=1,6)
   94 CONTINUE
  160 FORMAT(12F6.0)
      J=21
      DO95K=1,2
      READ(5,160) ((DE(K,L,M,J),L=1,2),M=1,6)
   95 CONTINUE
      J=22
      DO96K=1,2
      READ(5,160) ((DE(K,L,M,J),L=1,2),M=1,6)
   96 CONTINUE
      DO97J=1,5
      J15=J&15
      DO97K=1,2
      READ(5,160) ((DE(K,L,M,J15),L=1,2),M=1,6)
   97 CONTINUE
      DO201J=1,10
      J5=J&5
      DO201K=1,2
      READ(5,160) ((DE(K,L,M,J5),L=1,2),M=1,6)
  201 CONTINUE
      IF(N-1)99,202,203
  202 DO204J=1,22
      DO204K=1,6
      DO204M=1,2
      ZDE(M,K,J)=.5*(DE(1,M,K,J)&DE(2,M,K,J))-AS(M,K,J)/CF(M,ICF(J))
      KX=DE(1,M,K,J)-DE(2,M,K,J)
      IF(KX)3000,3001,3002
 3000 KX=-KX
      GO TO 3002
 3001 KDIFF(M,KX&1)=KDIFF(M,KX&1)&1
      GO TO 204
 3002 IF(KX-30)3001,3004,3004
 3004 KDIFF(M,31)=KDIFF(M,31)&1
  204 CONTINUE
      DO209J=1,9
      ZDG(J)=.5*(DG(1,J)&DG(2,J))&10000.*DEFS(J)
  209 CONTINUE
C     PROGRAM CHECK
C     PROGRAM CHECK
C     PROGRAM CHECK
C     IF THIS CARD INSERTED NO CHECK ON ZERO READINGS
      GO TO 98
C     DEFLECTIONS
  205 DO211J=1,9
      IF(DG(1,J))212,213,212
  212 IF(DG(2,J))214,215,214
  214 DEFS(J)=(ZDG(J)-.5*(DG(1,J)&DG(2,J))-DGC(N,J))/10000.
      GO TO 211
  215 DEFS(J)=(ZDG(J)-DG(1,J)-DGC(N,J))/10000.
      GO TO 211
  213 IF(DG(2,J))216,217,216
  216 DEFS(J)=(ZDG(J)-DG(2,J)-DGC(N,J))/10000.
      GO TO 211
  217 DEFS(J)=0.
  211 CONTINUE
      IF(PS)173,174,173
  174 PD=0.
      GO TO 175
  173 PD=100.*(1.-PF/PS)
  175 DO 218J=1,22
      DO218K=1,6
      DO228L=1,2
      IF(DE(1,L,K,J))248,219,248
  248 IF(DE(2,L,K,J))221,220,221
  221 AS(L,K,J)=CF(L,ICF(J))*(.5*(DE(1,L,K,J)&DE(2,L,K,J))-ZDE(L,K,J)-
     1TC(L,I,ICF(J)))
      GO TO 228
  220 AS(L,K,J)=CF(L,ICF(J))*(DE(1,L,K,J)-ZDE(L,K,J)-TC(L,I,ICF(J)))
      GO TO 228
  219 AS(L,K,J)=0.
  228 CONTINUE
      IF(AS(1,K,J))222,223,222
  222 IF(AS(2,K,J))224,225,224
  224 AVS(K,J)=.5*(AS(1,K,J)&AS(2,K,J))
      GO TO 218
  223 IF(AS(2,K,J))226,227,226
  225 AVS(K,J)=AS(1,K,J)
      GO TO 218
  226 AVS(K,J)=AS(2,K,J)
      GO TO 218
  227 AVS(K,J)=0.
  218 CONTINUE
C     CURVATURES
      DO229J=1,22
      IF(AVS(5,J))166,167,166
  166 IF(AVS(2,J))168,167,168
  167 CURV(J)=0.
      GO TO 229
  168 CURV(J)=(AVS(5,J)-AVS(2,J))/(1000000.*(D-DD))
  229 CONTINUE
      PA=.5*(PS&PF)
C     BENDING MOMENTS
      DO231J=1,10
      GO TO (232,233,234,235,236,237,238,239,240,241),J
  232 XSW=26.
  242 BMS(J)=BM1(J)&BMSW(J)&.5*PA*XSW/1000.
      BMS(21-J)=BMS(J)
      GO TO 231
  233 XSW=30.
      GO TO 242
  234 XSW=34.
      GO TO 242
  235 XSW=38.
```

```
      GO TO 242
  236 XSW=42.
      GO TO 242
  237 XSW=45.
      GO TO 242
  238 XSW=47.
      GO TO 242
  239 XSW=49.
      GO TO 242
  240 XSW=51.
      GO TO 242
  241 XSW=53.
      GO TO 242
  231 CONTINUE
      BMS(21)=BM1(21)&BMSW(21)&25.*PA/1000.
      BMS(22)=BMS(21)
      GO TO 246
  245 CONTINUE
   98 CONTINUE
   99 CONTINUE
  764 FORMAT(1H ,21HNORTH READER SIDE 1  ,5A4)
  765 FORMAT(1H ,21HSOUTH READER SIDE 2  ,5A4//////)
      WRITE(6,3100)
 3100 FORMAT(1H1,64X,16HREADINGS QUALITY//////)
      WRITE(6,3101)GUFF1,GUFF2
 3101 FORMAT(1H ,11HDIFFERENCES,6X,5A4,6X,5A4///)
      DO3102M=1,30
      MM1=M-1
      WRITE(6,3105)MM1,(KDIFF(J,M),J=1,2)
 3102 CONTINUE
 3105 FORMAT(1H ,4X,I3,14X,I4,21X,I4)
      WRITE(6,3106)(KDIFF(J,31),J=1,2)
 3106 FORMAT(1H ,4X,10H30 OR MORE,7X,I4,21X,I4)
      DO3200J=1,2
      KFACT=0
      DO3201M=1,31
      KFACT=KFACT&(M-1)*KDIFF(J,M)*KDIFF(J,M)
 3201 CONTINUE
      FACT=KFACT
      SD(J)=SQRT(FACT/DENOM)
 3200 CONTINUE
      WRITE(6,3202)(SD(J),J=1,2)
 3202 FORMAT(1H1,7HSTD DEV,13X,F6.3,19X,F6.3)
  121 FORMAT(1H ,33X,12HMICROSTRAINS///)
  122 FORMAT(1H ,34X,10HROW NUMBER//)
  123 FORMAT(1H ,6HCOLUMN,9X,1H1,11X,1H2,11X,1H3,11X,1H4,11X,1H5,11X,1H6
     1//)
  124 FORMAT(1H ,I4,3X,6I12)
  125 FORMAT(1H ,////34X,10HOTHER DATA///)
  126 FORMAT(1H ,6HCOLUMN,5X,6HMOMENT,9X,4HCURV,17X,4HPOSN,7X,5HDEFLN//)
  127 FORMAT(1H ,2X,I2,6X,F8.3,6X,F9.6,16X,I2,6X,F9.6)
  128 FORMAT(1H ,2X,I2,6X,F8.3,6X,F9.6)
  129 FORMAT(1H ,2X,I2,6X,F8.3,6X,F9.6,15X,15HLONGIT MOVEMENT)
  130 FORMAT(1H ,2X,I2,6X,F8.3,6X,F9.6,15X,4HWEST,5X,F9.6)
```



```
  131 FORMAT(1H ,2X,I2,6X,F8.3,6X,F9.6,15X,4HEAST,5X,F9.6)
  132 FORMAT(1H ,2X,I2,6X,F8.3,6X,F9.6,21X,4HLOAD)
  133 FORMAT(1H ,2X,I2,6X,F8.3,6X,F9.6,15X,5HSTART,7X,F6.0)
  134 FORMAT(1H ,2X,I2,6X,F8.3,6X,F9.6,15X,6HFINISH,6X,F6.0)
  135 FORMAT(1H ,2X,I2,6X,F8.3,6X,F9.6,15X,9H(AGE DROP,4X,F5.2//////)
      END
```

PROGRAM 7.3 'INCLINO'

```
C     ************************************************************************
C
C     INCLINOMETER READINGS REDUCTION
C
C     ************************************************************************
      DIMENSION RDG(4),ZRDG(4),DIFF(4),RAD(4),K1(4),K2(4),K3(4)
      PI=3.1415927
      READ(5,100) KN,NR
  100 FORMAT(I2,I3)
      WRITE(6,101) KN
  101 FORMAT(1H1,43X,30HINCLINOMETER READINGS FOR BEAM,I3)
      WRITE(6,102)
  102 FORMAT(1H1,2HLS,10X,11HLOCATION  1,18X,11HLOCATION  2,18X,11HLOCAT
     1ION  3,18X,11HLOCATION  4////)
      WRITE(6,103)
      DO20I=1,NR
      READ(5,104) LS,(RDG(N),N=1,4)
      IF(I-1)20,1,2
    1 DO12N=1,4
      ZRDG(N)=RDG(N)
      RAD(N)=0.
      K1(N)=0
      K2(N)=0
   12 K3(N)=0
      GO TO 13
    2 DO3N=1,4
      IF(RDG(N))6,7,6
    7 RAD(N)=9999999.
      K1(N)=99999
      K2(N)=99999
      K3(N)=99999
      GO TO 3
    6 DIFF(N)=RDG(N)-ZRDG(N)
      RAD(N)=DIFF(N)/3.
      DEG=RAD(N)*180./PI
      K1(N)=DEG
      TEMP=K1(N)
      AMIN=(DEG-TEMP)*60.
      IF(AMIN)4,5,5
    4 AMIN=-AMIN
    5 K2(N)=AMIN
      TEMP=K2(N)
      SEC=(AMIN-TEMP)*60.
      K3(N)=SEC
    3 CONTINUE
   13 WRITE(6,105) LS,((RDG(N),RAD(N),K1(N),K2(N),K3(N)),N=1,4)
   20 CONTINUE
  103 FORMAT(1H ,4(5X,3HRDG,6X,3HRAD,7X,5HANGLE)///)
  104 FORMAT(I2,4F6.4)
105   FORMAT(1H ,I2,4(F7.4,3X,F7.4,2X,I3,I3,I3,2X))
      END
```

PROGRAM 7.4 'DATALIST'

```
C     ************************************************************************
C
C     PROGRAM FOR DATA PRINT-OUT
C
C     ************************************************************************
      DIMENSION GUFF1(5),GUFF2(5),GUFF3(4),GUFF(20)
      READ(5,100) KODE,ICHT1
  100 FORMAT(I1,78X,I1)
      READ(5,101) GUFF1,ICHT2
      READ(5,101) GUFF2,ICHT3
  101 FORMAT(5A4,59X,I1)
      READ(5,102)KN,NS,GUFF3,NDGC,ICHT4
  102 FORMAT(I2,I4,4A4,I3,52X,I3)
      WRITE(6,103) KN
  103 FORMAT(1H1,29X,21HINPUT DATA FOR BEAM  ,I3)
      WRITE(6,104)
  104 FORMAT(1H1,12HGENERAL DATA///)
      WRITE(6,105) KODE,ICHT1
  105 FORMAT(1H ,I1,78X,I1)
      WRITE(6,106) GUFF1,ICHT2
      WRITE(6,106) GUFF2,ICHT3
      WRITE(6,120)KN,NS,GUFF3,NDGC,ICHT4
  120 FORMAT(1H ,I2,I4,4A4,I3,53X,I2)
  106 FORMAT(1H ,5A4,59X,I1)
      DO1I=1,3
      READ(5,107) GUFF
      WRITE(6,108) GUFF
    1 CONTINUE
  107 FORMAT(20A4)
  108 FORMAT(1H ,20A4)
      WRITE(6,409)
  409 FORMAT(1H1,23HTEMPERATURE CORRECTIONS///)
      DO2I=1,NS
      READ(5,107) GUFF
      WRITE(6,108) GUFF
    2 CONTINUE
      WRITE(6,109)
  109 FORMAT(1H1,19HCALIBRATION FACTORS///)
      READ(5,107) GUFF
      WRITE(6,108) GUFF
      IF(NDGC)4,4,3
    3 WRITE(6,110)
  110 FORMAT(1H1,22HDIAL GAUGE CORRECTIONS///)
      DO5I=1,NDGC
      READ(5,107) GUFF
      WRITE(6,108) GUFF
    5 CONTINUE
    4 WRITE(6,111)
  111 FORMAT(1H1,21HLOADS AND DIAL GAUGES///)
      N=2*NS
      DO6I=1,N
      READ(5,107) GUFF
      WRITE(6,108) GUFF
    6 CONTINUE
```

```
      IF(KN-66)11,12,12
11    IF(KN-46)16,12,17
17    IF(KN-47)16,12,16
16    N=1&NS
12    DO 7I=1,5
      WRITE(6,112) I
      DO 7J=1,N
      READ(5,107) GUFF
      WRITE(6,108) GUFF
    7 CONTINUE
  112 FORMAT(1H1,6HCOLUMN,I4///)
      DO8I=1,2
      I20=I&20
      WRITE(6,112) I20
      DO 8J=1,N
      READ(5,107) GUFF
      WRITE(6,108) GUFF
    8 CONTINUE
      DO9I=1,5
      I15=I&15
      WRITE(6,112) I15
      DO 9J=1,N
      READ(5,107) GUFF
      WRITE(6,108) GUFF
    9 CONTINUE
      DO10I=1,10
      I5=I&5
      WRITE(6,112) I5
      DO10J=1,N
      READ(5,107) GUFF
      WRITE(6,108) GUFF
   10 CONTINUE
      END
```

APPENDIX C

MATERIALS, EQUIPMENT AND TESTING PROCEDURE FOR BAUSCHINGER EFFECT

C.1 TEST SPECIMENS

Deformed, structural-grade reinforcing steel of $\frac{1}{2}$", $\frac{5}{8}$", $\frac{3}{4}$", and $\frac{7}{8}$" diameters was used for these experiments and machined as shown in Figure C.1. The diameter of the reduced section of the specimens was 0.25" for $\frac{1}{2}$" and $\frac{5}{8}$" diameter bars and 0.50" for other sizes. Corresponding thread sizes were $\frac{3}{8}$" N.F. and $\frac{5}{8}$" N.F. respectively.

The specimens were screwed into circular end plates, and clamp plates which were recessed to the diameter of the end plates, were then bolted to the base plate and bottom loading plate, as shown in Plate C.1.

Yield and ultimate stresses, as obtained from the machined gauge length, are listed in Table D.1.

C.2 TESTING EQUIPMENT AND PROCEDURE

C.2.1 Loading Frame

The loading frame used for these tests is shown in Plate C.2.

Design of the loading frame was based on the need for

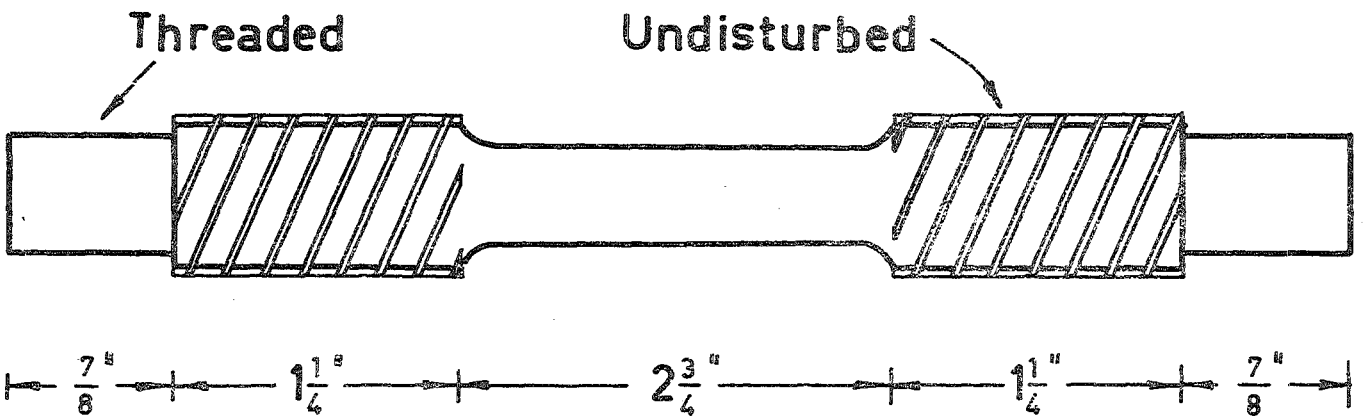

FIG.C.1 - BAUSCHINGER TEST SPECIMEN

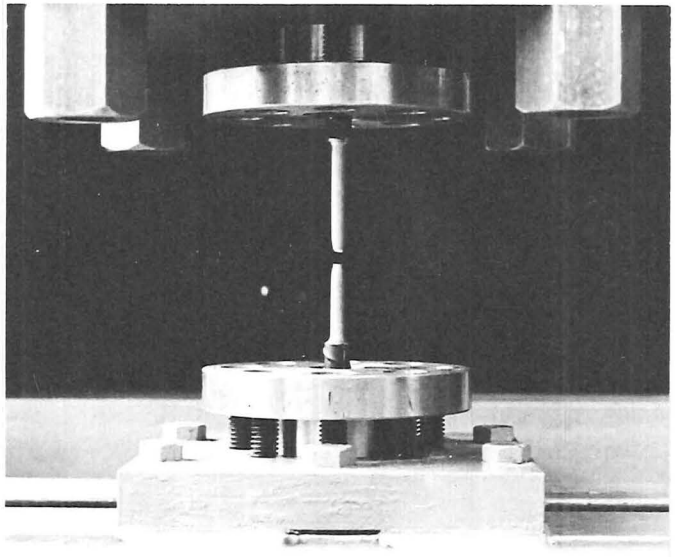

PLATE C1 - SPECIMEN MOUNTING

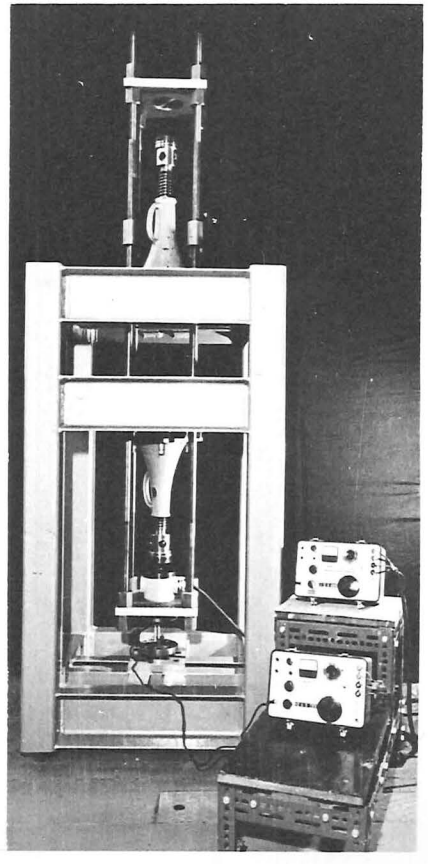

PLATE C2 - BAUSCHINGER TEST RIG

rigidity, and stresses in the components during load application were very low. Considerable care was taken with the construction of the frame to ensure that friction between hanger rods and the frame, and eccentricity of loading did not become significant during loading of the specimens. Despite this, difficulties were experienced with eccentricity during compression loading of some early specimens.

C.2.2 Load Application and Measurement

Load was applied by means of screw jacks as their use afforded strain control when loading into the plastic range. Compression load was applied directly to the specimen using the bottom jack, and tension was applied by activating the top jack and so transferring the stress through the four hanger rods.

The load was measured with Type PR9226, Philips 5-ton or 2-ton load cells, depending on the specimen size. The cells were calibrated on an Avery 25,000 lb Universal Testing Machine through a Budd Strain Bridge. The gauge factor on the bridge was selected as that which gave 1 microstrain reading for each 1 lb. load applied to the cell. Repeatable results were obtained from several trials. Recesses were provided in the top and bottom loading plates to maintain concentricity of loading.

A thrust bearing between the screw jack and load cell took up the rotation in the jack.

C.2.3 Loading Sequence

No fixed loading sequence was observed, the aim being to study as many factors as possible (e.g. unloading and reloading from compression and tension stresses after the Bauschinger Effect had been initiated). Also a large range of initial plastic strains was required for the analyses described in Chapter 3.

From the initial tests, it was noted that the machine behaved more accurately if the hanger system was aligned by yielding the specimen in tension first. Consequently, very few specimens were studied in which compression caused first yield. Also the behaviour of the machine was such that unloading characteristics could not be observed. This was probably due to friction in the frame and satisfactory results were obtained only when an increasing stress was being applied to the specimen. Indications were, however (Chapter 3), that the unloading behaviour of the steel was elastic with a modulus approximately equal to the initial elastic slope.

C.2.4 Specimen Yield Stresses

It was observed that yield stresses obtained using mechanical jacks were consistently 3,000 - 5,000 p.s.i. lower than those obtained on machined specimens from the same reinforcing bar but using an Avery hydraulic testing machine (Table D.1). The ultimate stresses, by comparison, were almost identical. That the yield points were not

distinct indicates that this may have been due to eccentricity of loading.

C.3 STRAIN MEASUREMENT

Strain was measured with an Instron G-51-14 strain-gauge extensometer which has a 2" gauge length and 50 per cent maximum strain. This extensometer was calibrated to a Budd Strain Bridge using a micrometer device. A very low gauge factor on the bridge enabled strain measurements of 1 microstrain to be obtained. However, the accuacy of these measurements was reflected in standard deviations which ranged between 31 and 167 microstrains.

As provision for compression strain was necessary, the extensometer was mounted on the specimen such that the initial gauge length was greater than 2". Coupled with this, the extensometer was mounted when an initial strain of ϵ_1 was imposed in the specimen by the hanger weight. Therefore the extensometer readings obtained directly from the bridge had to be corrected for these factors. The correction procedure was as follows:

The extensometer was mounted on the specimen with a distance between points of $(2 + x)$ inches. The initial strain reading, ϵ_o, will be $x/2$ corresponding to an initial actual strain of ϵ_1, the strain induced by the weight of the hanger.

$$\therefore \epsilon_o = \frac{x}{2} \qquad \ldots\ldots(C.1)$$

For an elongation of y" in the specimen, and using the sign convention tension positive, then the resulting actual strain, ϵ_a, is given by:

$$\epsilon_a = \frac{y}{2 + x} + \epsilon_1 \qquad \ldots\ldots(C.2)$$

where ϵ_1 is negative in this case.

Also, the measured strain, ϵ_r, is:

$$\epsilon_r = \frac{x + y}{2} \qquad \ldots\ldots(C.3)$$

From Equation (C.1): $x = 2\epsilon_o$

and from Equation (C.3): $y = 2\epsilon_r - x = 2(\epsilon_r - \epsilon_o)$

$$\therefore \epsilon_a = \frac{\epsilon_r - \epsilon_o}{1 + \epsilon_o} + \epsilon_1 \qquad \ldots\ldots(C.4)$$

APPENDIX D

MATERIALS, EQUIPMENT AND TESTING PROCEDURE FOR REINFORCED CONCRETE BEAMS

D.1 MATERIALS

D.1.1 Concrete

A commercially-prepared mix with 3 per cent air-entrainment was supplied by Certified Concrete Limited, Christchurch, and was used for all beams of this series. The aggregate used was Waimakariri River gravel which is a well-rounded greywacke stone. The maximum aggregate size was $\frac{1}{2}$" and ordinary Portland Cement was used. The mix proportions by weight were:

Water : cement : aggregate = .53:1.0:5.8

It was anticipated that this mix would produce a 4,000 p.s.i. concrete at 28 days and would therefore be a typical construction concrete. In fact, cylinder tests carried out at the time of beam experiments (age 33-251 days), showed the mix to produce cylinder strengths ranging between 4,645 p.s.i., and 7,485 p.s.i.

Placing

Beams were poured in pairs and compacted on an "Allam"

vibrating table working at 3,000 c.p.m. Only one beam mould was mounted on the table at any one time and placement of concrete was usually completed within five minutes. Control specimens for each beam were also mounted on the table, therefore receiving vibration identical to that of the beam.

Thus two beams and associated control specimens were poured with the same mix.

Control Specimens

For each beam, three 6" cubes, three 6" diameter x 12" cylinders, and three 12" x 3" x 3" modulus of rupture prisms were cast in machined steel forms. These were tested immediately prior to the start of the beam experiment. The cylinders were capped at both ends with dental-quality plaster and loaded at 2,000 p.s.i./minute to failure. The cubes were uncapped and were loaded at the same rate. Modulus of rupture specimens were tested very slowly and were simply-supported over 9", point loads being applied 3" from the supports. Despite this, the variation in modulus of rupture values in any one batch was comparatively high.

For some beam pairs, a shrinkage control block, 24" x $8\frac{1}{2}$" x 5", was cast. Stainless steel discs for Demountable Mechanical (Demec) gauges[18] were inserted into these blocks as the concrete set and zero readings taken as soon as the concrete was sufficiently hardened. A 60" x 8" x 5" section of a test beam was used to provide temperature compensation for the shrinkage readings. Shrinkage control blocks were

cured in exactly the same way as the beams, being stripped and removed from the fog room at the same time.

The shrinkage tests did not prove very satisfactory qualitatively as the magnitudes of the shrinkage strains were not sufficiently large in comparison with the accuracy of the Demec gauges, and the magnitude of the Temperature corrections. The tests did show however, that little shrinkage took place whilst the concrete was in the fog-room, but that very large shrinkage strains occurred within the twelve hour period after removing the concrete from the fog-room. Figure D1 shows the results of one of these tests.

In addition to these control specimens, a further experiment was carried out on the concrete mix. Four cylinders were cast with each of three beams pairs, and tested at 7, 14, 28 and 90 days respectively. Demec readings were taken at equal intervals around the circumference of the cylinders on 4"-gauge lengths at midheight. The resulting stress-strain curves were compared with Ritter's parabola and it was verified that the stress-strain response of concrete up to maximum stress closely approximated a parabola.

Curing

Following concrete placement, the beams and control specimens were cured in a fog-room with a controlled atmosphere at 100 per cent relative humidity at a temperature of

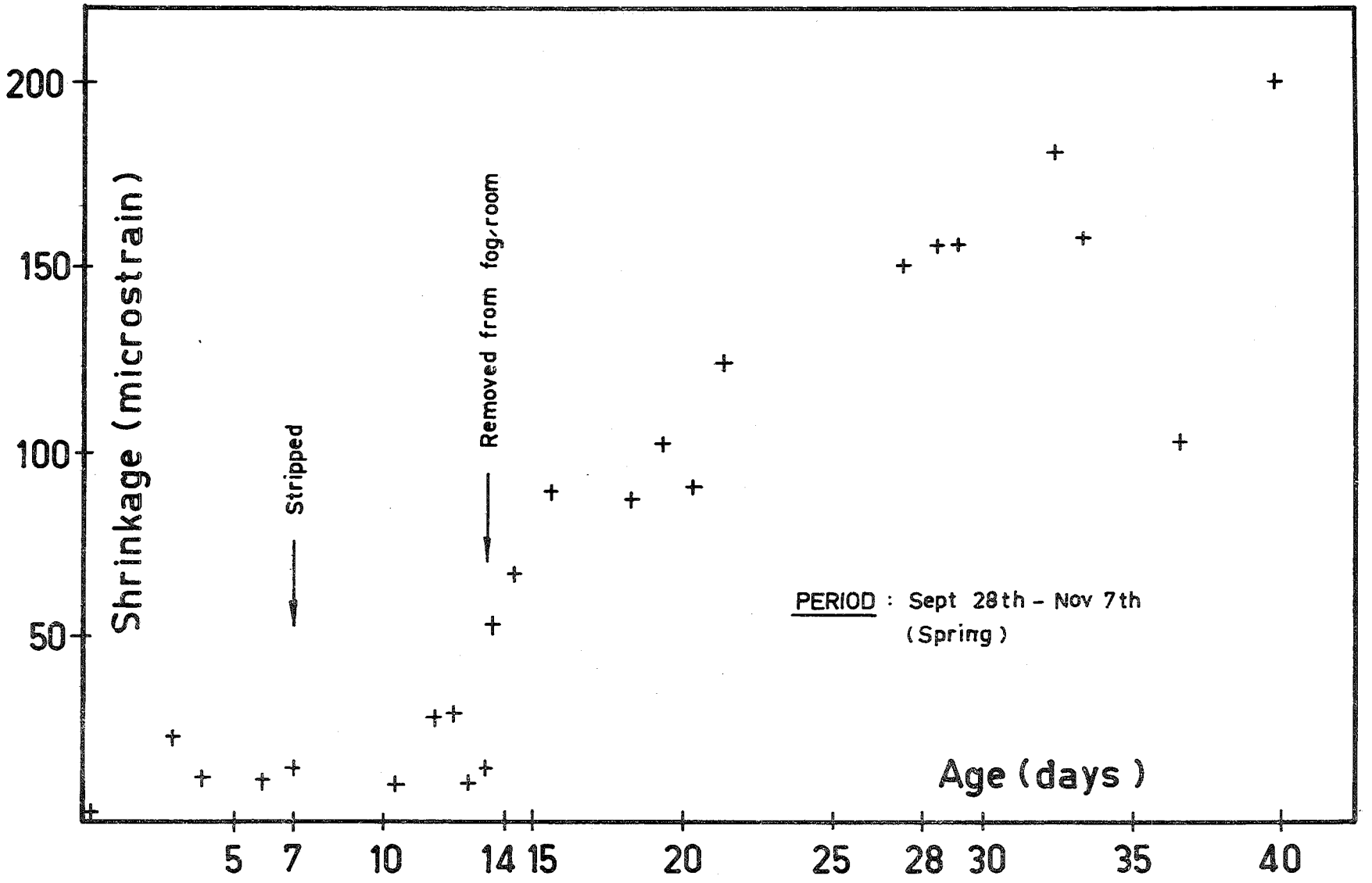

FIG. D.1 - SHRINKAGE STRAINS FOR BEAMS 66 & 67

68°F. Beams and specimens were stripped of their moulds seven days after pouring and remained in the fog-room for a further seven days. In the interval between fog curing and testing, the beams and control specimens were allowed to dry in the laboratory.

D.1.2 Steel

(i) Longitudinal beam steel

Deformed reinforcing steel of $\frac{1}{2}$", $\frac{5}{8}$", $\frac{3}{4}$" and $\frac{7}{8}$" diameters was used for longitudinal beam steel. The steel complies with A.S.T.M. A305-56T, NZSS 1963:1962, and C.P.114. Within all size groups, bars were from the same batch. Nevertheless, preliminary tests showed the variation of properties between bars within these groups to be too great to use this common feature with reliability. Each bar was cut into two 9' - 10" lengths for use in the beams and the remainder was used for control specimens and for Bauschinger tests.

$\frac{1}{2}$" diameter bars: From each $\frac{1}{2}$" diameter bar, three 10" specimens were tested undisturbed, using a Baty mechanical extensometer with a 2" gauge length. These tension tests gave yield and ultimate strengths for each bar, together with Young's Modulus, the strain hardening strain, and fracture strain. The average values of these parameters were used to describe the bar. Of all parameters, the ultimate stress showed the least variation from coupon to coupon.

$\frac{5}{8}$", $\frac{3}{4}$" and $\frac{7}{8}$" diameter bars: Each of the larger bars was subjected to two tests. Three specimens from each bar were tested undisturbed in tension to obtain the yield and ultimate forces. A further three specimens were machined and tested in tension according to ASTM A370-61T and extensometer readings recorded. These tests revealed slightly lower yield stresses for machined specimens than for undisturbed specimens and ultimate stresses that were rather higher.

The higher yield stresses observed in the undisturbed samples and the less distinct yield point, was attributed to the case hardening associated with forming the deformations. By assuming that this effect became negligible at ultimate load, it was possible to obtain the "effective" areas of the deformed bars by comparing ultimate loads for undisturbed and machined specimens. These effective areas were found to be 94 per cent, 95 per cent, $93\frac{1}{2}$ per cent, and $95\frac{1}{2}$ per cent, respectively, of the nominal areas of the $\frac{1}{2}$", $\frac{5}{8}$", $\frac{3}{4}$" and $\frac{7}{8}$" diameter bars. More precise measurements of similar deformed bars have been made at this University and produce areas that agree within 2 per cent to those above, thus confirming to some extent anyway, the case-hardening assumption. Yield and ultimate stresses for the beam steel were computed from undisturbed yield and ultimate loads and effective areas. Table D1 summarises

TABLE D.1

STEEL PROPERTIES

Nom. Dia.	Bar Number	Undisturbed F_u (lb)	Undisturbed F_y (lb)	A.S.T.M. Test f_u (p.s.i.)	A.S.T.M. Test f_y (p.s.i.)	Bauschinger Test f_u (p.s.i.)	Bauschinger Test f_y (p.s.i.)	$A_{eff} = \frac{F_u}{f_u}$ (sq.in.)	Undisturbed f_u (p.s.i.)	Undisturbed f_y (p.s.i.)
$\frac{1}{2}$"	6	12808	8892			**	45320		68950	47700
	7	12898	8942						69950	48450
	8	12710	8835			**	45570		69000	47950
	9	12930	8825			**	44760		70050	47900
	10	12853	9087			**	44210		69700	49200
	11	12813	8900			70000	46290	.1830	69600	48250
	12	12700	8800			69000	48100	.1841	68950	47700
	13	12865	9017			70200	48750	.1833	69950	48800
	14	12980	8967			70200	45980	.1849	70500	48650
	16	12857	8867			**	48420		69700	48050
	17	12868	8883			69100	47630	.1862	69850	48050
	18	12849	8817			**	51240		69700	47800
	20	12643	8767			**	48030		68500	47500
$\frac{5}{8}$"	21	20373	14300	69950	48250	70500	43860	.2908	70000	49100
$\frac{3}{4}$"	25	28983	19333	68450	46000	**	42530*		70200	47000
	26	28067	18817	66950	44200	68000	41590	.4128	67900	45700
	27	27850	19083	66450	45050	67700	41660	.4144	67600	46200
$\frac{7}{8}$"	29	41133	26467	71500	47200	71450	42700	.5757	71700	46100
	30	40617	26300	70550	45500	**	42360*		70950	45800
	31	40817	26900	71100	46150				71200	47000

** Buckling failure; * Compression yield.

Notes:
1. Undisturbed F_u and F_y, and A.S.T.M. f_u and f_y are average values from three coupons.
2. Effective areas are found from undisturbed F_u and Bauschinger Test f_u.
3. Undisturbed f_u and f_y values are obtained from undisturbed F_u and F_y and average effective areas.

the properties of the longitudinal reinforcing steels used in these experiments.

(ii) Stirrup Steel

Plain $\frac{1}{4}$" diameter reinforcing steel was used for all stirrups in this investigation. From each length of steel, three 10" specimens were cut and tension-tested for yield and ultimate stresses. The remainder of each bar was made into about 16 stirrups, bundled and numbered. All stirrups were manufactured and coupons tested before any beams were made so that, for beams requiring more than one bundle of stirrups, yield stresses of bundles could be matched. However, this was proved an unnecessary precaution as the first 8 stirrups on each side of the column stub were from the same bundle, and it was in this region that uniformity was most important.

D.2 BEAM MANUFACTURE

D.2.1 Manufacture of Reinforcing Cages

As mentioned in Chapter 7, it was very important that reliable steel strains be obtained from the experiments and to facilitate this, metal lugs were spot-welded to all longitudinal reinforcing bars so that strain measurements could be made. The lugs were of $\frac{1}{4}$" diameter mild steel cut to 1" lengths and twenty-one were required for each bar. As the lugs were difficult to handle and as they had to be welded in place accurately, a jig was manufactured to simplify

this operation.

The jig consisted of a length of angle section welded to a steel base plate, such that a cradle for the longitudinal bars was formed. A top plate had $\frac{1}{4}$" diameter holes drilled corresponding to the required lug positions and each hole was provided with a screw so that the lugs could be held firmly in the top plate. The top and bottom plates were then clamped together and the lugs spot-welded to the reinforcing bar rib as illustrated in Plate D1.

The beam having a comparatively small cross-section, necessitated accurately-made stirrups, and since a large number were required, a special stirrup-bender was made for the purpose (Plate D2). Five adjustable levers on a cross bar proved very satisfactory for determining bending points and after a few trials and minor adjustments to the position of these levers, stirrups could be quickly and accurately produced. The bending radius was only $\frac{3}{8}$" since it was desired that $\frac{1}{2}$" diameter longitudinal bars fit snugly into the corners. Despite this, no stirrup distress resulted from the small radius in any beam sections at failure. Internal stirrup dimensions were 3" x 6", giving 1" cover to all longitudinal steel.

The stirrups and longitudinal steel were then tied together, rather than welded, as this is the more common procedure in practice. Metal straps that fitted over the

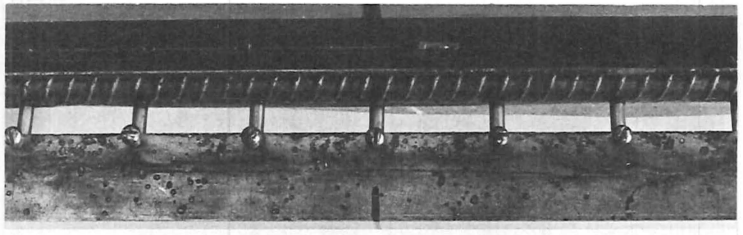

PLATE D1 - JIG FOR STRAIN LUGS

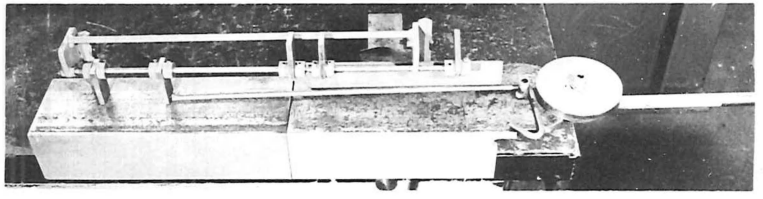

PLATE D2 - STIRRUP BENDER

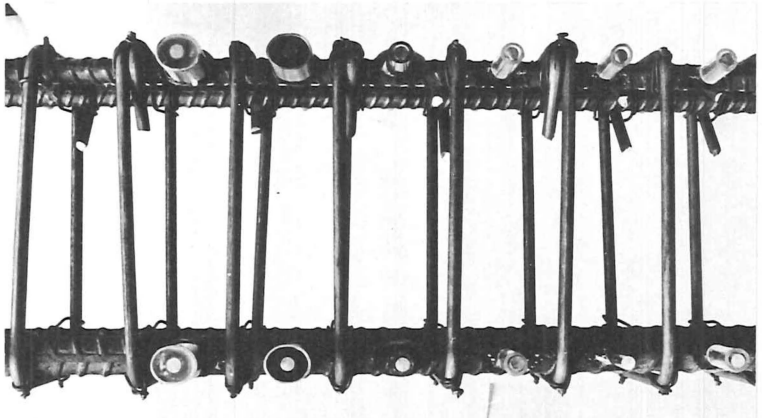

PLATE D4 - LUG WATERPROOFING

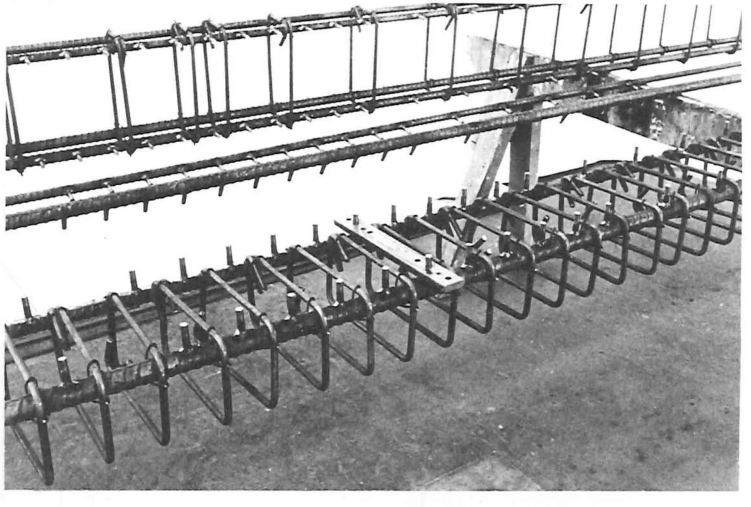

PLATE D3 - REINFORCING CAGES

lugs (Plate D3) ensured that spacing between top and bottom steel was correct and that lugs were perpendicular to the sides of the beam and therefore perpendicular to the plane of bending. All stirrup hooks were attached to the top steel and alternated between each top bar.

The final stage in the preparation of the reinforcing cage involved removing surplus welding metal from the bars and preparing the strain gauge lugs for waterproofing. $\frac{3}{4}$" metal tubes were squashed elliptical to $\frac{1}{2}$" minimum diameter and affixed to the main bars with "Mastik", a plastic, waterproof material. The tubes were so placed that each enclosed a lug and so that the maximum diameter was parallel to the bar. The lugs were then sheathed with polythene tubing and the tubes filled with wax to prevent cement entering. A pilot beam, using plain reinforcing steel, indicated that allowance for relative movement of steel to concrete should be made; hence the elliptical tubes. All beams in this investigation, however, used deformed bars and no slip was observed. The tubes were sufficiently thick to transfer concrete forces across the core holes formed.

Plate D4 illustrates the various phases of this operation.

When preparing the beam for testing, it was a simple matter to remove the wax and polythene tubing from the core holes. The lugs worked extremely well and no problems

were encountered.

Plate D5 shows the Beam 26 reinforcing cage in the mould prior to pouring.

D.2.2 Beam Moulds

Two identical steel beam moulds were constructed. The beams were 10' - 0" x 8" x 4 15/16" with a central 20" x 8" x 4 15/16" column stub. The form for the base and ends of the beam was 5" x $2\frac{1}{2}$" channel, which after cleaning and grinding, was reduced in width to 4 15/16". The sides of the mould, which were bolted to the channel, were of $\frac{1}{4}$" plate stiffened by 2" x 2" angle welded near the top surface.

The box for the central column stub posed some problems as, initially it was intended to use a 9"-wide column stub. 9" x 3" channel was used and 4 15/16"-wide slots cut to allow the mould to be moved over the beam shanks when being stripped. $\frac{1}{4}$" plates formed the sides of the stub. A pilot test showed that the most valuable data was at the stub face. Since the stub was wider than the beam this data was difficult to obtain, so 2" timber fillers were screwed to the $\frac{1}{4}$" side plates to reduce the stub width to that of the beam.

As provision for a stub meant that the bottom of the mould was not flat, it was necessary to provide the moulds with "feet". These were placed such that deflections in

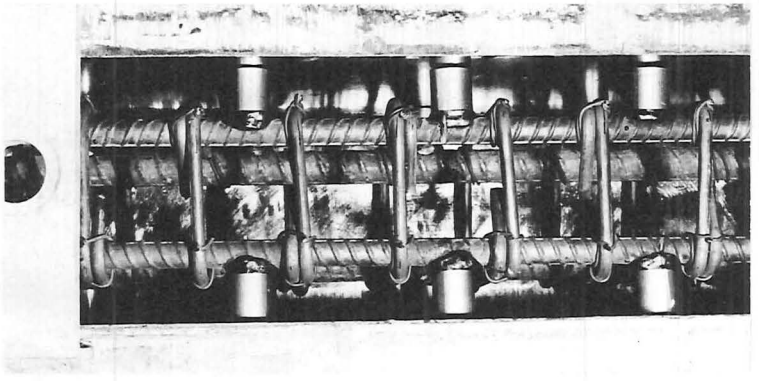

PLATE D5 - CAGE IN PLACE IN MOULD

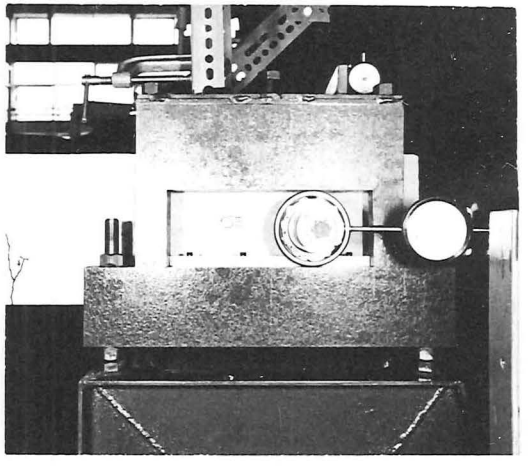

PLATE D8 - END SUPPORT

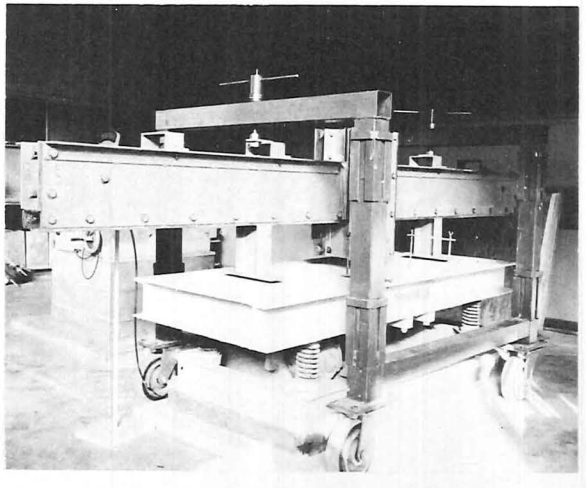

PLATE D6 - BEAM TRANSPORTATION

the mould would be minimal when filled with wet concrete. Again, this was probably an unnecessary precaution as deformations of the order of only 0.0001" were involved. The feet were drilled with holes so that the moulds could be bolted to the vibrating table.

Before assembling the moulds, the concrete-forming surfaces were given two thin coats of clear varnish. Following mould assembly, all joints were taped with PVC electrical tape and the surfaces given a light coat of mould oil using a soft cloth. This procedure prevented leakage and provided a very good finish to beam surfaces.

D.2.3 Transporting the Beams

The usual practice of moving beams and beam moulds with rollers could not be applied to these beams owing to the protruding column stub. A special gantry trolley was made for the purpose of moving the beams either with or without moulds, in places where other means were not available.

The trolley is illustrated in Plate D6.

D.3 TESTING EQUIPMENT AND PROCEDURE

D.3.1 Loading Frame

The design of the loading frame was based on minimum deformations and most components were subjected to stresses of less than 5,000 p.s.i. under the worst conditions of loading. Deflection measurements performed during a

preliminary test showed the frame to be very rigid.

The loading frame is shown in Plate D7.

D.3.2 Load Application and Measurement

Load was applied to the top and bottom of the column stub by means of screw jacks. These were considered more suitable than hydraulic jacks as deflection control was possible when loading into the plastic range. Further, by applying constant deflections instead of constant load, the creep occurred mainly in the magnitude of load, rather than in all the strain and deflection readings.

The load was measured with a Philips 5-ton load cell, type PR9226, which was situated between the screw jack and the column stub. $\frac{1}{2}$" steel plates were plastered to the top and bottom of the column stub and these were provided with $\frac{1}{8}$" deep seats for the load cell.

The load cell was calibrated on an Avery 25,000 lb Universal Testing Machine with a Budd Strain Bridge. The gauge factor on the bridge was selected as that which gave 1 microstrain reading for each 1 lb load applied to the cell. Repeatable results were obtained from several trials.

A thrust bearing between the screw jack and the load cell took up the rotation in the screw jack.

D.3.3 Support Conditions

As the beams were to be loaded cyclically, it was necessary to provide for both upward and downward reaction

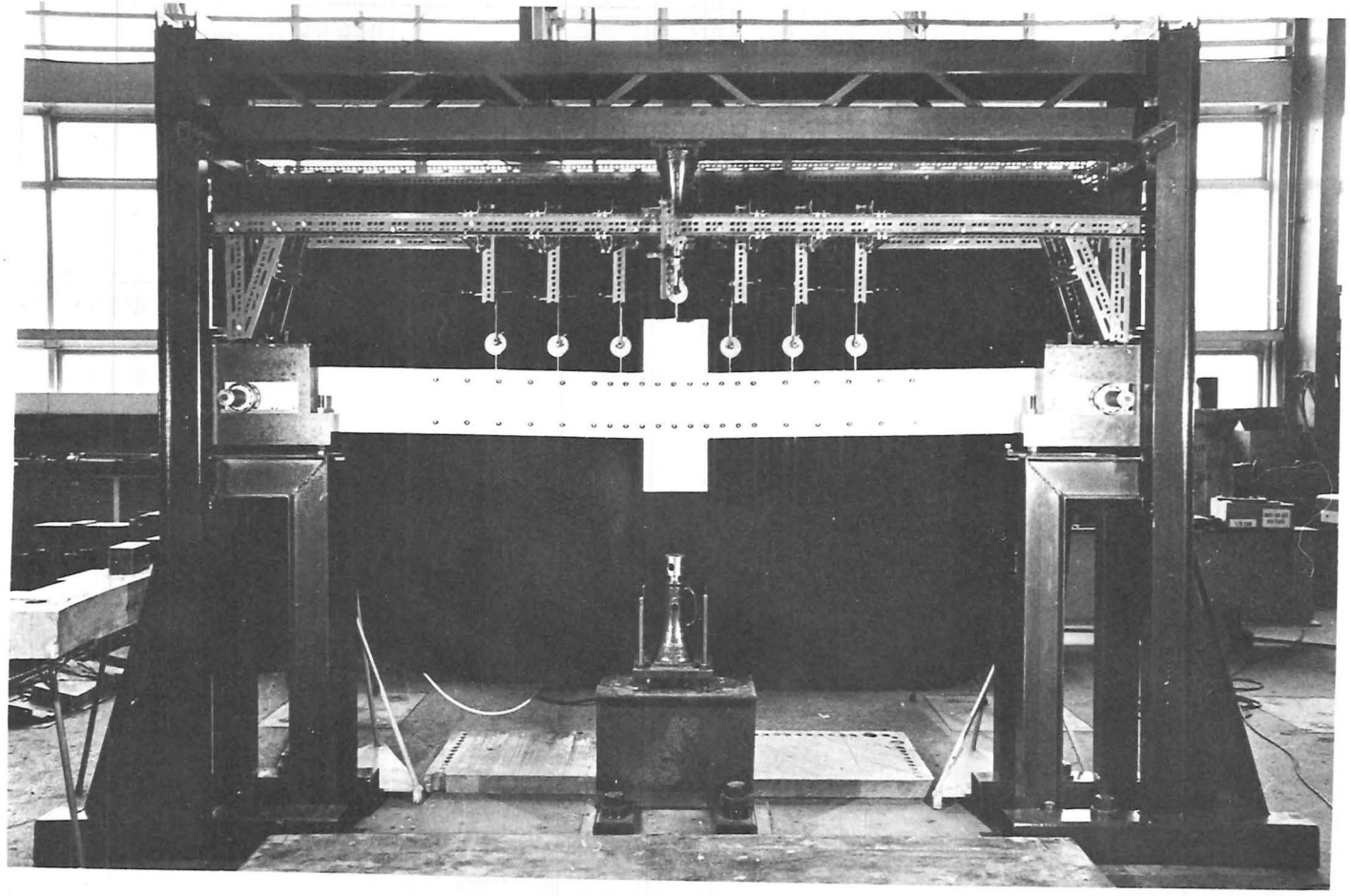

PLATE D7 - LOADING FRAME

at the end supports, and to allow longitudinal movement of the beam. To facilitate this, rather complex end supports were required.

The beams were cast with steel tubes at beam mid-depth and centred 6" from the ends of the beam. These tubes were machined to 2" diameter inside and were carefully sealed and waterproofed to prevent concrete intrusion during and subsequent to pouring. $\frac{1}{2}$" x 2" diameter steel plates were placed at the open ends of the tubes, and these and the mould sides were drilled so that a bolt located the tubes correctly in the beam mould. Each tube was spot-welded to stirrups on each side.

During testing, axles were inserted into the tubes and grubber screws locked these in place. The axle diameter was reduced to $1\frac{1}{2}$" at 2" from the beam sides, and roller bearings fitted on to the ends of these axles. The bearings fitted neatly into a milled groove in the rigid support box. Although the locating bolts kept the tubes placed in the beam during pouring, it was found necessary to alter slightly the relative position of the support boxes for each beam in order to avoid torsion at testing, and the position of these boxes was made adjustable. Plate D8 illustrates one of the end supports.

D.3.4 Crack Detection

Prior to testing, each beam was white-washed to simplify crack-detection. At each load increment cracks were observed

with x5 magnification hand microscopes, and marked with a felt-tipped pen to give better definition on the photographs. Cracks were marked on only one side of each beam, the other being left unmarked so that visual assessment of damage was not impaired.

D.3.5 Steel and Concrete Strain Readings

Steel and concrete strains were measured on each side of the beam by means of Demountable Mechanical (Demec) gauges. These gauges have a large strain range and are known to work reliably under cyclic straining (c.f. E.R.S.G.). For all beams, columns of 2" gauge length covered the central 20" of the beam and outside these were five 4"-gauge lengths.

The strains were measured between stainless steel discs drilled with a No. 60 hole and fixed to the steel lugs and concrete with sealing wax. In the first few beams tested, each column of gauge lengths had 6 rows; concrete gauge points being placed $\frac{3}{4}$" above and below each of the steel gauge points. These concrete gauges were later found to be of little value following cyclic loading, and only the rows near the top and bottom of the beam were retained. Concrete strains were read only when that face was in compression.

As two of the 2" gauge lengths had their common disc right at the beam-stub joint, measurements with a 4" Demec

gauge were made over the pair since it was felt that these common discs would drop off soon after cracking and valuable readings would be lost. In most cases, however, this did not eventuate and, as mentioned above, the concrete gauges did not provide any useful data anyway.

A beam shank from a test beam was supported on rollers and used to provide temperature compensation readings for the Demec gauges. Corrections as high as 215 microstrains were recorded.

Strains were measured on both sides of the beam and temperature corrected readings averaged to obtain curvatures. Variations in strain reading from one side of the beam to the other were very low until steel yield occurred. At this stage, steel in one side of the beam would usually deform more than that on the other. However, at yield the stresses were independent of strain and on reversal, the difference in strain from the unloading point was more important than absolute strain, and so it can be assumed that steel stresses were approximately equal.

The gauge positions and all other instrumentation is illustrated schematically in Figure D2.

D.3.6 Deflection

Nine 2"-travel, 0.001" dial gauges were mounted to obtain deflection readings. Two of these were used to measure the longitudinal movement of the beam and were mounted off heavy steel stands; the foot of each gauge being in contact with

the axle. The remaining seven dial gauges provided actual beam deflections and were affixed to a rigid "Dexion" frame which was securely attached to the end support boxes, thus giving deflections relative to the pinned end supports. A calculation showed the deformation in the box to be negligible and the neat fit of the roller bearings in their boxes provided continuity of deflection readings for both upward and downward loading. Of these seven dial gauges, one was seated on the loading plate at the top of the column stub and the others were seated on aluminium strips glued to the top surface of the beam. Therefore deflections were obtained at three points on each beam shank. The placing of these six dial gauges varied from beam to beam and the exact positions are shown in Table D2 and Figure D2.

D.3.7 Rotations

In addition to the nine dial gauges, four inclinometer stations were provided to give rotations at selected points. Two of these were at the top and bottom loading plates on the stub while the others were centred 18" from the free ends of the beam. The beam inclinometer readings could be used to provide additional deflection values as, being situated 12" from the support, the beams were still exhibiting elastic behaviour at these stations.

As mentioned in Chapter 7, the asymmetrical behaviour of these beams resulted in rotation of the column stub.

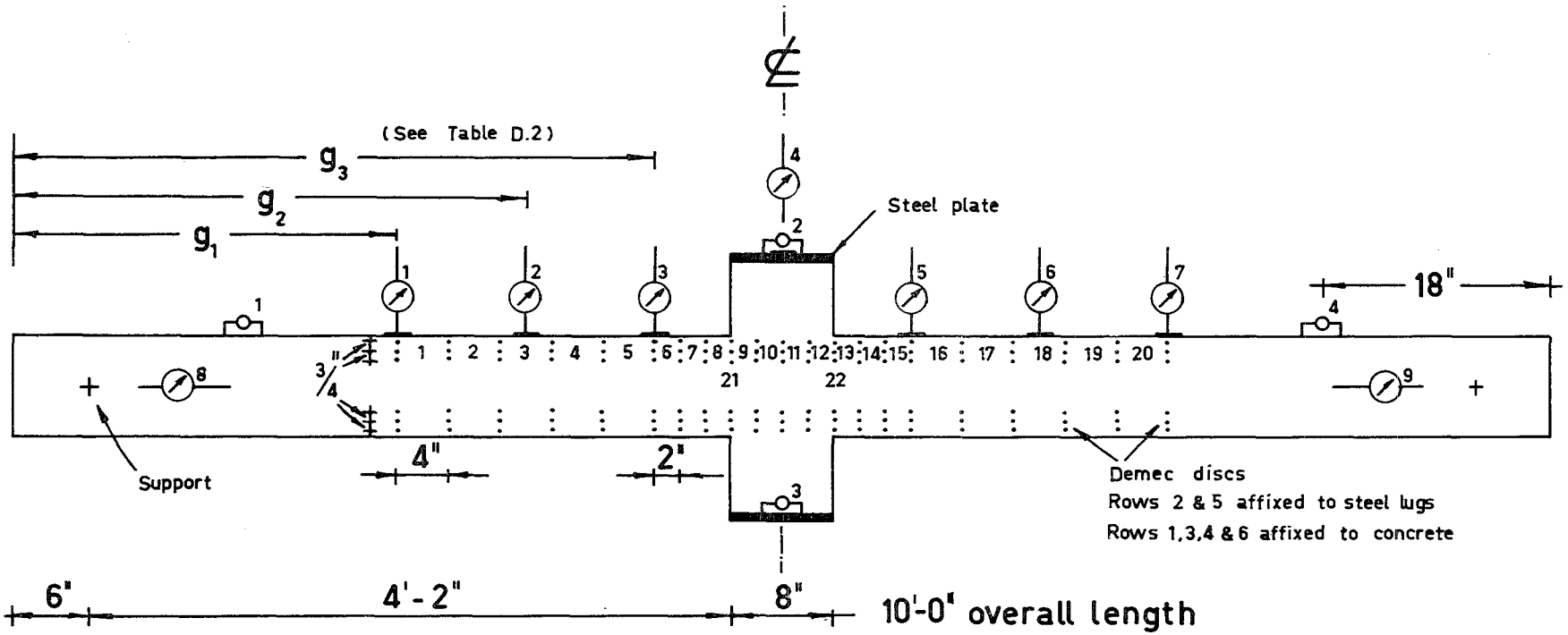

FIG. D.2 - INSTRUMENTATION OF BEAMS

TABLE D.2

BEAM INSTRUMENTATION

Beam Mark	Age at Test (Days)	g_1 (See Fig. D.2)	g_2	g_3	Demec Rows 3 & 4
24	47	29	41	53	Not present
26	245	30	42	53	"
27	63	29	41	53	"
44	108	29	41	53	"
46	51	21	39	47	Present
47	39	37	45	53	"
64	251	30	42	53	Not present
65	240	30	42	53	"
67	33	37	45	53	Present

The column stub inclinometer readings provided rotations that could be averaged and used to correct the deflections for symmetrical behaviour.

D.3.8 Age of Beams at Test

The tests were up to 5 days in duration and beam ages at testing varied from 33 to 251 days as shown in Table D2.

D.3.9 Sequence of Operations

For the initial "zero" readings, when the uncracked beam was subjected only to self-weight loading, the following sequence of operations was observed:-

1. Temperature compensation readings,
2. Dial gauges,
3. Demec gauges, column by column,
4. Temperature compensation readings,
5. Inclinometer stations,
6. Demec gauges, column by column,
7. Dial gauges,
8. Temperature compensation readings.

Demec gauges were read twice for two reasons: firstly, to ensure that important initial readings were accurate; secondly, as a means of determning the accuracy (i.e. repeatability) that could be expected from the Demec gauges. The standard deviations so obtained were of the order of 7 microstrains for all beams and for all Demec gauge operators.

For all other load stages, the procedure was:-

1. Increase or decrease deflection and read

initial load,

2. Record load at 30 second intervals for 2 minutes and mark cracks,
3. Inclinometer readings and complete crack detection,
4. Record load,
5. Dial gauges,
6. Demec gauges, column by column,
7. Dial gauges,
8. Record load.

Temperature compensation readings were taken at approximately half-hourly intervals and interpolation provided values for each load increment.

The quantity of Demec readings varied from increment to increment. At the end or beginning of a day's testing, or at any other time when the beam was subjected only to self-weight loading, all Demec positions were read. During yield, when the applied load was changing very little, only the 2" gauge lengths were measured; the deformations in the 4" gauge lengths, and in fact in many of the 2" gauge lengths, changing very little during such plastic deformation. As mentioned earlier, concrete gauges were read only when the loading imposed compression at that gauge, and then only at selected gauges: on average every second increment.

Inclinometer readings were also taken at selected load stages but all stations were read when the beam was in the plastic range, i.e. when large deflections were taking place.

Of the creep that occurred in the load value, most occurred within $\frac{1}{2}$ min. of application. Change in magnitude of loading before and after dial and Demec gauge readings was less than 2 per cent in the worst case. It is interesting to note that during unloading, creep resulted in a small increase in load in every case.